EPA-R4-73-016a

March 1973

Environmental Monitoring Series

Atmospheric Turbulence and the Dispersal of Atmospheric Pollutants

Office of Research and Monitoring
U.S. Environmental Protection Agency
Washington, D.C. 20460

EPA-R4-73-016a

Atmospheric Turbulence and the Dispersal of Atmospheric Pollutants

by

Coleman duP. Donaldson

Aeronautical Research Associates of Princeton, Inc.
50 Washington Road
Princeton, New Jersey 08540

Contract No. 68-02-0014
Program Element No. A-11009

EPA Project Officer: Kenneth L. Calder

Meteorology Laboratory
National Environmental Research Center
Research Triangle Park, North Carolina 27711

Prepared for

OFFICE OF RESEARCH AND MONITORING
U. S. ENVIRONMENTAL PROTECTION AGENCY
WASHINGTON, D.C. 20460

March 1973

This report has been reviewed by the Environmental Protection Agency and approved for publication. Approval does not signify that the contents necessarily reflect the views and policies of the Agency, nor does mention of trade names or commercial products constitute endorsement or recommendation for use.

PREFACE

In February 1971, Aeronautical Research Associates of Princeton, Inc. (A.R.A.P.) was awarded a small contract by the Environmental Protection Agency to assess the practicality of developing a theory for the dispersal of pollutants by the atmosphere - a theory which would be more fundamental than existing eddy diffusion or K methods. The method to be used was a second-order closure scheme under development at A.R.A.P. by Dr. Coleman duP. Donaldson and his colleagues. Since it appeared, on first application of this method, that a powerful new technique might be successfully developed for computing the dispersive power of the atmosphere under arbitrary meteorological conditions, a further contract was awarded to A.R.A.P. to continue the development of the method. A portion of this extension of the effort was to be applied towards a partial funding of the preparation of a monograph which would bring together a connected account of the derivation of the appropriate equations for the model of atmospheric turbulence and transport. The task is a difficult one for our work is not complete. Although the basic equations will not change, it is expected that, as our investigation proceeds, changes will be made in the nature and/or complexity of the models that are used to obtain a closure of the basic equations. A great deal remains to be done before a completely satisfactory model with associated programs is in hand. It is felt, however, that a working paper which gives a detailed progress report on the present state of A.R.A.P.'s atmospheric model will be useful. It should be pointed out that the work reported here has been the result of funding from many sources, including internal corporate support. Particular acknowledgement should be made of the support received from the National Aeronautics and Space Administration and the Air Force Office of Scientific Research, in addition to the Environmental Protection Agency.

TABLE OF CONTENTS

NOMENCLATURE

$a, b, c_1, c_2, c_3, c_2', c_3'$	constants
A, B, Q	general dependent variables
A_{ik}	constant tensor
C_1, C_2, C_3, C_4	constants
C_α	general species concentration
C_p	specific heat at constant pressure
$\mathscr{D}$	diffusion coefficient
f	Coriolis parameter, $2\Omega \sin \phi$
g	acceleration due to gravity
g_i	general acceleration vector
h	enthalpy
k	conductivity
L	local integral scale; Monin-Obukhov length scale
L_a	typical atmospheric length scale
L_s	typical motional length scale
M	Mach number
p	pressure
P	superequilibrium solution parameter defined in Eq. (7.45)
$Pr = \mu C_p/k$	Prandtl number
$q = K^{1/2}$	$\sqrt{\overline{u_m' u_m'}}$
r, ϕ, z	cylindrical coordinate system
R	gas constant
$Re = \rho_o u_j L_s/\mu_o$	Reynolds number
Re_{Λ_1}	$\rho q \Lambda_1/\mu$
$Ri = \frac{g}{T_o} \frac{\partial \bar{T}}{\partial z} \Big/ \left(\frac{\partial \bar{u}}{\partial z}\right)^2$	Richardson number
$Ri_{crit} = \frac{1 + b}{4b(1 + 3b)}$	critical Richardson number for superequilibrium flow
$Sc = \rho\mathscr{D}/\mu$	Schmidt number
t	time
T	temperature
T_{ij}, T_{ijk}	general tensors of rank two and three, respectively

u, v, w	velocity components
u_i	general velocity vector
UU, VV, WW, etc.	nondimensional representations of $\overline{u'u'}$, $\overline{v'v'}$, $\overline{w'w'}$, etc. (c.f., Eq. (7.30))
x, y, z	Cartesian coordinate system
x_i	general coordinate system
y_k	average length vector
α	constant slope of Λ_1 near $z = 0$
β	constant
γ	ratio of specific heats
σ	spread
δ_{char}	characteristic mean motion scale
δ_{ij}	Kronecker delta
Δ	difference
ε	small distance
η	constant
κ	von Kármán's constant
$\lambda, \Lambda, \Lambda_\alpha$	scalar length scales
μ, μ^*	first and second coefficients of viscosity, respectively
$\upsilon = \mu/\rho$	kinematic viscosity
ξ_k	length difference vector
ρ	density
τ_{ij}	stress tensor
$\tau_t = -\rho\overline{u'w'}$	turbulent shear stress
ϕ	latitude
Ω	Earth's angular rotation

Subscripts

A, B	general vector position notation
c	concentration correlation value
char	characteristic value
g	geostrophic wind condition
j, k	distance discretization designation
n	time discretization designation
t	background turbulence value
o	atmospheric equilibrium condition

1. INTRODUCTION

In 1967, the author, in order to study some aspects of the problem of boundary layer transition, constructed a model of transition [Ref. 1] by a rather simple second-order closure of the time-averaged equations for an incompressible fluid whose motion consists of a mean and a fluctuating part. While the study of the growth of disturbances during transition was of some interest in itself, the aspect of the transition model that most intrigued the author was the fact that it produced, if let run long enough so that transition was complete, a turbulent boundary layer that had some of the characteristics of real boundary layers. This result started the writer and his colleagues on an effort to construct a viable computational model of turbulent shear layers along the general lines of the model of transition. It was recognized that the method of approach was not new. Indeed, the idea was surely understood by Reynolds, who first formulated the equations upon which it is based [Ref. 2]. At that time, however, it was quite beyond practical application since no computational technology was available to provide solutions to the equations involved, even had a closure scheme been formulated.

In 1942, Kolmogorov [Ref. 3] and in 1945, Prandtl and Wieghardt [Ref. 4] specifically formulated the method along the lines that are pursued by a number of investigators at the present time. Two of the earliest to follow these leads were Chou [Ref. 5] and Rotta [Ref. 6]. All of these early formulations and discussions fell short of any practical results for, again, computational facilities and techniques were not available to solve the sets of equations which resulted.

With the advent of the 1960's, the development of digital computers had advanced to the point where one could reasonably expect to develop a practical means of computing turbulent shear layers by means of some sort of second-order closure techniques. A rather large group of related methods appeared within a short time from 1965 through 1970 [Refs. 7 through 15].

Since 1970 the development of computer programs which exploit some form of second-order closure scheme to compute turbulent shear flows or boundary layer transition has proceeded apace, and no attempt will be made here to summarize these efforts.

In January of 1970, the author and Dr. Harold Rosenbaum presented a paper on the generation of atmospheric clear air turbulence [Ref. 16]. In this paper, the first invariant model of an incompressible turbulent shear layer developed at A.R.A.P. was extended to the case of a thin atmospheric shear layer with arbitrary stability. It was mentioned in that paper that there would be no real difficulty in extending the model and program that had been developed to permit the calculation of the dispersal of passive atmospheric pollutants in the atmospheric boundary layer under arbitrary stability conditions.

Subsequently, A.R.A.P. received moderate support from both EPA and NASA to develop programs for computing the dispersal of pollutants in the atmospheric boundary layer. The support from EPA was directed towards the solution of the dispersal of pollutants from a line source, while that from NASA was directed towards the dispersal from a point source of pollutant material. While these efforts were underway, additional studies at A.R.A.P. were carried out; these were aimed at further understanding and improvement of the models used in the closure of the equation of motion at second order.

In this paper we will present the derivation of the set of equations on which the A.R.A.P. model of atmospheric turbulence and transport is based and, in addition, discuss the process which was used to obtain the present closure model and the values of the basic parameters which appear therein. Following these discussions, the relationship of the present second-order closure method for computing turbulent transport to eddy diffusivity or K theory models will be discussed by showing that what is essentially K theory can be obtained from a second-order closure scheme as a well-defined limiting case. Finally, some typical examples of computations using the present model will be presented.

2. EQUATIONS FOR AN ATMOSPHERIC SHEAR LAYER

The equations which we shall take to govern the motion of a compressible, nonchemically-reacting perfect gas are:

the perfect gas law

$$\tilde{p} = \tilde{\rho}\tilde{R}\tilde{T} \tag{2.1}$$

the continuity equation*

$$\frac{\partial \tilde{\rho}}{\partial t} + \frac{\partial}{\partial x_j}(\tilde{\rho}\tilde{u}_j) = 0 \tag{2.2}$$

the momentum equation

$$\frac{\partial \tilde{\rho}\tilde{u}_i}{\partial t} + \frac{\partial}{\partial x_j}(\tilde{\rho}\tilde{u}_j\tilde{u}_i) = -\frac{\partial \tilde{p}}{\partial x_i} + \frac{\partial}{\partial x_j}\tilde{\tau}_{ij} - \tilde{\rho}g_i \tag{2.3}$$

where the stress due to molecular diffusion is given by

$$\tilde{\tau}_{ij} = \tilde{\mu}\left(\frac{\partial \tilde{u}_i}{\partial x_j} + \frac{\partial \tilde{u}_j}{\partial x_i}\right) + \delta_{ij}\tilde{\mu}^* \frac{\partial \tilde{u}_m}{\partial x_m} \tag{2.4}$$

the energy equation

$$\frac{\partial \tilde{\rho}\tilde{h}}{\partial t} + \frac{\partial}{\partial x_j}(\tilde{\rho}\tilde{u}_j\tilde{h}) = \frac{\partial \tilde{p}}{\partial t} + \tilde{u}_j\frac{\partial \tilde{p}}{\partial x_j} + \frac{\partial}{\partial x_j}\left(\tilde{k}\frac{\partial \tilde{T}}{\partial x_j}\right) + \tilde{\tau}_{ij}\frac{\partial \tilde{u}_i}{\partial x_j} \tag{2.5}$$

and the species conservation equation

$$\frac{\partial}{\partial t}(\tilde{\rho}\tilde{C}_\alpha) + \frac{\partial}{\partial x_j}(\tilde{\rho}\tilde{u}_j\tilde{C}_\alpha) = \frac{\partial}{\partial x_j}\left(\tilde{\rho}\tilde{\mathcal{D}}\frac{\partial}{\partial x_j}\tilde{C}_\alpha\right) \tag{2.6}$$

In what follows, we will be interested in the development of turbulence and the transport of matter in a thin layer of the atmosphere. We will assume that the matter to be transported in the atmosphere is not too highly concentrated, so that it makes no first-order effect upon the heat capacity or gas constant of the air in which it is carried. In this case, if we designate the heat capacity as C_{p_o} and the gas constant as R_o, we may

*In this equation and those that follow, the summation convention of tensor analysis is used; i.e., repeated indices in any expression indicate that one is to sum over these indices.

write (2.1) as

$$\tilde{p} = \tilde{\rho} R_o \tilde{T} \tag{2.7}$$

and (2.5) as

$$C_{p_o}\left[\frac{\partial}{\partial t}\tilde{\rho}\tilde{T} + \frac{\partial}{\partial x_j}(\tilde{\rho}\tilde{u}_j\tilde{T})\right] = \frac{\partial \tilde{p}}{\partial t} + \tilde{u}_j\frac{\partial \tilde{p}}{\partial x_j} + \frac{\partial}{\partial x_j}\tilde{k}\frac{\partial \tilde{T}}{\partial x_j} + \tilde{\tau}_{ij}\frac{\partial \tilde{u}_i}{\partial x_j} \tag{2.8}$$

Since the Mach number M of the flow in which we will be interested is small, we may neglect the last term on the right-hand side of (2.8) since this term represents the heat generated by the dissipation of the motion and is of order M^2 compared with the other terms in the equation. The final form of the energy equation is, then,

$$C_{p_o}\left[\frac{\partial \tilde{\rho}\tilde{T}}{\partial t} + \frac{\partial}{\partial x_j}(\tilde{\rho}\tilde{u}_j\tilde{T})\right] = \frac{\partial \tilde{p}}{\partial t} + \tilde{u}_j\frac{\partial \tilde{p}}{\partial x_j} + \frac{\partial}{\partial x_j}\left(\tilde{k}\frac{\partial \tilde{T}}{\partial x_j}\right) \tag{2.9}$$

Following the usual practice for obtaining the equations for the motion of an atmospheric shear layer [Refs. 17 and 18], we will consider the atmosphere to be in a state slightly removed from an adiabatic atmosphere at rest. We consider then an expansion of the equations presented above according to the following scheme:

$$\tilde{p} = p_o + p$$

$$\tilde{\rho} = \rho_o + \rho$$

$$\tilde{T} = T_o + T$$

$$\tilde{u}_j = 0 + u_j$$

$$\tilde{C}_\alpha = C_{\alpha_o} + C_\alpha$$

$$\tilde{\mu} = \mu_o + \mu$$

$$\tilde{\mu}^* = \mu_o^* + \mu^*$$

$$\tilde{k} = k_o + k$$

$$\tilde{\rho}\tilde{\mathscr{D}} = \rho_o \mathscr{D}_o + \rho \mathscr{D}_o + \rho_o \mathscr{D} + \rho \mathscr{D} \tag{2.10}$$

If we expand the gas law (2.7) according to this scheme, we have

$$p_o = \rho_o R_o T_o \tag{2.11}$$

and

$$p = R_o \left(\rho_o T + \rho T_o + \rho T \right) \tag{2.12}$$

The continuity equation (2.2) yields

$$\frac{\partial \rho_o}{\partial t} = 0 \tag{2.13}$$

which agrees with our assumption, and

$$\frac{\partial \rho}{\partial t} + \frac{\partial}{\partial x_j} \left(\rho_o u_j + \rho u_j \right) = 0 \tag{2.14}$$

The momentum equation (2.3) yields

$$\frac{\partial p_o}{\partial x_i} = - \rho_o g_i \tag{2.15}$$

and

$$(\rho_o + \rho) \frac{\partial u_i}{\partial t} + (\rho_o + \rho) u_j \frac{\partial u_i}{\partial x_j} + \left\{ u_i \left[\frac{\partial \rho}{\partial t} + \frac{\partial}{\partial x_j} \left(\rho_o u_j + \rho u_j \right) \right] \right\}$$

$$= - \frac{\partial p}{\partial x_i} - \rho g_i + \frac{\partial}{\partial x_j} \left[(\mu_o + \mu) \left(\frac{\partial u_i}{\partial x_j} + \frac{\partial u_j}{\partial x_i} \right) + \right.$$

$$\left. + \delta_{ij} (\mu_o^* + \mu^*) \frac{\partial u_m}{\partial x_m} \right] \tag{2.16}$$

This equation may be simplified further by noting that in the first two terms on the left-hand side of the equation we may

neglect ρ compared to ρ_o. Likewise on the right-hand side, we may neglect μ compared to μ_o and μ^* compared to μ_o^*. In addition, the term on the left-hand side in curly brackets is zero by virtue of (2.14) so that we may write

$$\rho_o \frac{\partial u_i}{\partial t} + \rho_o u_j \frac{\partial u_i}{\partial x_j} = -\frac{\partial p}{\partial x_i} - \rho g_i + \frac{\partial}{\partial x_j}\left[\mu_o\left(\frac{\partial u_i}{\partial x_j} + \frac{\partial u_j}{\partial x_i}\right)\right] + \frac{\partial}{\partial x_i}\mu_o^* \frac{\partial u_m}{\partial x_m} \quad (2.17)$$

Expansion of the energy equation (2.9) yields

$$\frac{\partial}{\partial x_j}\left(k_o \frac{\partial T_o}{\partial x_j}\right) = \left(C_{p_o} - R_o\right)\rho_o \frac{\partial T_o}{\partial t} \cong 0 \quad (2.18)$$

and

$$C_{p_o}(\rho_o + \rho)\frac{\partial T}{\partial t} + C_{p_o}(\rho_o + \rho)u_j \frac{\partial T}{\partial x_j} + \left\{C_{p_o}(T_o + T)\left[\frac{\partial \rho}{\partial t} + \frac{\partial}{\partial x_j}\left(\rho_o u_j + \rho u_j\right)\right]\right\} = u_j\left[\frac{\partial p_o}{\partial x_j} - C_{p_o}(\rho_o + \rho)\frac{\partial T_o}{\partial x_j}\right] + \frac{\partial p}{\partial t} + u_j \frac{\partial p}{\partial x_j} + \frac{\partial}{\partial x_j}\left[(k_o + k)\frac{\partial T}{\partial x_j} + k\frac{\partial T_o}{\partial x_j}\right] \quad (2.19)$$

In this equation, as in the momentum equation, we may neglect ρ compared to ρ_o in the first two terms, and the term in curly brackets is zero by virtue of (2.14). On the right-hand side of the equation, the term in square brackets may be neglected since the basic atmosphere is isentropic; i.e.,

$$\frac{\partial p_o}{\partial x_j} = \rho_o C_{p_o}\frac{\partial T_o}{\partial x_j} = \frac{p_o}{T_o}\frac{C_{p_o}}{R_o}\frac{\partial T_o}{\partial x_j} \quad (2.20)$$

and, by the thin layer approximation we are using, the remaining term in the square brackets is small compared to the term kept in the second term on the left-hand side of the equation.

The two terms on the right-hand side containing p, namely,

$$\frac{\partial p}{\partial t} + u_j \frac{\partial p}{\partial x_j}$$

represent the heating of the fluid due to the motion and are of order M^2 compared to the other terms in the equation and so may be neglected. Finally, by neglecting k compared with k_o in the last term on the right-hand side, the energy equation becomes

$$C_{p_o}\rho_o \frac{\partial T}{\partial t} + C_{p_o}\rho_o u_j \frac{\partial T}{\partial x_j} = \frac{\partial}{\partial x_j}\left(k_o \frac{\partial T}{\partial x_j} + k \frac{\partial T_o}{\partial x_j}\right) \tag{2.21}$$

Substitution of the expansion (2.10) into the species conservation equation (2.6) results in

$$\rho_o \frac{\partial C_\alpha}{\partial t} + (\rho_o + \rho)u_j \frac{\partial C_\alpha}{\partial x_j} + \left(C_{\alpha_o} + C_\alpha\right)\left[\frac{\partial \rho}{\partial t} + \frac{\partial}{\partial x_j}\left(\rho_o u_j + \rho u_j\right)\right]$$

$$= \frac{\partial}{\partial x_j}\left[\rho_o \mathscr{D}_o \frac{\partial C_\alpha}{\partial x_j} + \rho \mathscr{D}_o \frac{\partial C_\alpha}{\partial x_j} + \rho_o \mathscr{D} \frac{\partial C_\alpha}{\partial x_j} + \rho \mathscr{D} \frac{\partial C_\alpha}{\partial x_j}\right] \tag{2.22}$$

Since the basic atmosphere is all air, $\partial C_{\alpha_o}/\partial x_j = 0$. Using this result, (2.22) may be written to the same order of accuracy as the other equations we have derived as

$$\rho_o \frac{\partial C_\alpha}{\partial t} + \rho_o u_j \frac{\partial C_\alpha}{\partial x_j} = \frac{\partial}{\partial x_j}\left[\rho_o \mathscr{D}_o \frac{\partial C_\alpha}{\partial x_j}\right] \tag{2.23}$$

We now return to the equations that result from the perfect gas law, namely, (2.11) and (2.12), and note that we may write

$$\frac{p}{p_o} = \frac{T}{T_o} + \frac{\rho}{\rho_o} + \frac{\rho T}{\rho_o T_o} \tag{2.24}$$

or to the order of accuracy of our other equations

$$\frac{p}{p_o} = \frac{T}{T_o} + \frac{\rho}{\rho_o} \tag{2.25}$$

Now we note that the changes in p will be of the order of $\rho_o u_j^2$, so that

$$\frac{T}{T_o} + \frac{\rho}{\rho_o} = 0\left(\frac{u_j^2}{R_o T_o}\right) = 0(\gamma M^2) \tag{2.26}$$

We will, therefore, neglect the effects of motion-induced pressure changes on the variation of density and take

$$\rho = -\frac{\rho_o}{T_o} T \tag{2.27}$$

This latter assumption is related to, and entirely consistent with, our neglect of the pressure work terms in the energy equation.

We may now combine (2.14), (2.21), and (2.27) to find an expression for the divergence of the velocity field. If (2.27) is substituted into (2.14), we obtain, after some manipulation,

$$-\rho_o \frac{\partial T}{\partial t} - \rho_o u_j \frac{\partial T}{\partial x_j} + (T_o - T)\frac{\partial}{\partial x_j}(\rho_o u_j) + \rho_o u_j \frac{T}{T_o}\frac{\partial T_o}{\partial x_j} = 0 \tag{2.28}$$

Neglecting T compared with T_o in the third term on the right-hand side of this expression allows us to write

$$\rho_o T_o \frac{\partial u_j}{\partial x_j} + \rho_o T_o u_j\left[\frac{\partial \ell n \rho_o}{\partial x_j} + \frac{T}{T_o}\frac{\partial \ell n T_o}{\partial x_j}\right] = \rho_o \frac{\partial T}{\partial t} + \rho_o u_j \frac{\partial T}{\partial x_j} \tag{2.29}$$

In (2.29) we may neglect the term $(T/T_o)(\partial \ell n T_o/\partial x_j)$ compared to $\partial \ell n \rho_o/\partial x_j$. If the resulting equation is compared with (2.21), one finds that

$$\frac{\partial u_j}{\partial x_j} = -\frac{u_j}{\rho_o}\frac{\partial \rho_o}{\partial x_j} + \frac{R_o}{C_{p_o}}\frac{1}{p_o}\frac{\partial}{\partial x_j}\left[k_o \frac{\partial T}{\partial x_j} + k \frac{\partial T_o}{\partial x_j}\right] \tag{2.30}$$

This equation states that there must be a divergence of velocity at a point where a volume of air is moving in the vertical direction (the direction of the gradient of ρ_o) so that air can expand or contract to the pressure level of the equilibrium

atmosphere. It also states that any atmospheric element gaining or losing heat by conduction to the air immediately surrounding it must expand or contract so as to maintain its pressure at that of the equilibrium atmosphere.

It may be useful to gather together the equations we have just discussed. For the atmosphere at rest, we have

$$p_o = R_o \rho_o T_o \tag{2.11}$$

$$\frac{\partial p_o}{\partial x_i} = -\rho_o g_i \tag{2.15}$$

$$\frac{\partial}{\partial x_j}\left(k_o \frac{\partial T_o}{\partial x_j}\right) = \left(C_{p_o} - R_o\right)\rho_o \frac{\partial T_o}{\partial t} \cong 0 \tag{2.18}$$

and

$$\frac{\partial p_o}{\partial x_j} = \rho_o C_{p_o} \frac{\partial T_o}{\partial x_j} \tag{2.20}$$

For the disturbed flow, we have

$$\rho_o \frac{\partial u_i}{\partial t} + \rho_o u_j \frac{\partial u_i}{\partial x_j} = -\frac{\partial p}{\partial x_i} - \rho g_i + \frac{\partial}{\partial x_j}\left[\mu_o\left(\frac{\partial u_i}{\partial x_j} + \frac{\partial u_j}{\partial x_i}\right)\right] + \frac{\partial}{\partial x_i}\ \mu_o^* \frac{\partial u_m}{\partial x_m} \tag{2.17}$$

$$C_{p_o}\rho_o \frac{\partial T}{\partial t} + C_{p_o}\rho_o u_j \frac{\partial T}{\partial x_j} = \frac{\partial}{\partial x_j}\left[k_o \frac{\partial T}{\partial x_j} + k \frac{\partial T_o}{\partial x_j}\right] \tag{2.21}$$

$$\rho_o \frac{\partial C_\alpha}{\partial t} + \rho_o u_j \frac{\partial C_\alpha}{\partial x_j} = \frac{\partial}{\partial x_j}\left[\rho_o \mathscr{D}_o \frac{\partial C_\alpha}{\partial x_j}\right] \tag{2.23}$$

$$\rho = -\frac{\rho_o}{T_o} T \tag{2.27}$$

and

$$\frac{\partial u_j}{\partial x_j} = -\frac{u_j}{\rho_o}\frac{\partial \rho_o}{\partial x_j} + \frac{R_o}{C_{p_o}}\frac{1}{p_o}\frac{\partial}{\partial x_j}\left[k_o \frac{\partial T}{\partial x_j} + k \frac{\partial T_o}{\partial x_j}\right] \tag{2.30}$$

One recognizes immediately an inconsistency in the equations for the basic atmosphere. Combination of (2.15) and (2.20) yields

$$\frac{\partial T_o}{\partial x_i} = - \frac{g_i}{C_{p_o}} \tag{2.31}$$

which gives, if $g_i = g\delta_{i3}$,

$$\frac{\partial T_o}{\partial x_1} = \frac{\partial T_o}{\partial x_2} = 0 \tag{2.32}$$

and

$$\frac{\partial T_o}{\partial x_3} = - \frac{g}{C_{p_o}} = \text{constant} \tag{2.33}$$

which is the normal adiabatic lapse rate. Since by (2.18) we must also have

$$k_o \frac{\partial T_o}{\partial x_3} = \text{constant}$$

the equations for the basic atmosphere are slightly inconsistent since k_o is, in general, a function of T_o . This inconsistency is such that the assumption of no time variation of T_o is negated, since (2.18) states that, in general,

$$\rho_o \left(C_{p_o} - R_o \right) \frac{\partial T_o}{\partial t} = \frac{\partial}{\partial x_j} \left(k_o \frac{\partial T_o}{\partial x_j} \right) \tag{2.18}$$

The inconsistency, however, is of small practical consequence since (2.18) yields a time rate of change of T_o which is enormously slower than the rates of change involved in practical computations of atmospheric motion.

The equations given above are greatly simplified if one considers that the region of the atmosphere in which one is interested is of small extent compared to the scale of the atmosphere. In this case, the variations in the molecular transport coefficients can, indeed, be neglected in the equations and, in

addition, as will be shown below, the divergence of the velocity field does not play a significant role in controlling the motions that occur.

We begin with an order of magnitude analysis of (2.30). Let us define a typical scale of the atmosphere as

$$L_a = \left(\frac{1}{\rho_o} \frac{\partial \rho_o}{\partial z} \right)^{-1} \tag{2.34}$$

and a much smaller scale typical of the motion in question as L_s . Equation (2.30) may then be written

$$\frac{\partial u_j}{\partial x_j} = - \frac{u_j}{L_a} \left[1 - O\left(\frac{R_o}{C_{p_o}} \frac{L_a}{u_j} \frac{1}{p_o} \frac{\frac{k_o \Delta T}{L_s} + \frac{k T_o}{L_a}}{L_s} \right) \right] \tag{2.35}$$

which may be written

$$\frac{\partial u_j}{\partial x_j} = - \frac{u_j}{L_a} \left\{ 1 - O\left[\frac{k_o}{\mu_o C_{p_o}} \cdot \frac{\mu_o}{\rho_o u_j L_s} \cdot \left(\frac{\Delta T}{T_o} \frac{L_a}{L_s} + \frac{k}{k_o} \right) \right] \right\} \tag{2.36}$$

In general we will have $L_a \Delta T / L_s T_o$ of order ten or less* and, since the Prandtl number $\mu_o C_{p_o} / k_o$ is of order unity and k/k_o is small, (2.36) may be written

$$\frac{\partial u_j}{\partial x_j} = - \frac{u_j}{L_a} \left[1 - O\left(\frac{10}{Re} \right) \right] \tag{2.37}$$

Here the Reynolds number Re is defined as $\rho_o u_j L_s / \mu_o$. We see then that unless the scale in question is so small that Re is of order ten the primary cause of divergence of the velocity field is the basic density gradient in the undisturbed atmosphere, and we may write (2.30) as

$$\frac{\partial u_j}{\partial x_j} = - \frac{u_j}{\rho_o} \frac{\partial \rho_o}{\partial x_j} \tag{2.38}$$

---

* T_o / L_a is of order 1°/100 meters and, in general, we will be interested in atmospheric flows with lapse rates up to the order of 10°/100 meters

In the equations of motion, the velocity divergence enters through the viscous term

$$\frac{\partial}{\partial x_j}\left[\mu_o\left(\frac{\partial u_i}{\partial x_j}+\frac{\partial u_j}{\partial x_i}\right)+\delta_{ij}\mu_o^*\frac{\partial u_k}{\partial x_k}\right]$$

$$=\frac{\partial}{\partial x_j}\left[\mu_o\left(\frac{\partial u_i}{\partial x_j}+\frac{\partial u_j}{\partial x_i}\right)-\delta_{ij}\frac{\mu_o^* u_k}{\rho_o}\frac{\partial \rho_o}{\partial x_k}\right] \tag{2.39}$$

The order of magnitude of the term on the left in the square brackets is $\mu_o u_j/L_s$ while that on the right is of order $\mu_o u_j/L_a$. It is clear then that we may neglect the effect of velocity divergence in the viscous terms of the momentum equation.

It will be convenient to write terms in the equations of motion such as $\rho_o u_j(\partial u_i/\partial x_j)$ and $\rho_o u_j(\partial T/\partial x_j)$, etc., in the form

$$\rho_o u_j\frac{\partial Q}{\partial x_j}=\rho_o\frac{\partial}{\partial x_j}(Qu_j)-\rho_o Q\frac{\partial u_j}{\partial x_j}$$

$$=\rho_o\left(\frac{\partial}{\partial x_j}Qu_j+\frac{Qu_j}{\rho_o}\frac{\partial \rho_o}{\partial x_j}\right) \tag{2.40}$$

Here again it is clear that the first term on the right-hand side of (2.40) is of order $u_j Q/L_s$ while the second term on the right-hand side is of order $u_j Q/L_a$. We may, therefore, write

$$\rho_o u_j\frac{\partial Q}{\partial x_j}=\rho_o\frac{\partial}{\partial x_j}(u_j Q) \tag{2.41}$$

in manipulating the equations. In view of the foregoing discussion, we may further simplify (2.38) to

$$\frac{\partial u_j}{\partial x_j}=0 \tag{2.42}$$

In what follows, we will adopt the shear layer approximation with the result that the coefficients of molecular diffusion can be taken constant in the equations of motion and the velocity field is effectively divergence free. We will make one more simplification, a simplification that is often made in analyses of aerodynamic heat and mass transfer phenomena. In view of the fact that the Prandtl number $\mu C_p/k$ and the Schmidt number $\mu/\rho\mathscr{D}$ for air are of order one (see Table 2.1 below), we will greatly simplify the equations of motion if we assume that these numbers are indeed equal to one, and write

$$k_o = \mu_o C_{p_o} \tag{2.43}$$

and

$$\rho_o \mathscr{D}_o = \mu_o \tag{2.44}$$

Table 2.1 Prandtl and Schmidt Numbers for Several Gases at 0°C and 1 Atmosphere

Gas	$Pr = \mu C_p/k$	$Sc = \mu/\rho\mathscr{D}$
Ne	0.66	0.73
A	0.67	0.75
N_2	0.71	0.74
CH_4	0.74	0.70
O_2	0.72	0.74
CO_2	0.75	0.71
H_2	0.71	0.73
Au	0.71	0.74

3. EQUATIONS FOR TURBULENT SHEAR LAYERS

If the assumptions listed in the previous section are adopted, the equations for an atmospheric shear layer may be written:

$$p_o = \rho_o R_o T_o \tag{3.1}$$

$$\frac{\partial p_o}{\partial x_i} = - \rho_o g_i \tag{3.2}$$

$$\frac{\partial p_o}{\partial x_i} = C_{p_o} \rho_o \frac{\partial T_o}{\partial x_i} = - \rho_o g_i \tag{3.3}$$

$$\rho_o \frac{\partial u_i}{\partial t} + \rho_o u_j \frac{\partial u_i}{\partial x_j} = - \frac{\partial p}{\partial x_i} + \frac{\rho_o}{T_o} g_i T + \mu_o \frac{\partial^2 u_i}{\partial x_j^2} \tag{3.4}$$

$$\rho_o \frac{\partial T}{\partial t} + \rho_o u_j \frac{\partial T}{\partial x_j} = \mu_o \frac{\partial^2 T}{\partial x_j^2} \tag{3.5}$$

$$\rho_o \frac{\partial C_\alpha}{\partial t} + \rho_o u_j \frac{\partial C_\alpha}{\partial x_j} = \mu_o \frac{\partial^2 C_\alpha}{\partial x_j^2} \tag{3.6}$$

$$\rho = - \frac{\rho_o}{T_o} T \tag{3.7}$$

and

$$\frac{\partial u_j}{\partial x_j} = 0 \tag{3.8}$$

A set of equations, generally referred to as the Boussinesq equations for a stratified fluid, is usually found in treatises on atmospheric motion. That set reduces to (3.1) through (3.8) when it is assumed that the Prandtl number and the Schmidt number are both equal to one, as discussed in Section 2.

Following the technique used by Reynolds [Ref. 2], we now develop the equations for the mean properties of a turbulent atmospheric shear layer. To do this, we express the physical variables as the sum of a mean value of the variable and an

instantaneous fluctuation about that mean according to the following scheme:

$$\begin{aligned} p &= \bar{p} + p' \\ T &= \bar{T} + T' \\ \rho &= \bar{\rho} + \rho' \\ u_i &= \bar{u}_i + u_i' \\ C_\alpha &= \bar{C}_\alpha + C_\alpha' \end{aligned} \tag{3.9}$$

In these expressions, a bar over a quantity indicates the average value of that quantity, while the prime denotes the instantaneous fluctuation of the quantity about its mean.

The continuity equation (3.8) immediately yields the two results:

$$\frac{\partial \bar{u}_j}{\partial x_j} = 0 \tag{3.10}$$

and

$$\frac{\partial u_j'}{\partial x_j} = 0 \tag{3.11}$$

(3.11) implies the further result

$$u_j' \frac{\partial Q'}{\partial x_j} = \frac{\partial (u_j' Q')}{\partial x_j} \tag{3.12}$$

This relation is used frequently in the manipulations that follow.

If (3.9) is used in the momentum equation, the result is

$$\begin{aligned} \rho_o \left(\frac{\partial \bar{u}_i}{\partial t} + \frac{\partial u_i'}{\partial t} \right) + \rho_o \left(\bar{u}_j \frac{\partial \bar{u}_i}{\partial x_j} + \bar{u}_j \frac{\partial u_i'}{\partial x_j} + u_j' \frac{\partial \bar{u}_i}{\partial x_j} + u_j' \frac{\partial u_i'}{\partial x_j} \right) \\ = - \frac{\partial \bar{p}}{\partial x_i} - \frac{\partial p'}{\partial x_i} + \frac{\rho_o g_i}{T_o} (\bar{T} + T') \\ + \mu_o \frac{\partial^2 \bar{u}_i}{\partial x_j^2} + \mu_o \frac{\partial^2 u_i'}{\partial x_j^2} \end{aligned} \tag{3.13}$$

If this equation is averaged, we obtain

$$\rho_o \frac{\partial \bar{u}_i}{\partial t} + \rho_o \bar{u}_j \frac{\partial \bar{u}_i}{\partial x_j} = - \frac{\partial \bar{p}}{\partial x_i} + \frac{\rho_o}{T_o} g_i \bar{T} + \mu_o \frac{\partial^2 \bar{u}_i}{\partial x_j^2} - \rho_o \frac{\partial \overline{u_i' u_j'}}{\partial x_j} \qquad (3.14)$$

This is the usual equation for the mean motion of an atmospheric layer. It is seen that the turbulence has introduced an effective stress, the Reynolds stress, which is of magnitude $\rho_o \overline{u_i' u_j'}$.

We may obtain an equation for the velocity fluctuations by subtracting (3.14) from (3.13); thus,

$$\rho_o \frac{\partial u_i'}{\partial t} + \rho_o \left(\bar{u}_j \frac{\partial u_i'}{\partial x_j} + u_j' \frac{\partial \bar{u}_i}{\partial x_j} + u_j' \frac{\partial u_i'}{\partial x_j} - \overline{u_j' \frac{\partial u_i'}{\partial x_j}} \right)$$

$$= - \frac{\partial p'}{\partial x_i} + \frac{\rho_o}{T_o} g_i T' + \mu_o \frac{\partial^2 u_i'}{\partial x_j^2} \qquad (3.15)$$

From this equation we can obtain an equation for the Reynolds stress correlation $\overline{u_i' u_k'}$. If (3.15) is multiplied through by u_k' and time averaged, one obtains

$$\rho_o \overline{u_k' \frac{\partial u_i'}{\partial t}} + \rho_o \left(\bar{u}_j \overline{u_k' \frac{\partial u_i'}{\partial x_j}} + \overline{u_j' u_k'} \frac{\partial \bar{u}_i}{\partial x_j} + \overline{u_k' u_j' \frac{\partial u_i'}{\partial x_j}} \right)$$

$$= - \overline{u_k' \frac{\partial p'}{\partial x_i}} + \frac{\rho_o}{T_o} g_i \overline{u_k' T'} + \mu_o \overline{u_k' \frac{\partial^2 u_i'}{\partial x_j^2}} \qquad (3.16)$$

If the indices i and k in (3.16) are interchanged and the resulting equation added to (3.16), there results, after some rearrangement

$$\rho_o \frac{\partial \overline{u_i' u_k'}}{\partial t} + \rho_o \bar{u}_j \frac{\partial \overline{u_i' u_k'}}{\partial x_j} = - \rho_o \overline{u_i' u_j'} \frac{\partial \bar{u}_k}{\partial x_j} - \rho_o \overline{u_k' u_j'} \frac{\partial \bar{u}_i}{\partial x_j}$$

$$- \rho_o \frac{\partial}{\partial x_j} (\overline{u_i' u_j' u_k'}) - \frac{\partial}{\partial x_i} (\overline{p' u_k'}) - \frac{\partial}{\partial x_k} (\overline{p' u_i'})$$

$$+ \overline{p' \left(\frac{\partial u_i'}{\partial x_k} + \frac{\partial u_k'}{\partial x_i} \right)} + \frac{\rho_o}{T_o} \left(\overline{g_i u_k' T'} + \overline{g_k u_i' T'} \right)$$

$$+ \mu_o \frac{\partial^2 \overline{u_i' u_k'}}{\partial x_j^2} - 2\mu_o \overline{\frac{\partial u_i'}{\partial x_j} \frac{\partial u_k'}{\partial x_j}} \qquad (3.17)$$

This is the standard equation for the Reynolds stress correlation and has been discussed at great length in various texts on atmospheric motion [see, for example, Ref. 17].

We will briefly review the nature of this equation. The two terms on the left-hand side represent ρ_o times the substantive derivative (rate of change following the motion) of the correlation $\overline{u_i' u_k'}$. On the right-hand side, the first two terms

$$- \rho_o \overline{u_i' u_j'} \frac{\partial \bar{u}_k}{\partial x_j} - \rho_o \overline{u_k' u_j'} \frac{\partial \bar{u}_i}{\partial x_j}$$

are called the production terms. They represent the production of new correlations by the interaction of the turbulence with the variation of the mean velocity field as well as the modification of existing correlations by the variation of the mean field (stream tube stretching effects).

The term

$$\rho_o \frac{\partial}{\partial x_j} (\overline{u_i' u_j' u_k'})$$

represents the diffusion of the correlation $\overline{u_i' u_k'}$ by the turbulent velocity fluctuations and is called, appropriately, the velocity diffusion term.

The next two terms

$$\frac{\partial}{\partial x_i}\left(\overline{p'u_k'}\right) + \frac{\partial}{\partial x_k}\left(\overline{p'u_i'}\right)$$

are called the pressure diffusion terms. They are the least understood of all the terms in (3.17) because of the great difficulty associated with experimentally measuring a pressure-velocity correlation. In general, they have been found not to play a dominant role in the development of a two-dimensional, truly incompressible, turbulent shear layer.

The sixth expression on the right-hand side of (3.17)

$$\overline{p'\left(\frac{\partial u_i'}{\partial x_k} + \frac{\partial u_k'}{\partial x_i}\right)}$$

is called the tendency-towards-isotropy term. This nomenclature stems from the fact that, while the term appears in each of the equations for the separate energy components in a truly incompressible turbulent flow, i.e., in the equations for $\overline{u_1'^2}$, $\overline{u_2'^2}$, and $\overline{u_3'^2}$, it drops out of the equation for the total energy $\overline{u_1'^2} + \overline{u_2'^2} + \overline{u_3'^2}$ by virtue of the vanishing of the divergence of the turbulent velocity field. The term must then, for incompressible flows, represent a rearrangement of the turbulent energy among the various components of velocity.

The seventh term on the right-hand side of (3.17), namely,

$$\frac{\rho_o}{T_o}\left(g_i\overline{u_k'T'} + g_k\overline{u_i'T'}\right)$$

represents the production or reduction of the correlation $\overline{u_i'u_k'}$ due to the interaction of fluctuations in velocity with fluctuations in temperature.

The term

$$\mu_o \frac{\partial^2\overline{u_i'u_k'}}{\partial x_j^2}$$

in (3.17) is obviously the diffusion of the correlation $\overline{u_i'u_k'}$ by the action of molecular viscosity.

Finally, the term

$$-2\mu_o \overline{\frac{\partial u_i'}{\partial x_j}\frac{\partial u_k'}{\partial x_j}}$$

is called the dissipation term and represents, in the equations of $\overline{u_1'^2}$, $\overline{u_2'^2}$, and $\overline{u_3'^2}$, the conversion of these energies to heat by the action of molecular viscosity.

We will return to a discussion of the nature of these terms later in this paper when we discuss how some of these terms might be modeled.

If the Reynolds scheme (3.9) is applied to the energy equation, the result is

$$\rho_o\left(\frac{\partial \bar{T}}{\partial t} + \frac{\partial T'}{\partial t}\right) + \rho_o\left(\bar{u}_j \frac{\partial \bar{T}}{\partial x_j} + \bar{u}_j \frac{\partial T'}{\partial x_j} + u_j' \frac{\partial \bar{T}}{\partial x_j} + u_j' \frac{\partial T'}{\partial x_j}\right)$$

$$= \mu_o \frac{\partial^2 \bar{T}}{\partial x_j^2} + \mu_o \frac{\partial^2 T'}{\partial x_j^2} \tag{3.18}$$

When this equation is averaged, one obtains

$$\rho_o \frac{\partial \bar{T}}{\partial t} + \rho_o \bar{u}_j \frac{\partial \bar{T}}{\partial x_j} = \mu_o \frac{\partial^2 \bar{T}}{\partial x_j^2} - \rho_o \frac{\partial}{\partial x_j}\left(\overline{u_j'T'}\right) \tag{3.19}$$

Here again, the turbulence produces an increased heat transfer whose magnitude is $\rho_o C_{p_o} \overline{u_j'T'}$. The equation for the temperature fluctuation is

$$\rho_o \frac{\partial T'}{\partial t} + \rho_o\left(\bar{u}_j \frac{\partial T'}{\partial x_j} + u_j' \frac{\partial \bar{T}}{\partial x_j} + u_j' \frac{\partial T'}{\partial x_j} - \overline{u_j' \frac{\partial T'}{\partial x_j}}\right) = \mu_o \frac{\partial^2 T'}{\partial x_j^2} \tag{3.20}$$

We can obtain an equation for the heat transfer correlation $\overline{u_k'T'}$ in the following way. First, multiply (3.20) by u_k' and time average to obtain

$$\rho_o \overline{u_k' \frac{\partial T'}{\partial t}} + \rho_o\left(\bar{u}_j \overline{u_k' \frac{\partial T'}{\partial x_j}} + \overline{u_j' u_k'} \frac{\partial \bar{T}}{\partial x_j} + \overline{u_j' u_k' \frac{\partial T'}{\partial x_j}}\right)$$

$$= \mu_o \overline{u_k' \frac{\partial^2 T'}{\partial x_j^2}} \tag{3.21}$$

Next multiply the equation for $\partial u_k'/\partial t$ [i.e., (3.15)] with i replaced by k, by T' and obtain

$$\rho_o \overline{T' \frac{\partial u_k'}{\partial t}} + \rho_o \left(\bar{u}_j \overline{T' \frac{\partial u_k'}{\partial x_j}} + \overline{u_j' T'} \frac{\partial \bar{u}_k}{\partial x_j} + \overline{u_j' T' \frac{\partial u_k'}{\partial x_j}} \right)$$

$$= - \overline{T' \frac{\partial p'}{\partial x_k}} + \frac{\rho_o}{T_o} g_k \overline{T'^2} + \mu_o \overline{T' \frac{\partial^2 u_k'}{\partial x_j^2}} \qquad (3.22)$$

If (3.21) and (3.22) are added, one obtains, after some rearrangement,

$$\rho_o \frac{\partial}{\partial t} (\overline{u_k' T'}) + \rho_o \bar{u}_j \frac{\partial}{\partial x_j} (\overline{u_k' T'}) = - \rho_o \overline{u_j' u_k'} \frac{\partial \bar{T}}{\partial x_j} - \rho_o \overline{u_j' T'} \frac{\partial \bar{u}_k}{\partial x_j}$$

$$- \rho_o \frac{\partial}{\partial x_j} (\overline{u_j' u_k' T'}) - \frac{\partial}{\partial x_k} (\overline{p' T'}) + \overline{p' \frac{\partial T'}{\partial x_k}}$$

$$+ \frac{\rho_o}{T_o} g_k \overline{T'^2} + \mu_o \frac{\partial^2 \overline{u_k' T'}}{\partial x_j^2} - 2\mu_o \overline{\frac{\partial u_k'}{\partial x_j} \frac{\partial T'}{\partial x_j}} \qquad (3.23)$$

By analogy with the Reynolds stress equation, we may identify the various terms in this equation for the heat transport correlation. The two terms on the left-hand side represent ρ_o times the derivative following a particle trajectory of the correlation $\overline{u_k' T'}$. The first two terms on the right-hand side are production terms. The first of these represents production of $\overline{u_k' T'}$ by the interaction of the turbulent velocities and the variation of the mean temperature field, while the other term represents production due to the interaction of heat transport correlations and the variation of the mean velocity field.

The third term on the right-hand side of (3.23) is the diffusion of the correlation $\overline{u_k' T'}$ by the turbulent velocity.

The fourth term is the equivalent of the pressure diffusion term in the Reynolds stress correlation equation and will be referred to as the pressure diffusion term. Similarly, the

term $\overline{p'\partial T'/\partial x_k}$ represents a "tendency towards isotropy" or a tendency for the pressure fluctuations to eliminate any correlation between u_k' and T'.

The term

$$\frac{\rho_o}{T_o} g_k \overline{T'^2}$$

represents the production of temperature transport correlation in the direction of gravitational acceleration due to the fluctuations in temperature of the flow.

The term

$$\mu_o \frac{\partial^2 \overline{u_k'T'}}{\partial x_j^2}$$

is obviously the diffusion of $\overline{u_k'T'}$ by molecular action, while the final term

$$- 2\mu_o \overline{\frac{\partial u_k'}{\partial x_j} \frac{\partial T'}{\partial x_j}}$$

represents the role played by molecular viscosity in correlating or uncorrelating the velocity and temperature fluctuations. In most cases, the effect is one of uncorrelation. In spite of the fact that this last term is not always dissipative, it is nonetheless referred to as the dissipative term.

In (3.23), the correlation $\overline{T'^2}$ occurs. It is easy to obtain an equation for this second-order correlation. To do so, we multiply (3.20) by $2T'$ and average. The result is

$$\rho_o \frac{\partial \overline{T'^2}}{\partial t} + \rho_o \bar{u}_j \frac{\partial \overline{T'^2}}{\partial x_j} = - 2\rho_o \overline{u_j'T'} \frac{\partial \bar{T}}{\partial x_j} - \rho_o \frac{\partial}{\partial x_j}\left(\overline{u_j'T'^2}\right) + \mu_o \frac{\partial^2 \overline{T'^2}}{\partial x_j^2} - 2\mu_o \overline{\frac{\partial T'}{\partial x_j} \frac{\partial T'}{\partial x_j}} \qquad (3.24)$$

This equation is similar to the two previous equations for second-order correlations with the exception that there are no pressure diffusion or tendency-to-isotropy terms. It is clear

then that the only way that temperature fluctuations can be destroyed in a flow of constant temperature is by the action of molecular diffusivity.

When the Reynolds scheme is applied to the species conservation equation, one obtains

$$\rho_o \left(\frac{\partial \bar{C}_\alpha}{\partial t} + \frac{\partial C'_\alpha}{\partial t} \right) + \rho_o \left(\bar{u}_j \frac{\partial \bar{C}_\alpha}{\partial x_j} + \bar{u}_j \frac{\partial C'_\alpha}{\partial x_j} + u'_j \frac{\partial \bar{C}_\alpha}{\partial x_j} + u'_j \frac{\partial C'_\alpha}{\partial x_j} \right)$$

$$= \mu_o \frac{\partial^2 \bar{C}_\alpha}{\partial x_j^2} + \mu_o \frac{\partial^2 C'_\alpha}{\partial x_j^2} \tag{3.25}$$

Averaging the equation results in

$$\rho_o \frac{\partial \bar{C}_\alpha}{\partial t} + \rho_o \bar{u}_j \frac{\partial \bar{C}_\alpha}{\partial x_j} = \mu_o \frac{\partial^2 \bar{C}_\alpha}{\partial x_j^2} - \rho_o \frac{\partial}{\partial x_j} (\overline{u'_j C'_\alpha}) \tag{3.26}$$

As before, we can obtain equations for $\overline{C'_\alpha u'_k}$ and $\overline{C'^2_\alpha}$. They are

$$\rho_o \frac{\partial \overline{u'_k C'_\alpha}}{\partial t} + \rho_o \bar{u}_j \frac{\partial}{\partial x_j} (\overline{u'_k C'_\alpha}) = - \rho_o \overline{u'_j u'_k} \frac{\partial \bar{C}_\alpha}{\partial x_j} - \rho_o \overline{u'_j C'_\alpha} \frac{\partial \bar{u}_k}{\partial x_j}$$

$$- \rho_o \frac{\partial}{\partial x_j} (\overline{u'_j u'_k C'_\alpha}) - \frac{\partial}{\partial x_k} (\overline{p' C'_\alpha}) + \overline{p' \frac{\partial C'_\alpha}{\partial x_k}}$$

$$+ \frac{\rho_o}{T_o} g_k \overline{C'_\alpha T'} + \mu_o \frac{\partial^2 \overline{u'_k C'_\alpha}}{\partial x_j^2} - 2\mu_o \overline{\frac{\partial u'_k}{\partial x_j} \frac{\partial C'_\alpha}{\partial x_j}} \tag{3.27}$$

and

$$\rho_o \frac{\partial \overline{C'^2_\alpha}}{\partial t} + \rho_o \bar{u}_j \frac{\partial}{\partial x_j} \left(\overline{C'^2_\alpha} \right) = - 2\rho_o \overline{u'_j C'_\alpha} \frac{\partial \bar{C}_\alpha}{\partial x_j}$$

$$- \rho_o \frac{\partial}{\partial x_j} \left(\overline{u'_j C'^2_\alpha} \right) + \mu_o \frac{\partial^2 \overline{C'^2_\alpha}}{\partial x_j^2} - 2\mu_o \overline{\frac{\partial C'_\alpha}{\partial x_j} \frac{\partial C'_\alpha}{\partial x_j}} \tag{3.28}$$

It will be seen that because of the gravitational term $(\rho_o/T_o)g_k\overline{C'_\alpha T'}$ in (3.27) it will be necessary to have an equation for $\overline{C'_\alpha T'}$ if a closed set of equations is to be realized. This equation is derived in the usual manner and is

$$\rho_o \frac{\partial}{\partial t}(\overline{C'_\alpha T'}) + \rho_o \bar{u}_j \frac{\partial}{\partial x_j}(\overline{C'_\alpha T'}) =$$

$$= -\rho_o \overline{u'_j C'_\alpha} \frac{\partial \bar{T}}{\partial x_j} - \rho_o \overline{u'_j T'} \frac{\partial \bar{C}_\alpha}{\partial x_j} - \rho_o \frac{\partial}{\partial x_j}(\overline{u'_j C'_\alpha T'})$$

$$+ \mu_o \frac{\partial^2 \overline{C'_\alpha T'}}{\partial x_j^2} - 2\mu_o \frac{\partial \overline{C'_\alpha}}{\partial x_j} \frac{\partial \overline{T'}}{\partial x_j} \qquad (3.29)$$

We need not discuss these last three equations in detail for they are almost identical in form to the equations for $\overline{u'_k T'}$ and $\overline{T'^2}$.

Let us now collect the equations we have derived for the production of turbulence and the dispersal of pollutants in an atmospheric shear layer.

Making use of the notation

$$\frac{D}{Dt} = \frac{\partial}{\partial t} + \bar{u}_j \frac{\partial}{\partial x_j} \qquad (3.30)$$

and writing $\mu_o/\rho_o = \upsilon_o$, we have

$$\frac{D\bar{u}_i}{Dt} = -\frac{1}{\rho_o}\frac{\partial \bar{p}}{\partial x_i} + \upsilon_o \frac{\partial^2 \bar{u}_i}{\partial x_j^2} - \frac{\partial}{\partial x_j}\overline{u'_i u'_j} + \frac{1}{T_o} g_i \bar{T} \qquad (3.31)$$

$$\frac{D\bar{T}}{Dt} = \upsilon_o \frac{\partial^2 \bar{T}}{\partial x_j^2} - \frac{\partial}{\partial x_j}\overline{u'_j T'} \qquad (3.32)$$

$$\frac{D\bar{C}_\alpha}{Dt} = \upsilon_o \frac{\partial^2 \bar{C}_\alpha}{\partial x_j^2} - \frac{\partial}{\partial x_j}\overline{u'_j C'_\alpha} \qquad (3.33)$$

and

$$\frac{\partial \bar{u}_i}{\partial x_i} = 0 \tag{3.34}$$

$$\begin{aligned}\frac{D\overline{u_i'u_k'}}{Dt} = &- \overline{u_j'u_k'}\,\frac{\partial \bar{u}_i}{\partial x_j} - \overline{u_j'u_i'}\,\frac{\partial \bar{u}_k}{\partial x_j} - \frac{\partial}{\partial x_j}\left(\overline{u_i'u_j'u_k'}\right) \\ &- \frac{1}{\rho_o}\frac{\partial}{\partial x_k}\left(\overline{p'u_i'}\right) - \frac{1}{\rho_o}\frac{\partial}{\partial x_i}\left(\overline{p'u_k'}\right) + \overline{\frac{p'}{\rho_o}\left(\frac{\partial u_i'}{\partial x_k} + \frac{\partial u_k'}{\partial x_i}\right)} \\ &+ \frac{1}{T_o}\left(g_i\overline{u_k'T'} + g_k\overline{u_i'T'}\right) \\ &+ \nu_o\frac{\partial^2\overline{u_i'u_k'}}{\partial x_j^2} - 2\nu_o\,\overline{\frac{\partial u_i'}{\partial x_j}\frac{\partial u_k'}{\partial x_j}}\end{aligned} \tag{3.35}$$

$$\begin{aligned}\frac{D\overline{u_k'T'}}{Dt} = &- \overline{u_j'u_k'}\,\frac{\partial \bar{T}}{\partial x_j} - \overline{u_j'T'}\,\frac{\partial \bar{u}_k}{\partial x_j} - \frac{\partial}{\partial x_j}\left(\overline{u_j'u_k'T'}\right) \\ &- \frac{1}{\rho_o}\frac{\partial}{\partial x_k}\left(\overline{p'T'}\right) + \overline{\frac{p'}{\rho_o}\frac{\partial T'}{\partial x_k}} \\ &+ \frac{1}{T_o}g_k\overline{T'^2} + \nu_o\frac{\partial^2\overline{u_k'T'}}{\partial x_j^2} - 2\nu_o\,\overline{\frac{\partial u_k'}{\partial x_j}\frac{\partial T'}{\partial x_j}}\end{aligned} \tag{3.36}$$

$$\begin{aligned}\frac{D\overline{T'^2}}{Dt} = &- 2\overline{u_j'T'}\,\frac{\partial \bar{T}}{\partial x_j} - \frac{\partial}{\partial x_j}\,\overline{u_j'T'^2} \\ &+ \nu_o\frac{\partial^2\overline{T'^2}}{\partial x_j^2} - 2\nu_o\,\overline{\frac{\partial T'}{\partial x_j}\frac{\partial T'}{\partial x_j}}\end{aligned} \tag{3.37}$$

$$\frac{D\overline{u_k'C_\alpha'}}{Dt} = - \overline{u_j'u_k'} \frac{\partial \bar{C}_\alpha}{\partial x_j} - \overline{u_j'C_\alpha'} \frac{\partial \bar{u}_k}{\partial x_j} - \frac{\partial}{\partial x_j} (\overline{u_j'u_k'C_\alpha'})$$

$$- \frac{1}{\rho_o} \frac{\partial}{\partial x_k} (\overline{p'C_\alpha'}) + \overline{\frac{p'}{\rho_o} \frac{\partial C_\alpha'}{\partial x_k}}$$

$$+ \frac{1}{T_o} g_k \overline{C_\alpha'T'} + \nu_o \frac{\partial^2 \overline{u_k'C_\alpha'}}{\partial x_j^2} - 2\nu_o \overline{\frac{\partial u_k'}{\partial x_j} \frac{\partial C_\alpha'}{\partial x_j}} \qquad (3.38)$$

$$\frac{D\overline{C_\alpha'T'}}{Dt} = - \overline{u_j'C_\alpha'} \frac{\partial \bar{T}}{\partial x_j} - \overline{u_j'T'} \frac{\partial \bar{C}_\alpha}{\partial x_j} - \frac{\partial}{\partial x_j} (\overline{u_j'C_\alpha'T'})$$

$$+ \nu_o \frac{\partial^2 \overline{C_\alpha'T'}}{\partial x_j^2} - 2\nu_o \overline{\frac{\partial C_\alpha'}{\partial x_j} \frac{\partial T'}{\partial x_j}} \qquad (3.39)$$

$$\frac{D\overline{C_\alpha'^2}}{Dt} = - 2\overline{u_j'C_\alpha'} \frac{\partial \bar{C}_\alpha}{\partial x_j} - \frac{\partial}{\partial x_j} \left(\overline{u_j'C_\alpha'^2} \right)$$

$$+ \nu_o \frac{\partial^2 \overline{C_\alpha'^2}}{\partial x_j^2} - 2\nu_o \overline{\frac{\partial C_\alpha'}{\partial x_j} \frac{\partial C_\alpha'}{\partial x_j}} \qquad (3.40)$$

It will be noted that if some means can be found to model in (3.35) through (3.40)

(1) the velocity diffusion terms

(2) the terms containing pressure fluctuations, i.e.,

(a) the tendency-towards-isotropy terms

(b) the pressure diffusion terms

and (3) the dissipation terms

in terms of the mean variables and/or the second-order correlations of the variables, then the set of equations given above is closed and a solution can, in principle, be found for the mean quantities $\bar{u}_i$, $\bar{T}$, and $\bar{C}_\alpha$, as well as for all the second-order correlations except $\overline{p'^2}$.

In the following sections we shall discuss the problem of choosing such a model. Before going on to this, however, a discussion of the solutions of the above equations is in order.

First, let us assume that the motion in question is laminar. In that case, all the fluctuations are zero and the equations needed to solve for the motion alone, i.e., for the five unknowns $\bar{u}_1$, $\bar{u}_2$, $\bar{u}_3$, $\bar{T}$, and $\bar{p}$ are (3.31), (3.32), and (3.34). Since (3.31) is a vector equation, it yields 3 scalar equations for $\bar{u}_1$, $\bar{u}_2$, and $\bar{u}_3$ so that, together with (3.32) and (3.34), there are five equations for the five unknowns. Once the motion is known, the mass fraction (concentration) field for each species α may be found from the α equations given by (3.33).

If the motion is turbulent and a viable second-order closure model can be found, the unknowns involved in the solution for the motion are $\bar{u}_1$, $\bar{u}_2$, $\bar{u}_3$, $\bar{T}$, $\bar{p}$, $\overline{u_1'u_1'}$, $\overline{u_2'u_2'}$, $\overline{u_3'u_3'}$, $\overline{u_1'u_2'} = \overline{u_2'u_1'}$, $\overline{u_1'u_3'} = \overline{u_3'u_1'}$, $\overline{u_2'u_3'} = \overline{u_3'u_2'}$, $\overline{u_1'T'}$, $\overline{u_2'T'}$, $\overline{u_3'T'}$, and $\overline{T'^2}$. There are then 15 unknowns. One obtains the 15 equations required to solve for the motion as follows:

from (3.31)	3 equations
from (3.32)	1 equation
from (3.34)	1 equation
from (3.35)	6 equations
from (3.36)	3 equations
from (3.37)	1 equation

for a total of 15 equations.

Once the motion is solved for the concentration field for any of the α, each species involved may be solved by solving five simultaneous equations for the unknowns $\bar{C}_\alpha$, $\overline{C_\alpha'u_1'}$, $\overline{C_\alpha'u_2'}$, $\overline{C_\alpha'u_3'}$, and $\overline{C_\alpha'T'}$ obtained

from (3.33)	1 equation
from (3.38)	3 equations
and from (3.39)	1 equation

Once this solution has been obtained, the variance of the fluctuations of mass fraction of the α species may be obtained from a solution of (3.40).

4. SELECTION OF MODELS

In order to construct models of the four types of terms referred to in Section 3 so as to form a closed set of equations for solving for the motion of the atmosphere and its ability to disperse pollutants, one can be guided by some very general principles which reduce the number of models that might be investigated. Once models that adhere to these general principles have been selected, resort must be had to a comparison of computed results with experimental data in order to refine the models or to determine the numerical values of certain parameters which occur in the construction of the models. At the present time, there are more models for closure of the equations of motion at the second-order correlations than there are principal investigators working on the problem. This occurs because each investigator generally has an option or two that he is currently trying out. In our own work, we have tried to start from the simplest model that would satisfy the general principles and increase the complexity of the model only if experimental data indicate that more complexity is needed.

The basic principles that must be observed in selecting a model are the following:

(1) The model must be of tensor form so that it is invariant under an arbitrary transformation of coordinate systems. The model must have all the tensor properties and, in addition, all the symmetries of the term which it replaces.

(2) The model must be invariant under a Galilean transformation.

(3) The model must have the dimensional properties of the term it replaces.

(4) The model must be such as to satisfy all the conservation relationships known to govern the variables in question.

With these basic principles, let us try to determine the simplest models possible for the various terms that must be modeled in (3.35) through (3.40).

We will start with the velocity diffusion terms. We wish to model the tensor $\overline{u_i'u_j'u_k'}$ in terms of the second-order correlations $\overline{u_i'u_k'}$. The simplest tensor of rank three that can be obtained from the second-order correlation $\overline{u_i'u_k'}$ that is of the form T_{ijk} is $\partial(\overline{u_i'u_k'})/\partial x_j$. The tensor $\overline{u_i'u_j'u_k'}$ is symmetric in all three indices so that our model must be symmetric in these indices. We therefore choose

$$\overline{u_i'u_j'u_k'} \sim \frac{\partial}{\partial x_i}(\overline{u_j'u_k'}) + \frac{\partial}{\partial x_j}(\overline{u_i'u_k'}) + \frac{\partial}{\partial x_k}(\overline{u_i'u_j'}) \qquad (4.1)$$

This expression has all the tensor character necessary for the model but is not dimensionally correct. To make the dimensions correct, we must multiply the right-hand side of (4.1) by a scalar with dimensions of length times velocity. The simplest scalar velocity we can form from the second-order velocity correlations is

$$q = \sqrt{\overline{u_m'u_m'}}$$

If we multiply this expression by a scalar length, say, Λ_2, which is to be related to the scale of the mean motion or to the scale of the turbulence, we can form a simple model of the triple correlation $\overline{u_i'u_j'u_k'}$. Thus,

$$\overline{u_i'u_j'u_k'} = -\Lambda_2 q\left[\frac{\partial}{\partial x_i}(\overline{u_j'u_k'}) + \frac{\partial}{\partial x_j}(\overline{u_i'u_k'}) + \frac{\partial}{\partial x_k}(\overline{u_i'u_j'})\right] \qquad (4.2)$$

In (4.2) we have included a minus sign to ensure that turbulent energy will be diffused down the gradient or from regions of high turbulent intensity to regions of low intensity.

Let us consider a model for the triple correlation $\overline{u_j'u_k'T'}$. From the second-order correlation $\overline{u_k'T'}$ we can form a tensor of form T_{jk} with the necessary symmetry. Thus,

$$T_{jk} = \frac{\partial}{\partial x_j}(\overline{u_k'T'}) + \frac{\partial}{\partial x_k}(\overline{u_j'T'}) \qquad (4.3)$$

This expression does not have the dimensions of $\overline{u_j' u_k' T'}$, so we write

$$\overline{u_j' u_k' T'} = - \Lambda_2 q \left[\frac{\partial}{\partial x_j} (\overline{u_k' T'}) + \frac{\partial}{\partial x_k} (\overline{u_j' T'}) \right] \tag{4.4}$$

Here we might have chosen a scale length other than Λ_2. But, as we shall see later, in order to keep the model simple it will be necessary to choose as few scale lengths as possible. We therefore take Λ_2 as the scale for all velocity diffusion terms unless experimental results later show that the model must be more complicated.

In modeling the term $\overline{u_i' u_j' T'}$ we might have chosen a term of the following form:

$$\text{const } \overline{u_i' u_j'} \sqrt{\overline{T'^2}}$$

We have chosen not to do this since we want this diffusion term to be a gradient type of diffusion.

By analogy with the velocity diffusion expressions (4.2) and (4.4), we will choose to model the four remaining triple correlations that appear in the velocity diffusion terms as

$$\overline{u_j' u_k' C_\alpha'} = - \Lambda_2 q \left[\frac{\partial}{\partial x_k} (\overline{u_j' C_\alpha'}) + \frac{\partial}{\partial x_j} (\overline{u_k' C_\alpha'}) \right] \tag{4.5}$$

$$\overline{u_j' T'^2} = - \Lambda_2 q \frac{\partial}{\partial x_j} \overline{T'^2} \tag{4.6}$$

$$\overline{u_j' C_\alpha' T'} = - \Lambda_2 q \frac{\partial}{\partial x_j} \overline{C_\alpha' T'} \tag{4.7}$$

$$\overline{u_j' C_\alpha'^2} = - \Lambda_2 q \frac{\partial}{\partial x_j} \overline{C_\alpha'^2} \tag{4.8}$$

Consider now the tendency-towards-isotropy term in the equation for $\overline{u_i' u_k'}$. We wish to model

$$\overline{\frac{p'}{\rho_o}\left(\frac{\partial u_i'}{\partial x_k} + \frac{\partial u_k'}{\partial x_i}\right)}$$

This expression is a second-order tensor of form T_{ik} . The simplest tensor of this form that can be formed from the second-order correlations is obviously the second-order correlation $\overline{u_i'u_k'}$ itself. We therefore start by taking

$$\overline{\frac{p'}{\rho_o}\left(\frac{\partial u_i'}{\partial x_k} + \frac{\partial u_k'}{\partial x_i}\right)} \sim \overline{u_i'u_k'} \tag{4.9}$$

The correlation $\overline{u_i'u_k'}$ has all the tensor and symmetry properties we wish, but it does not have the proper dimensions. We can remedy this by multiplying $\overline{u_i'u_k'}$ by the scalar q/Λ_1 where Λ_1 is a new scale length. We then have

$$\overline{\frac{p'}{\rho_o}\left(\frac{\partial u_i'}{\partial x_k} + \frac{\partial u_k'}{\partial x_i}\right)} = \frac{q}{\Lambda_1}\,\overline{u_i'u_k'}$$

This cannot be correct, for if we set i equal to k , the left-hand side of the supposed equation vanishes in an incompressible fluid while the right-hand side does not. This can be remedied by taking

$$\overline{\frac{p'}{\rho_o}\left(\frac{\partial u_i'}{\partial x_k} + \frac{\partial u_k'}{\partial x_i}\right)} = -\frac{q}{\Lambda_1}\left(\overline{u_i'u_k'} - \frac{\delta_{ik}}{3}\,q^2\right) \tag{4.10}$$

The minus sign in this expression is chosen so that in the absence of other influences, the turbulent energy will be equilibrated between the various components of velocity. The model was first given by Rotta [Ref. 6]. We could have included a term in (4.10) proportional to the mean strain [Crow, Ref. 43], but for our initial simple model, we choose not to do so.

We must now model the "tendency-towards-isotropy" terms that appear in the equations for $\overline{u_k'T'}$ and $\overline{u_k'C_\alpha'}$. By analogy with the tendency towards isotropy of the stress correlation for $i \neq k$, we adopt the following models:

$$\overline{\frac{p'}{\rho_o}\frac{\partial T'}{\partial x_k}} = -\frac{q}{\Lambda_1}\overline{u_k'T'} \tag{4.11}$$

and

$$\overline{\frac{p'}{\rho_o}\frac{\partial C_\alpha'}{\partial x_k}} = -\frac{q}{\Lambda_1}\overline{u_k'C_\alpha'} \tag{4.12}$$

Here again, more generality can be put into the model by selecting the scales in these last two equations to be different than the Λ_1 of the isotropy term for the stress correlation equation. Whether this should be done or not will depend upon the agreement between computed results and experimental data. For the time being, we will use the same scale in each of the isotropy terms.

As mentioned previously, the pressure diffusion terms are difficult to model since so little is known concerning them.* We will, however, choose a model of the terms which will be essentially nonproductive; i.e., the model will depend upon the gradient of the quantity in the equation for which we are trying to model the pressure diffusion term. Thus, we choose

$$\overline{p'u_k'} = -\rho_o q\Lambda_3 \frac{\partial}{\partial x_i}\overline{u_i'u_k'} \tag{4.13}$$

$$\overline{p'T'} = -\rho_o q\Lambda_3 \frac{\partial}{\partial x_i}\overline{u_i'T'} \tag{4.14}$$

and

$$\overline{p'C_\alpha'} = -\rho_o q\Lambda_3 \frac{\partial}{\partial x_i}\overline{u_i'C_\alpha'} \tag{4.15}$$

In these expressions, since we expect the pressure diffusion effect to be small, we expect that Λ_3 will be small compared, say, to Λ_1. We have chosen a negative sign so that the model, as written, will represent a transfer of the quantity in question down the gradient.†

---

*Our knowledge of these terms is limited for, to date, it has not been possible to simultaneously measure the fluctuation of pressure and velocity at a point in a flowing medium.

†It should be noted that in some recent studies using a model which is essentially that described here, Prof. Paul Libby has reported somewhat better agreement of computations with experimental results if a small Λ_3 is used and the signs of the right-hand sides of (4.13), (4.14), and (4.15) are reversed.

To model the correlations appearing in the dissipation terms, namely,

$$\overline{\frac{\partial u_i'}{\partial x_j}\frac{\partial u_k'}{\partial x_j}}\ ,\quad \overline{\frac{\partial u_k'}{\partial x_j}\frac{\partial T'}{\partial x_j}}\ ,\quad \overline{\frac{\partial T'}{\partial x_j}\frac{\partial T'}{\partial x_j}}\ ,\quad \overline{\frac{\partial u_k'}{\partial x_j}\frac{\partial C_\alpha'}{\partial x_j}}\ ,$$

$$\overline{\frac{\partial C_\alpha'}{\partial x_j}\frac{\partial T'}{\partial x_j}}\ ,\ \text{and}\ \ \overline{\frac{\partial C_\alpha'}{\partial x_j}\frac{\partial C_\alpha'}{\partial x_j}}$$

it would appear that the simplest model that can account for all of these terms is

$$\overline{\frac{\partial A'}{\partial x_j}\frac{\partial B'}{\partial x_j}} = \frac{\overline{A'B'}}{\lambda^2} \tag{4.16}$$

where λ is another scalar length.

Here again we have the same question that was raised before; i.e., should not the λ's in each term be different? The answer to this must again be "yes" if comparison between computed results and experimental data requires it. As in the other cases, we will, for the present, try to develop the simplest possible model and will therefore make use of only one λ in all the dissipation terms. In later sections of this report, we will return to the question of modeling these dissipation terms in light of the results found with the model adopted here.

If the models we have described above are placed into the equations for a turbulent atmospheric shear layer, (3.31) through (3.40), we obtain the following set of modeled equations:

$$\frac{D\bar{u}_i}{Dt} = \nu_o \frac{\partial^2 \bar{u}_i}{\partial x_j^2} - \frac{\partial}{\partial x_j}\overline{u_i'u_j'} + \frac{1}{T_o} g_i \bar{T} - \frac{1}{\rho_o}\frac{\partial \bar{p}}{\partial x_i} \tag{4.17}$$

$$\frac{D\bar{T}}{Dt} = \nu_o \frac{\partial^2 \bar{T}}{\partial x_j^2} - \frac{\partial}{\partial x_j}\overline{u_j'T'} \tag{4.18}$$

$$\frac{D\bar{C}_\alpha}{Dt} = \nu_o \frac{\partial^2 \bar{C}_\alpha}{\partial x_j^2} - \frac{\partial}{\partial x_j} \overline{u_j' C_\alpha'} \tag{4.19}$$

$$\frac{\partial \bar{u}_i}{\partial x_i} = 0 \tag{4.20}$$

$$\begin{aligned}\frac{D\overline{u_i'u_k'}}{Dt} = &- \overline{u_j'u_k'} \frac{\partial \bar{u}_i}{\partial x_j} - \overline{u_j'u_i'} \frac{\partial \bar{u}_k}{\partial x_j} + \frac{1}{T_o}\left(g_i \overline{u_k'T'} + g_k \overline{u_i'T'}\right) \\ &+ \frac{\partial}{\partial x_j}\left[\Lambda_2 q \left(\frac{\partial \overline{u_i'u_j'}}{\partial x_k} + \frac{\partial \overline{u_j'u_k'}}{\partial x_i} + \frac{\partial \overline{u_k'u_i'}}{\partial x_j}\right)\right] \\ &+ \frac{\partial}{\partial x_i}\left(\Lambda_3 q \frac{\partial}{\partial x_j} \overline{u_j'u_k'}\right) + \frac{\partial}{\partial x_k}\left(\Lambda_3 q \frac{\partial}{\partial x_j} \overline{u_j'u_i'}\right) \\ &- \frac{q}{\Lambda_1}\left(\overline{u_i'u_k'} - \frac{\delta_{ik}}{3} q^2\right) + \nu_o \frac{\partial^2 \overline{u_i'u_k'}}{\partial x_j^2} - 2\nu_o \frac{\overline{u_i'u_k'}}{\lambda^2}\end{aligned} \tag{4.21}$$

$$\begin{aligned}\frac{D\overline{u_k'T'}}{Dt} = &- \overline{u_j'u_k'} \frac{\partial \bar{T}}{\partial x_j} - \overline{u_j'T'} \frac{\partial \bar{u}_k}{\partial x_j} + \frac{1}{T_o} g_k \overline{T'^2} \\ &+ \frac{\partial}{\partial x_j}\left[\Lambda_2 q \left(\frac{\partial}{\partial x_k} \overline{u_j'T'} + \frac{\partial}{\partial x_j} \overline{u_k'T'}\right)\right] + \frac{\partial}{\partial x_k}\left(\Lambda_3 q \frac{\partial}{\partial x_j} \overline{u_j'T'}\right) \\ &- \frac{q}{\Lambda_1} \overline{u_k'T'} + \nu_o \frac{\partial^2 \overline{u_k'T'}}{\partial x_j^2} - 2\nu_o \frac{\overline{u_k'T'}}{\lambda^2}\end{aligned} \tag{4.22}$$

$$\begin{aligned}\frac{D\overline{T'^2}}{Dt} = &- 2\overline{u_j'T'} \frac{\partial \bar{T}}{\partial x_j} + \frac{\partial}{\partial x_j}\left(\Lambda_2 q \frac{\partial}{\partial x_j} \overline{T'^2}\right) \\ &+ \nu_o \frac{\partial^2 \overline{T'^2}}{\partial x_j^2} - 2\nu_o \frac{\overline{T'^2}}{\lambda^2}\end{aligned} \tag{4.23}$$

$$\frac{D\overline{u_k'C_\alpha'}}{Dt} = - \overline{u_j'u_k'} \frac{\partial \bar{C}_\alpha}{\partial x_j} - \overline{u_j'C_\alpha'} \frac{\partial \bar{u}_k}{\partial x_j} + \frac{1}{T_o} g_k \overline{C_\alpha'T'}$$

$$+ \frac{\partial}{\partial x_j} \left[\Lambda_2 q \left(\frac{\partial}{\partial x_j} \overline{u_k'C_\alpha'} + \frac{\partial}{\partial x_k} \overline{u_j'C_\alpha'} \right) \right]$$

$$+ \frac{\partial}{\partial x_k} \left(\Lambda_3 q \frac{\partial}{\partial x_j} \overline{u_j'C_\alpha'} \right)$$

$$- \frac{q}{\Lambda_1} \overline{u_k'C_\alpha'} + \nu_o \frac{\partial^2 \overline{u_k'C_\alpha'}}{\partial x_j^2} - 2\nu_o \frac{\overline{u_k'C_\alpha'}}{\lambda^2} \qquad (4.24)$$

$$\frac{D\overline{C_\alpha'T'}}{Dt} = - \overline{u_j'C_\alpha'} \frac{\partial \bar{T}}{\partial x_j} - \overline{u_j'T'} \frac{\partial \bar{C}_\alpha}{\partial x_j} + \frac{\partial}{\partial x_j} \left(\Lambda_2 q \frac{\partial}{\partial x_j} \overline{C_\alpha'T'} \right)$$

$$+ \nu_o \frac{\partial^2 \overline{C_\alpha'T'}}{\partial x_j^2} - 2\nu_o \frac{\overline{C_\alpha'T'}}{\lambda^2} \qquad (4.25)$$

$$\frac{D\overline{C_\alpha'^2}}{Dt} = - 2\overline{u_j'C_\alpha'} \frac{\partial \bar{C}_\alpha}{\partial x_j} + \frac{\partial}{\partial x_j} \left(\Lambda_2 q \frac{\partial}{\partial x_j} \overline{C_\alpha'^2} \right)$$

$$+ \nu_o \frac{\partial^2 \overline{C_\alpha'^2}}{\partial x_j^2} - 2\nu_o \frac{\overline{C_\alpha'^2}}{\lambda^2} \qquad (4.26)$$

In the pressure diffusion terms, ρ_o has been taken out of the derivative by the same reasoning that led to (2.41) from (2.40). This set of modeled equations is solved according to the procedure described at the end of Section 3.

For thin shear layers, these equations can be further simplified by making"boundary layer" assumptions. First we introduce the notation

$$\begin{array}{lll} x_1 = x & x_2 = y & x_3 = z \\ u_i = u & u_2 = v & u_3 = w \\ g_1 = 0 & g_2 = 0 & g_3 = g \end{array} \qquad (4.27)$$

Then we assume that the vertical component of the mean velocity is small compared to the other components

$$\bar{w} << \bar{u} \quad \text{or} \quad \bar{v} \tag{4.28}$$

and that derivatives with respect to z are large

$$\frac{\partial Q}{\partial z} >> \frac{\partial Q}{\partial x} \ , \ \frac{\partial Q}{\partial y} \tag{4.29}$$

The equations are of particularly simple form if, for example, the problem is time dependent and all mean variables (excepting $\bar{p}$) are independent of x and y ; that is, if $\bar{u} = \bar{u}(z,t)$, $\bar{T} = \bar{T}(z,t)$, $\overline{u'w'} = \overline{u'w'}(z,t)$, etc. In this case we must have $(1/\rho_o)(\partial\bar{p}/\partial x)$ and $(1/\rho_o)(\partial\bar{p}/\partial y)$ (which are functions of z alone) specified as functions of time, and we find that the vertical momentum equation becomes

$$\frac{\partial \bar{p}}{\partial z} = - \rho g \tag{4.30}$$

while continuity gives $\bar{w} = 0$.

For this problem, since the pollutants involved have been assumed to be passive, we have a coupled set of thirteen partial differential equations for the thirteen variables:

$$\bar{u}(z,t) \ , \ \bar{v}(z,t) \ , \ \bar{T}(z,t) \ , \ \overline{u'u'}(z,t) \ , \ \overline{v'v'}(z,t) \ ,$$

$$\overline{w'w'}(z,t) \ , \ \overline{u'w'}(z,t) \ , \ \overline{v'w'}(z,t) \ , \ \overline{u'v'}(z,t) \ ,$$

$$\overline{u'T'}(z,t) \ , \ \overline{v'T'}(z,t) \ , \ \overline{w'T'}(z,t) \ , \ \overline{T'^2}(z,t) \ .$$

If initial conditions on these quantities as functions of z are given at some time, say, $t = 0$, the equations can be solved for the development in time of the mean quantities and the correlations. Once the turbulence characteristics of the atmosphere are known as functions of z and t , one is then able to solve for the transport of the pollutants by solving a coupled set of five equations for $\bar{C}_\alpha(z,t)$, $\overline{C'_\alpha u'}(z,t)$, $\overline{C'_\alpha v'}(z,t)$, $\overline{C'_\alpha w'}(z,t)$, and $\overline{C'_\alpha T'}(z,t)$. Once these quantities are known, the variance of the fluctuation in C_α can be determined by

solving the final equation for $\overline{C_\alpha'^2}(z,t)$. These solutions can be obtained, of course, providing that initial conditions on these quantities as functions of z are provided at some time.

Of particular interest is the steady dispersal of passive pollutants in an atmosphere that has reached a given steady state of turbulence. Since the equations for the atmospheric motion and for the dispersal of pollutants are decoupled, one can first solve for the atmospheric turbulence that would be generated by known profiles of velocity and temperature, say, $\bar{u} = \bar{u}(z)$, $\bar{v} = 0$, $\bar{w} = 0$, and $\bar{T} = \bar{T}(z)$, and then solve for the steady dispersal of pollutant material in this atmosphere. The turbulence characteristics of the atmosphere used for these latter computations are those found by holding $\bar{u}(z)$ and $\bar{T}(z)$ fixed in the equations for the second-order correlations $\overline{u_i'u_k'}$, $\overline{u_k'T'}$, and $\overline{T'^2}$ (these equations are (4.21), (4.22), and (4.23), respectively) and observing the resulting distributions at large times. These distributions, as we shall see, are independent of the initial conditions on these variables used to state the calculations at $t = 0$.

It must be borne in mind that in order to perform the calculations just mentioned, it is necessary to have equations for the scales Λ_1 , Λ_2 , Λ_3 , and λ or have these scales given as functions of z and t .

Before we can proceed further, it is necessary to make more precise the details of the model of turbulent atmospheric flow that has just been presented. To do this, we must construct models for some well-known flows and compare the results with experimental data. In this way we will determine relationships between the various scales Λ_α and λ , by choosing these parameters so as to give the best results for the widest number of experimental observations and determine in this way the property of these flows which is related to these scales.

To make the calculations necessary to carry out the comparison between experimental results and calculations suggested

above, it is necessary to have computer programs which accurately solve the sets of equations we have discussed. A general template for the solution of such systems of equations has been developed at A.R.A.P. over the past few years. A description of these numerical techniques is contained in Appendix A.

5. SEARCH FOR MODEL PARAMETERS

It is easy to verify that equations (4.17) through (4.26) reduce to the equations for a low Mach number, constant density medium if we assume $\overline{T} \equiv 0$, $T' \equiv 0$, $C' \equiv 0$. They may therefore be used to calculate the generation of turbulence in a classical incompressible shear layer for which a great deal of detailed experimental data are available. The detailed model of turbulent flow that we will use in later sections of this report was developed by comparing computations with experimental results for three shear flows:

(1) the axially symmetric free jet;

(2) the two-dimensional free shear layer; and

(3) the flat plate boundary layer.

To calculate the first of these flows in cylindrical coordinates (r,ϕ,z) with velocities (u,v,w), one finds that in the appropriate boundary layer form the equations are

$$\frac{\partial \bar{u}}{\partial r} + \frac{\bar{u}}{r} + \frac{\partial \bar{w}}{\partial z} = 0 \tag{5.1}$$

$$\bar{u}\,\frac{\partial \bar{w}}{\partial r} + \bar{w}\,\frac{\partial \bar{w}}{\partial z} = \nu\left(\frac{\partial^2 \bar{w}}{\partial r^2} + \frac{1}{r}\,\frac{\partial \bar{w}}{\partial r}\right) - \frac{\partial \overline{u'w'}}{\partial r} - \frac{\overline{u'w'}}{r} \tag{5.2}$$

$$\begin{aligned}
\bar{u}\,\frac{\partial \overline{u'u'}}{\partial r} + \bar{w}\,\frac{\partial \overline{u'u'}}{\partial z} = {} & \frac{\partial}{\partial r}\left[(3\Lambda_2 + 2\Lambda_3)q\,\frac{\partial \overline{u'u'}}{\partial r}\right] \\
& + \frac{\Lambda_2 q}{r}\left(3\,\frac{\partial \overline{u'u'}}{\partial r} - 2\,\frac{\partial \overline{v'v'}}{\partial r}\right) \\
& + \frac{2}{r}\,\frac{\partial}{\partial r}\left[\Lambda_3 q(\overline{u'u'} - \overline{v'v'})\right] \\
& - \frac{(4\Lambda_2 + 2\Lambda_3)q}{r^2}\,(\overline{u'u'} - \overline{v'v'}) \\
& - \frac{q}{\Lambda_1}\left(\overline{u'u'} - \frac{q^2}{3}\right) + \nu\left[\frac{\partial^2 \overline{u'u'}}{\partial r^2} + \frac{1}{r}\,\frac{\partial \overline{u'u'}}{\partial r}\right. \\
& \left. - \frac{2}{r^2}\,(\overline{u'u'} - \overline{v'v'}) - \frac{2\overline{u'u'}}{\lambda^2}\right]
\end{aligned} \tag{5.3}$$

$$\bar{u}\frac{\partial\overline{v'v'}}{\partial r} + \bar{w}\frac{\partial\overline{v'v'}}{\partial z} = \frac{\partial}{\partial r}\left(\Lambda_2 q\frac{\partial\overline{v'v'}}{\partial r}\right) + \frac{3\Lambda_2 q}{r}\frac{\partial\overline{v'v'}}{\partial r}$$

$$+ \frac{2}{r}\frac{\partial}{\partial r}\left[\Lambda_2 q(\overline{u'u'} - \overline{v'v'})\right] + \frac{2\Lambda_3 q}{r}\frac{\partial\overline{u'u'}}{\partial r}$$

$$+ \frac{(4\Lambda_2 + 2\Lambda_3)q}{r^2}(\overline{u'u'} - \overline{v'v'}) - \frac{q}{\Lambda_1}\left(\overline{v'v'} - \frac{q^2}{3}\right)$$

$$+ \nu\left[\frac{\partial^2\overline{v'v'}}{\partial r^2} + \frac{1}{r}\frac{\partial\overline{v'v'}}{\partial r} + \frac{2}{r^2}(\overline{u'u'} - \overline{v'v'})\right.$$

$$\left. - \frac{2\overline{v'v'}}{\lambda^2}\right] \qquad (5.4)$$

$$\bar{u}\frac{\partial\overline{w'w'}}{\partial r} + \bar{w}\frac{\partial\overline{w'w'}}{\partial z} = -2\overline{u'w'}\frac{\partial\bar{w}}{\partial r} + \frac{\partial}{\partial r}\left(\Lambda_2 q\frac{\partial\overline{w'w'}}{\partial r}\right) + \frac{\Lambda_2 q}{r}\frac{\partial\overline{w'w'}}{\partial r}$$

$$- \frac{q}{\Lambda_1}\left(\overline{w'w'} - \frac{q^2}{3}\right)$$

$$+ \nu\left(\frac{\partial^2\overline{w'w'}}{\partial r^2} + \frac{1}{r}\frac{\partial\overline{w'w'}}{\partial r} - \frac{2\overline{w'w'}}{\lambda^2}\right) \qquad (5.5)$$

$$\bar{u}\frac{\partial\overline{u'w'}}{\partial r} + \bar{w}\frac{\partial\overline{u'w'}}{\partial z} = -\overline{u'u'}\frac{\partial\bar{w}}{\partial r} + \frac{\partial}{\partial r}\left[(2\Lambda_2 + \Lambda_3)q\frac{\partial\overline{u'w'}}{\partial r}\right]$$

$$+ \frac{2\Lambda_2 q}{r}\frac{\partial\overline{u'w'}}{\partial r} + \frac{1}{r}\frac{\partial}{\partial r}(\Lambda_3 q\overline{u'w'})$$

$$- \frac{(2\Lambda_2 + \Lambda_3)q}{r^2}\overline{u'w'} - \frac{q}{\Lambda_1}\overline{u'w'}$$

$$+ \nu\left(\frac{\partial^2\overline{u'w'}}{\partial r^2} + \frac{1}{r}\frac{\partial\overline{u'w'}}{\partial r} - \frac{\overline{u'w'}}{r^2} - \frac{2\overline{u'w'}}{\lambda^2}\right) \qquad (5.6)$$

For the second and third flows, if u is taken as the free stream velocity in the x direction and z the direction normal to x in which large gradients in u exist, the appropriate equations are

$$\frac{\partial \bar{u}}{\partial x} + \frac{\partial \bar{w}}{\partial z} = 0 \tag{5.7}$$

$$\bar{u}\frac{\partial \bar{u}}{\partial x} + \bar{w}\frac{\partial \bar{u}}{\partial z} = \nu\frac{\partial^2 \bar{u}}{\partial z^2} - \frac{\partial \overline{u'w'}}{\partial z} \tag{5.8}$$

$$\bar{u}\frac{\partial \overline{u'u'}}{\partial x} + \bar{w}\frac{\partial \overline{u'u'}}{\partial z} = -2\overline{u'w'}\frac{\partial \bar{u}}{\partial z} + \frac{\partial}{\partial z}\left(\Lambda_2 q \frac{\partial \overline{u'u'}}{\partial z}\right) - \frac{q}{\Lambda_1}\left(\overline{u'u'} - \frac{q^2}{3}\right) + \nu\left(\frac{\partial^2 \overline{u'u'}}{\partial z^2} - \frac{2\overline{u'u'}}{\lambda^2}\right) \tag{5.9}$$

$$\bar{u}\frac{\partial \overline{v'v'}}{\partial x} + \bar{w}\frac{\partial \overline{v'v'}}{\partial z} = \frac{\partial}{\partial z}\left(\Lambda_2 q \frac{\partial \overline{v'v'}}{\partial z}\right) - \frac{q}{\Lambda_1}\left(\overline{v'v'} - \frac{q^2}{3}\right) + \nu\left(\frac{\partial^2 \overline{v'v'}}{\partial z^2} - \frac{2\overline{v'v'}}{\lambda^2}\right) \tag{5.10}$$

$$\bar{u}\frac{\partial \overline{w'w'}}{\partial x} + \bar{w}\frac{\partial \overline{w'w'}}{\partial z} = \frac{\partial}{\partial z}\left[(3\Lambda_2 + 2\Lambda_3)q \frac{\partial \overline{w'w'}}{\partial z}\right] - \frac{q}{\Lambda_1}\left(\overline{w'w'} - \frac{q^2}{3}\right) + \nu\left(\frac{\partial^2 \overline{w'w'}}{\partial z^2} - \frac{2\overline{w'w'}}{\lambda^2}\right) \tag{5.11}$$

$$\bar{u}\frac{\partial \overline{u'w'}}{\partial x} + \bar{w}\frac{\partial \overline{u'w'}}{\partial z} = -\overline{w'w'}\frac{\partial \bar{u}}{\partial z} + \frac{\partial}{\partial z}\left[(2\Lambda_2 + \Lambda_3)q \frac{\partial \overline{u'w'}}{\partial z}\right] - \frac{q}{\Lambda_1}\overline{u'w'} + \nu\left(\frac{\partial^2 \overline{u'w'}}{\partial z^2} - \frac{2\overline{u'w'}}{\lambda^2}\right) \tag{5.12}$$

It is a fact established by careful experimental observation that both the free jet and the two-dimensional free shear layer become, after a transient due to initial conditions, self-similar turbulent flows at high Reynolds numbers. If (5.1) through (5.6) and (5.7) through (5.12) are to permit self-similar solutions for the free jet and the free shear layer, respectively, it is necessary that certain relationships exist between the scale length Λ_α , λ , and the characteristic scale of the mean motion δ_{char} . It can be shown that these relations are

$$\Lambda_1 = c_1 \delta_{char} \tag{5.13}$$

$$\Lambda_2 = c_2 \Lambda_1 = c_2' \delta_{char} \tag{5.14}$$

$$\Lambda_3 = c_3 \Lambda_1 = c_3' \delta_{char} \tag{5.15}$$

and

$$\lambda = \Lambda_1 / \sqrt{a + b \mathrm{Re}_{\Lambda_1}} \tag{5.16}$$

where

$$\mathrm{Re}_{\Lambda_1} = \rho q \Lambda_1 / \mu \tag{5.17}$$

The relation (5.16) between the dissipative scale λ and the isotropy scale Λ_1 is required so that as the Reynolds number of the flow increases, dissipation will keep pace with the other productive and diffusive terms in the equation so that a self-similar flow can result. This form of the relationship between λ and Λ_1 has been used in the past by Glushko [Ref. 7].

For self-similar free turbulent flows, the structure given above is all that is needed to compute a turbulent shear layer or a free jet, provided the five constants, c_1 , c_2 , c_3 , a , and b , are given. To find these constants, we must resort to the comparison of calculated flow fields with experimental results.

If we wish to compute a boundary layer flow, we must consider an additional problem. When a wall is present in a shear flow, we wish to apply the boundary condition at the wall that

$$(\overline{u_i' u_k'})_{z=0} = 0$$

where z is measured normal to the surface. In addition, there should be no diffusion of $\overline{u_i' u_k'}$ through the surface so that the flux of $\overline{u_i' u_k'}$ due to viscosity, namely, $\mu \partial \overline{u_i' u_k'}/\partial z$, must be zero at $z = 0$ and thus $\partial \overline{u_i' u_k'}/\partial z = 0$ at $z = 0$. Thus it is reasonable to assume that near the wall

$$\overline{u_i' u_k'} = A_{ik} z^{1+\eta} \tag{5.18}$$

where A_{ik} is a constant and η is a positive constant. But if there is no diffusion through the wall, then all that is diffused towards the wall by viscosity at $z = \varepsilon$ is dissipated in the region between $z = \varepsilon$ and $z = 0$. (It is easily verified that all other terms in the model equation for $\overline{u_i' u_k'}$ are negligible if ε is small enough.) Thus,

$$2\mu \int_0^{\varepsilon} \frac{\overline{u_i' u_k'}}{\lambda^2} \, dz = \mu \left(\frac{\partial \overline{u_i' u_k'}}{\partial z} \right)_{z=\varepsilon}$$

or, using (5.18)

$$2 \int_0^{\varepsilon} \frac{z^{1+\eta}}{\lambda^2} \, dz = (1 + \eta)\varepsilon^{\eta}$$

If this relation is to hold for all $\varepsilon \to 0$, we must have

$$\lambda = \alpha z \tag{5.19}$$

where $\alpha^2 = 2/(1 + \eta)\eta$. Thus, near a solid surface, we always assume, in applying our model, that (5.19) holds in the region near the wall.

It is convenient to express this result in terms of Λ_1. Near a wall, (5.16) becomes

$$\lambda = \Lambda_1/\sqrt{a} \tag{5.20}$$

Using (5.19) we may write

$$\Lambda_1 = \alpha \sqrt{a} z \tag{5.21}$$

Thus, for boundary layer flows, α is another number which must be found from experimental results.

In our first attempts to construct a model of turbulent shear flows [Refs. 10 and 16], the following assumptions were made in order to construct the simplest possible model of boundary layer flows:

(1) It was assumed that all the large lambdas associated with inviscid modeling were equal; i.e., $\Lambda_1 = \Lambda_2 = \Lambda_3 = \Lambda$.

(2) It was assumed that α was equal to one.

(3) In the outer portion of a boundary layer, Λ was taken to be a constant c_1 times $\delta_{.99}$ ($\delta_{.99}$ is the value of z for which $\bar{u}$ is 99% of the free stream velocity). This value was assumed to hold, independent of z, as the wall was approached, until Λ became equal to $\sqrt{a}$ times z. For smaller values of z, Λ was taken equal to $\sqrt{a}\, z$.

With these assumptions, (5.7) through (5.12) were solved with various choices for the parameters a, b, and $c_1 = \Lambda/\delta_{.99}$ to produce a developing turbulent boundary layer on a flat plate. It was determined that the following choice of parameters

$$c_1 = \Lambda/\delta_{.99} = 0.064$$
$$a = 2.5 \qquad (5.22)$$
$$b = 0.125$$

yielded a fair representation of a turbulent boundary layer. The mean velocity profile and the behavior of skin friction with Reynolds number were adequately represented. The distributions of the second-order correlations within the boundary layer were reasonable.

The results of this original parameter search were used to compute a number of other turbulent flows in order to demonstrate the method [Refs. 19 and 20].

Before proceeding with further applications, it was considered necessary that a more detailed parameter search be made. In particular, two free turbulent flows - the free jet and the free shear layer - should be calculated to determine the values of the parameters c_2, c_3, a and b that would best

fit the experimental results for both flows. The value of c_1 being the ratio of Λ_1 to some arbitrarily defined characteristic length in each case is not an invariant of the problem and was to be chosen with fixed values of the other parameters to obtain best results in each case. Once these studies were complete, the model would be used to compute turbulent boundary layer flows so that, by comparison with experimental results, values for c_1 and α could be made for this flow. Hopefully, all flows could be described in a reasonable way by a single choice of the basic model parameters c_2, c_3, a, and b, and (where appropriate) α. The values of local Λ_1 determined from the values of c_1 in each case were then to be compared with the local magnitude of the integral scale L in each case. If it was found that the value of c_1 represented a choice that amounted to

$$\Lambda = \text{const } L = \beta L \tag{5.23}$$

then it would be assumed that a reasonably invariant model had been determined.

Application of Model to Free Shear Flows

Our search for a new model of turbulent shear layers began with an attempt to describe the axially symmetric free jet with the original turbulence model obtained for a boundary layer flow. This model, as mentioned previously, was one for which $\Lambda_1 = \Lambda_2 = \Lambda_3 = \Lambda$. This choice leaves three parameters to be determined. They are $c_1 = \Lambda/\delta_{char}$ and the two constants a and b in the expression

$$\lambda = \Lambda/\sqrt{a + b \cdot Re_\Lambda}$$

The method of searching for values of these parameter was as follows. The equations for a free jet were programmed so as to solve the system of equations for a free jet developing in the axial direction. At an arbitrary initial station in the axial direction, a mean velocity profile and profiles of the pertinent second-order correlations were arbitrarily assumed. For a given choice of model parameters (in this case, a, b, and $c_1 = \Lambda/r_{.5}$

where $r_{.5}$ is the radius for which $\bar{u}$ is one-half the centerline value), the free jet equations were solved for the development of the jet downstream of the initial distributions. In all cases, essentially self-similar solutions were obtained far downstream of the start of the calculation. If a set of parameters could be found so that the resulting self-similar flow agreed with experimental measurements with respect to the rate of spread, as well as with respect to mean velocity and correlation distributions, it would then be assumed that a reasonable turbulence model had been achieved.

Actually such calculations were carried out for both free jets and two-dimensional free shear layers. With the single Λ model, it was found that no combinations of parameters a, b, and c_1 could produce an adequate description of either a free jet or a free shear layer. In general, it was found that if the parameters were adjusted so as to give an adequate rate of spread of the mean profile (i.e., if the level of the turbulent shear correlation was large enough) the spread of the correlations $\overline{u_i'u_k'}$ by diffusion was always too large. This general result is illustrated in Figure 5.1 where it is seen that, if the general level of the shear correlation $\overline{u'w'}$ were to match the experimental data of Wygnanski and Fiedler [Ref. 21] in the region of maximum shear, it is clear that far too long a tail of $\overline{u'w'}$ at large r would result. This was a very general result for free shear flows and forces us to consider a more complicated model.

The difficulty that was experienced with the constant Λ model was the existence of too much diffusion relative to the rate of loss of correlations, either by dissipation or the tendency towards isotropy. To correct this difficulty in the studies reported here, the diffusion lengths Λ_2 and Λ_3 were made smaller than Λ_1. An idea of the effect of reducing the diffusion lengths relative to the isotropy length can be seen from Figure 5.2. Here the rms value of the longitudinal velocity fluctuation w' that has been calculated for several choices of model parameters is plotted versus radius in a self-

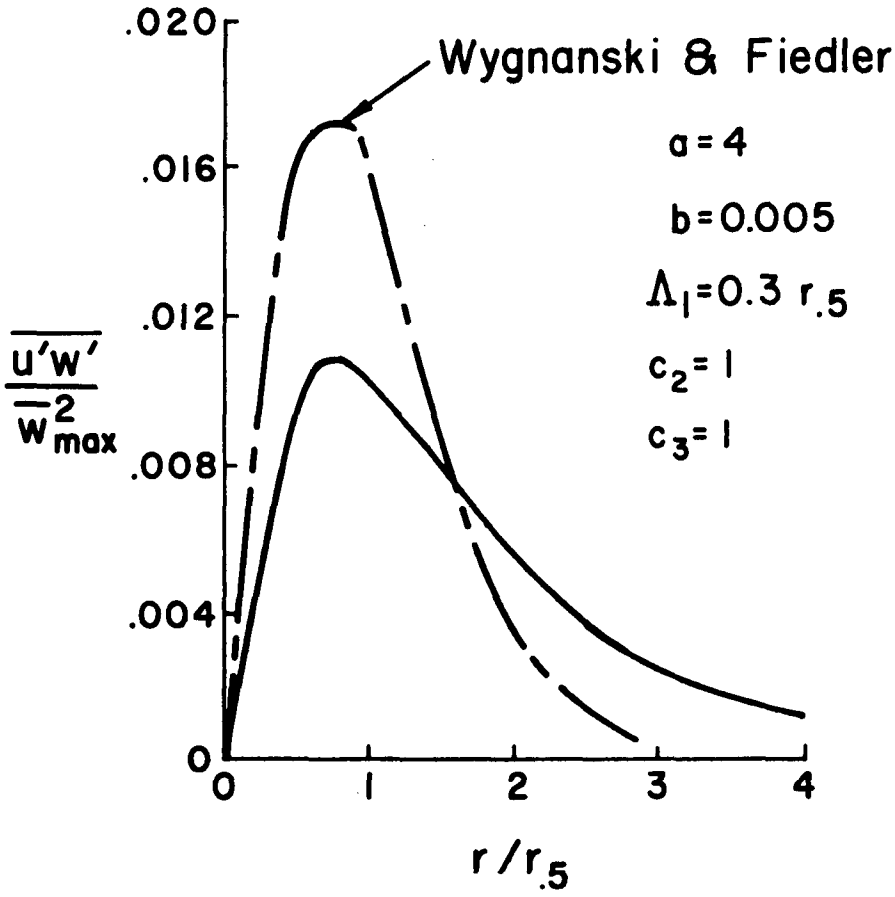

Figure 5.1. Result of a free jet computation with a single Λ model of turbulence

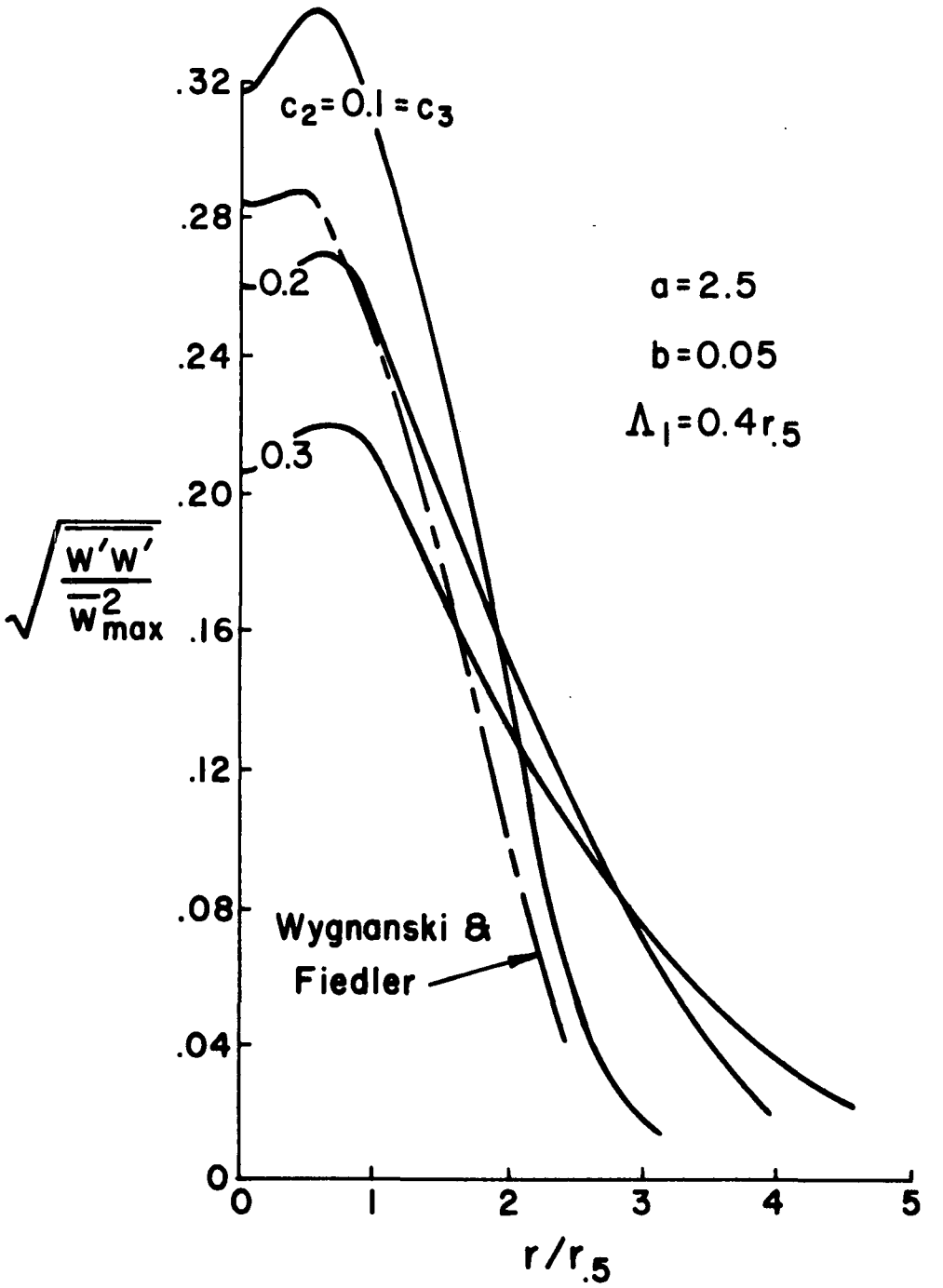

Figure 5.2. Behavior of solutions for a self-similar free jet when the parameter $c_2 = \Lambda_2/\Lambda_1 = \Lambda_3/\Lambda_1$ is varied

similar free jet. Note that as the diffusion lengths Λ_2 and Λ_3 (which are c_2 times Λ_1) are reduced, the amount of diffusion is obviously reduced and the levels of turbulence on the jet centerline are appreciably increased.

The effect of the choice of the scale of the isotropy length Λ_1 can be seen from Figure 5.3. The distribution of longitudinal turbulence intensity is shown as a function of radius for two choices of Λ_1 relative to the local value of $r_{.5}$. It is seen that the levels are much lower for the smaller Λ_1 than for the larger value. This is what one might expect because of the increased dissipation as well as the increased loss of shear correlation by the tendency towards isotropy when the scale Λ_1 and, hence, λ is made smaller.

The effect of neglecting pressure diffusion can be seen in Figure 5.4; the longitudinal velocity fluctuations in a free jet are shown as a function of radial position for a given choice of model parameters a, b, c_1, and c_2 for two choices of c_3. One choice is $c_3 = c_2$ and the second is $c_3 = 0$, i.e., neglect of pressure diffusion. It is seen that for this choice of the other parameters the effect of neglecting pressure diffusion is not large.

Having given some idea of how some of the various parameters entering the model for turbulent shear layers affect the solutions, we must now discuss the selection of an actual set of parameters. If one considers only a single type of shear flow that one wishes to model, say, the free jet, it is possible to choose a whole spectrum of models which will give a good description of the mean spread of the free jet and the distribution of, say, the longitudinal turbulent velocity field. To illustrate this point, we may refer to Figure 5.5. Here we see that two profiles of longitudinal velocity fluctuation can be obtained with radically different choices of b and Λ_1. It is observed that if one chooses small b one must also choose a small value of Λ_1 relative to a characteristic scale of the jet. What then is the basic difference between these two solutions? It is this. For the solution with small b and small

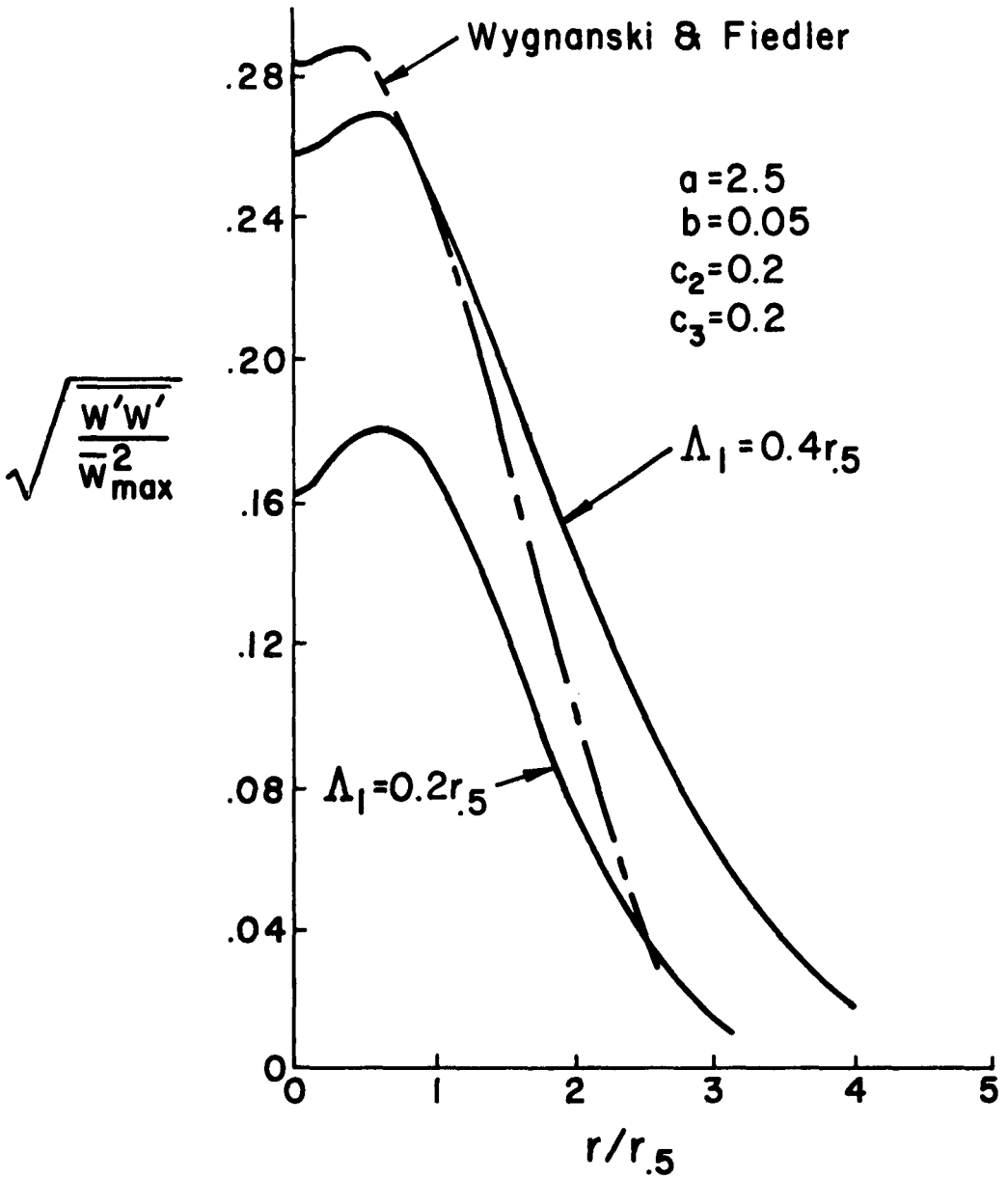

Figure 5.3. Effect of variation of the isotropy scale Λ_1 on characteristics of a self-similar free jet

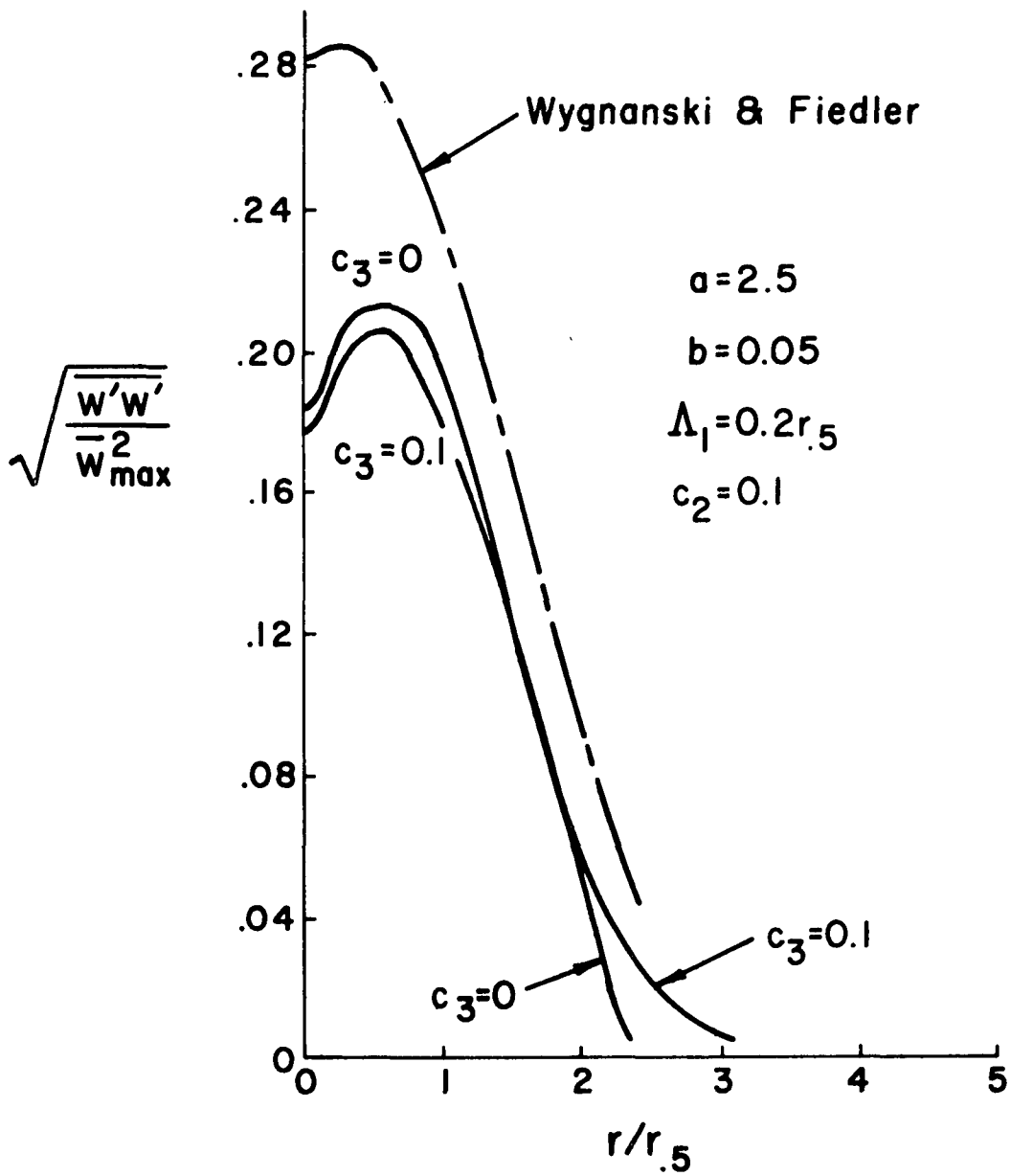

Figure 5.4. The effect of neglecting pressure diffusion when calculating a self-similar free jet

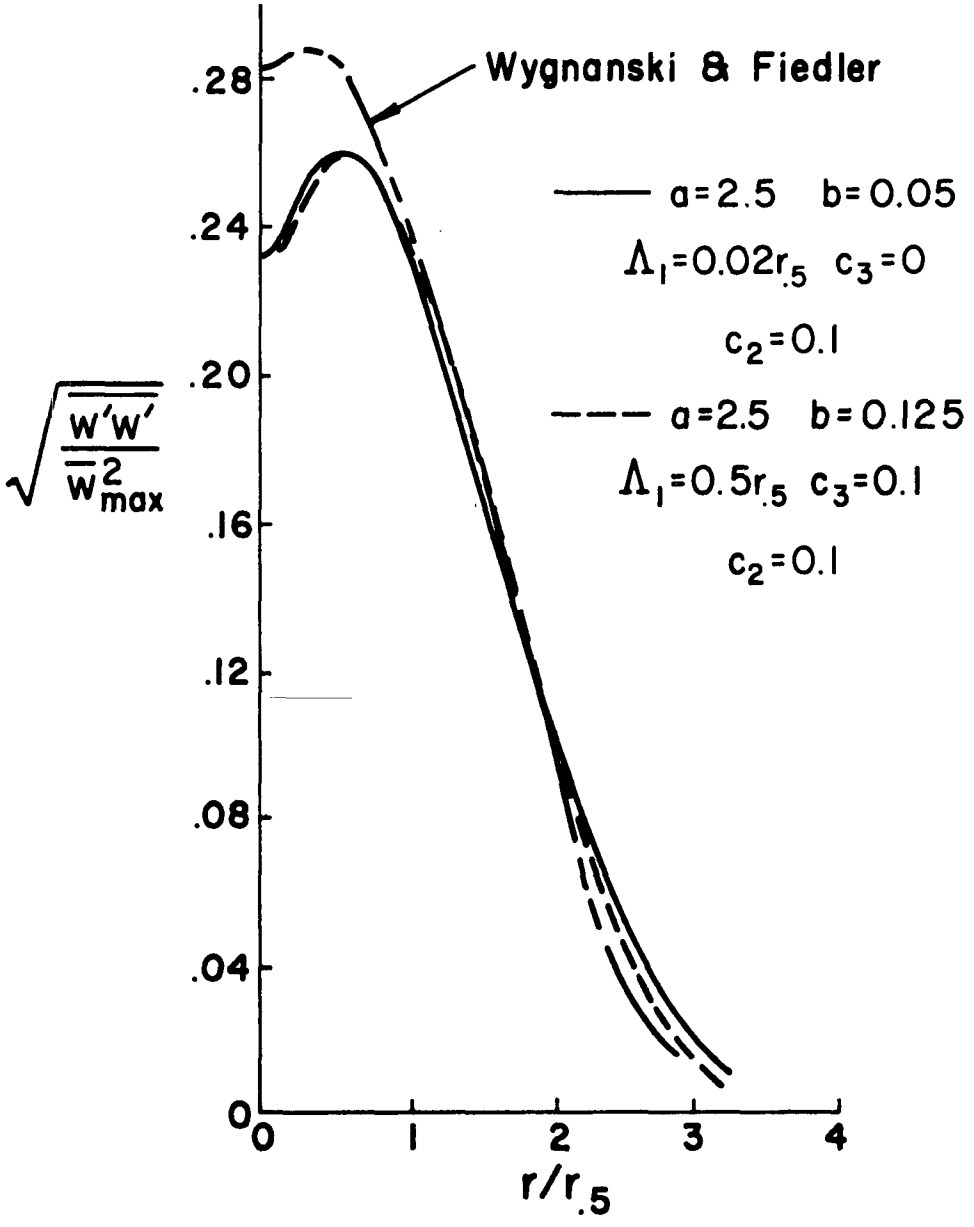

Figure 5.5. Two choices of model parameters that yield almost the same distributions of $\overline{w'w'}$ for a self-similar free jet

Λ_1 , the balance of the production of turbulence is more by dissipation and less by diffusion than for the other case. Also for the case of small b and small Λ_1 , the solutions are more isotropic on the jet centerline than for the other case.

The choice between the two models exhibited in Figure 5.5 must be made on the basis of the degree of diffusion and the degree of isotropy desired in the calculated result. This is a difficult decision to make, for existing experimental data do not agree as to how isotropic free jets are on their centerline, as will be seen later. There is another way that one can decide between two different models. If one uses the same model to compute two different turbulent flows having essentially different geometries, the model which gives the best results for both flows is, since we are seeking an invariant model, the one to choose.

As mentioned previously, we have computed self-similar solutions for a free shear layer as well as for an axially symmetric free jet. Actually a search for model parameters for each type of flow was carried out. As a result of these studies, it was determined that, insofar as the parameter studies have proceeded at this point, the following model for free turbulent shear flows gave the best results:

$$\begin{aligned} a &= 2.5 \\ b &= 0.125 \\ c_2 &= 0.1 \\ c_3 &= 0.1 \end{aligned} \tag{5.24}$$

Also, the value

$$c_1 = \Lambda_1/\delta_{char} = 0.50 \tag{5.25}$$

was found best for both flows, although it was not part of the plan to have a common value of c_1 . As mentioned above, for the free jet,

$$\delta_{char} = r_{.5} \tag{5.26}$$

The characteristic length for the free shear layer was taken as

$$\delta_{char} = z_{.25} - z_{.75} \tag{5.27}$$

which is the distance normal to the flow in the shear layer from the point where the velocity is one-quarter the external driving velocity to where it is three-quarters this velocity.

In Figures 5.6 through 5.13, we show comparisons with experimental data of the velocity correlation profiles computed for both a free jet and a free shear layer using the model parameters given above. The experimental results are taken from the work of Wygnanski and Fiedler [Refs. 21 and 22], Gibson [23], and Donaldson, Snedeker, and Margolis [24].

Figures 5.6 and 5.7 show the longitudinal fluctuations in a free jet and free shear layer, respectively. The agreement between model calculations and experiment is good in both cases. For the free jet in Figure 5.6, it would perhaps have been desirable to have a little more diffusion (larger Λ_1 and larger b) in the model in an attempt to reduce the overshoot in $\overline{w'w'}$ near the centerline of the jet.

Figures 5.8 and 5.9 show distributions of normal fluctuations in both the free jet and the free shear layer. Here we note the agreement with experimental data is not so good. There appears to be a little too much diffusion for these cases. Also note the very large discrepancy between measured normal fluctuations on the centerline, as reported in three separate experiments. The data of Gibson show the components of turbulent velocity to be essentially isotropic on the jet centerline, while those of Wygnanski and Fiedler and Donaldson, Snedeker, and Margolis do not. From the results shown in Figure 5.8, it would appear that if one were to desire more isotropy, one would wish to choose a smaller value of Λ_1 and, hence, a smaller value of b . This is opposite to the conclusion drawn from Figure 5.6.

Figures 5.10 and 5.11 show the sidewise components of turbulence for the free jet and free shear layer, respectively. The agreement between experiment and computed results is better for the free jet than for the free shear layer. The reason for this behavior is not known.

In Figures 5.12 and 5.13, we show the shear correlations for the free jet and the free shear layer. The agreement in both cases

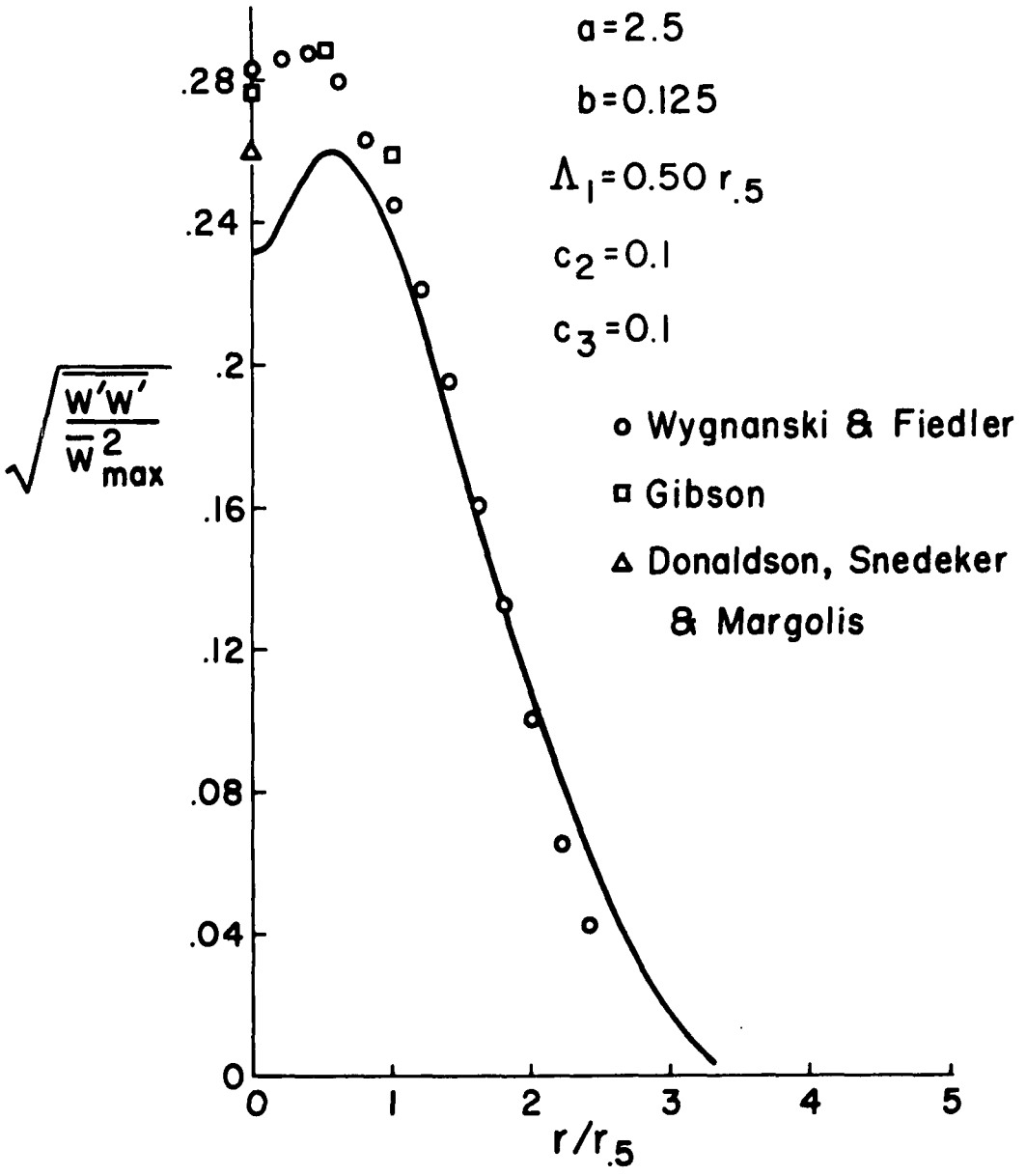

Figure 5.6. Comparison of experimental results and model predictions for the longitudinal velocity correlations in a free jet

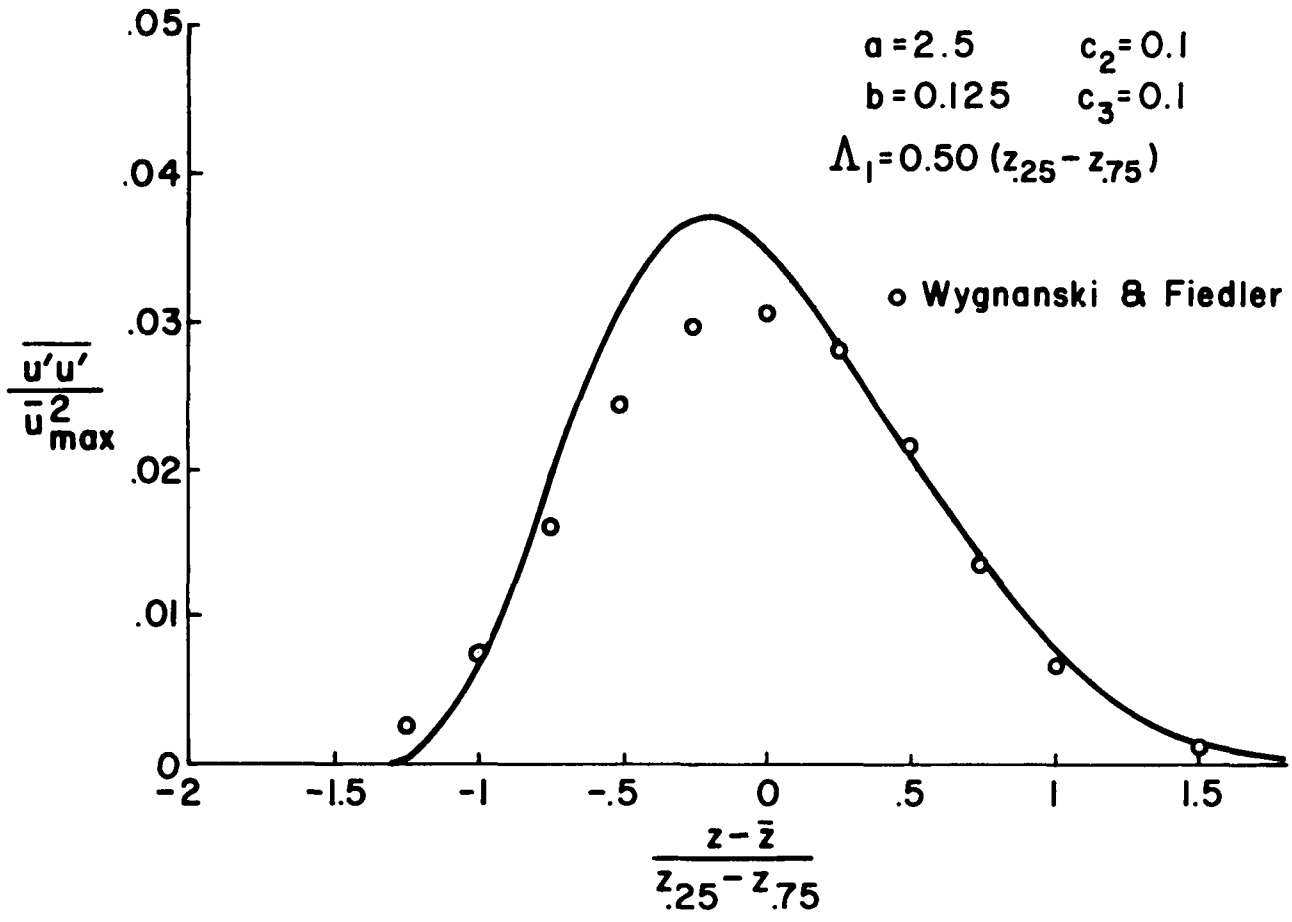

Figure 5.7. Comparison of experimental results and model predictions for the longitudinal velocity correlations in a free shear layer

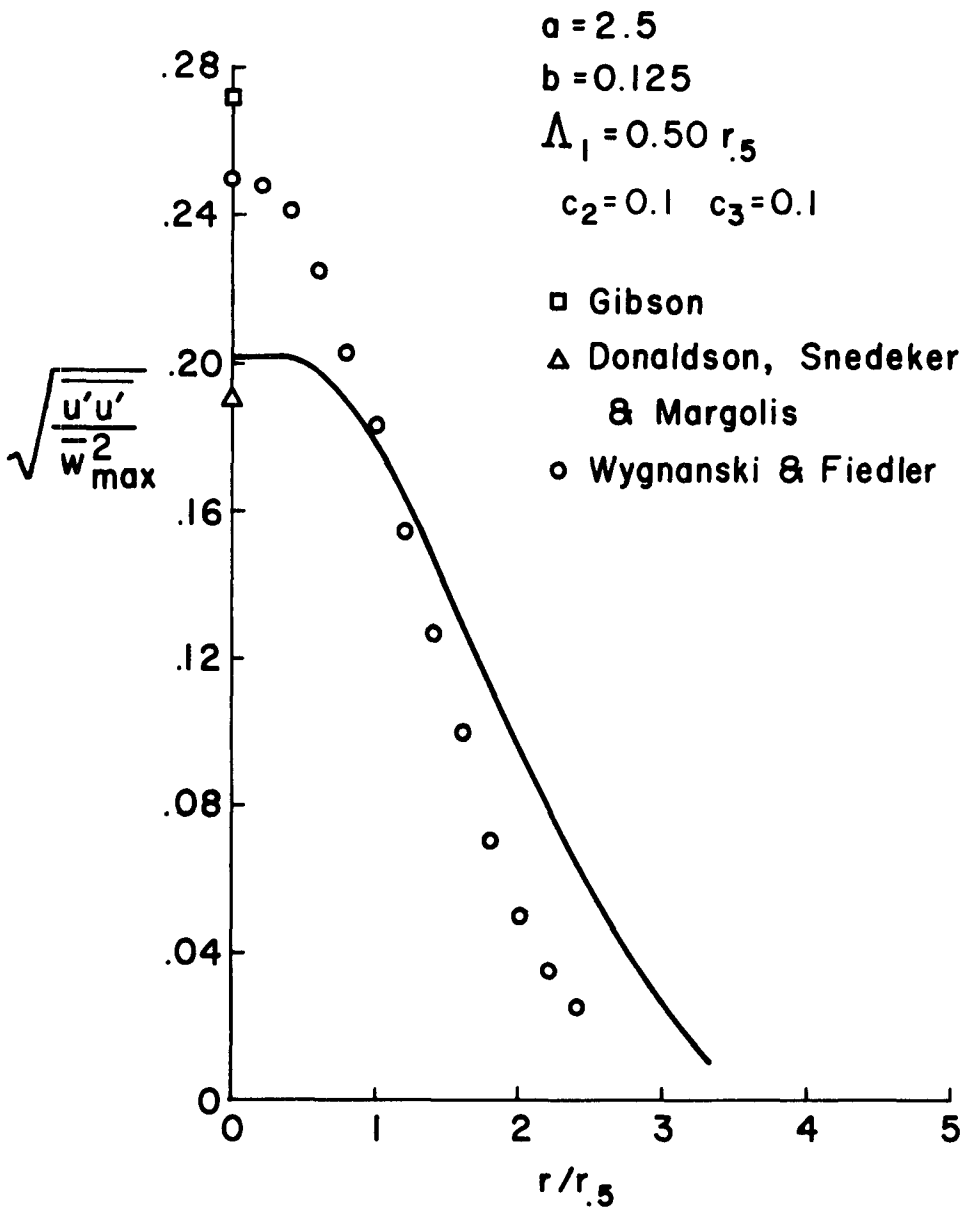

Figure 5.8. Comparison of experimental results and model predictions for the radial velocity fluctuations in a free jet

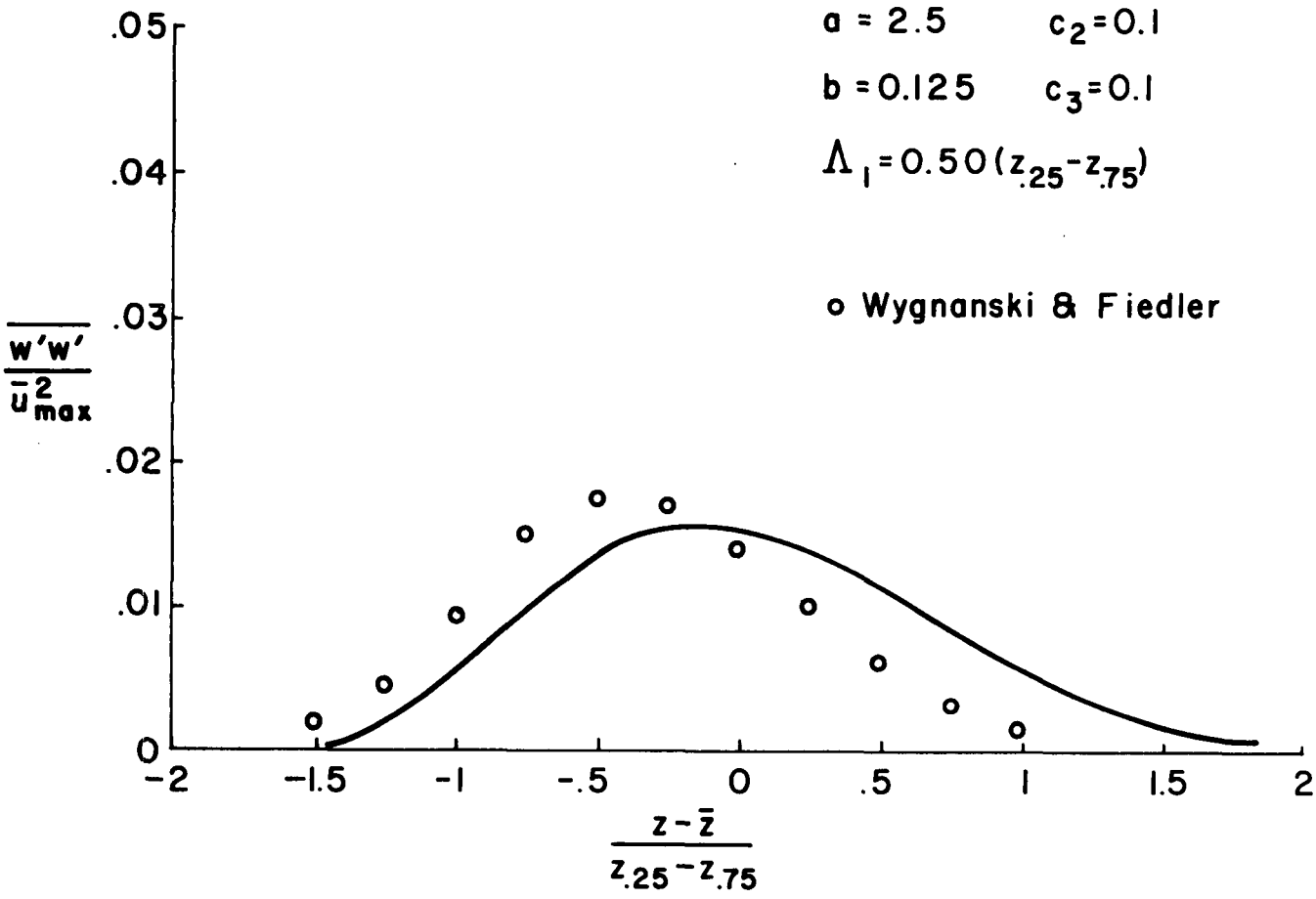

Figure 5.9. Comparison of experimental results and model predictions for the normal velocity fluctuations in a free shear layer

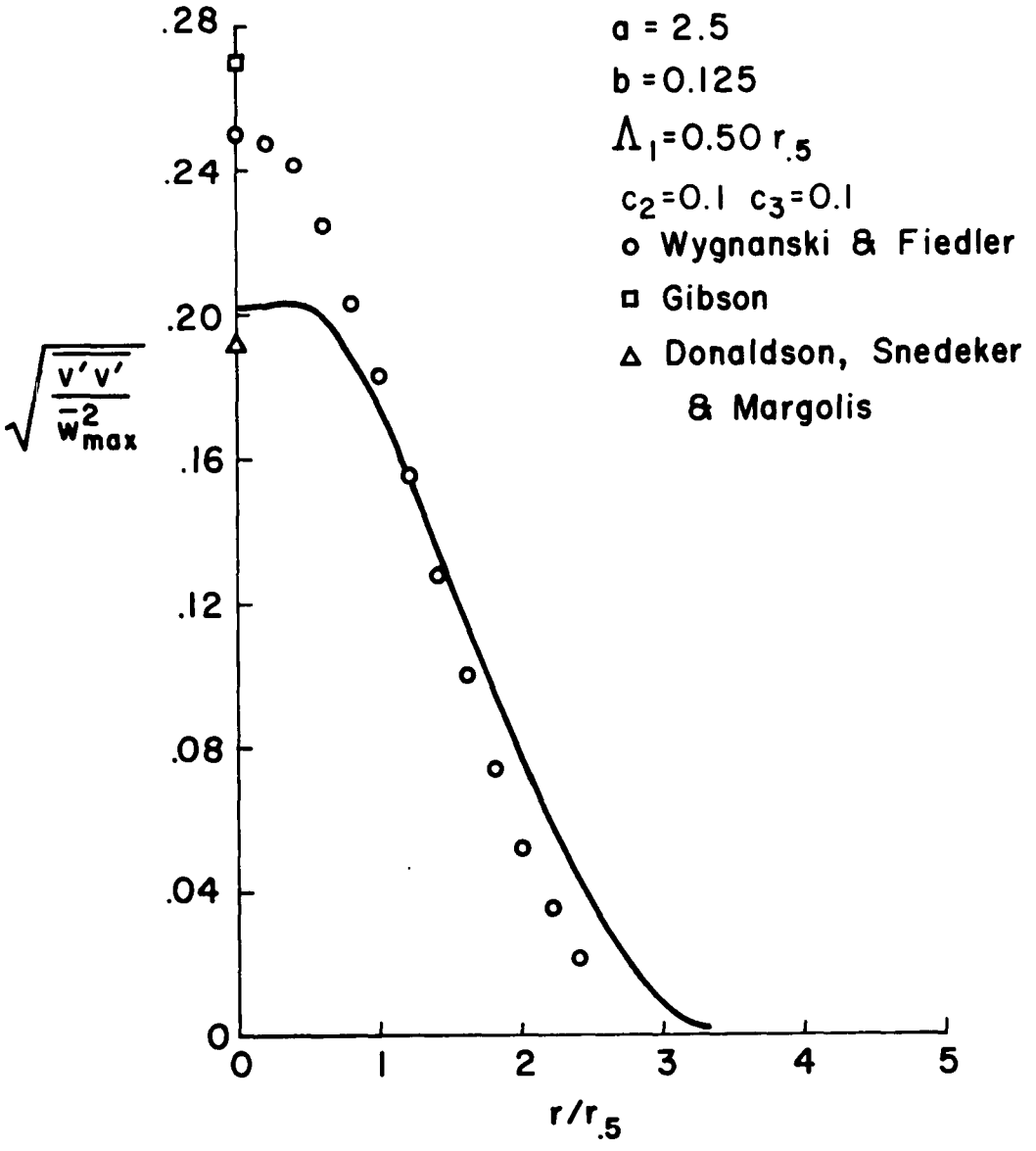

Figure 5.10. Comparison of experimental results and model predictions for the sidewise fluctuations in a free jet

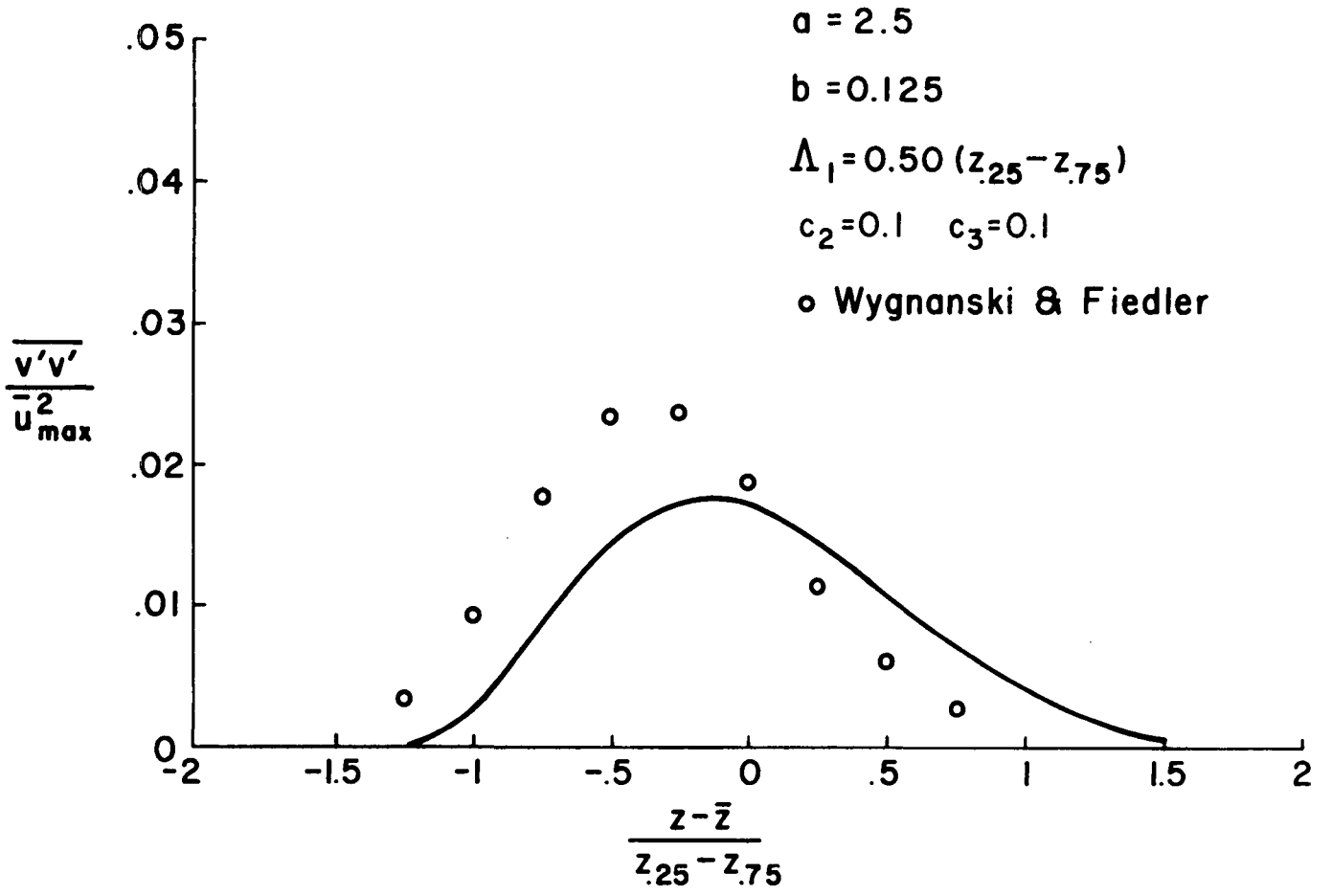

Figure 5.11. Comparison of experimental results and model predictions for the sidewise fluctuations in a free shear layer

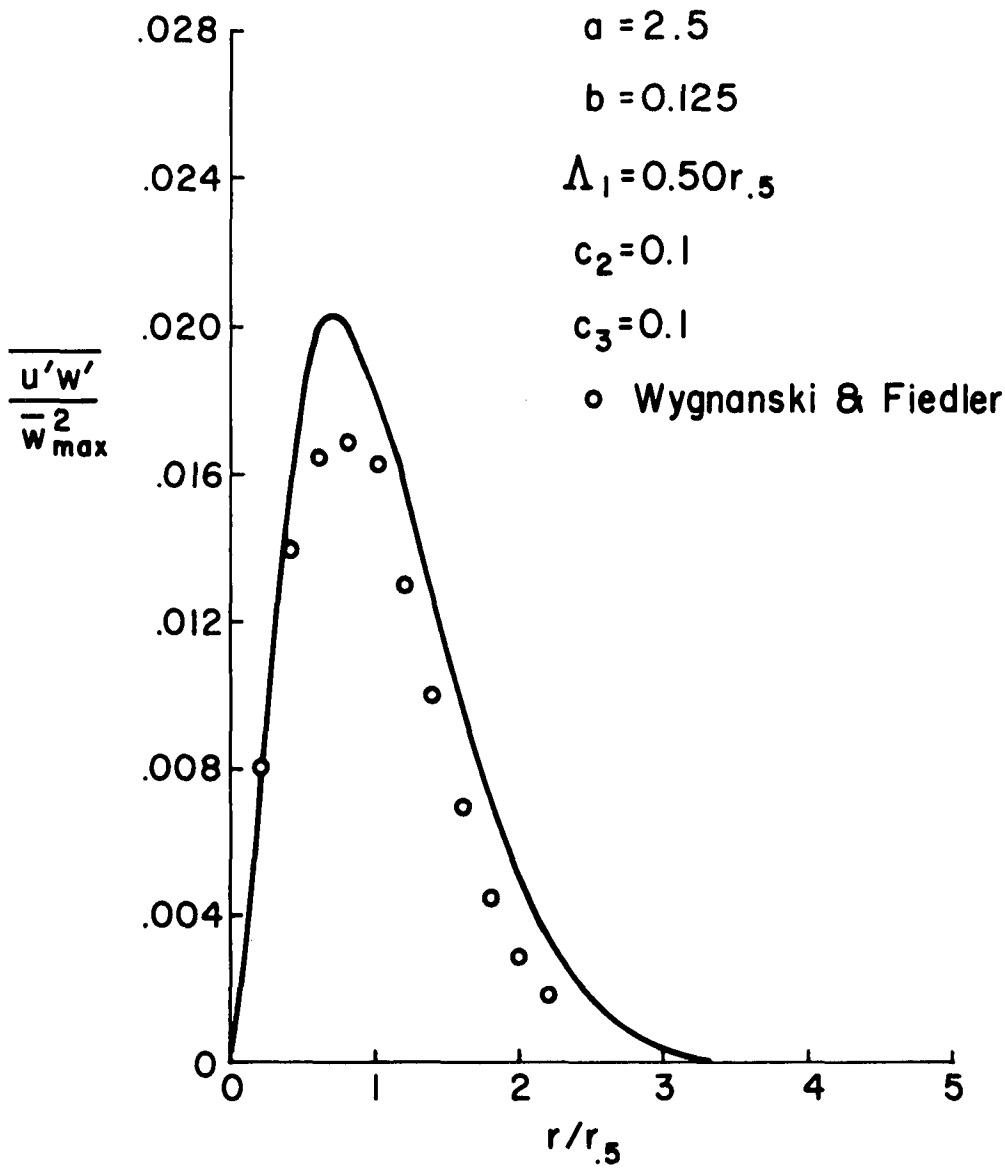

Figure 5.12. Comparison of experimental results and model predictions for the shear correlation in a free jet

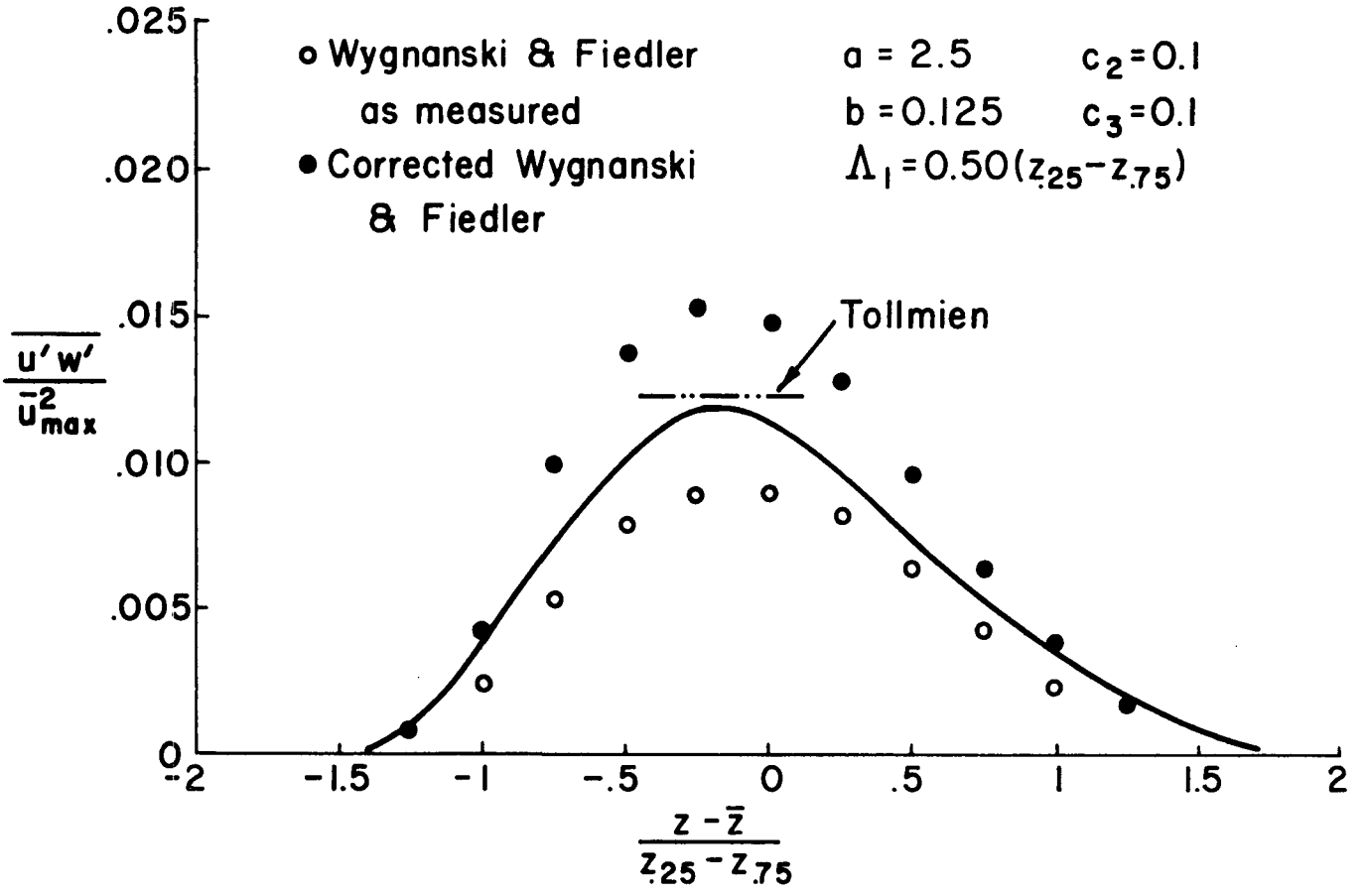

Figure 5.13. Comparison of experimental results and model computations for the shear correlation in a free shear layer

is fair. It should be noted that the experimental values of shear correlation from Ref. 21 have been shown as reported (the open circles) in Figure 5.13 and also as corrected by us (the solid symbols) so as to agree with the measured rate of spread of the free shear layer. A comparison of the measured shear and that inferred from the mean velocity profiles was reported by Wygnanski and Fiedler but apparently their computations contained an error. Also shown in Figure 5.13 is the level of shear that may be inferred from the mean spread of the free shear layer studied by Tollmien [Ref. 25] and Prandtl [Ref. 26] many years ago. It is seen from the results presented in Figures 5.12 and 5.13 that the model gives a fairly good representation of the shear in both the free jet and the free shear layer.

A careful study of Figures 5.6 through 5.13 shows that it really is necessary to study further the problem of choice of model parameters. However, before this is done, it appears desirable to have at hand experimental data which one can rely on to be truly representative of the basic flow which is being calculated. It is difficult to choose a more sophisticated model until the question of the degree of isotropy on the center-line of a free jet is settled. In addition, one should at this point determine if the model just found for free shear layers can be used for a model of the outer regions of a boundary layer and give reasonable results.

Before turning to the problem of the turbulent boundary layer, it will be instructive to find a relationship between the values of Λ_1 used in the free shear layer and the free jet calculations and the general magnitude of the integral scales measured for such flows. In the computations that have been made, it has been assumed that Λ_1 is constant across a free jet or a free shear layer at any given longitudinal position and, in magnitude, proportional to the local scale of the mean flow. It is well known that the integral scales of such flows are, in general, proportional to the local mean scales, but the actual value of the integral scale varies across the layer.

In Table 5.1 we present the values of integral scale within a free jet, as reported by Wygnanski and Fiedler. The integral scale tabulated is the longitudinal integral scale

$$L = \frac{1}{\overline{w'w'}(z_1)} \int_0^\infty \overline{w'(z_1)w'(z_2)}\, d(z_2 - z_1) \tag{5.28}$$

for the free jet.

Table 5.1. Integral Scales in a Free Jet [Ref. 21]

Radial Position r/x	Dimensionless Scale $L/r_{.5}$	Scale Ratio Λ_1/L
0	0.448	1.12
.05	0.595	0.84
.10	0.726	0.69
.15	0.850	0.59
.20	0.855	0.58

Also shown in Table 5.1 is the ratio of the computational scale Λ_1 to the local integral scale L. Thus a typical value for this ratio for the free jet is

$$\Lambda_1/L = 0.69 \tag{5.29}$$

For the free shear layer, similar results are given in Table 5.2. These experimental values are also due to Wygnanski and Fiedler. The longitudinal integral scale is, in this case, defined by

$$L = \frac{1}{\overline{u'u'}(x_1)} \int_0^\infty \overline{u'(x_1)u'(x_2)}\, d(x_2 - x_1) \tag{5.30}$$

Table 5.2. Integral Scales in a Free Shear Layer [Ref. 22]

Location in Jet	Dimensionless Scales L/x	$L/(z_{.25} - z_{.75})$	Scale Ratio Λ_1/L
Inner Region	0.098	0.846	0.59
Center	0.103	0.883	0.57
Outer Region	0.147	1.27	0.39

A typical value of Λ_1/L for a free shear layer appears to be approximately

$$\Lambda_1/L = 0.55 \tag{5.31}$$

Before proceeding further, it must be demonstrated that if the present model is applied to a boundary layer, useful results will be obtained for the same choice of model parameters that has been made for free turbulent shear flows.

Application of Model to Boundary Layers

If the model of turbulent shear flows is to be applied to a boundary layer, the parameters c_2, c_3, a , and b are known. But, since the characteristic length in a boundary layer is arbitrary (as it is in the free jet and the free shear layer), we are at liberty to choose c_1 , i.e., the ratio between Λ_1 and the characteristic length (which, in this case, we take equal to $\delta_{.99}$, the thickness of the layer in which the velocity reaches 99% of its free stream value).

As discussed previously, one other parameter enters the problem, namely, α , the coefficient appearing in (5.19). We have, then,

$$\Lambda_1 = \alpha\sqrt{a}\, z \tag{5.32}$$

for $0 \leq z \leq c_1\delta_{.99}/(\alpha\sqrt{a})$ and

$$\Lambda_1 = c_1\delta_{.99} \tag{5.33}$$

for $z > c_1\delta_{.99}/(\alpha\sqrt{a})$

With only these two parameters α and c_1 to determine, the search is not difficult. The model that has been found is the following:

$$\begin{aligned} a &= 2.5 \\ b &= 0.125 \\ c_2 &= 0.1 \\ c_3 &= 0.1 \\ c_1 &= \Lambda_1/\delta_{.99} = 0.15 \\ \alpha &= 0.7/\sqrt{a} = 0.443 \end{aligned} \tag{5.34}$$

The ability of this model of a turbulent shear layer to predict the known mean properties of turbulent boundary layers is shown in Figures 5.14 through 5.16. In Figure 5.14, we show the skin friction developed by our model as it proceeds from a disturbed laminar layer to a fully turbulent layer. Also shown are the laminar skin friction law and the turbulent law proposed by Coles [Ref. 27] which is a good fit to experimental data. It is no great surprise that the general levels of skin friction we computed agree well with experimental findings inasmuch as the values of α and c_1 were chosen to get these levels correct. Of more importance is the nearly exact following of the trend of skin friction with Reynolds number by the model computations.

Figure 5.15 shows a comparison of the computed mean velocity profiles developed by the model in the vicinity of the wall and the well-known law of the wall as proposed by Coles [27]. It may be seen that the law of the wall is not quite achieved by the present selection of model parameters. However, the results are sufficiently accurate to be encouraging.

In Figure 5.16, we compare the experimentally determined velocity defect law proposed by Coles [27] with the results of our model computations. It is seen that once the turbulent boundary layer is well established, the computational model gives a fairly good representation of the outer regions of the turbulent boundary layer.

With these results in hand, we must now consider the relationship of the computational scales used to the longitudinal integral scales that are found in the outer regions of turbulent boundary layers. For this purpose, we may use the measurements of Grant [Ref. 28]. When the experimental correlations reported by Grant for $y/\delta_o = 0.66$ * in a turbulent boundary layer are integrated to give the longitudinal integral scale, one obtains $L/\delta_o \simeq 0.3$. Since for our calculations, $\delta_o/\delta_{.99} \simeq 0.83$, we find that $L/\delta_{.99} \simeq 0.25$. Since the computational scale

*Grant defined δ_o as that height in the boundary layer where the velocity defect was equal to the friction velocity.

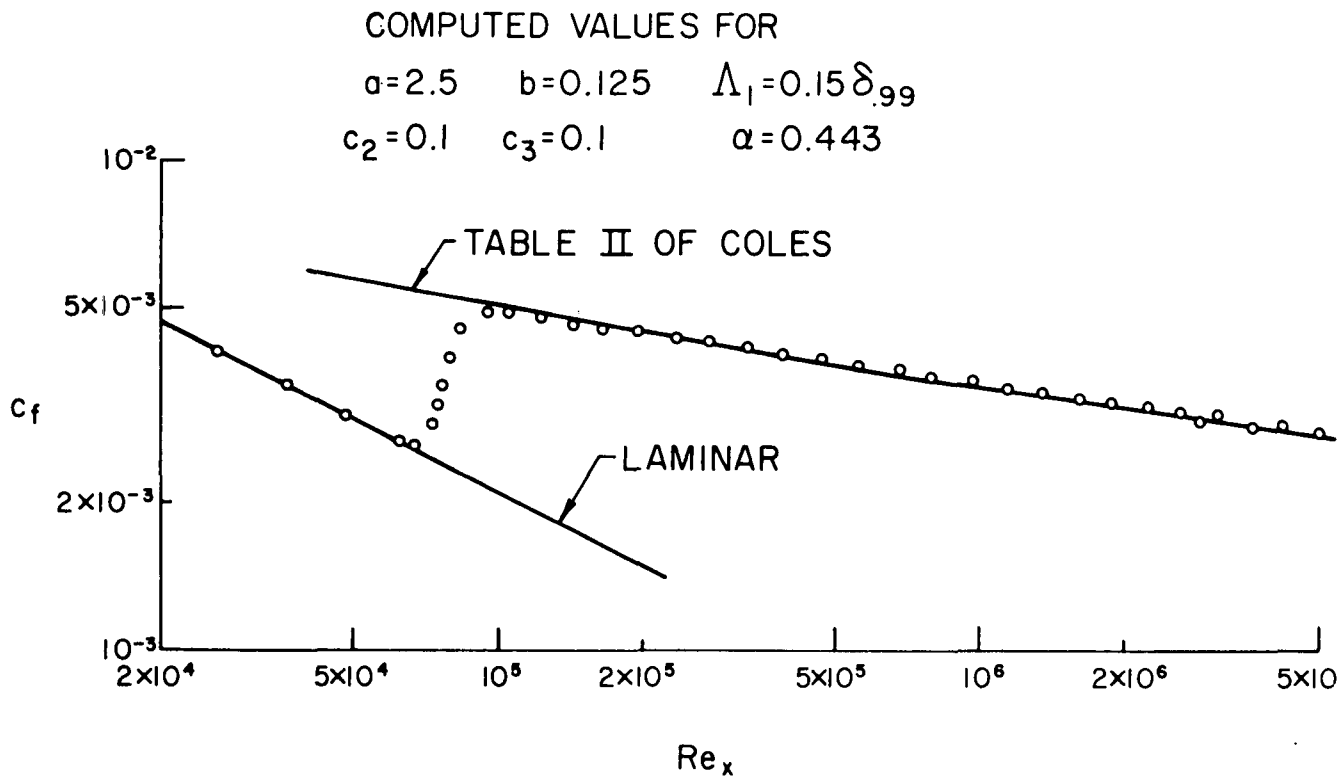

Figure 5.14. Computed variation of coefficient of friction with Reynolds number

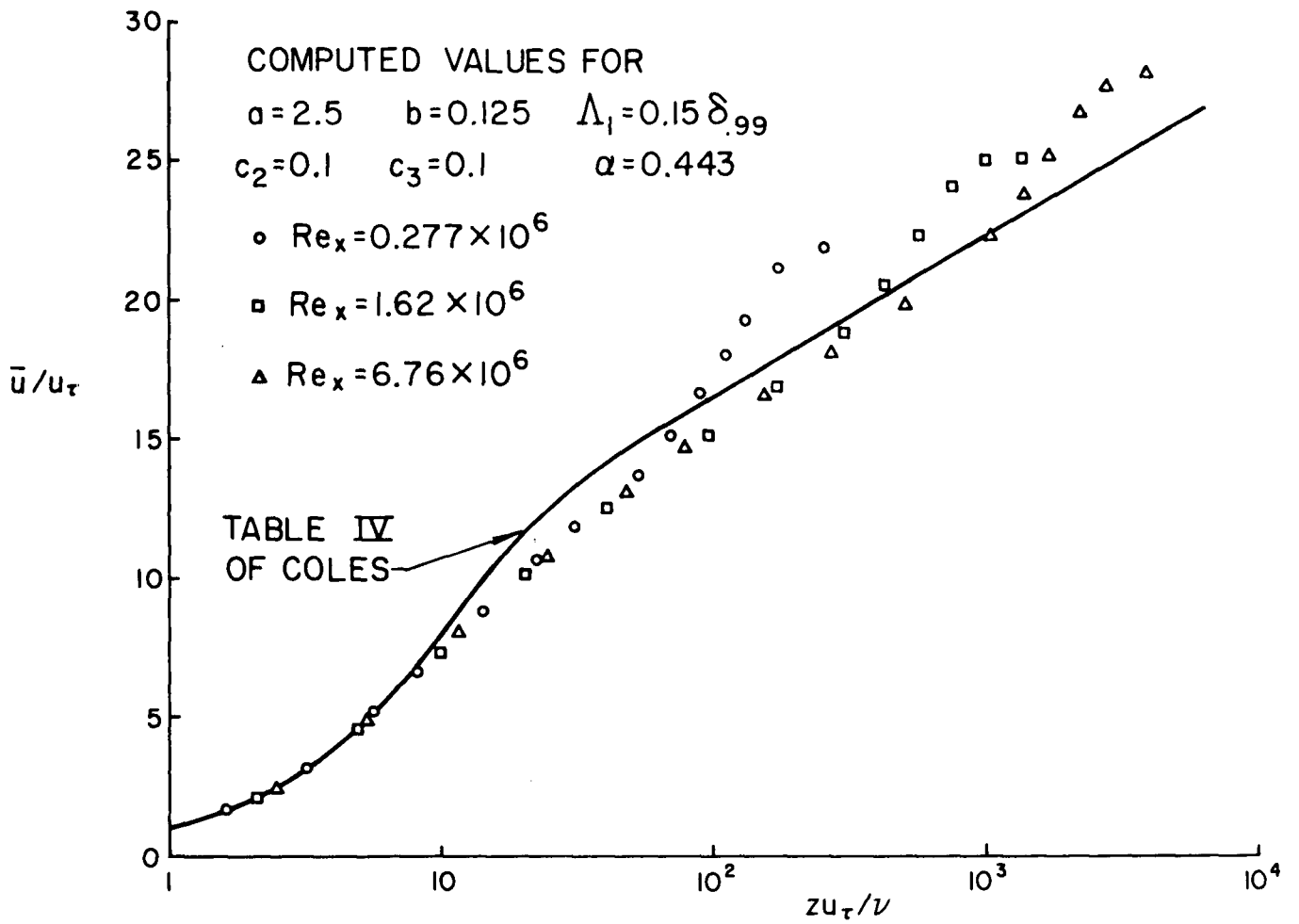

Figure 5.15. Computed velocity profiles for three Reynolds numbers. Computation started at Re_x = 20,000. The reference velocity u_τ is defined by $\tau_{wall} = \rho u_\tau^2$.

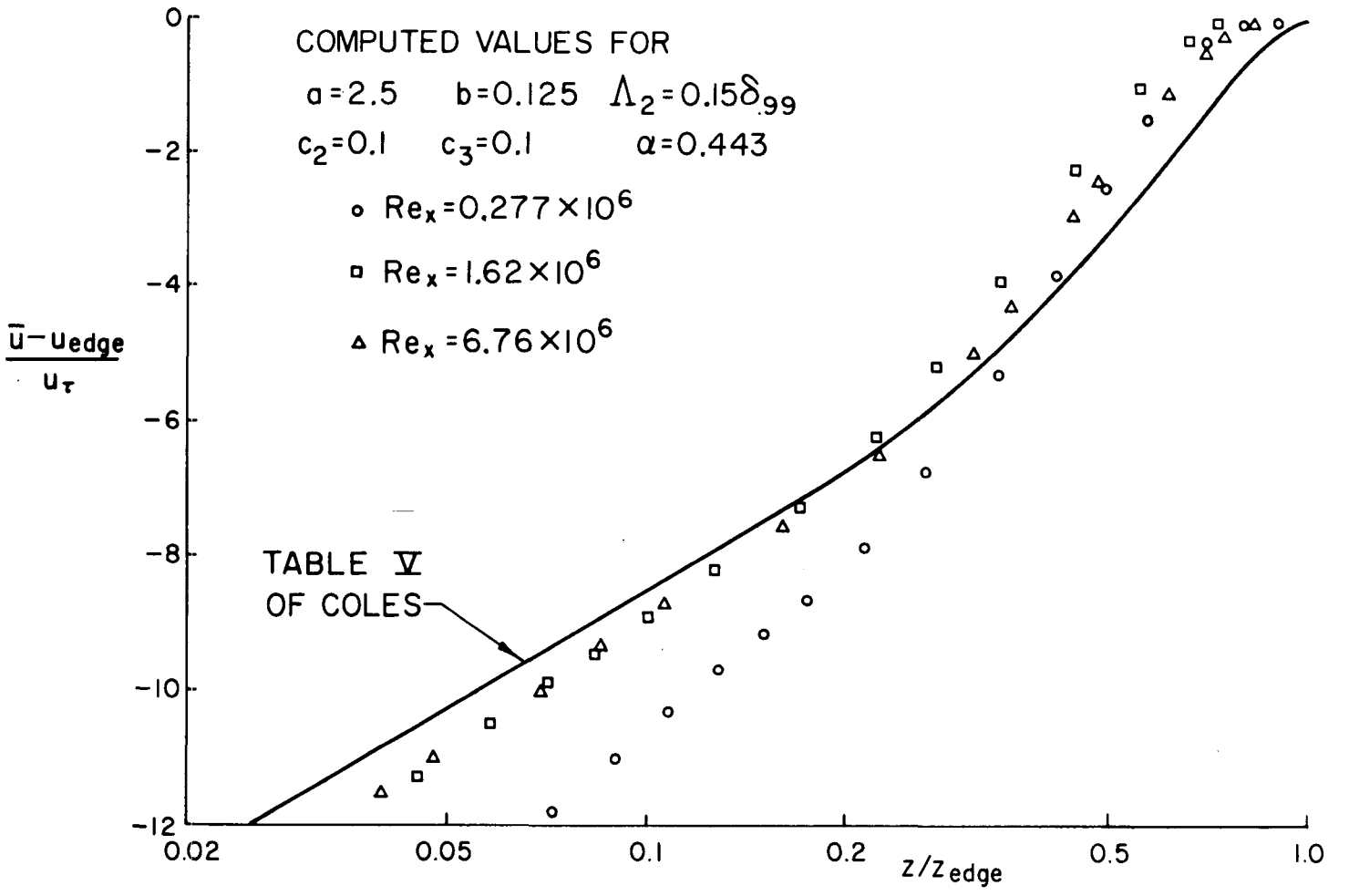

Figure 5.16. Computed velocity defects for three Reynolds numbers. Computation started at Re_x = 20,000. The reference velocity u_τ is defined by $\tau_{wall} = \rho u_\tau^2$.

used was $\Lambda_1/\delta_{.99} = 0.15$, we find that

$$\Lambda_1/L \simeq 0.6 \tag{5.35}$$

This is a most welcome result since it shows that, for all the turbulent flows we have investigated, the ratio of the proper computational scale to the longitudinal integral scale is approximately the same.

Some Comments on Second-Order Modeling Techniques

The method of modeling turbulent shear flows which we have just described was developed, as we have previously pointed out, in order to attempt calculations of turbulent flows other than the classical shear layers that were discussed in the previous sections. The author and his colleagues have applied the model to the calculation of the decay of a turbulent line vortex [Ref. 29], to the generation of turbulence in the earth's atmosphere [Refs. 16 and 20], and to the dispersal of pollutants by the atmosphere [Ref. 30]. Since these computations were carried out with the original oversimplified constant Λ model discussed previously, one must not take the numerical values obtained too seriously; nevertheless, these computations did give some most interesting results and insights. Certainly the utility of the method was demonstrated and it appears that it, and others like it, should be carefully studied and refined in the next few years. The first order of business should be a continuance of the types of parameter studies that we have just described, for as large a spectrum of shear flows as can be reliably measured. In this way, we would hope to develop a model with the broadest capability possible.

It is here that one runs into the difficulties that were touched upon previously in connection with the free jet and the free shear layer. It would be very helpful indeed if the research community could agree on canonical free jet and free shear layer experiments which could be performed by several investigators. The purpose of these experiments would be to

strive for agreement between experimentalists as to what the characteristics of such flows were and to explain any discrepancies that might exist. Before very much refinement of turbulent shear flow models can be accomplished, it appears that we are going to have to have a more precise definition of what the models must predict.

6. AN EQUATION FOR THE SCALE Λ_1

Although our work has not proceeded so far as to couple an equation for the scale Λ_1 to the rest of the model equations when making shear layer computations, it is our intention to do so in the near future. For the sake of completeness, then, we outline here the derivation of an equation for the scale length Λ_1.

We have seen in Section 5 that Λ_1 is related to the integral scale L defined by (5.30). Since this scale depends on an integral of the two-point correlation

$$\overline{u_i'(x_1)u_k'(x_2)} = \overline{(u_i')_A(u_k')_B} \tag{6.1}$$

we will start with an equation for this quantity.

Starting with (3.15), equations for $(u_i')_A$ and $(u_k')_B$ may be written. Much as in the derivation of (3.17), these may be combined to give

$$\begin{aligned}
&\frac{\partial}{\partial t}\overline{(u_i')_A(u_k')_B} + \overline{(u_k')_B(u_j')_A}\left(\frac{\partial \bar{u}_i}{\partial x_j}\right)_A + \overline{(u_i')_A(u_j')_B}\left(\frac{\partial \bar{u}_k}{\partial x_j}\right)_B \\
&\quad + (\bar{u}_j)_A\left(\frac{\partial}{\partial x_j}\right)_A\overline{(u_i')_A(u_k')_B} + (\bar{u}_j)_B\left(\frac{\partial}{\partial x_j}\right)_B\overline{(u_i')_A(u_k')_B} \\
&\quad + \left(\frac{\partial}{\partial x_j}\right)_A\overline{(u_i')_A(u_j')_A(u_k')_B} + \left(\frac{\partial}{\partial x_j}\right)_B\overline{(u_i')_A(u_j')_B(u_k')_B} \\
&= -\frac{1}{\rho_o}\left(\frac{\partial}{\partial x_i}\right)_A\overline{p_A'(u_k')_B} - \frac{1}{\rho_o}\left(\frac{\partial}{\partial x_k}\right)_B\overline{p_B'(u_i')_A} \\
&\quad + \nu_o\left(\frac{\partial^2}{\partial x_j \partial x_j}\right)_A\overline{(u_i')_A(u_j')_B} + \nu_o\left(\frac{\partial^2}{\partial x_j \partial x_j}\right)_B\overline{(u_i')_A(u_k')_B} \\
&\quad + \frac{g_i}{T_o}\overline{T_A'(u_k')_B} + \frac{g_k}{T_o}\overline{T_B'(u_i')_A}
\end{aligned} \tag{6.2}$$

In this notation, a variable at one point is considered a constant with respect to differentiation at another point. For example,

$$(u_j')_B\left(\frac{\partial}{\partial x_j}\right)_A (u_i')_A = \left(\frac{\partial}{\partial x_j}\right)_A [(u_j')_A (u_j')_B] \tag{6.3}$$

We introduce new variables. Let

$$y_k = \tfrac{1}{2}[(x_k)_A + (x_k)_B] \tag{6.4}$$

and

$$\xi_k = (x_k)_B - (x_k)_A \tag{6.5}$$

In terms of these variables, the contraction of (6.2) can be written

$$\begin{aligned}
&\frac{\partial}{\partial t}\,\overline{(u_i')_A(u_i')_B} + \frac{1}{2}\left[(\bar{u}_j)_A + (\bar{u}_j)_B\right]\frac{\partial}{\partial y_j}\,\overline{(u_i')_A(u_i')_B} \\
&\quad + \left[(\bar{u}_j)_B - (\bar{u}_j)_A\right]\frac{\partial}{\partial \xi_j}\,\overline{(u_i')_A(u_i')_B} + \frac{1}{2}\left[\overline{(u_i')_B(u_j')_A}\cdot\right. \\
&\quad \left.\cdot\,\frac{\partial(\bar{u}_i)_A}{\partial y_j} + \overline{(u_i')_A(u_j')_B}\,\frac{\partial(\bar{u}_i)_B}{\partial y_j}\right] + \overline{(u_i')_A(u_j')_B}\,\frac{\partial(\bar{u}_i)_B}{\partial \xi_j} \\
&\quad - \overline{(u_i')_B(u_j')_A}\,\frac{\partial(\bar{u}_i)_A}{\partial \xi_j} + \frac{1}{2}\,\frac{\partial}{\partial y_j}\left[\overline{(u_i')_A(u_j')_A(u_i')_B}\right. \\
&\quad \left. + \overline{(u_i')_A(u_j')_B(u_i')_B}\right] + \frac{\partial}{\partial \xi_j}\left[\overline{(u_i')_A(u_j')_B(u_i')_B}\right. \\
&\quad \left. - \overline{(u_i')_A(u_j')_A(u_i')_B}\right] = \\
&\quad = \frac{1}{2\rho_o}\,\frac{\partial}{\partial y_i}\left[\overline{p_A'(u_i')_B} + \overline{p_B'(u_i')_A}\right] - \frac{1}{\rho_o}\,\frac{\partial}{\partial \xi_i}\left[\overline{p_B'(u_i')_A}\right. \\
&\quad \left. - \overline{p_B'(u_i')_B}\right] + \frac{\nu_o}{2}\,\frac{\partial^2}{\partial y_j \partial y_j}\overline{(u_i')_A(u_i')_B} \\
&\quad + 2\nu_o\,\frac{\partial^2}{\partial \xi_j \partial \xi_j}\overline{(u_i')_A(u_i')_B} + \frac{g_i}{\bar{T}_o}\left[\overline{T_A'(u_i')_B} + \overline{T_B'(u_i')_A}\right]
\end{aligned} \tag{6.6}$$

This equation may now be integrated with respect to ξ_k from 0 to $+\infty$. The process is discussed in Ref. 31 and the reader is referred to this paper for more detail. The resulting equation is very complex and it is not necessary to reproduce it here, since it is clear from the structure of (6.6) that the simplest model equation for Λ_1, for the case of a simple parallel shear flow, will be of the form

$$\frac{Dq^2\Lambda_1}{Dt} = - C_1\overline{u'w'}\Lambda_1 \frac{\partial \bar{u}}{\partial z} + C_2 \frac{\partial}{\partial z}\left(q\Lambda_2 \frac{\partial}{\partial z} q^2\Lambda_1\right)$$

$$+ \frac{\nu}{2}\frac{\partial^2}{\partial z^2}(q^2\Lambda_1) - C_3 2\nu \frac{q^2\Lambda_1}{\lambda^2} + C_4 \frac{g}{T_o}\overline{w'T'}\Lambda_1 \qquad (6.7)$$

Here the C's are constants that remain to be determined by matching computed solutions with experimental data.

This equation is almost identical to that used by Rodi and Spalding [Ref. 15] in their calculation of turbulence in free jets. There is, of course, an additional term, namely,

$$C_4 \frac{g}{T_o}\overline{w'T'}\Lambda_1$$

which represents the tendency of atmospheric stability to increase or decrease the scale of atmospheric turbulence depending on whether the atmosphere is unstable, with $\overline{w'T'} > 0$, or stable, with $\overline{w'T'} < 0$.

It is clear that one might derive equations for a whole host of scales. For example, equations might be derived for the integral scale of the temperature fluctuations by writing the equation for $\overline{T'_A T'_B}$ and proceeding as above, or the integral scale of the concentration fluctuation by use of the equation for $\overline{(C'_\alpha)_A (C'_\alpha)_B}$.

How might these equations be used? Since, as we have seen, we always need to have available in our calculations a length Λ_1 (or several Λ_1's, if a more complicated model of turbulence

is desired), we could, rather than relate these Λ_1's directly to some locally defined mean scale of the motion, carry along equations, such as (6.7) for the required Λ_1's and add these equations to the group of equations that are to be solved simultaneously.

Although such a procedure should be the ultimate aim of any second-order closure scheme, we will not try, in this report, to couple an equation for the scale Λ_1 to the equations for the second-order correlations. We have chosen to proceed in this way, as mentioned previously, because it permits one to observe the sensitivity of the modeled equations to various choices of Λ_1. An ability to observe this sensitivity has been and continues to be useful in studying the general characteristics of solutions to turbulent shear flows by invariant modeling.

7. RELATION OF SECOND-ORDER MODELS TO K THEORY

Before we begin a discussion of the calculation of atmospheric flows using the invariant second-order modeling scheme that has been described here, it is instructive to relate this model to the classical eddy diffusivity or K models of turbulent transport. To do this, we first write out the model equations [(4.17) through (4.26)] for an essentially parallel shear flow in the atmosphere; that is, we assume $\bar{u} = \bar{u}(z)$, $\bar{v} = \partial/\partial y = 0$, $\bar{w} \ll \bar{u}$, and $\partial/\partial x \ll \partial/\partial z$. The result is

$$\frac{D\bar{u}}{Dt} = \nu_o \frac{\partial^2 \bar{u}}{\partial z^2} - \frac{\partial \overline{u'w'}}{\partial z} \tag{7.1}$$

$$\frac{\partial \bar{p}}{\partial z} = \frac{g\rho_o \bar{T}}{T_o} - \rho_o \frac{\partial \overline{w'w'}}{\partial z} \tag{7.2}$$

$$\frac{D\bar{T}}{Dt} = \nu_o \frac{\partial^2 \bar{T}}{\partial z^2} - \frac{\partial \overline{w'T'}}{\partial z} \tag{7.3}$$

$$\frac{D\bar{C}_\alpha}{Dt} = \nu_o \frac{\partial^2 \bar{C}_\alpha}{\partial z^2} - \frac{\partial \overline{w'C'_\alpha}}{\partial z} \tag{7.4}$$

$$\frac{\partial \bar{u}}{\partial x} = \frac{\partial \bar{w}}{\partial z} = 0 \tag{7.5}$$

$$\begin{aligned}\frac{D\overline{u'u'}}{Dt} = &- 2\overline{u'w'}\frac{\partial \bar{u}}{\partial z} + \frac{\partial}{\partial z}\left(\Lambda_2 q \frac{\partial \overline{u'u'}}{\partial z}\right) \\ &- \frac{q}{\Lambda_1}\left(\overline{u'u'} - \frac{q^2}{3}\right) \\ &+ \nu_o \frac{\partial^2 \overline{u'u'}}{\partial z^2} - 2\nu_o \frac{\overline{u'u'}}{\lambda^2}\end{aligned} \tag{7.6}$$

$$\begin{aligned}\frac{D\overline{v'v'}}{Dt} = &\frac{\partial}{\partial z}\left(\Lambda_2 q \frac{\partial \overline{v'v'}}{\partial z}\right) \\ &- \frac{q}{\Lambda_1}\left(\overline{v'v'} - \frac{q^2}{3}\right) \\ &+ \nu_o \frac{\partial^2 \overline{v'v'}}{\partial z^2} - 2\nu_o \frac{\overline{v'v'}}{\lambda^2}\end{aligned} \tag{7.7}$$

$$\frac{D\overline{w'w'}}{Dt} = \frac{2g}{T_o}\,\overline{w'T'} + 3\,\frac{\partial}{\partial z}\left(\Lambda_2 q\,\frac{\partial\overline{w'w'}}{\partial z}\right) + 2\,\frac{\partial}{\partial z}\left(\Lambda_3 q\,\frac{\partial\overline{w'w'}}{\partial z}\right)$$

$$- \frac{q}{\Lambda_1}\left(\overline{w'w'} - \frac{q^2}{3}\right)$$

$$+ \nu_o\,\frac{\partial^2\overline{w'w'}}{\partial z^2} - 2\nu_o\,\frac{\overline{w'w'}}{\lambda^2} \qquad (7.8)$$

$$\frac{D\overline{u'w'}}{Dt} = -\,\overline{w'w'}\,\frac{\partial\bar{u}}{\partial z} + \frac{g}{T_o}\,\overline{u'T'} + 2\,\frac{\partial}{\partial z}\left(\Lambda_2 q\,\frac{\partial\overline{u'w'}}{\partial z}\right)$$

$$+ \frac{1}{\rho_o}\,\frac{\partial}{\partial z}\left(\rho_o\Lambda_3 q\,\frac{\partial\overline{u'w'}}{\partial z}\right)$$

$$- \frac{q}{\Lambda_1}\,\overline{u'w'}$$

$$+ \nu_o\,\frac{\partial^2\overline{u'w'}}{\partial z^2} - 2\nu_o\,\frac{\overline{u'w'}}{\lambda^2} \qquad (7.9)$$

$$\frac{D\overline{u'T'}}{Dt} = -\,\overline{u'w'}\,\frac{\partial\bar{T}}{\partial z} - \overline{w'T'}\,\frac{\partial\bar{u}}{\partial z} + \frac{\partial}{\partial z}\left(\Lambda_2 q\,\frac{\partial\overline{u'T'}}{\partial z}\right)$$

$$- \frac{q}{\Lambda_1}\,\overline{u'T'}$$

$$+ \nu_o\,\frac{\partial^2\overline{u'T'}}{\partial z^2} - 2\nu_o\,\frac{\overline{u'T'}}{\lambda^2} \qquad (7.10)$$

$$\frac{D\overline{w'T'}}{Dt} = -\,\overline{w'w'}\,\frac{\partial\bar{T}}{\partial z} + \frac{g}{T_o}\,\overline{T'^2} + 2\,\frac{\partial}{\partial z}\left(\Lambda_2 q\,\frac{\partial\overline{w'T'}}{\partial z}\right)$$

$$+ \frac{1}{\rho_o}\,\frac{\partial}{\partial z}\left(\rho_o\Lambda_3 q\,\frac{\partial\overline{w'T'}}{\partial z}\right)$$

$$- \frac{q}{\Lambda_1}\,\overline{w'T'}$$

$$+ \nu_o\,\frac{\partial^2\overline{w'T'}}{\partial z^2} - 2\nu_o\,\frac{\overline{w'T'}}{\lambda^2} \qquad (7.11)$$

$$\frac{D\overline{T'^2}}{Dt} = -2\overline{w'T'}\frac{\partial\bar{T}}{\partial z} + \frac{\partial}{\partial z}\left(\Lambda_2 q \frac{\partial\overline{T'^2}}{\partial z}\right) + \nu_o \frac{\partial^2\overline{T'^2}}{\partial z^2} - 2\nu_o \frac{\overline{T'^2}}{\lambda^2} \tag{7.12}$$

$$\frac{D\overline{u'C'_\alpha}}{Dt} = -\overline{u'w'}\frac{\partial\bar{C}_\alpha}{\partial z} - \overline{w'C'_\alpha}\frac{\partial\bar{u}}{\partial z} + \frac{\partial}{\partial z}\left(\Lambda_2 q \frac{\partial\overline{u'C'_\alpha}}{\partial z}\right) - \frac{q}{\Lambda_1}\overline{u'C'_\alpha} + \nu_o \frac{\partial^2\overline{u'C'_\alpha}}{\partial z^2} - 2\nu_o \frac{\overline{u'C'_\alpha}}{\lambda^2} \tag{7.13}$$

$$\frac{D\overline{w'C'_\alpha}}{Dt} = -\overline{w'w'}\frac{\partial\bar{C}_\alpha}{\partial z} + \frac{g}{T_o}\overline{C'_\alpha T'} + 2\frac{\partial}{\partial z}\left(\Lambda_2 q \frac{\partial\overline{w'C'_\alpha}}{\partial z}\right) + \frac{1}{\rho_o}\frac{\partial}{\partial z}\left(\rho_o \Lambda_3 q \frac{\partial\overline{w'C'_\alpha}}{\partial z}\right) - \frac{q}{\Lambda_1}\overline{w'C'_\alpha} + \nu_o \frac{\partial^2\overline{w'C'_\alpha}}{\partial z^2} - 2\nu_o \frac{\overline{w'C'_\alpha}}{\lambda^2} \tag{7.14}$$

$$\frac{D\overline{C'_\alpha T'}}{Dt} = -\overline{w'C'_\alpha}\frac{\partial\bar{T}}{\partial z} - \overline{w'T'}\frac{\partial\bar{C}_\alpha}{\partial z} + \frac{\partial}{\partial z}\left(\Lambda_2 q \frac{\partial\overline{C'_\alpha T'}}{\partial z}\right) + \nu_o \frac{\partial^2\overline{C'_\alpha T'}}{\partial z^2} - 2\nu_o \frac{\overline{C'_\alpha T'}}{\lambda^2} \tag{7.15}$$

$$\frac{D\overline{C'^2_\alpha}}{Dt} = -2\overline{w'C'_\alpha}\frac{\partial\bar{C}_\alpha}{\partial z} + \frac{\partial}{\partial z}\left(\Lambda_2 q \frac{\partial\overline{C'^2_\alpha}}{\partial z}\right) + \nu_o \frac{\partial^2\overline{C'^2_\alpha}}{\partial z^2} - 2\nu_o \frac{\overline{C'^2_\alpha}}{\lambda^2} \tag{7.16}$$

In addition, we have $\overline{u'v'} = \overline{v'w'} = \overline{v'T'} = \overline{v'C'_\alpha} = 0$.

Equations (7.1) through (7.5) define the mean variables $\bar{u}$, $\bar{w}$, $\bar{T}$, $\bar{C}_\alpha$, and $\bar{p}$. In these equations the second-order transport correlations $\overline{u'w'}$, $\overline{w'T'}$, and $\overline{w'C'_\alpha}$ appear. In older methods of turbulent transport calculations, these correlations are related, by analogy to molecular transport, to the gradients of the mean velocity, temperature, and concentration fields. This assumption is equivalent to saying that the second-order transport correlations have no "memory," i.e., do not have dynamic or rate equations which govern their behavior. This assumption also implies that the second-order correlations at a point have no knowledge of what is going on in contiguous elements in the flow. Since we may look at each of (7.6) through (7.16) as a rate equation for the particular species in question (in the sense of chemical kinetic equations), we should be able to recover traditional turbulent transport theory (eddy transport theory or K theory) by a suitable limiting process applied to (7.6) through (7.16).

The suitable limiting process requires the following assumptions:

(1) Since the dynamics of the correlations (species) are not important, we will make the assumption that the correlations (species) are in local equilibrium. That is, we will assume, in a manner precisely analogous to the assumption of local chemical equilibrium in a flowing gas, that

$$\frac{D}{Dt} \equiv 0 \tag{7.17}$$

(2) In view of the fact that in eddy diffusivity theories the turbulent transport at a point has no knowledge of the value of transport at another point, we must neglect all the diffusive terms in the dynamic equations for the correlations.

(3) Since eddy diffusivity or K theory is a large Reynolds number theory, we must assume in arriving at our equations that the Reynolds number is large. We will assume, therefore, that

$$\lambda^2 = \frac{\Lambda_1^2}{a + b\frac{q\Lambda_1}{\nu_o}} \simeq \frac{\nu_o \Lambda_1}{bq} \tag{7.18}$$

Thus, to relate our present model to K theories, we must seek the equilibrium, nondiffusive limit of (7.6) through (7.16). Because of the high Reynolds number, nondiffusive, and equilibrium assumptions, we refer to the resulting equations as the "superequilibrium" equations. This word aptly describes the flow we are studying.

The superequilibrium equations for the correlations are

$$0 = -2\overline{u'w'}\frac{\partial \bar{u}}{\partial z} - \frac{q}{\Lambda_1}(1 + 2b)\overline{u'u'} + \frac{q^3}{3\Lambda_1} \tag{7.19}$$

$$0 = -\frac{q}{\Lambda_1}(1 + 2b)\overline{v'v'} + \frac{q^3}{3\Lambda_1} \tag{7.20}$$

$$0 = \frac{2g}{T_o}\overline{w'T'} - \frac{q}{\Lambda_1}(1 + 2b)\overline{w'w'} + \frac{q^3}{3\Lambda_1} \tag{7.21}$$

$$0 = -\overline{w'w'}\frac{\partial \bar{u}}{\partial z} + \frac{g}{T_o}\overline{u'T'} - \frac{q}{\Lambda_1}(1 + 2b)\overline{u'w'} \tag{7.22}$$

$$0 = -\overline{u'w'}\frac{\partial \bar{T}}{\partial z} - \overline{w'T'}\frac{\partial \bar{u}}{\partial z} - \frac{q}{\Lambda_1}(1 + 2b)\overline{u'T'} \tag{7.23}$$

$$0 = -\overline{w'w'}\frac{\partial \bar{T}}{\partial z} + \frac{g}{T_o}\overline{T'^2} - \frac{q}{\Lambda_1}(1 + 2b)\overline{w'T'} \tag{7.24}$$

$$0 = -2\overline{w'T'}\frac{\partial \bar{T}}{\partial z} - 2b\frac{q}{\Lambda_1}\overline{T'^2} \tag{7.25}$$

$$0 = -\overline{u'w'}\frac{\partial \bar{C}_\alpha}{\partial z} - \overline{w'C'_\alpha}\frac{\partial \bar{u}}{\partial z} - \frac{q}{\Lambda_1}(1 + 2b)\overline{C'_\alpha u'} \tag{7.26}$$

$$0 = -\overline{w'w'}\frac{\partial \bar{C}_\alpha}{\partial z} + \frac{g}{T_o}\overline{C'_\alpha T'} - \frac{q}{\Lambda_1}(1 + 2b)\overline{w'C'_\alpha} \tag{7.27}$$

$$0 = - \overline{w'C'_\alpha} \frac{\partial \bar{T}}{\partial z} - \overline{w'T'} \frac{\partial \bar{C}_\alpha}{\partial z} - 2b \frac{q}{\Lambda_1} \overline{C'_\alpha T'} \tag{7.28}$$

$$0 = - 2\overline{w'C'_\alpha} \frac{\partial \bar{C}_\alpha}{\partial z} - 2b \frac{q}{\Lambda_1} \overline{C'^2_\alpha} \tag{7.29}$$

(7.19) through (7.29) are algebraic equations for all of the correlations. It is easily seen that (7.19) through (7.25) are a coupled set of equations for the local state of turbulence and turbulence transport in the absence of pollutants. This occurs because we have assumed, in the derivation of the basic equations from which the present set was obtained, that the pollutants are passive. Knowing the state of turbulence from a solution of (7.19) through (7.25), we can obtain the vertical contaminant transport correlation $\overline{C'_\alpha w'}$ from a simultaneous solution of (7.27) and (7.28). The correlation $\overline{u'C'_\alpha}$ is obtained directly from (7.26) once $\overline{w'C'_\alpha}$ is known and, finally, the variance of the contaminant fluctuation is found directly from (7.29).

The solution of (7.19) through (7.29) can be obtained in a particularly elegant fashion if the following definitions are introduced into the equations. Let (for the case when $\partial\bar{u}/\partial z > 0$)

$$\begin{aligned}
\overline{u'u'} &= UU\Lambda_1^2 \left(\frac{\partial \bar{u}}{\partial z}\right)^2 & \overline{u'T'} &= UT\Lambda_1^2 \frac{\partial \bar{u}}{\partial z} \frac{\partial \bar{T}}{\partial z} \\
\overline{v'v'} &= VV\Lambda_1^2 \left(\frac{\partial \bar{u}}{\partial z}\right)^2 & \overline{w'T'} &= WT\Lambda_1^2 \frac{\partial \bar{u}}{\partial z} \frac{\partial \bar{T}}{\partial z} \\
\overline{w'w'} &= WW\Lambda_1^2 \left(\frac{\partial \bar{u}}{\partial z}\right)^2 & \overline{T'^2} &= TT\Lambda_1^2 \left(\frac{\partial \bar{T}}{\partial z}\right)^2 \\
\overline{u'w'} &= UW\Lambda_1^2 \left(\frac{\partial \bar{u}}{\partial z}\right)^2 & q^2 &= QQ\Lambda_1^2 \left(\frac{\partial \bar{u}}{\partial z}\right)^2
\end{aligned} \tag{7.30}$$

and likewise for the concentration correlations

$$\overline{u'C'_\alpha} = UC\Lambda_1^2 \frac{\partial \bar{u}}{\partial z} \frac{\partial \bar{C}_\alpha}{\partial z} \qquad \overline{C'_\alpha T'} = CT\Lambda_1^2 \frac{\partial \bar{T}}{\partial z} \frac{\partial \bar{C}_\alpha}{\partial z} \tag{7.31}$$

$$\overline{w'C'_\alpha} = WC\Lambda_1^2 \frac{\partial \bar{u}}{\partial z} \frac{\partial \bar{C}_\alpha}{\partial z} \qquad \overline{C'^2_\alpha} = CC\Lambda_1^2 \left(\frac{\partial \bar{C}_\alpha}{\partial z} \right)^2$$

Note that

$$QQ = Q^2 = UU + VV + WW \tag{7.32}$$

Substitution of the definitions given in (7.30) and (7.31) into (7.19) through (7.29) results in

$$Q(1 + 2b)UU = \frac{Q^3}{3} - 2UW \tag{7.33}$$

$$Q(1 + 2b)VV = \frac{Q^3}{3} \tag{7.34}$$

$$Q(1 + 2b)WW = \frac{Q^3}{3} + 2RiWT \tag{7.35}$$

$$Q(1 + 2b)UW = - WW + RiUT \tag{7.36}$$

$$Q(1 + 2b)UT = - UW - WT \tag{7.37}$$

$$Q(1 + 2b)WT = - WW + RiTT \tag{7.38}$$

$$Q(2b)TT = - 2WT \tag{7.39}$$

for the atmospheric equations while for the contaminant equations, we have

$$Q(1 + 2b)UC = - UW - WC \tag{7.40}$$

$$Q(1 + 2b)WC = - WW + RiCT \tag{7.41}$$

$$Q(2b)CT = - WT - WC \tag{7.42}$$

$$Q(2b)CC = - 2WC$$

In these equations, Ri is the Richardson number

$$Ri = \frac{g}{T_o} \frac{\partial \bar{T}}{\partial z} \Big/ \left(\frac{\partial \bar{u}}{\partial z} \right)^2 \tag{7.44}$$

It is immediately obvious from (7.33) through (7.43) that all the nondimensional second-order correlations are a function only of the Richardson number and the parameter b from the second-order closure model. It will be remembered that the value of b determined in the parameter search reported previously is 0.125.

It is convenient to express the solution of (7.33) through (7.43) in terms of the parameter

$$P = \frac{1 - (4 + 15b)Ri + [1 + 2(2 - 9b)Ri + (4 + 9b)^2 Ri^2]^{1/2}}{6} \tag{7.45}$$

In terms of this parameter, the various correlations may be written

$$Q^2 = \frac{1}{b(1 + 2b)^2} P \tag{7.46}$$

$$UU = \frac{(P + bRi)[P + (1 + 4b)Ri] + 2b[P + (1 + b)Ri]}{3(1 + 2b)(P + bRi)[P + (1 + 4b)Ri]} Q^2 \tag{7.47}$$

$$VV = \frac{1}{3(1 + 2b)} Q^2 \tag{7.48}$$

$$WW = \frac{P + (1 + 2b)Ri}{3(1 + 2b)[P + (1 + 4b)Ri]} Q^2 \tag{7.49}$$

$$UW = -\frac{b}{3} \frac{P + (1 + b)Ri}{(P + bRi)[P + (1 + 4b)Ri]} Q^3 \tag{7.50}$$

$$UT = \frac{b}{3(1 + 2b)} \frac{2P + (1 + 2b)Ri}{(P + bRi)[P + (1 + 4b)Ri]} Q^2 \tag{7.51}$$

$$WT = -\frac{b}{3[P + (1 + 4b)Ri]} Q^3 \tag{7.52}$$

$$TT = \frac{1}{3[P + (1 + 4b)Ri]} Q^2 \tag{7.53}$$

$$UC = \frac{b}{3(1 + 2b)} \frac{2P + (1 + 2b)Ri}{(P + bRi)[P + (1 + 4b)Ri]} Q^2 \tag{7.54}$$

$$WC = -\frac{b}{3[P + (1 + 4b)Ri]} Q^3 \tag{7.55}$$

$$CT = \frac{1}{3[P + (1 + 4b)Ri]} Q^2 \tag{7.56}$$

$$CC = \frac{1}{3[P + (1 + 4b)Ri]} Q^2 \tag{7.57}$$

It is clear from these equations that when the parameter $P = 0$, there is no turbulence ($Q^2 = 0$) and all the second-order correlations vanish. The critical value of the Richardson number for which this occurs is a function of b and is given by

$$Ri_{crit} = \frac{1 + b}{4b(1 + 3b)} \tag{7.58}$$

For $b = 0.125$, we find that the critical Richardson number is

$$Ri_{crit} = 1.636 \tag{7.59}$$

The behavior of all the nondimensional second-order correlations as functions of the Richardson number are plotted in Figures 7.1 through 7.5. From these figures the profound difference between turbulence and turbulent transport in stable and unstable atmospheres is obvious. Note particularly that the nondimensional vertical transport of matter and heat fall off far more rapidly than do the nondimensional turbulent energy components when a stable atmospheric situation is approached. In fact,

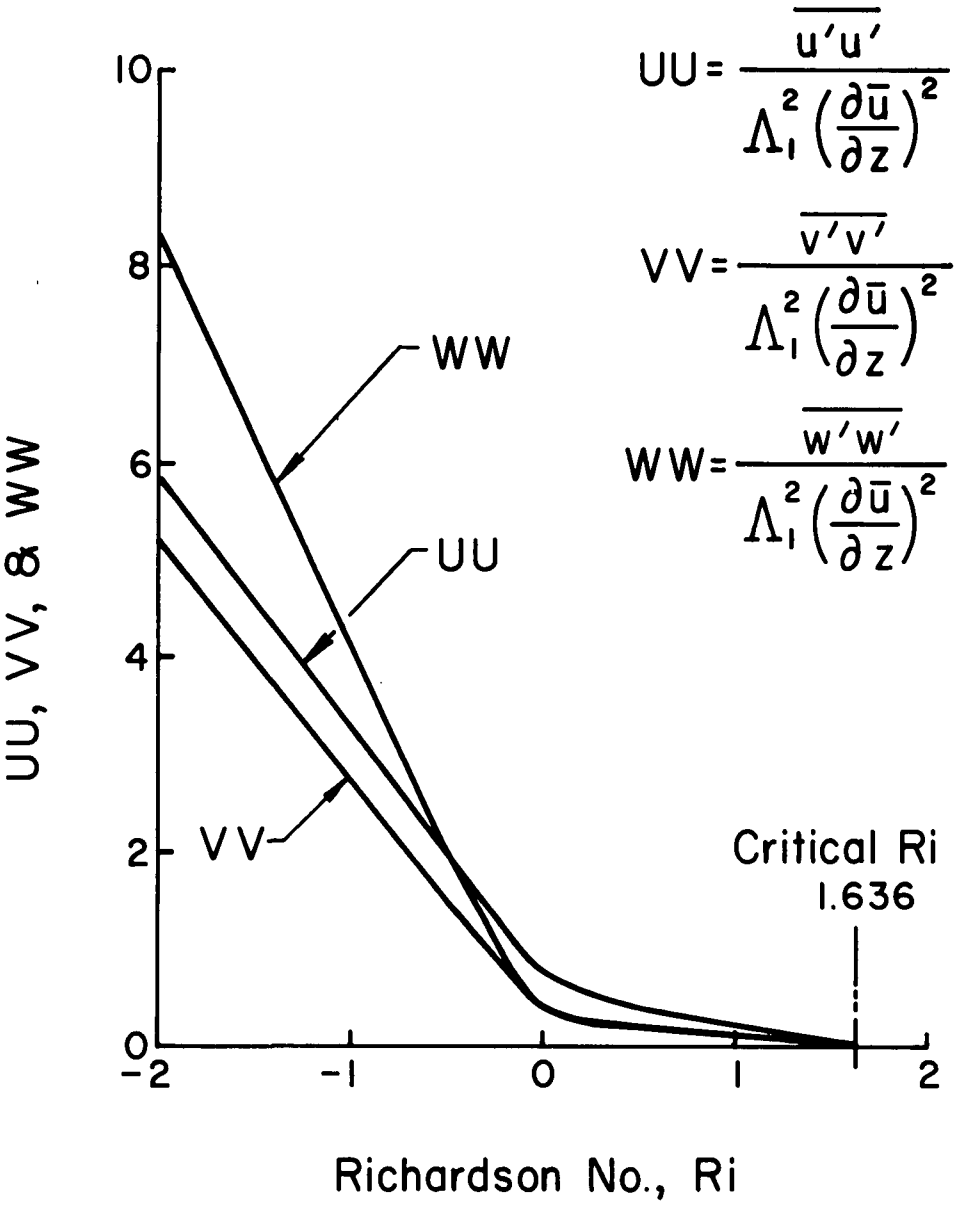

Figure 7.1. Superequilibrium values of the turbulence components as a function of the Richardson number for b = 0.125

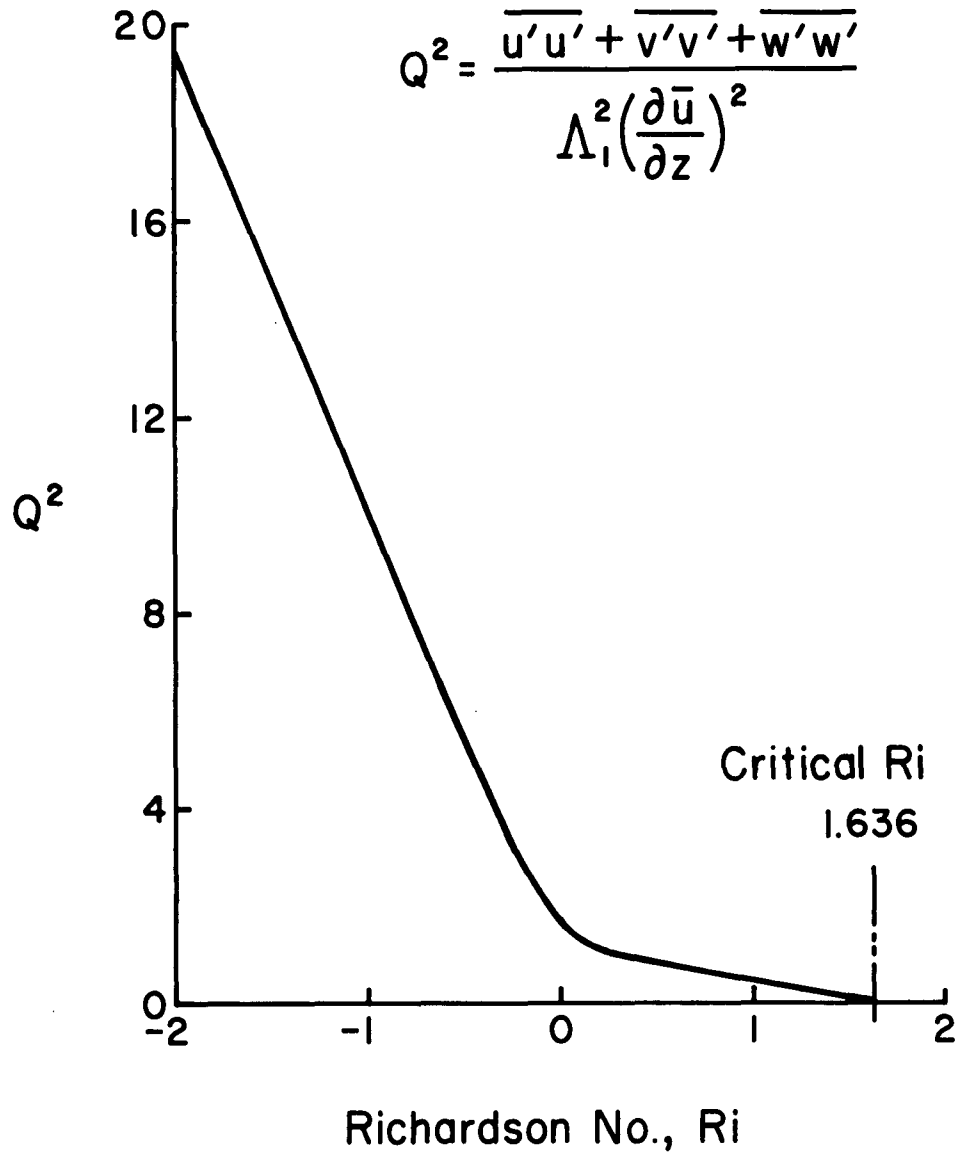

Figure 7.2. Superequilibrium value of the sum of the squares of the turbulent velocity fluctuations as a function of the Richardson number for b = 0.125

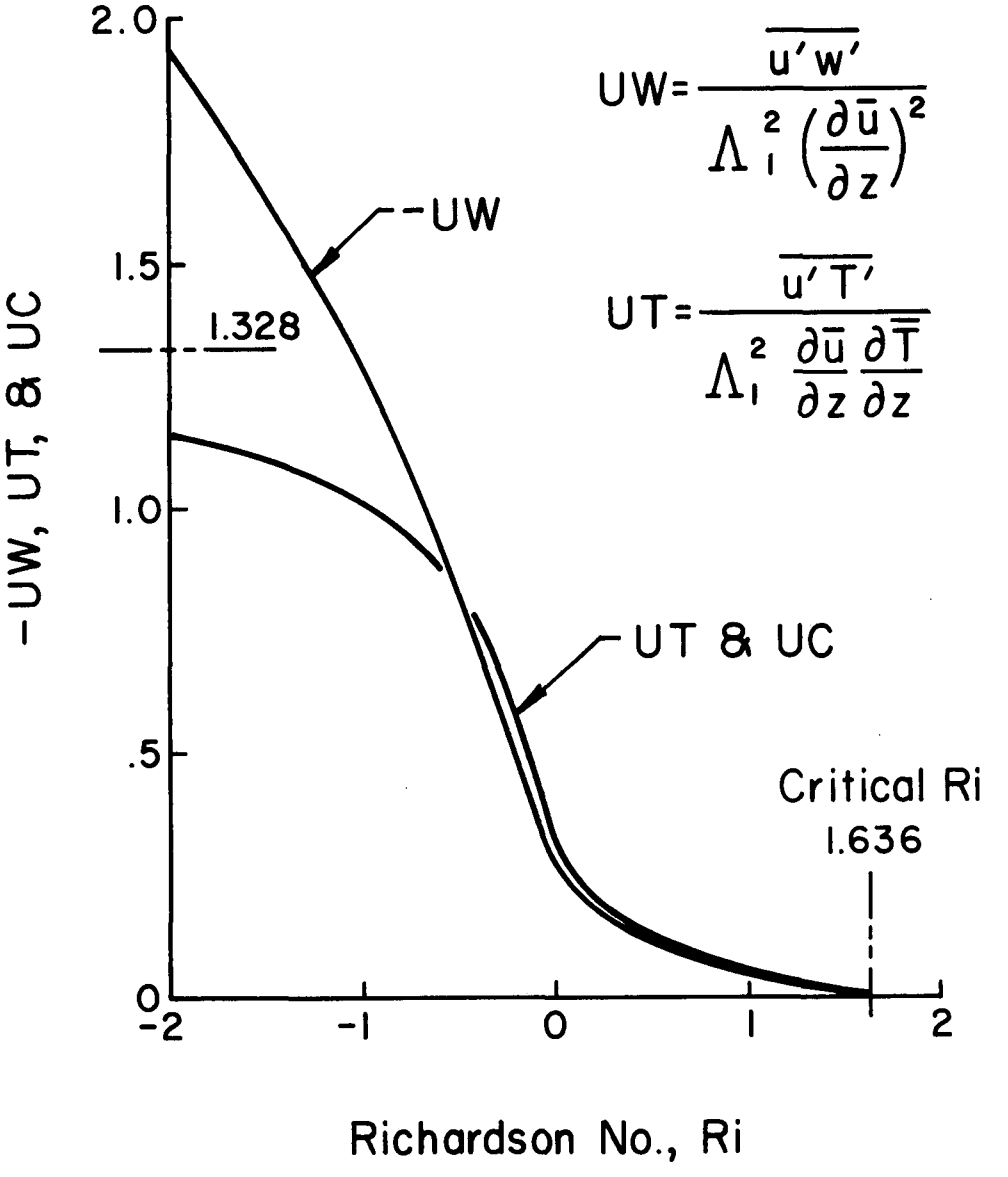

Figure 7.3. Superequilibrium values for shear and longitudinal heat and mass transfer correlations as functions of the Richardson number for $b = 0.125$. Note UT and UC approach the value 1.328 for $Ri = -\infty$.

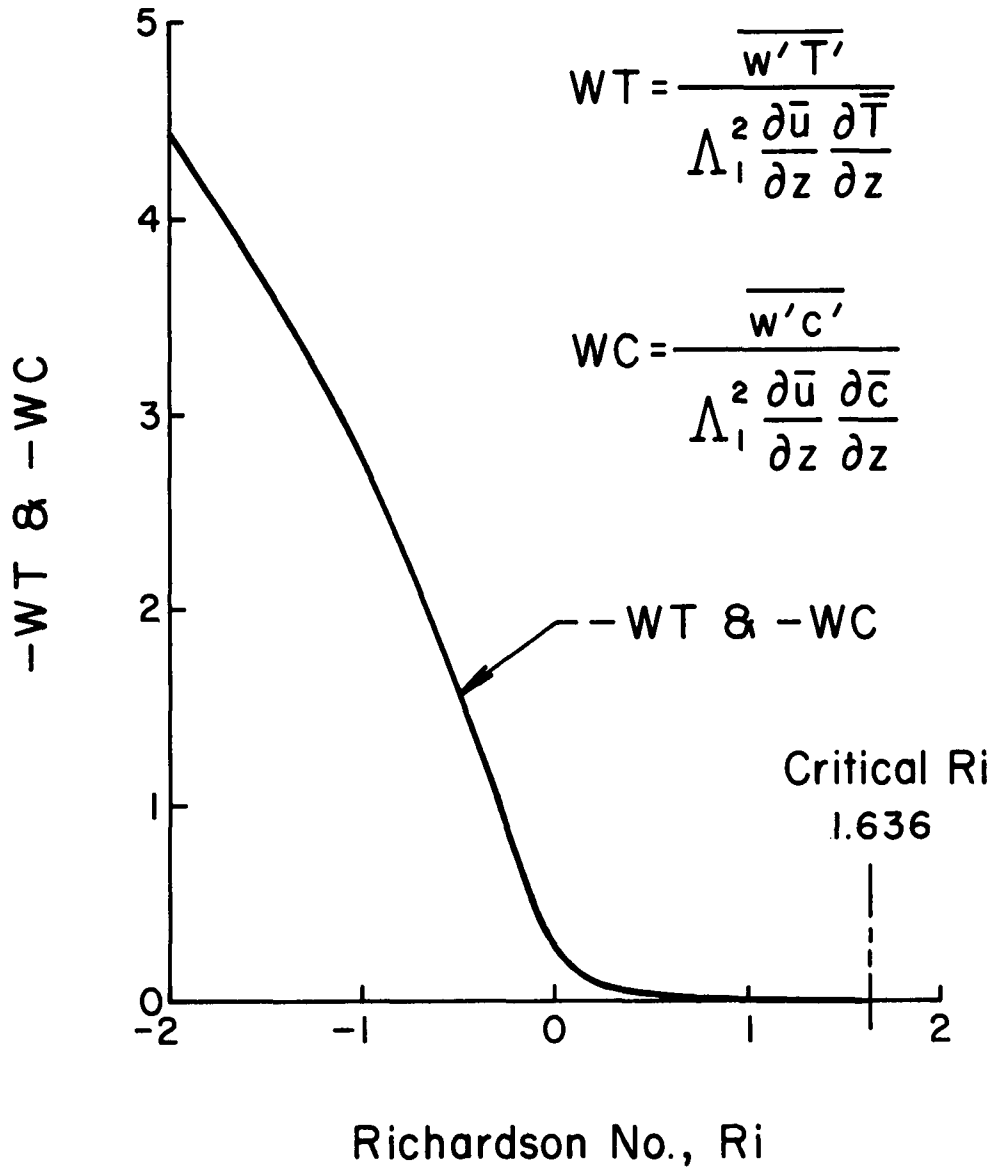

Figure 7.4. Superequilibrium values for vertical heat transfer and vertical mass transfer correlations as a function of the Richardson number for b = 0.125

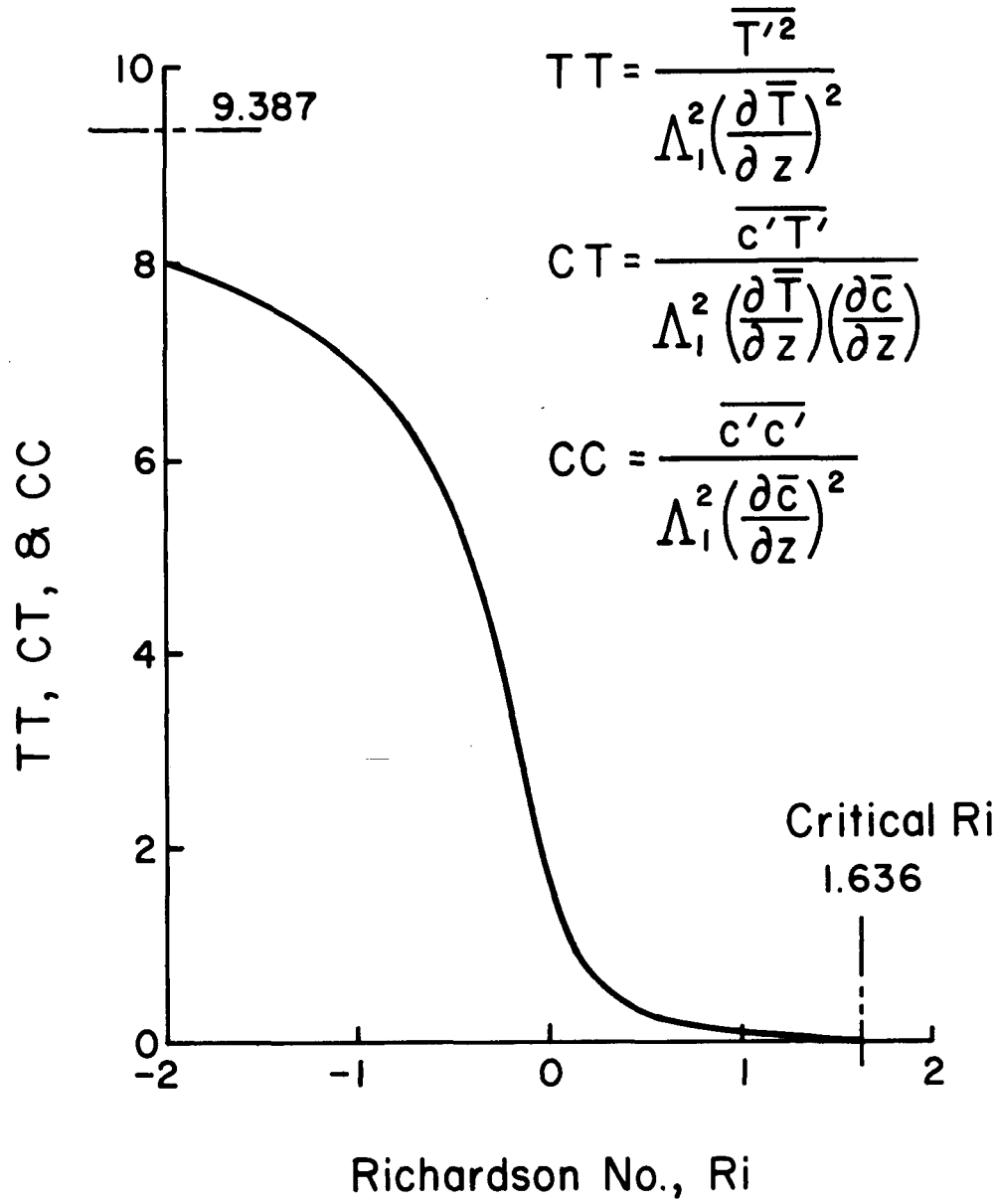

Figure 7.5. Superequilibrium values for TT, CT, and CC as functions of the Richardson number for b = 0.125. Note that these functions approach the limit 9.387 for Ri = $-\infty$.

above a Richardson number of one, vertical turbulent transport has almost ceased to exist although there is still some atmospheric turbulence.

It should be noted that the superequilibrium results just obtained specify the nondimensional values of second-order correlations. For example, assuming the value of $b = 0.125$ to be correct, a Richardson number of 0.10 would give

$$UW = - 0.2712 \tag{7.60}$$

$$WT = WC = - 0.2631 \tag{7.61}$$

The transports of momentum, heat, and matter would then be given by (for $\partial\bar{u}/\partial z > 0$)

$$- \rho_o \overline{u'w'} = 0.2712\rho_o \Lambda_1^2 \left(\frac{\partial \bar{u}}{\partial z}\right)^2 \tag{7.62}$$

$$- \rho_o C_{p_o} \overline{w'T'} = 0.2631\rho_o \Lambda_1^2 \frac{\partial \bar{u}}{\partial z} \frac{\partial \bar{T}}{\partial z} \tag{7.63}$$

$$- \rho_o \overline{w'C'} = 0.2631\rho_o \Lambda_1^2 \frac{\partial \bar{u}}{\partial z} \frac{\partial \bar{C}_\alpha}{\partial z} \tag{7.64}$$

It is clear from these expressions that the actual transport is not defined until the length scale Λ_1 is known. This is a difficulty with atmospheric flows, for unless Λ_1 is determined at a given altitude and the local Richardson number specified there, the transports are not known. In general, Λ_1 will depend at a given altitude on the Richardson number but can assume a range of values depending on the past history of the motion. While this range of values is limited so that the order of magnitude of the transport might be determined, there will always be a variation in transport proportional to the square of the variation in Λ_1 at any fixed Richardson number.

For classical laboratory flows, this problem does not exist. In this case, it is generally found that Λ_1 is proportional to the characteristic breadth of the layer under consideration while the gradients are proportional to a characteristic

velocity, temperature, or concentration difference divided by this characteristic breadth. Thus, for the classical shear flows

$$\Lambda_1^2 \left(\frac{\partial \bar{u}}{\partial z}\right)^2 = \delta_{char}^2 \left(\frac{\Delta \bar{u}_{char}}{\delta_{char}}\right)^2 = \text{const}\left(\Delta \bar{u}_{char}\right)^2 \tag{7.65}$$

and likewise

$$\Lambda_1^2 \frac{\partial \bar{u}}{\partial z} \frac{\partial \overline{T}}{\partial z} = \text{const}\ \Delta \bar{u}_{char}\ \Delta \overline{T}_{char} \tag{7.66}$$

and

$$\Lambda_1^2 \frac{\partial \bar{u}}{\partial z} \frac{\partial \overline{C}_\alpha}{\partial z} = \text{const}\ \Delta \bar{u}_{char}\ \Delta \overline{C}_{char} \tag{7.67}$$

For each type of flow, these constants are well defined. This type of simplicity is, alas, not true of the atmosphere,as we will try to demonstrate presently.

Before considering the problem of the scale Λ_1, it is instructive to compare the results of superequilibrium theory with certain well-known results from classical turbulent transport theory for the case when no gravitational effects are involved. To do this, we place the Richardson number equal to zero in the expressions given in (7.45) through (7.57). We obtain, for $b = 0.125$,

$$P = 0.3333 \tag{7.68}$$

$$Q^2 = \frac{1}{3b(1 + 2b)^2} = 1.7066 \tag{7.69}$$

$$UU = \frac{1 + 6b}{9b(1 + 2b)^3} = 0.7964 \tag{7.70}$$

$$VV = WW = \frac{1}{9b(1 + 2b)^3} = 0.4551 \tag{7.71}$$

$$UW = TW = CW = -\frac{\sqrt{3/b}}{9(1 + 2b)^3} = -0.2786 \tag{7.72}$$

$$UT = UC = \frac{2}{3(1 + 2b)^3} = 0.3413 \tag{7.73}$$

$$TT = CT = CC = \frac{1}{3b(1 + 2b)^2} = 1.7066 \tag{7.74}$$

First we note that superequilibrium theory indicates that $\overline{v'v'} = \overline{w'w'}$ and, further, that

$$\frac{\overline{u'u'}}{\overline{v'v'}} = \frac{\overline{u'u'}}{\overline{w'w'}} = \frac{UU}{VV} = \frac{UU}{WW} = 1 + 6b = 1.75 \tag{7.75}$$

Second, we note that the value of $-\overline{u'w'}/q^2$, which Bradshaw, Ferriss, and Atwell [Ref. 8] assume to be a constant equal to 0.15, is defined by superequilibrium theory to be

$$-\frac{UW}{Q^2} = \frac{1}{1 + 2b}\sqrt{\frac{b}{3}} = 0.163 \tag{7.76}$$

This is a rather surprisingly accurate result in view of the fact that the value of b was determined from very different considerations during the parameter search reported in Section 5.

We may also derive from superequilibrium theory the value of von Kárman's constant κ in his expression for the turbulent shear near a surface, namely,

$$\tau_t = -\rho\overline{u'w'} = \rho\kappa^2 z^2 \left(\frac{\partial \bar{u}}{\partial z}\right)^2 \tag{7.77}$$

From our results

$$\tau_t = -\rho UW\Lambda_1^2 \left(\frac{\partial \bar{u}}{\partial z}\right)^2$$

$$= +\frac{\sqrt{3/b}}{9(1 + 2b)^3}\rho\Lambda_1^2\left(\frac{\partial \bar{u}}{\partial z}\right)^2 \tag{7.78}$$

In Section 5 it was found that near a surface, Λ_1 is of the form $\Lambda_1 = \alpha z$, where the parameter search finds that

$\alpha = 0.7$. Letting

$$\Lambda_1 = 0.7z \tag{7.79}$$

we find that (7.78) gives

$$\tau_t = \frac{0.49\sqrt{3/b}}{9(1 + 2b)^3} \rho z^2 \left(\frac{\partial \bar{u}}{\partial z}\right)^2 \tag{7.80}$$

Comparison of (7.77) and (7.80) reveals that

$$\kappa^2 = \frac{0.49\sqrt{3/b}}{9(1 + 2b)^3} = 0.137 \tag{7.81}$$

or

$$\kappa = 0.37 \tag{7.82}$$

The value of von Kármán's constant is actually 0.4. Again, the agreement between results obtained by taking the equilibrium, nondiffusive limit of our second-order closure model of turbulent shear flow and classical mixing length theory is rather remarkable.

We now return to a discussion of the scale Λ_1. We ask whether superequilibrium theory might give some useful information about this scale. The answer is obtained by considering the equilibrium, high Reynolds number, nondiffusive form of (6.7). The result is

$$0 = - C_1 \overline{u'w'} \Lambda_1 \frac{\partial \bar{u}}{\partial z} - 2bC_3 q^3 \Lambda_1 + C_4 \frac{g}{T_o} \overline{w'T'} \Lambda_1 \tag{7.83}$$

Substitution in (7.83) of the definitions given in (7.30) results in

$$0 = - C_1 UW \Lambda_1^3 - 2bC_3 Q^3 \Lambda_1^3 + C_4 WTRi \Lambda_1^3 \tag{7.84}$$

We note that the scale Λ_1 may be cancelled from this equation. We may imply from this that the scale of turbulence cannot

depend upon purely local conditions but must depend to some extent upon the nearby elements of the flow. In the classical laboratory free shear flows (which are self-similar), the scale at two equivalent points is tied to the scale of the mean motion at these points, because the neighboring regions about these two points are equivalent; thus the effects of past history and diffusion are equivalent. This is not so in the atmosphere and, hence, the scale Λ_1 is not well defined.

In dealing with the atmosphere with classical K theories, we must then not only know the effect of local Richardson number on the nondimensional parameters UW , WT , WC, etc., but must also have some general information about nearby elements of the flow so that a scale can be determined.

The fact that the scale is undetermined under superequilibrium conditions is consistent with the experimental results of Rose [Refs. 33 and 34] who examined the behavior of turbulence introduced into regions of uniform shear. In these experiments it was found that the scale length tended to increase continuously as the observation station was moved downstream [Ref. 33] and that the level of turbulence, when the scale was large enough so that the turbulence was not dissipated, followed the scale of turbulence introduced into the shear layer.

A characteristic length used in similarity theory of atmospheric flows is the Monin-Obukhov length defined [see Ref. 32] as

$$L = - \frac{T_o \left| \overline{u'w'} \right|^{3/2}}{\kappa g \overline{w'T'}} \tag{7.85}$$

Substitutions of the definition given as (7.30) into (7.85) gives

$$L = - \frac{|UW|^{3/2}}{WT} \frac{\Lambda_1}{\kappa Ri} \tag{7.86}$$

If we substitute the expressions for UW and WT from (7.50) and (7.52) into (7.86), we obtain an equation for the ratio of

the Monin-Obukhov length to the scale Λ_1, namely,

$$\frac{L}{\Lambda_1} = \frac{1}{\kappa}\left(\frac{b}{3}\right)^{1/2} \frac{[P + (1 + b)Ri]^{3/2}}{Ri(P + bRi)^{3/2}[P + (1 + 4b)Ri]^{1/2}} \qquad (7.87)$$

This relationship is plotted in Figure 7.6.

The singular character of the relationship between L and Λ_1 at Ri = 0 and the very rapid variation of L/Λ_1 in the range of a Richardson number of general interest is apparent. The results presented are interesting but do not, alas, permit any further insight into that elusive parameter - the Monin-Obkuhov length.

For those familiar with atmospheric turbulence, the critical Richardson number of 1.636 found in this superequilibrium study is obviously too high. We have investigated the cause of this result in considerable detail. It seems clear from the excellent results of superequilibrium theory for neutral flows that this method of looking at the model equations is a powerful one. Indeed, it has been found that it is an excellent basis from which to decide upon the basic modeling that is to be used. We are presently changing our model so that the superequilibrium limit of the modified model will yield critical Richardson numbers more in agreement with experimental observations.

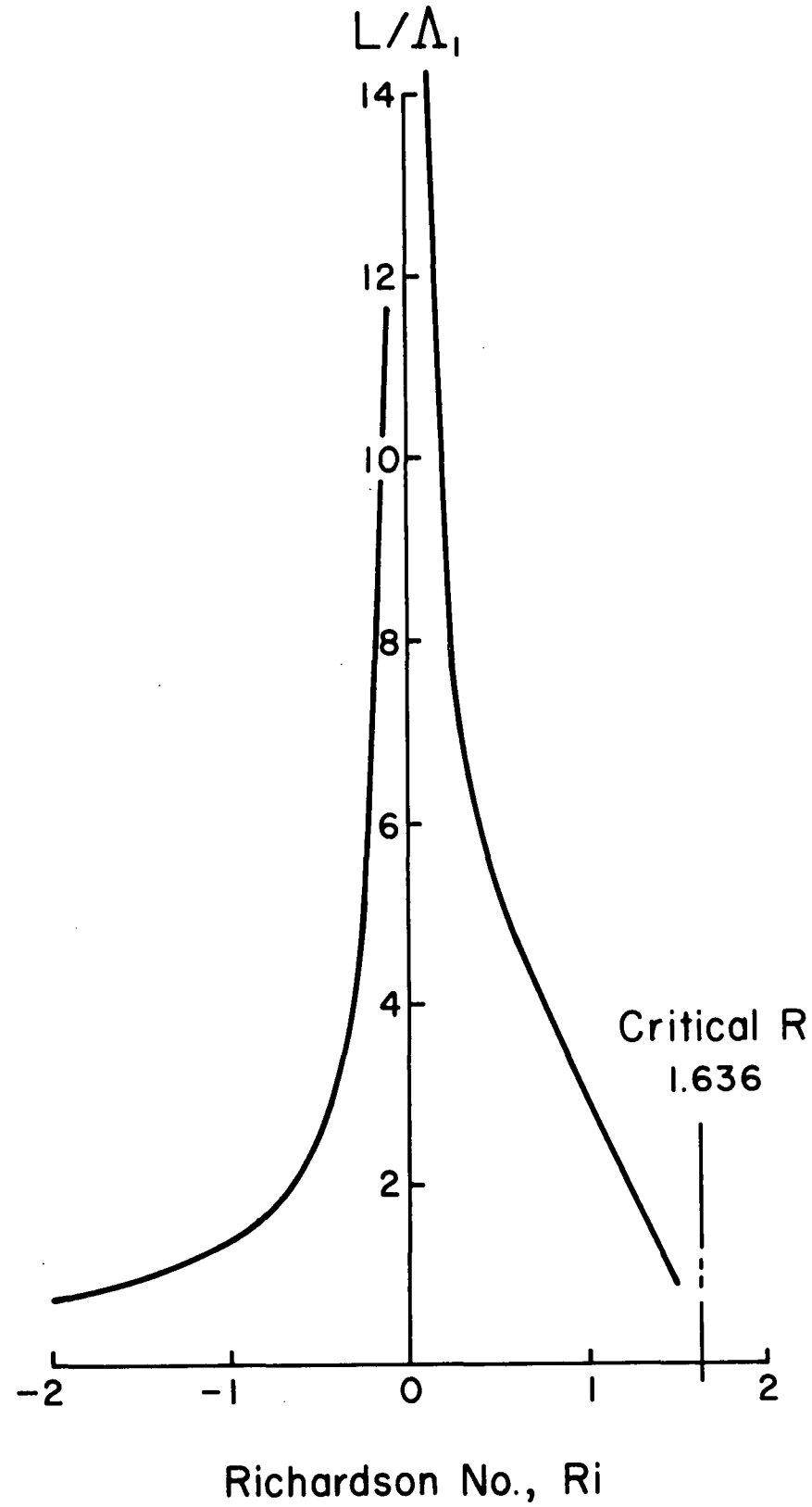

Figure 7.6. Relationship between Monin-Obukhov length L and the isotropy scale Λ_1 as a function of the Richardson number as given by superequilibrium theory for b = 0.125

8. APPLICATION OF SECOND-ORDER MODELING TO THE ATMOSPHERIC BOUNDARY LAYER

We will now take up the application of the second-order closure model of turbulent flow developed in Sections 4 and 5 to the problem of computing the atmospheric boundary layer. Before doing this, however, it is important to point out once again that the model used contains a minimal number of scale lengths. It is felt that the results obtained with this simple model are most instructive. One of the goals of our present studies is to obtain an answer to the question of just how sophisticated in the specification of the scale lengths one must get to obtain reliable predictions of the properties of turbulent flows in which the profiles of the mean velocity, temperature, and concentration are not related in a simple fashion as they are in the classical free turbulent flows.

To demonstrate the method, we will compute the state of atmospheric turbulence for several cases of motion in the atmospheric boundary layer for which measurements have been made of the mean velocity and the mean temperature profiles and of the average values of the second-order correlations $\overline{u'u'}$, $\overline{v'v'}$, $\overline{w'w'}$, $\overline{u'w'}$, $\overline{u'T'}$, $\overline{w'T'}$, and $\overline{T'^2}$. These data obtained for the Air Force Cambridge Research Laboratories were provided by Messrs. Wyngaard and Coté of AFCRL. The profiles of mean velocity and mean temperature for the three cases considered here are shown in Figures 8.1, 8.2, and 8.3.

To calculate by means of our model the turbulent energy and the fluxes of momentum and heat associated with these profiles, we will assume the mean velocity to be parallel to the surface in the xz plane. Thus, $\bar{v} = \bar{w} = 0$. We will also consider the motion to be independent of x and y and hence a function only of z (height) and t (time). Consequently, $\partial/\partial y = \partial/\partial x = 0$, and it is seen that the substantial (total) derivative $D/Dt = \partial/\partial t$. The mean velocity and temperature equations are then analogous to Eqs. (7.1) and (7.2) and are

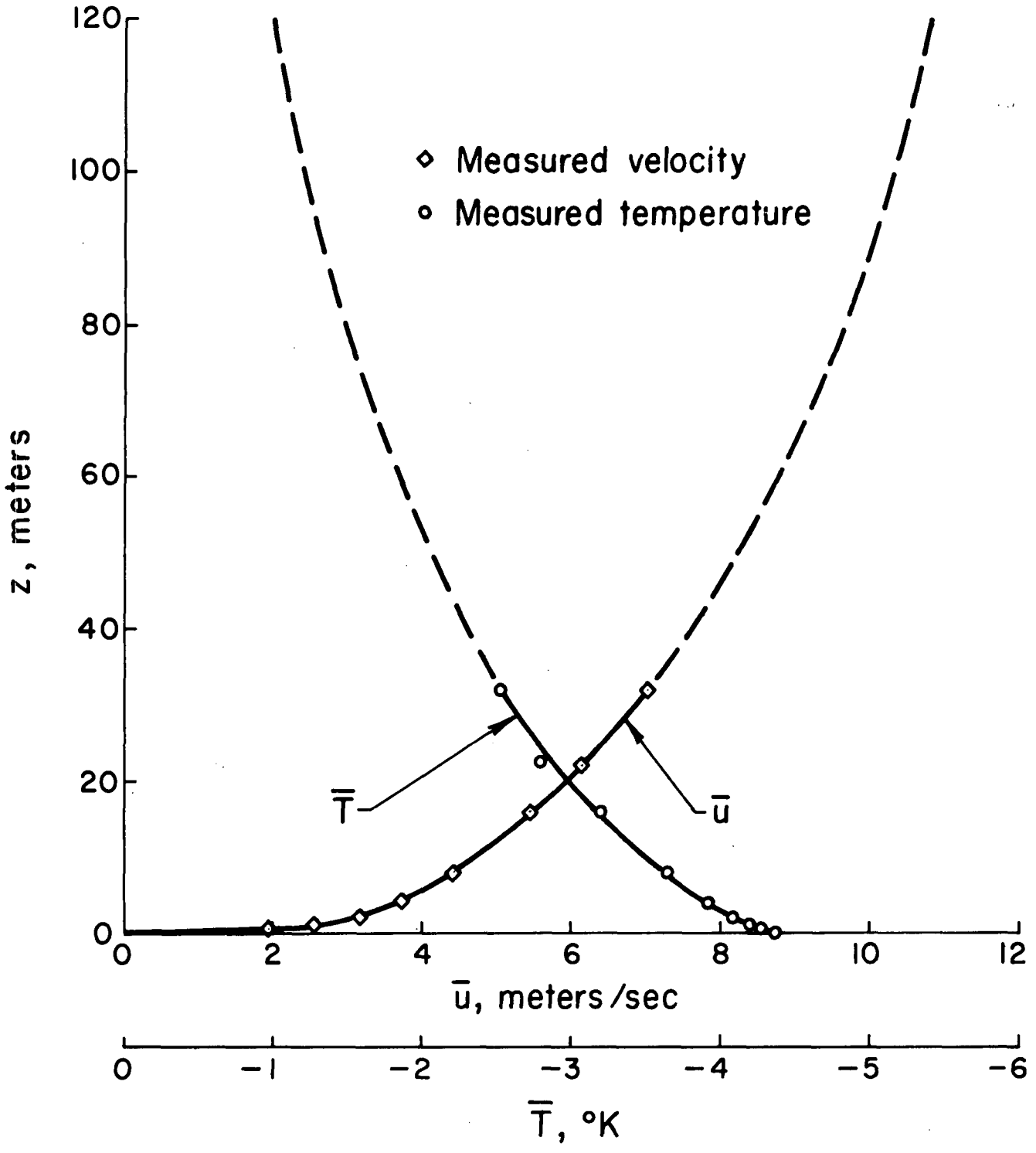

Figure 8.1. Mean velocity and mean temperature profiles for a stable atmospheric boundary layer (Wyngaard & Coté, Run 25). The solid lines are faired through the data points; the dashed curves are assumed continuations of the measured profiles for computational purposes.

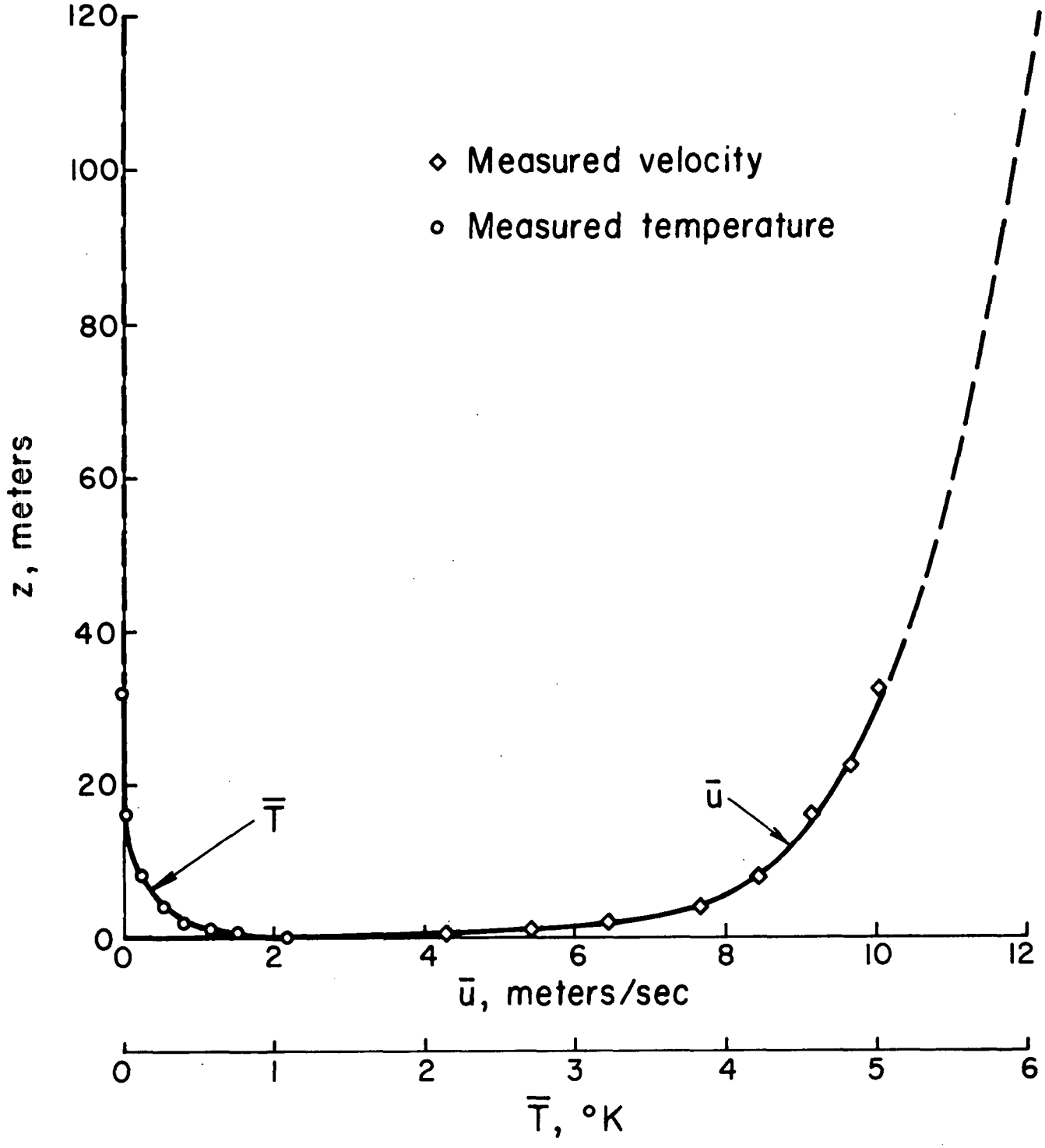

Figure 8.2. Mean velocity and mean temperature profiles for an atmospheric boundary layer that is neutrally stable except for a small unstable region near the surface (Wyngaard & Coté, Run 54). The solid lines are faired through the measured data points; the dashed lines are assumed continuations of the measured data for computational purposes.

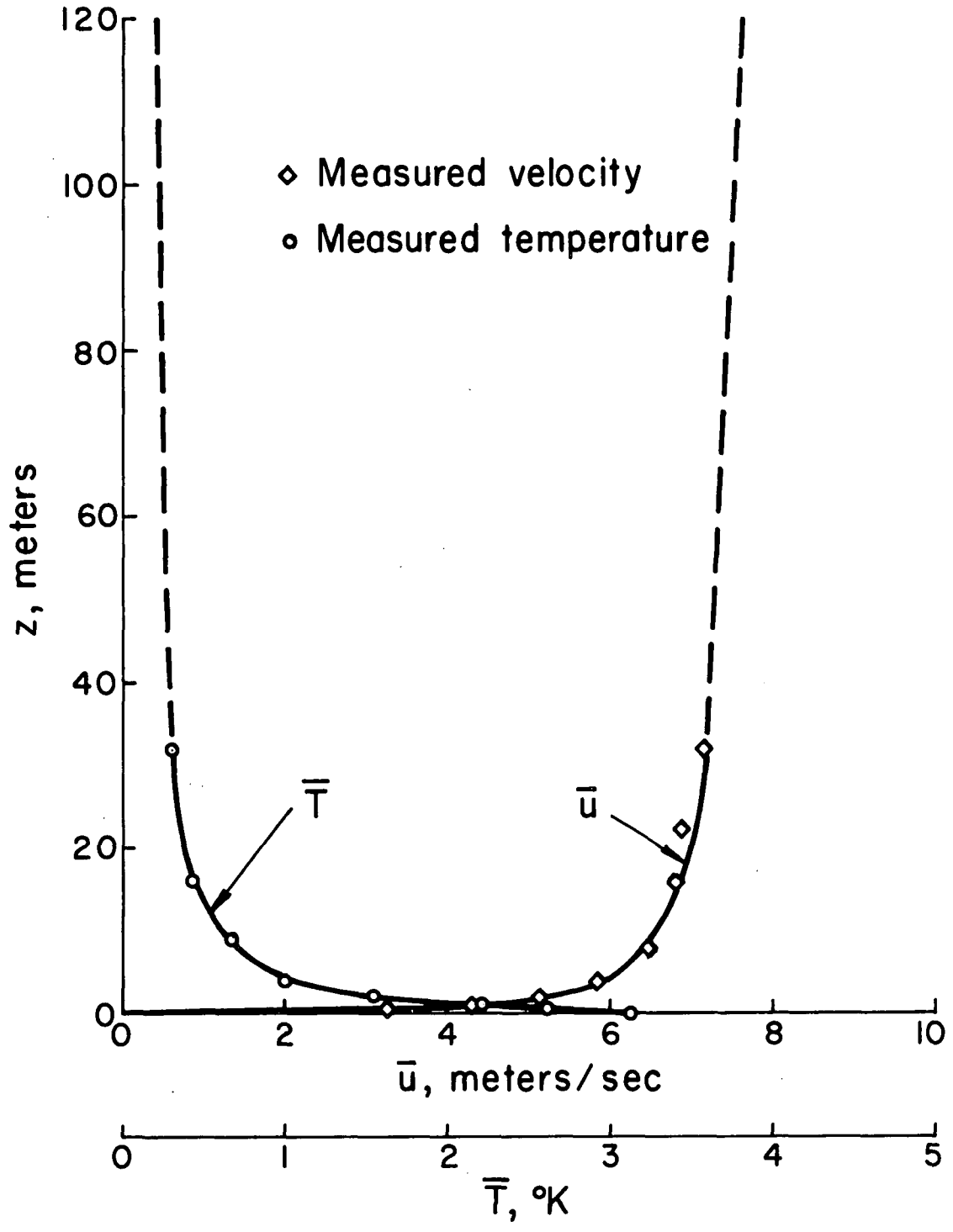

Figure 8.3. Mean velocity and mean temperature profiles for an unstable atmospheric boundary layer (Wyngaard & Coté, Run 40). The solid lines are faired through the measured data points; the dashed lines are assumed continuations of the measured profiles for computational purposes.

$$\frac{\partial \bar{u}}{\partial t} = \nu_o \frac{\partial^2 \bar{u}}{\partial z^2} - \frac{\partial \overline{u'w'}}{\partial z} - \frac{1}{\rho_o} \frac{\partial \bar{p}}{\partial x} \tag{8.1}$$

$$\frac{\partial \bar{T}}{\partial t} = \nu_o \frac{\partial^2 \bar{T}}{\partial z^2} - \frac{\partial \overline{w'T'}}{\partial z} + \dot{Q} \tag{8.2}$$

In (8.1) the pressure gradient $\partial\bar{p}/\partial x$ is included. Additionally, in (8.2) a term $\dot{Q}(z,t)$ has been added which represents any local source of heat that might be present in the atmosphere. The purpose of this term will be explained below.

The equations for the turbulent quantities are identical with (7.6) through (7.12) except of course that $D/Dt = \partial/\partial t$ on the left-hand side of all the equations.

In order to calculate the turbulence produced for the three cases of atmospheric motion given in Figures 8.1, 8.2, and 8.3, we may proceed as follows. First, we note that the profiles given were steady, at least on a time scale large compared to the time required for turbulent adjustment according to our model, as will be demonstrated later. If this is so, we may, in the equations for the double correlations, assume that $\bar{u}(z)$ and $\bar{T}(z)$ are the given profiles. These equations can then be solved for the time variations of these correlations assuming <u>any</u> initial distributions for the turbulent correlations themselves. The solution is continued until the derivatives of the correlations with respect to time approach zero. The resulting distributions of the second-order correlations are then taken to be the appropriate distributions for an atmosphere whose mean profiles of $\bar{u}(z)$ and $\bar{T}(z)$ are those given. Equations (8.1) and (8.2) may then be solved, assuming $\partial\bar{u}/\partial t = 0$ and $\partial\bar{T}/\partial t = 0$ for the distributions in z of the driving force $(1/\rho_o)(\partial p/\partial x)$ and the heat source $\dot{Q}$ necessary to maintain the atmosphere in its assumed state.

It is found that the steady state or equilibrium distributions of the second-order correlations found in this manner are independent of the assumed initial conditions on these variables.

For this reason, computations are generally run with a small level of isotropic turbulence introduced into the system, while the other correlations $\overline{u'w'}$, $\overline{u'T'}$, $\overline{w'T'}$, and $\overline{T'^2}$ are assumed to be zero initially.

These calculations can be illustrated by considering the case of the almost neutrally stable atmosphere shown in Figure 8.2. For this case, we choose the scale length Λ_1 in the following way. Near the surface (the flow is unstable only very near the surface), we choose $\Lambda_1 = 0.7z$ in accordance with the findings of our parameter search for the incompressible boundary layer. Also in accordance with the parameter search for the flat plate boundary layer, we take Λ_1 constant in the outer layers of the atmospheric boundary layer and, as a first guess, equal to 0.15 times a characteristic height of this layer. This is a somewhat difficult and arbitrary dimension to choose since the actual measurements of the mean velocity profile do not permit such a height to be chosen, and one must do the best one can with a continuation of the measured data. For this case it would appear that a characteristic height might be chosen as something like 110 to 120 meters. For this reason, we take, as a first guess at the scale length in the outer region, $\Lambda_1 = 17$ meters. With these assumptions, a computation of the turbulence and transport properties of the atmospheric boundary layer may be made according to the scheme outlined above. The results obtained are shown by the solid lines in Figures 8.4 and 8.5. It is seen that the order of magnitude of all quantities is estimated correctly. The agreement between the calculated and measured values of $\overline{u'w'}$ and $\overline{w'w'}$ is reasonably good. The agreement for $\overline{u'u'}$ and $\overline{v'v'}$ is not so good. It is interesting to note in this regard that the magnitudes of $\overline{u'u'}$ and $\overline{v'v'}$ as measured are alike, with $\overline{v'v'}$ more than twice $\overline{w'w'}$. In view of the structure of the governing equation, this latter experimental result is certainly surprising. The agreement between the measured results and computed values for the temperature correlations $\overline{u'T'}$, $\overline{w'T'}$,

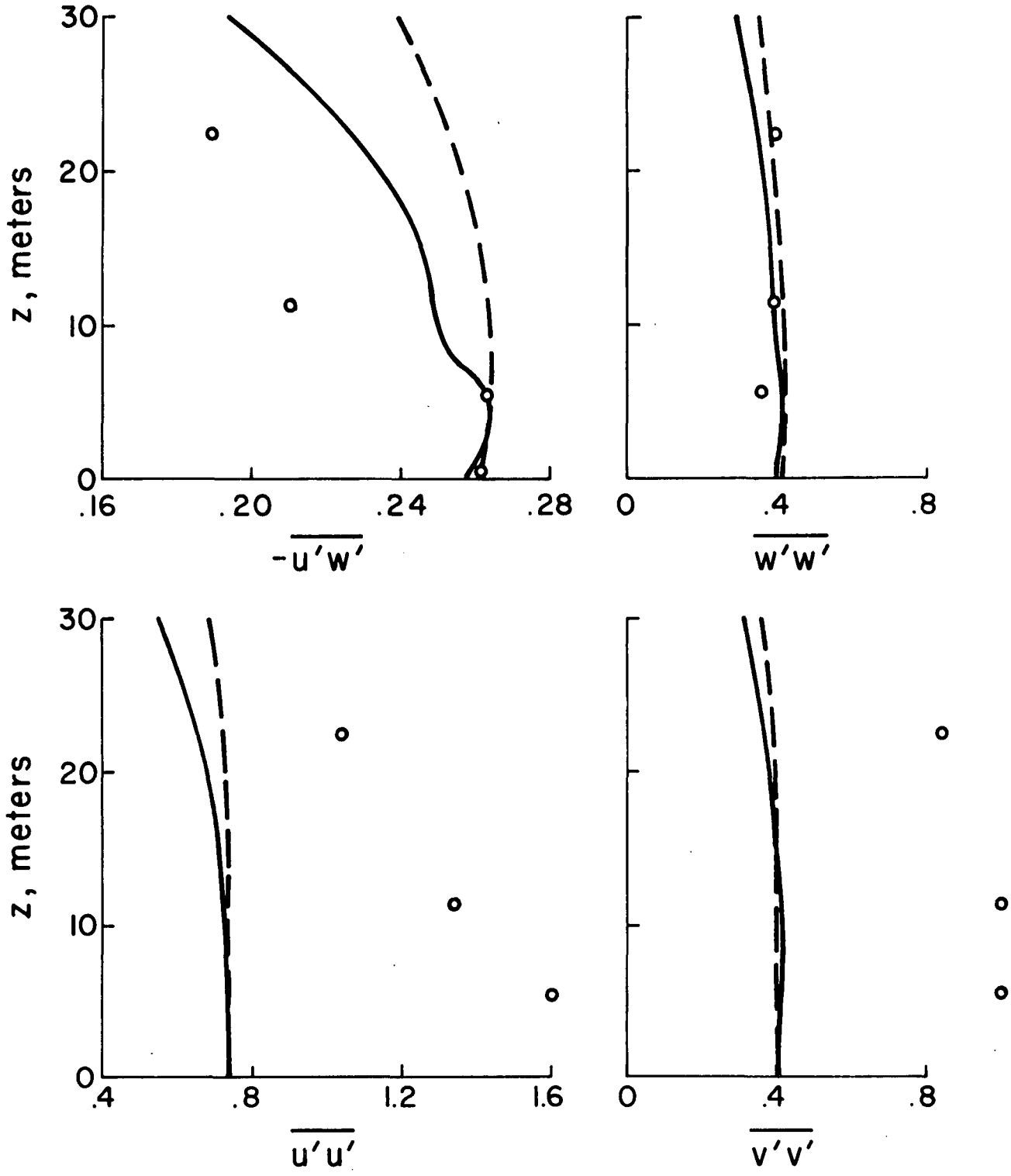

Figure 8.4. Steady state distributions of the velocity correlations for the profiles of mean velocity and temperature given in Figure 8.2. Near the surface, $\Lambda_1/z = \alpha = 0.7$. The solid lines are for $\Lambda_{1\ max}$ = 17 meters. The dashed lines are for $\Lambda_{1\ max}$ = 30 meters.

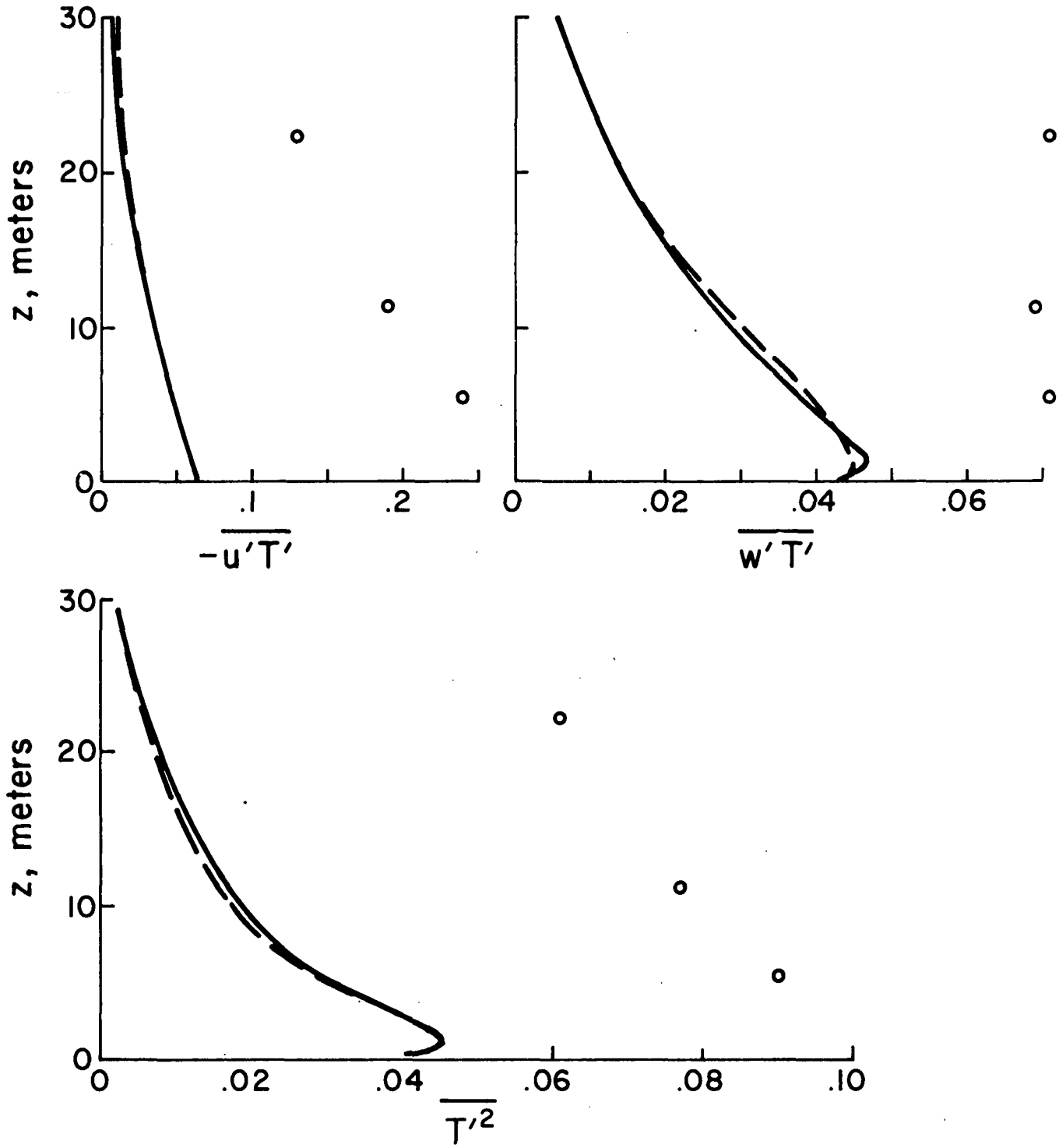

Figure 8.5. Steady state distributions of the temperature correlations for profiles of mean velocity and temperature given in Figure 8.2. Near the surface, $\Lambda_1/z = \alpha = 0.7$. The solid lines are for $\Lambda_{1\ max} = 17$ meters. The dashed lines are for $\Lambda_{1\ max} = 30$ meters.

and $\overline{T'^2}$ is poor. The measured correlations are, however, very small and the accuracy of these results may be somewhat questionable. For example, the measured vertical heat flux correlation is constant with height and extends far past the region where any significant potential temperature gradient exists.

An idea of the sensitivity of the computed results to the choice of the outer or maximum value of Λ_1 can be had by referring to the dashed lines in Figures 8.4 and 8.5. These results were obtained for an outer Λ_1 of 30 meters. The $\alpha = \Lambda_1/z$ near the wall was maintained at 0.7. It is seen that there is not a great change in the computed results below a height of 20 meters, as might be expected, since the Λ_1 's in both cases are equal below 17/0.7 = 24.3 meters. For the temperature correlations, there is essentially no chance since all potential temperature gradients are confined to the region below 24.3 meters.

An idea of the sensitivity of the computed results to the choice of $\alpha = \Lambda_1/z$ near the surface can be had by reference to Figures 8.6 and 8.7. Here the results shown by dashed curves were obtained with $\Lambda_1/z = \alpha = 1.0$ near the surface and $\Lambda_{1\ max} = 17$ meters. For reference the results obtained with $\alpha = 0.7$ and $\Lambda_{1\ max} = 17$ meters are again shown as solid curves. The effect of increasing α is very pronounced, as might be expected. It is interesting to note that even with this choice of parameters it was impossible to match the magnitude of $\overline{v'v'}$ and the temperature correlations. The magnitudes of $\overline{u'w'}$ and $\overline{w'w'}$ are now greatly overpredicted. Before making a comment on the accuracy of these results, it will be well to compare computed results for the profiles shown in Figures 8.1 and 8.3 with experimental data. First, however, some further discussion of the results that have been presented is in order.

First we note that the effect of increasing α is to increase the level of the correlations near the surface. For a fixed $\Lambda_{1\ max}$, the effect of increasing α is generally to

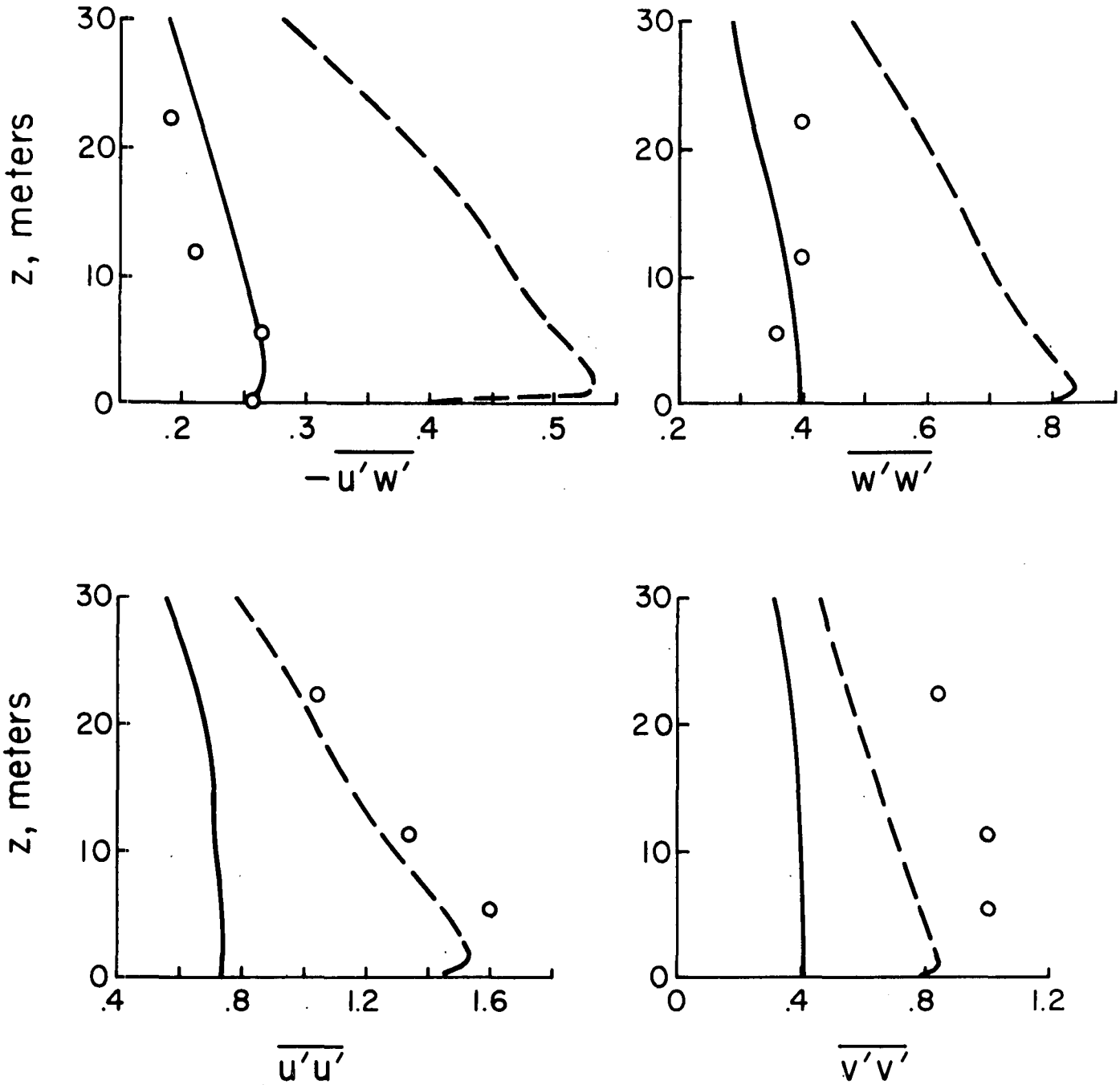

Figure 8.6. Steady state distributions of the velocity correlations for the profiles of mean velocity and temperature shown in Figure 8.2. Near the surface, $\Lambda_1/z = \alpha = 1.0$ for the dashed curves and for the solid curves $\alpha = 0.7$. In both cases $\Lambda_{1\ max} = 17$ meters.

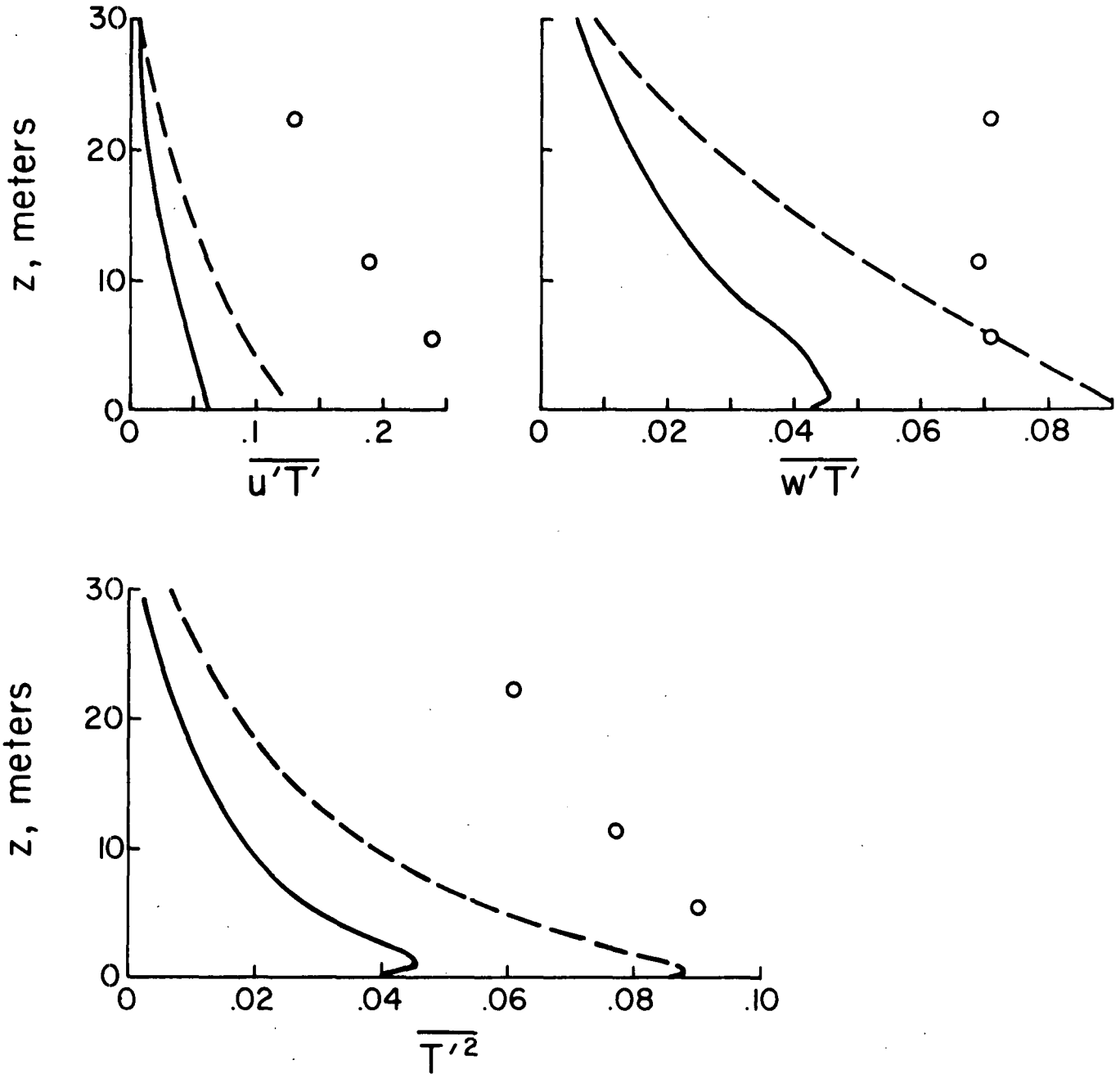

Figure 8.7. Steady state distributions of the temperature correlations for the profiles of mean velocity and temperature given in Figure 8.2. Near the surface, $\Lambda_1/z = \alpha = 1.0$ for the dashed curves and for the solid curves $\alpha = 0.7$. In both cases $\Lambda_{1\ max} = 17$ meters.

draw out and sharpen the maxima of the correlation distributions near the surface. Second, the effect of increasing $\Lambda_{1\ max}$ is to increase the correlations in the region above the height given by $\Lambda_{1\ max}/\alpha$. Both of these results are expected in view of the very strong role played by the scale Λ_1 in the super-equilibrium theory discussed in Section 7.

We may obtain information about the dynamics of atmospheric turbulence from the details of the steady state computations that are carried out to obtain the curves shown in Figures 8.4 through 8.7. Figure 8.8 shows the behavior of the shear correlation with time at two heights for the computations shown in Figures 8.4 and 8.5 with $\alpha = 0.7$ and $\Lambda_{1\ max} = 17$ meters. It is seen that the shear correlation, starting from a zero value, has been able to reach a near-equilibrium value in about 20 to 40 seconds. This characteristic time of the atmospheric profile in question is most interesting, for it indicates that the correlations should be able to track, in the sense of approximating the equilibrium solutions, changes in the mean profile which are accomplished in times large compared to 20 seconds. Since the measured mean profiles under consideration were essentially constant over a period of the order of thousands of seconds, one would expect that equilibrium calculations such as those we have made should be permissible.

Let us now turn to the effect of coupling the equations for the mean profiles to the equations for the second-order correlations. We may investigate this for the case we have been considering by choosing an appropriate $\Lambda_{1\ max}$ and α, computing out to equilibrium with the mean velocity and temperature profiles fixed, and then using the resulting turbulence profiles as initial conditions for considering the coupled equations. As an example of such a run, we consider the results shown in Figures 8.9 and 8.10. Here an equilibrium solution for the case shown in Figure 8.2 was obtained for the case when $\alpha = 0.7$ and $\Lambda_{1\ max} = 15$ meters. This result is shown as the reference lines in Figures 8.9 and 8.10. With these initial conditions, we then

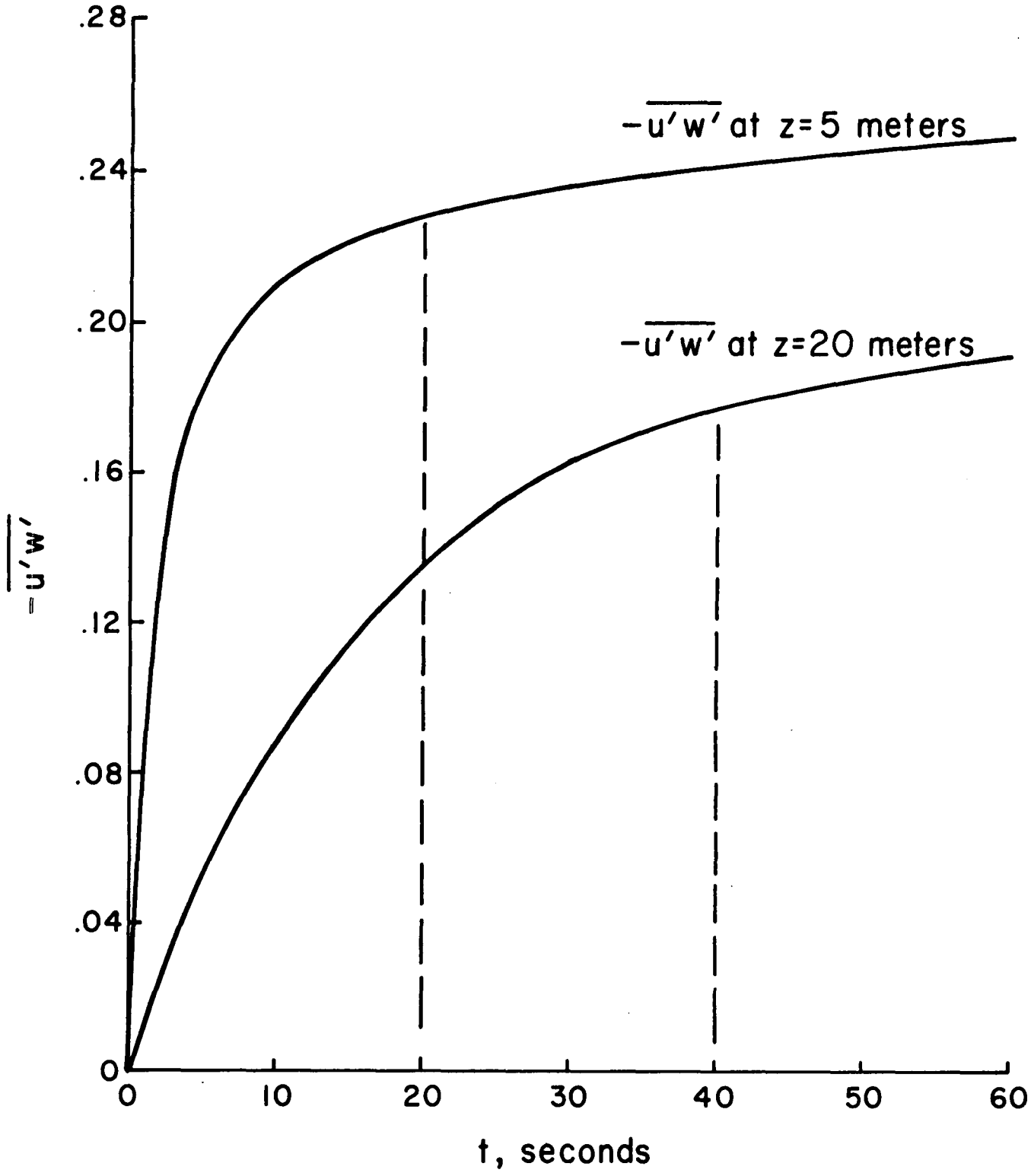

Figure 8.8. Approach of the shear correlation to its equilibrium value. Mean profiles are given in Figure 8.2. $\Lambda_{1\ max}$ = 17 meters and α = 0.7.

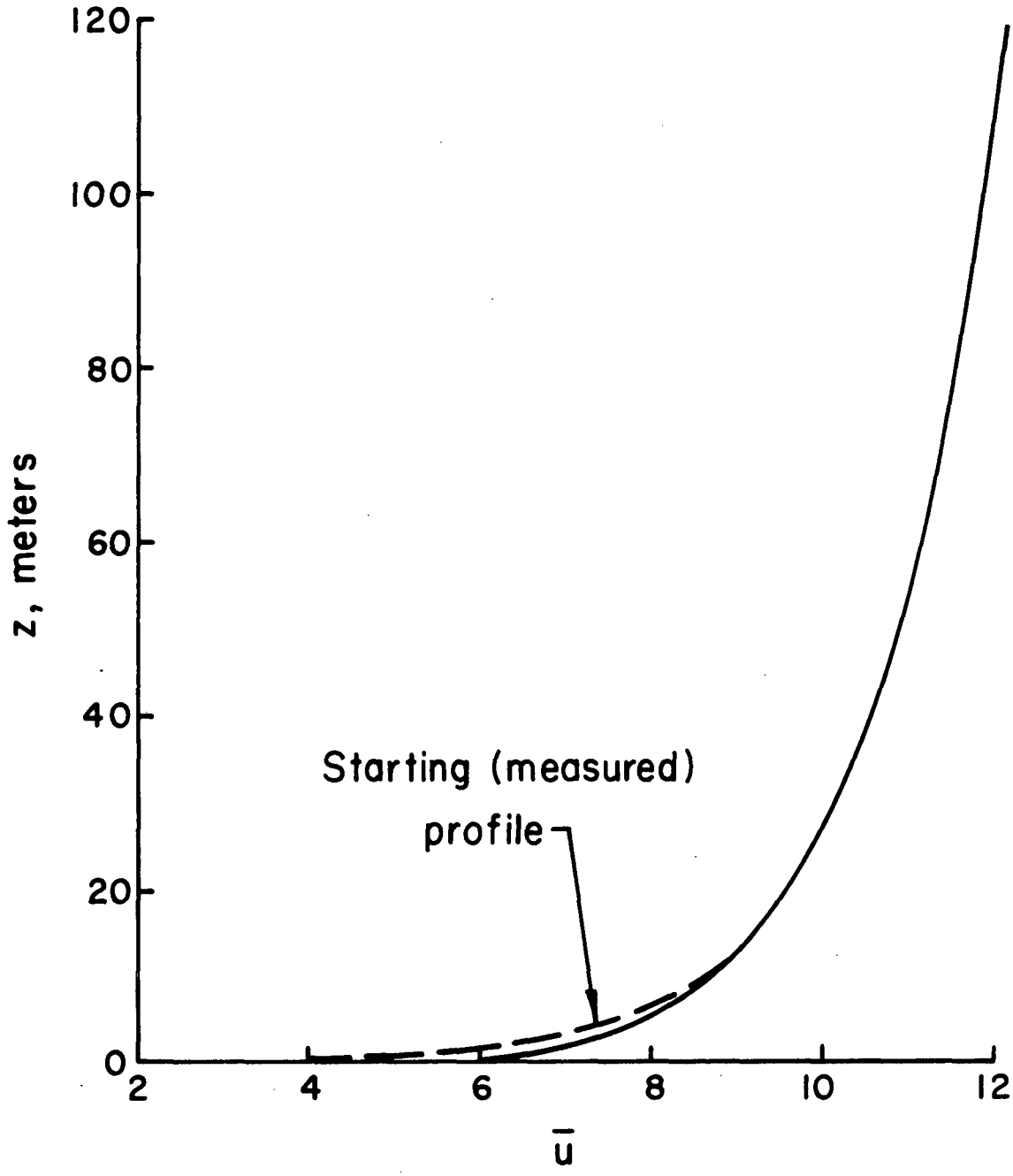

Figure 8.9. Effect of letting $\bar{u}$ profile run free for 10 seconds with $-\partial p/\partial x$ = 2 millibars/100 kilometers

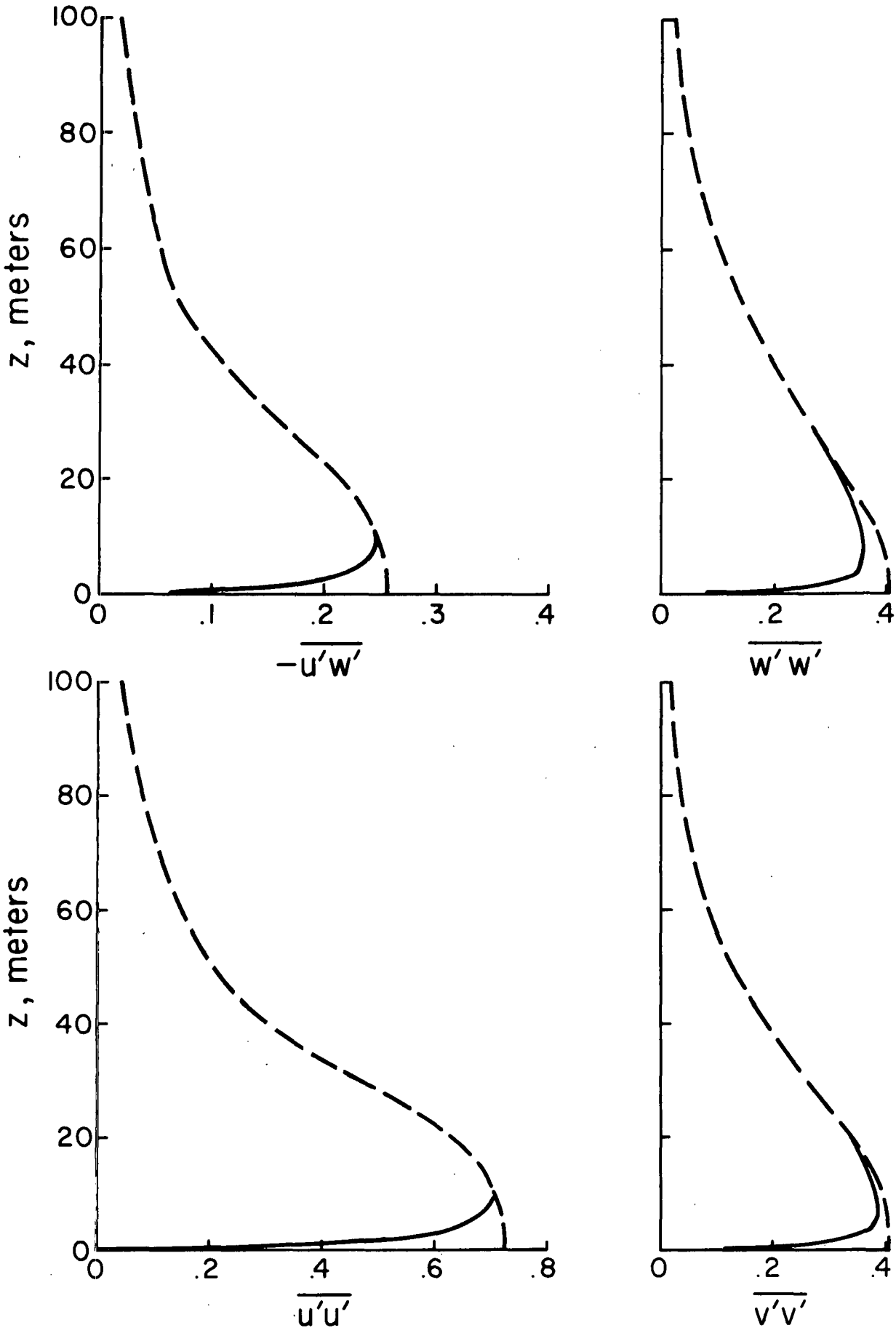

Figure 8.10. Effect of letting $\bar{u}$ profile run free for 10 seconds with $-\partial p/\partial x$ = 2 millibars/100 kilometers

ran with all of the equations solved in a coupled mode for a time of the order of the characteristic time of the turbulence, namely, 10 seconds. A uniform driving force of 2 millibars/ 100 kilometers was assumed to act. The results of this computation are shown as the solid lines in Figures 8.9 and 8.10. It is seen that for this case a very small change in the velocity profile caused a rather significant change in the distributions of the turbulent correlations close to the surface, i.e., within the first 5 meters. There was essentially no effect on the correlation profiles above a height of 10 meters. The results are identical for the mean temperature profile and the profiles of the temperature correlations although plots of these results are not presented. Additional calculations similar to those just discussed have been carried out for somewhat different conditions, including an attempt to add effects of surface roughness to the model. While these studies are not yet complete, it appears that, except for a region very close to the surface, it is possible to estimate the turbulent structure of an atmospheric boundary layer on the basis of an equilibrium solution, knowing the mean velocity and temperature profiles. Near the surface, this is also possible but, in this case, it is absolutely necessary to have some adequate model of the effect of surface roughness. A method for including the effects of roughness will be developed in Section 12 of this report.

We turn now to the calculation of the state of turbulence for the velocity and temperature profiles shown in Figure 8.1. For this case of a stable atmosphere, it is found that, if one assumes $\alpha = 0.7$ as seemed appropriate for neutral atmospheres, and if, further, one assumes $\Lambda_{1\,max}$ of the order of 0.15 times an estimate of the shear layer thickness, one greatly overestimates the level of turbulence and the magnitudes of the turbulent transport correlations. The answer is, as might be

expected, that the stable character of the atmosphere has greatly reduced the scale of the turbulent motion compared to the scale of the mean profiles. A search for values of α and $\Lambda_{1_{max}}$ which gave reasonable agreement of the computed results with experimental results yielded the values of $\alpha = 0.5$ and $\Lambda_{1_{max}} = 5$ meters. The equilibrium distributions computed for these values are shown in Figures 8.11 and 8.12. It can be seen that this choice of parameters gives the correct magnitude of all the correlations. In this case, the vertical heat transfer correlation $\overline{w'T'}$ as well as the turbulent shear and vertical velocity fluctuations are in agreement with experimental results. The temperature correlation $\overline{u'T'}$ is underpredicted, while $\overline{T'^2}$ is overpredicted.

The mean profiles for the case of an unstable atmosphere are given in Figure 8.3. Results of such calculations are shown in Figures 8.13 and 8.14. Here, reasonable agreement between experimental results and computations was found when $\alpha = 0.7$ and $\Lambda_{1_{max}}$ was taken to be 30 meters. The results show that all correlations are predicted within an order of magnitude. The predictions for $\overline{w'w'}$, $\overline{w'T'}$, and $\overline{T'^2}$ are good. That for $\overline{u'w'}$ is of the right magnitude, but the predicted distribution is poor. The predictions of $\overline{u'u'}$ and $\overline{v'v'}$ are low, as they have been in all cases. Of particular note here is the fact that the experimental results show $\overline{v'v'}$ to be larger than $\overline{w'w'}$ for an unstable shear layer! This is difficult to understand on the basis of the equations of motion, and there is certainly no way the model equations can yield this result. It is conceivable that the large values of $\overline{u'u'}$ and $\overline{v'v'}$ that were measured might have been due to a very slight torsional oscillation of the measuring tower. A comment is in order concerning the distribution of $\overline{u'w'}$. For this unstable case, the fairing of the mean velocity profile between the data points has a profound effect upon the outcome of the computations in view of the very large changes in the value of $\partial\bar{u}/\partial z$ that can result from the different fairings.

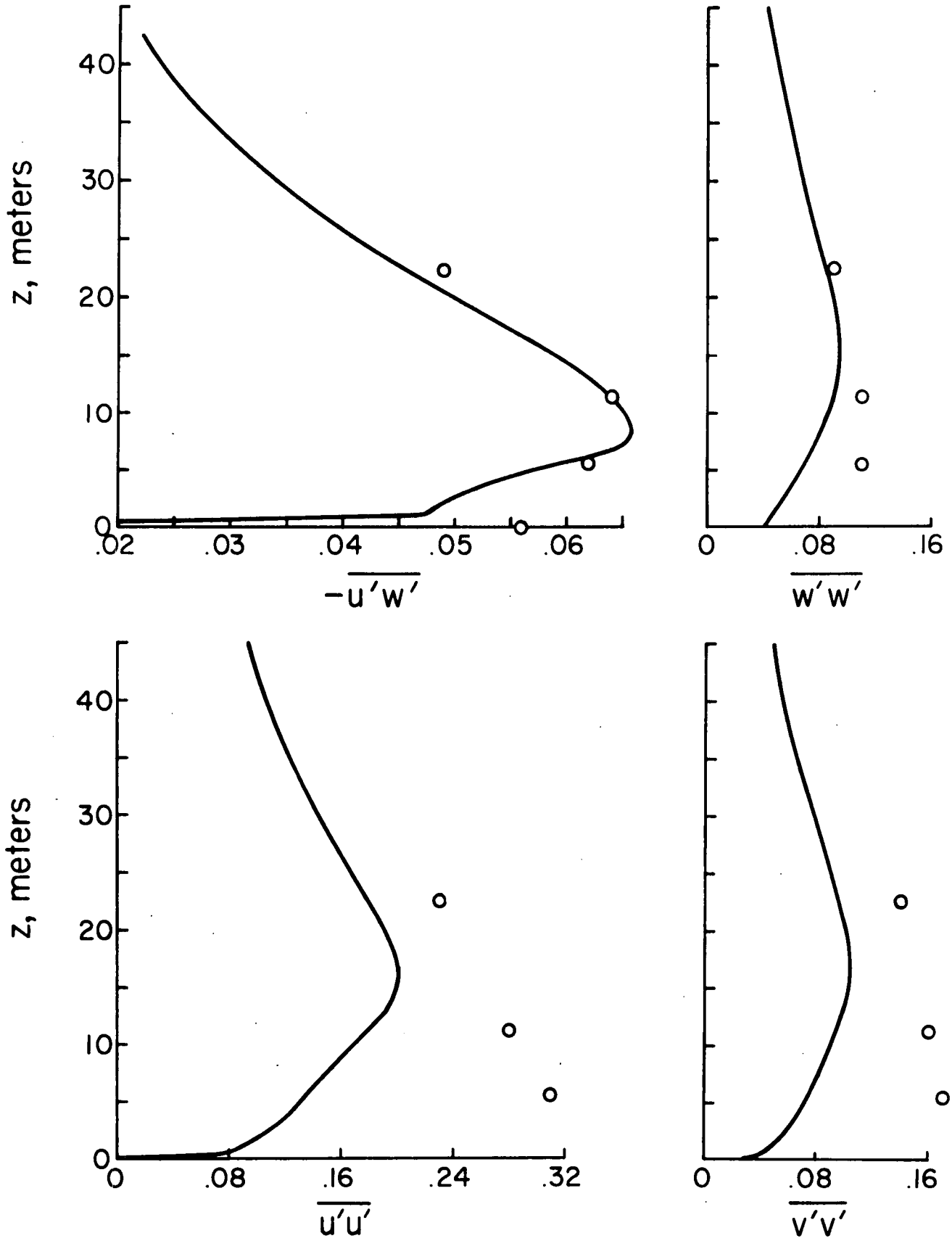

Figure 8.11. Steady state distributions of the velocity correlations for the profiles of mean velocity and temperature given in Figure 8.1. Near the surface, $\Lambda_1/z = \alpha = 0.5$ and $\Lambda_{1\ max} = 5$ meters .

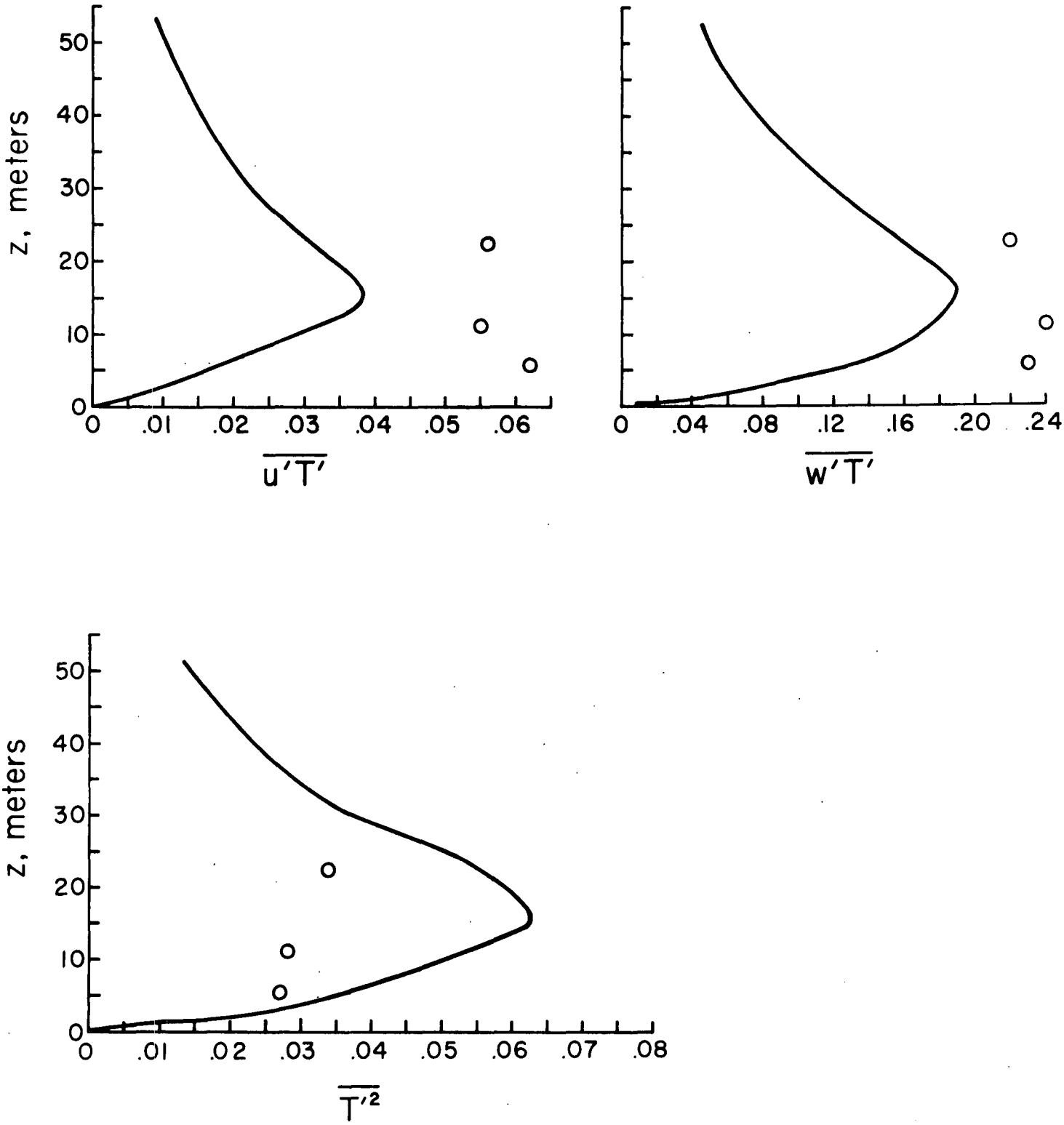

Figure 8.12. Steady state distributions of the temperature correlations for the profiles of mean velocity and temperature given in Figure 8.1. Near the surface, $\Lambda_1/z = \alpha = 0.5$ and $\Lambda_{1\ max} = 5$ meters.

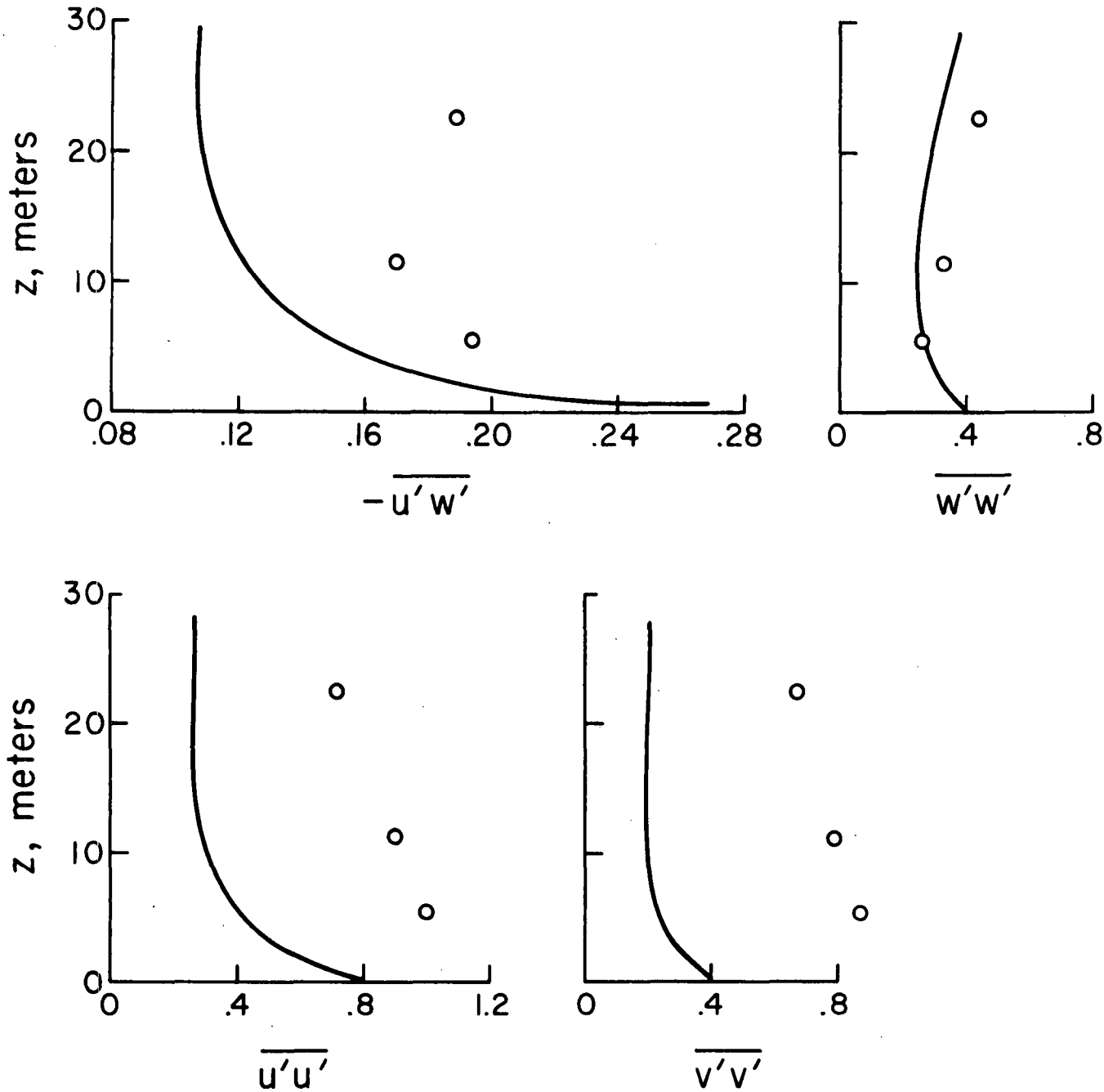

Figure 8.13. Steady state distributions of the velocity correlations for the profiles of mean velocity and temperature given in Figure 8.3. Near the surface, $\Lambda_1/z = \alpha = 0.7$ and $\Lambda_{1\ max} = 30$ meters.

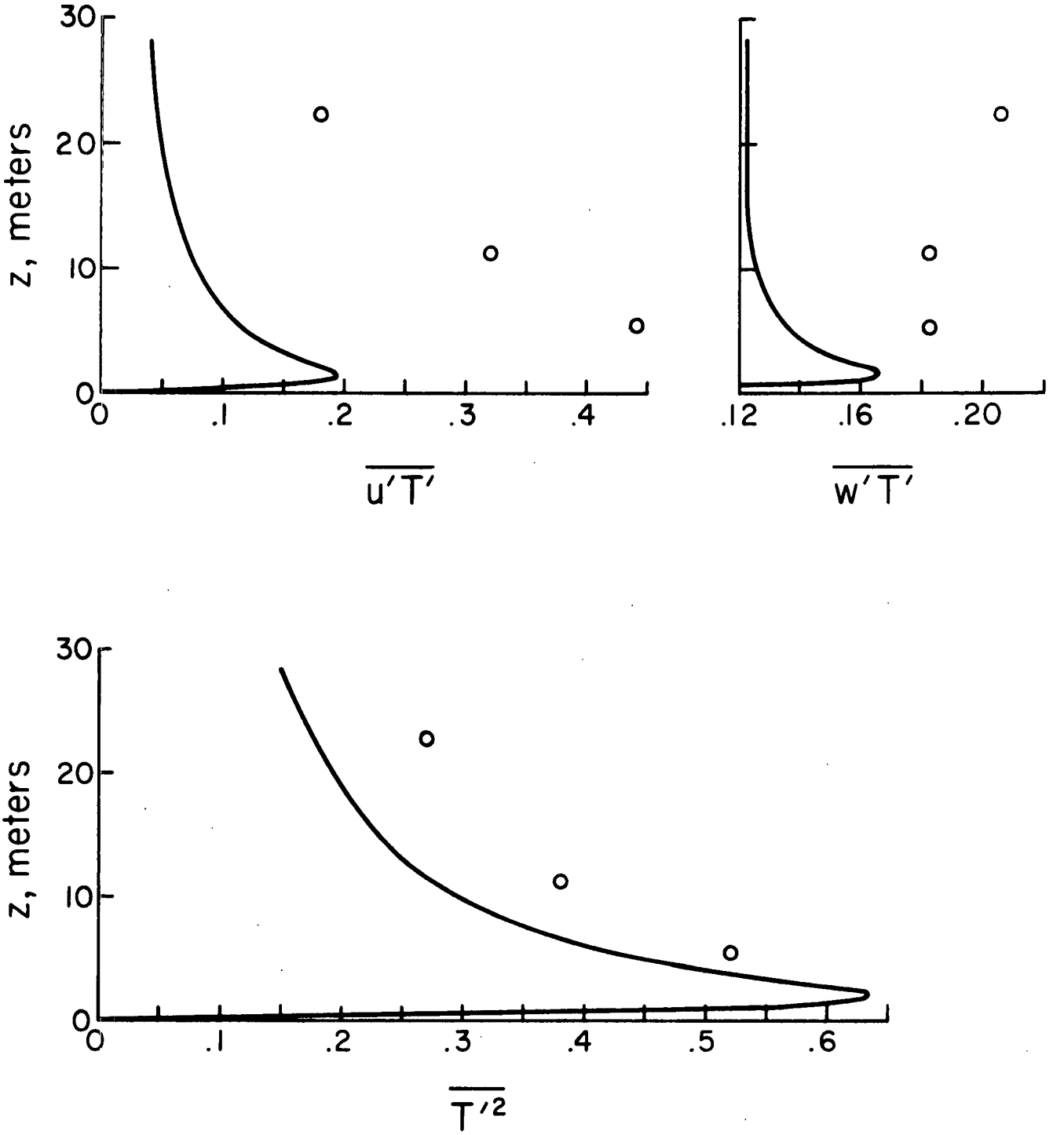

Figure 8.14. Steady state distributions of the temperature correlations for the profiles of mean velocity and temperature given in Figure 8.3. Near the surface, $\Lambda_1/z = \alpha = 0.7$ and $\Lambda_{1\ max} = 30$ meters.

Such fine points are rather academic in view of the profound effect of stability on the scale $\Lambda_{1\ max}$. We note here that $\Lambda_{1\ max}$ is, for this unstable case, far larger in relation to the characteristic thickness of the mean profile than it was for the neutral or stable case.

From the results presented above, it is clear that one will need a great deal of reliable and detailed experimental data on the atmospheric boundary layer if a completely satisfactory model is to be developed. Some of the work of developing this model to its ultimate form can be done by considering laboratory flows in which different gases are mixed in classical free jet and free shear layer experiments. Some headway can be made by considering the case of the compressible turbulent boundary layer. In the long run, however, it is going to be necessary to have many good sets of data from real atmospheric boundary layers if a high degree of confidence in the detailed prediction of any such model is to be developed.

9. DISPERSAL OF POLLUTANTS FROM A LINE SOURCE

We have already seen in Section 3 that the equations for the dispersal of a pollutant in a turbulent medium, under the assumptions made in this study, are decoupled from the equations for the generation of the turbulence field itself. If, then, one is given or can compute the turbulent structure of the earth's boundary layer, one can use the equations given in Section 3, namely, (3.33), (3.38), and (3.39) to compute the mean concentration field of the species α downstream from some source of pollutant. The uncoupled equation (3.40) may be solved at the same time for the variance of the concentration fluctuations $\overline{c_\alpha'^2}$. In this section we will demonstrate the nature of such calculations by discussing the dispersal of pollutants downstream of a line source for a few specially chosen cases of turbulent motion.

Let us assume that the mean and turbulent velocity and temperature fields are steady and of the form $\bar{u} = \bar{u}(z)$, $\bar{v} \equiv 0$, $\bar{w} \equiv 0$, $\bar{T} = \bar{T}(z)$, $\overline{u_i'u_k'} = \overline{u_i'u_k'}(z)$, $\overline{u_i'T'} = \overline{u_i'T'}(z)$, and $\overline{T'^2} = \overline{T'^2}(z)$. These are turbulent fields similar to the equilibrium atmospheric motions discussed in the previous section. Let us further assume that at $x = 0$ and in the vicinity of the height $z = z_o$, there exists a line source of a single pollutant species $\alpha = p$. Thus, at $x = 0$ we will assume that pollutant is introduced into the velocity field $\bar{u}(z)$ through the existence of an initial distribution of pollutant $\bar{C}_p(x,z)$ given by

$$\bar{C}_p(0,z) = \bar{C}_{p_o}(z) \tag{9.1}$$

This assumption requires us to specify, since $\sum_\alpha \bar{C}_\alpha = 1$, that the background or atmospheric species has, at $x = 0$, the distribution

$$\bar{C}_{\alpha_o} = \bar{C}_\alpha(0,z) = 1 - \bar{C}_{p_o}(z) \tag{9.2}$$

We should note here that it is quite possible, using the equations we have developed, to assume that at $x = 0$ the distribution of $\bar{u}$ is disturbed by the introduction of pollutants. In this case, we must solve for the mean and turbulent velocity and temperature fields downstream of $x = 0$ which are now of the form $\bar{u}(x,z)$, $\bar{T}(x,z)$, $\overline{u_i' u_k'}(x,z)$, etc., before calculating the dispersal of pollutants in this turbulent field. In what follows, in order to keep the exposition of the method as simple as possible, we will neglect the effect upon the background turbulent field of the introduction of the pollutants. In this case our problem becomes that of solving for the mean fields $\bar{C}_p(x,z)$ and $C_p'^2(x,z)$ by using (3.33), (3.38), (3.39) and (3.40) when the mean and turbulent velocity and temperature fields are known functions of z. Before displaying the forms that (3.33) and (3.38) through (3.40) take for the particular problem we have set, we will make one more simplifying assumption.

This final assumption is the usual thin layer or boundary layer assumption; i.e., that the gradients of variables in which we are interested are far larger in the z direction than in the x direction. Thus, in the equations, we will neglect derivatives with respect to x compared to those with respect to z. Since we are dealing with the dispersal of a line source located on the line $x = 0$, $z = z_o$ in a flow for which derivatives with respect to y are zero, we may also set $\partial/\partial y = 0$ in our equations. With these assumptions, our equations become

$$\bar{u} \frac{\partial \bar{C}_p}{\partial x} = \nu_o \frac{\partial^2 \bar{C}_p}{\partial z^2} - \frac{\partial}{\partial z} \overline{w' C_p'} \tag{9.3}$$

$$\bar{u} \frac{\partial \overline{w' C_p'}}{\partial x} = -\overline{w'^2} \frac{\partial \bar{C}_p}{\partial z} - \frac{\partial}{\partial z} \left(\overline{w'^2 C_p'} \right) - \frac{1}{\rho_o} \frac{\partial}{\partial z} \left(\overline{p' C_p'} \right) + \overline{\frac{p'}{\rho_o} \frac{\partial C_p'}{\partial z}}$$

$$+ \frac{1}{T_o} g \overline{C_p' T'} + \nu_o \frac{\partial^2 \overline{w' C_p'}}{\partial z^2} - 2\nu_o \overline{\frac{\partial w'}{\partial x_j} \frac{\partial C_p'}{\partial x_j}} \tag{9.4}$$

$$\bar{u}\,\frac{\partial\overline{C_p'T'}}{\partial x} = -\overline{w'C_p'}\,\frac{\partial\bar{T}}{\partial z} - \overline{w'T'}\,\frac{\partial\bar{C}_p}{\partial z} - \frac{\partial}{\partial z}\left(\overline{w'C_p'T'}\right)$$

$$+ \nu_o\,\frac{\partial^2\overline{C_p'T'}}{\partial z^2} - 2\nu_o\,\frac{\partial\overline{C_p'}}{\partial x_j}\,\frac{\partial\overline{T'}}{\partial x_j} \qquad (9.5)$$

$$\bar{u}\,\frac{\partial\overline{C_p'^2}}{\partial x} = -2\overline{w'C_p'}\,\frac{\partial\bar{C}_p}{\partial z} - \frac{\partial}{\partial z}\left(\overline{w'C_p'^2}\right)$$

$$+ \nu_o\,\frac{\partial^2\overline{C_p'^2}}{\partial z^2} - 2\nu_o\,\overline{\left(\frac{\partial C_p'}{\partial x_j}\right)^2} \qquad (9.6)$$

To this point, our equations are exact. In order to solve our problem, we introduce the models discussed in Section 4 into (9.4), (9.5), and (9.6) to obtain a closed set of equations. The modeled equations are

$$\bar{u}\,\frac{\partial\overline{w'C_p'}}{\partial x} = -\overline{w'w'}\,\frac{\partial\bar{C}_p}{\partial z} + \frac{\partial}{\partial z}\left\{(2\Lambda_2 + \Lambda_3)q\,\frac{\partial\overline{w'C_p'}}{\partial z}\right\} - \frac{q}{\Lambda_1}\,\overline{w'C_p'}$$

$$+ \frac{1}{T_o}\,g\overline{C_p'T'} + \nu_o\,\frac{\partial^2\overline{w'C_p'}}{\partial z^2} - 2\nu_o\,\frac{\overline{w'C_p'}}{\lambda^2} \qquad (9.7)$$

$$\bar{u}\,\frac{\partial\overline{C_p'T'}}{\partial x} = -\overline{w'C_p'}\,\frac{\partial\bar{T}}{\partial z} - \overline{w'T'}\,\frac{\partial\bar{C}_p}{\partial z} + \frac{\partial}{\partial z}\left\{\Lambda_2 q\,\frac{\partial\overline{C_p'T'}}{\partial z}\right\}$$

$$+ \nu_o\,\frac{\partial^2\overline{C_p'T'}}{\partial z^2} - 2\nu_o\,\frac{\overline{C_p'T'}}{\lambda^2} \qquad (9.8)$$

$$\bar{u}\,\frac{\partial\overline{C_p'^2}}{\partial x} = -2\overline{w'C_p'}\,\frac{\partial\bar{C}_p}{\partial z} + \frac{\partial}{\partial z}\left\{\Lambda_2 q\,\frac{\partial\overline{C_p'^2}}{\partial z}\right\} + \nu_o\,\frac{\partial^2\overline{C_p'^2}}{\partial z^2} - 2\nu_o\,\frac{\overline{C_p'^2}}{\lambda^2} \qquad (9.9)$$

In these equations, we recognize the scales Λ_1, Λ_2, Λ_3, and λ that were used in the equations which generated the turbulent velocity and temperature fields. In what follows we will use the same general model form as was used in the turbulence calculations; namely, $\Lambda_2 = \Lambda_3 = 0.1\Lambda_1$ and

$$\lambda = \Lambda_1/\sqrt{2.5 + 0.125 Re_{\Lambda_1}} \tag{9.10}$$

but we will investigate the consequence of various choices of the scale Λ_1. In Section 4 it was pointed out that to choose Λ_1 the same for both the calculation of turbulent velocity and concentration fields would, of course, be the simplest choice. Thus, following our rule of trying to find the simplest model, the consequence of such a choice should be studied. It is not hard to argue that this might cause some difficulty in the calculations. Consider, for example, the introduction of a thin stream of pollutant, say of the order of 0.1 meters thick, into a region of the atmosphere where the integral scale L of the velocity fluctuations was known to be of the order of 30 meters. Since Λ_1 for this velocity field is of the same order as L, we might guess that some difficulty would be experienced in the use of so large a Λ_1 in the equations for the concentration correlations. On the other hand, if the thickness of the pollutant layer was much larger than the scale of the atmospheric turbulence, it is difficult to see how the scale of, say, the velocity-concentration fluctuations could exceed by very much the scale of the background turbulence. With these preliminary thoughts in mind, let us turn to some actual calculations to see just how the choice of Λ_1 affects the solution of our equations.

To do this, let us consider a special case of turbulent diffusion. Let us consider the diffusion of a line source of pollutant into a region of homogeneous isotropic turbulence in a neutral atmosphere that is moving by the source at uniform velocity, i.e., $\bar{u}(z) \equiv$ constant. We will consider the consequences of making three choices of Λ_1 :

(a) Λ_1 is a constant and equal to the Λ_1 of the background turbulence into which the pollutant is dispersed.

(b) Λ_1 is proportional to the half-breadth of the concentration profile. In the calculations presented here, Λ_1 is taken equal to the half-breadth defined as the distance between the z for $\overline{C}_p = 3/4\overline{C}_{p_{max}}$ and the z for $\overline{C}_p = \overline{C}_{p_{max}}/4$.

(c) Λ_1 is proportional (equal in these calculations) to the half-breadth of the concentration profile while the Λ_1 so defined is less than the background Λ_1 and thereafter is constant and equal to the background Λ_1 .

For the purposes of these expository calculations, we have chosen a background Λ_1 equal to 15 meters. The turbulent field is assumed to pass the line source of pollutant material at 10 meters per second. The initial mean concentration of pollutant at $x = 0$ is taken to be a Gaussian profile with $\overline{C}_p(0,z_o) = 1$. The ratio of the square root of the second moment of this distribution to the zeroth moment was chosen to be 1 meter. This results in an initial half-breadth of .929 meters. It was assumed that at $x = 0$ the background turbulent field extended throughout the region occupied by the initial distribution of pollutant. In addition, it was assumed that initially $\overline{u_i'C_p'} \equiv 0$ and $\overline{C_p'^2} \equiv 0$.

Some results of solving for the mean concentration field downstream of the source described above in a turbulent field having $\left(\overline{u'^2}\right)^{1/2} = \left(\overline{v'^2}\right)^{1/2} = \left(\overline{w'^2}\right)^{1/2} = 0.1\bar{u}$ are given in Figures 9.1 and 9.2. These calculations were made under the assumption that Λ_1 was constant and equal to the Λ_1 of the background turbulence, namely, $\Lambda_1 = 15$ meters.

Figure 9.1 exhibits the behavior of the maximum concentration of pollutants $\overline{C}_{p_{max}}$ downstream of the source at $x = 0$. Figure 9.2 depicts the mean concentration profiles at various distances downstream of the line source. It will be noted in Figure 9.1 that very little reduction of concentration is apparent for some ten to twenty meters downstream of the source.

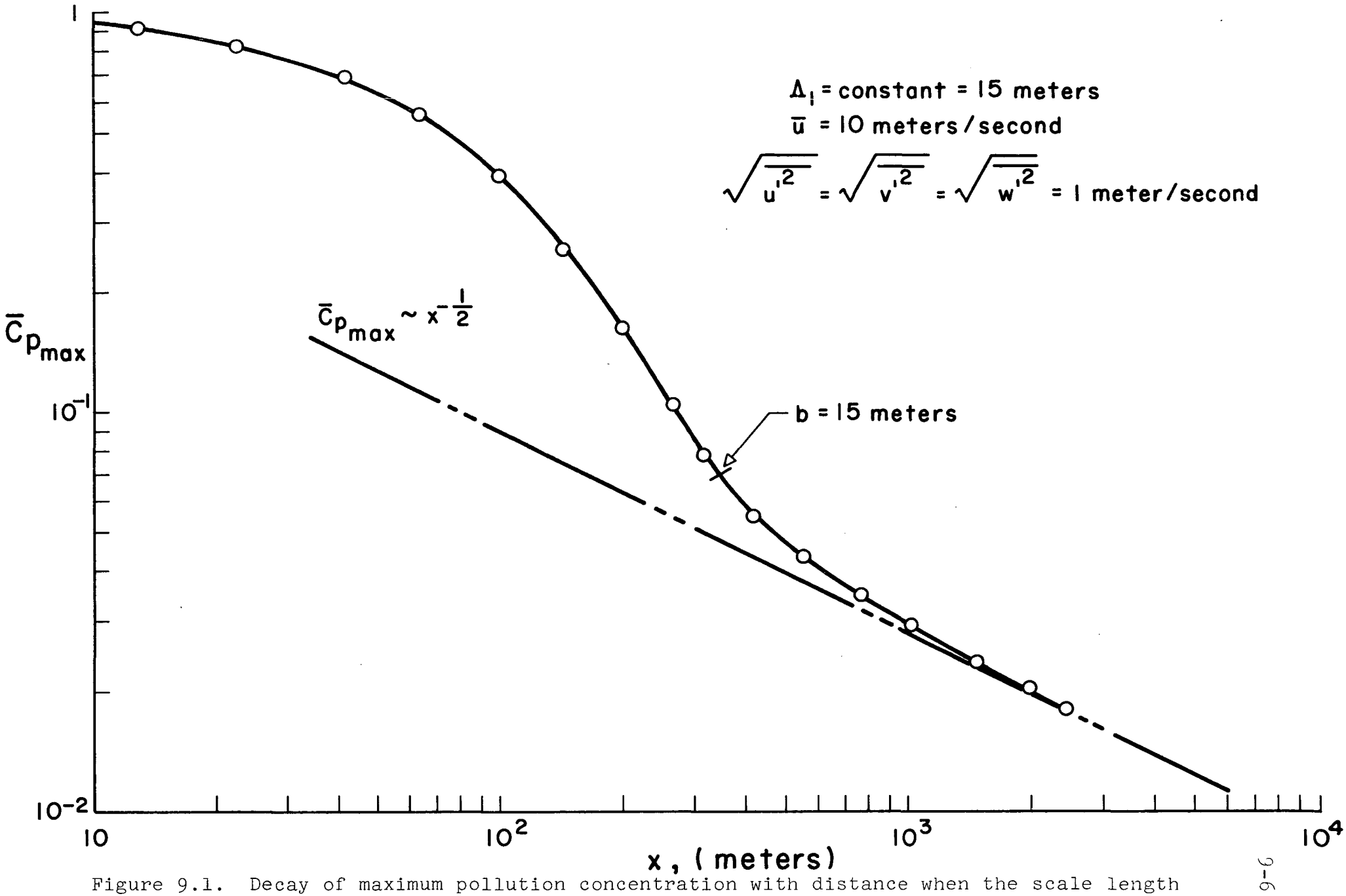

Figure 9.1. Decay of maximum pollution concentration with distance when the scale length Λ_1 is assumed constant

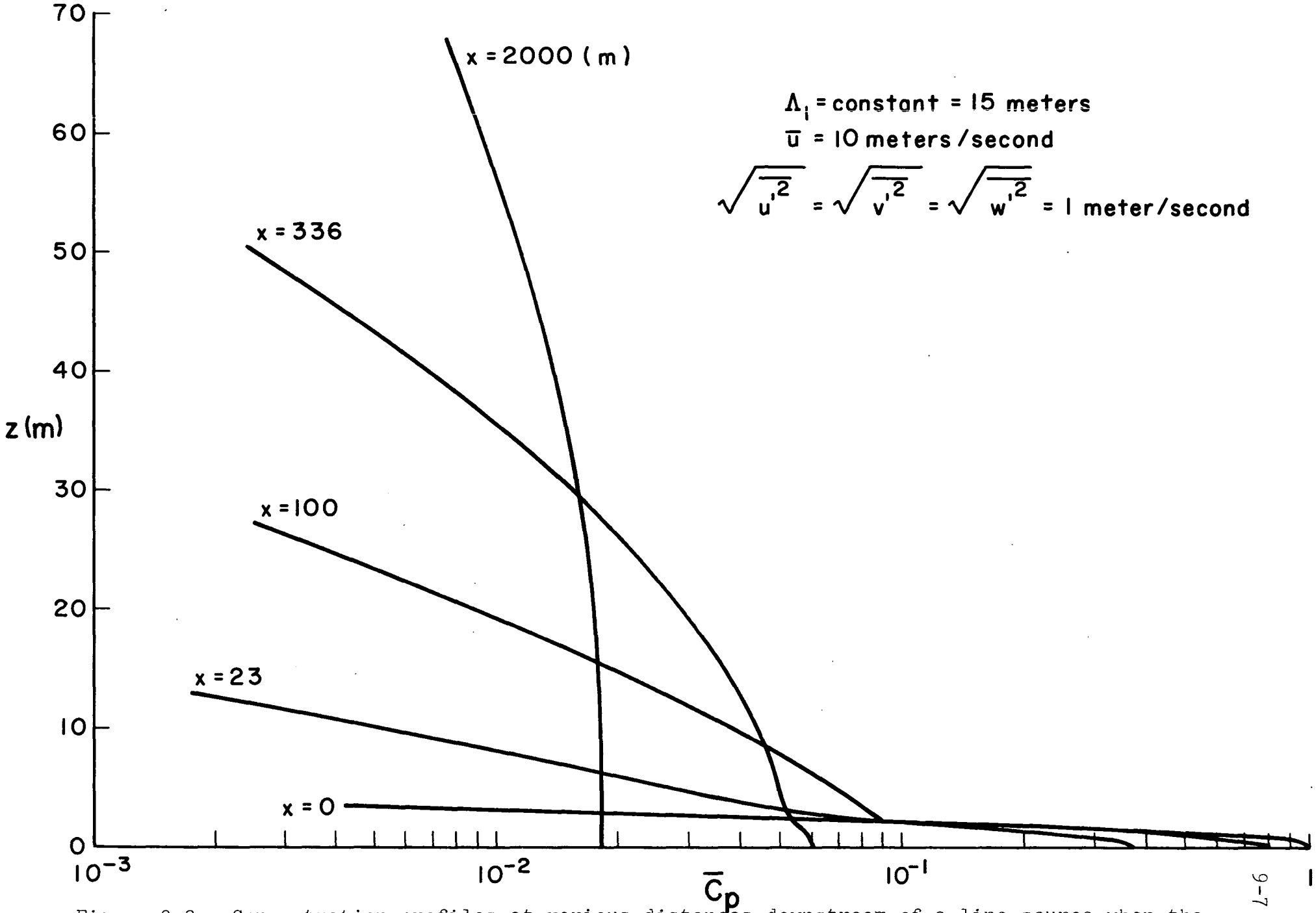

Figure 9.2. Concentration profiles at various distances downstream of a line source when the scale Λ_1 is assumed constant

This is because we have assumed that no turbulent transport $\overline{w'C_p'}$ existed at $x = 0$, and the dynamic equations for the production of this turbulent transport are such that for a mean concentration profile with a spread of approximately 1 meter and for a turbulence level of roughly 1 meter/second, it requires of the order of 1 second for the turbulent transport terms to adjust to their proper values. In the region from 60 to 300 meters downstream of the source, the decay of the centerline distribution is rapid and approaches a rate somewhat greater than x^{-1}. At some 420 meters downstream of the source, the half-breadth b of the concentration profile is equal to 15 meters. For larger distances than this, the rate of decay of the centerline concentration continues with the x^{-1} behavior. Eventually, when the half-breadth of the profile is considerably larger than the Λ_1 used in the computation, the rate of decay of the centerline concentration falls off as $x^{-1/2}$. This sort of behavior is to be expected at large distances from the source and has been observed in experimental studies [Ref. 35]. We will defer a detailed discussion of this phenomenon to the next section when we will discuss dispersion from a point source. Here we will take up the mid-range behavior of pollutant dispersal following the period of initial formation of the turbulent exchange correlation $\overline{w'C_p'}$.

To what do we ascribe the unrealistic behavior of $\overline{C}_{p_{max}}$ in the mid-range $100 < x < 300$ meters where the decay of $\overline{C}_{p_{max}}$ is greater than x^{-1}? This behavior has been traced to the unrealistic profiles of $\overline{C}_p$ that are initially generated due to the choice of $\Lambda_1 = 15$ meters in Eqs. (9.7), (9.8), and (9.9) when the half-breadth of the concentration profile is consderably less than this figure. These unrealistic profiles are evident in Figure 9.2. Note in this figure that for $x = 100$ meters and for $x = 336$ meters, the concentration profiles have a bump or "nose" near the region of maximum concentration. It is the elimination of this unrealistic nose in the region between

100 meters, where it is very pronounced, and 336 meters, where it has almost been eliminated, that causes $\overline{C}_{p_{max}}$ to decay faster than x^{-1}. Once the half-breadth of the pollution profile has exceeded 15 meters, this difficulty is eliminated and the concentration profiles behave properly.

A close examination of the details of the computation of the profiles in the formative and mid-range regions of concentration decay was made. This examination showed that the cause of the unrealistic profiles and decay behavior was the existence of too much diffusion in the equations for the correlations in the formative and mid-range regions of decay. The amount of this error was dependent on the ratio of the Λ_1 used in the calculations to the local half-breadth of the concentration profiles. For this reason, a second solution of this dispersal problem was run under the assumption that the Λ_1 in the calculations was always equal to the local half-breadth b of the concentration profile. The results of such a computation are shown in Figures 9.3 and 9.4.

From Figure 9.3, we see immediately that after a formative distance of the order of tens of meters, the decay of the maximum concentration of pollutant approaches a decay rate exactly proportional to x^{-1}. By extrapolating this decay rate back to $\overline{C}_{p_{max}} = 1$, one obtains an effective source position x_o of 26.5 meters which is really indicative in these calculations of a characteristic time for the formation of turbulent transport correlations, namely, $x_o/\bar{u}$ as 26.5/10 = 2.65 seconds.

Examination of Figure 9.4 shows that with the present choice of Λ_1 no difficulty in profile shape is encountered. We do note, however, that this choice of Λ_1 will never permit a far region decay where $\overline{C}_{p_{max}}$ is proportional to $x^{-1/2}$. Since we wish our decay rates to ultimately approach $x^{-1/2}$ as well as behave properly in the formative and mid-ranges of decay, it appears that the proper choice for Λ_1 is that Λ_1 be proportional to the concentration half-breadth b for all cases when

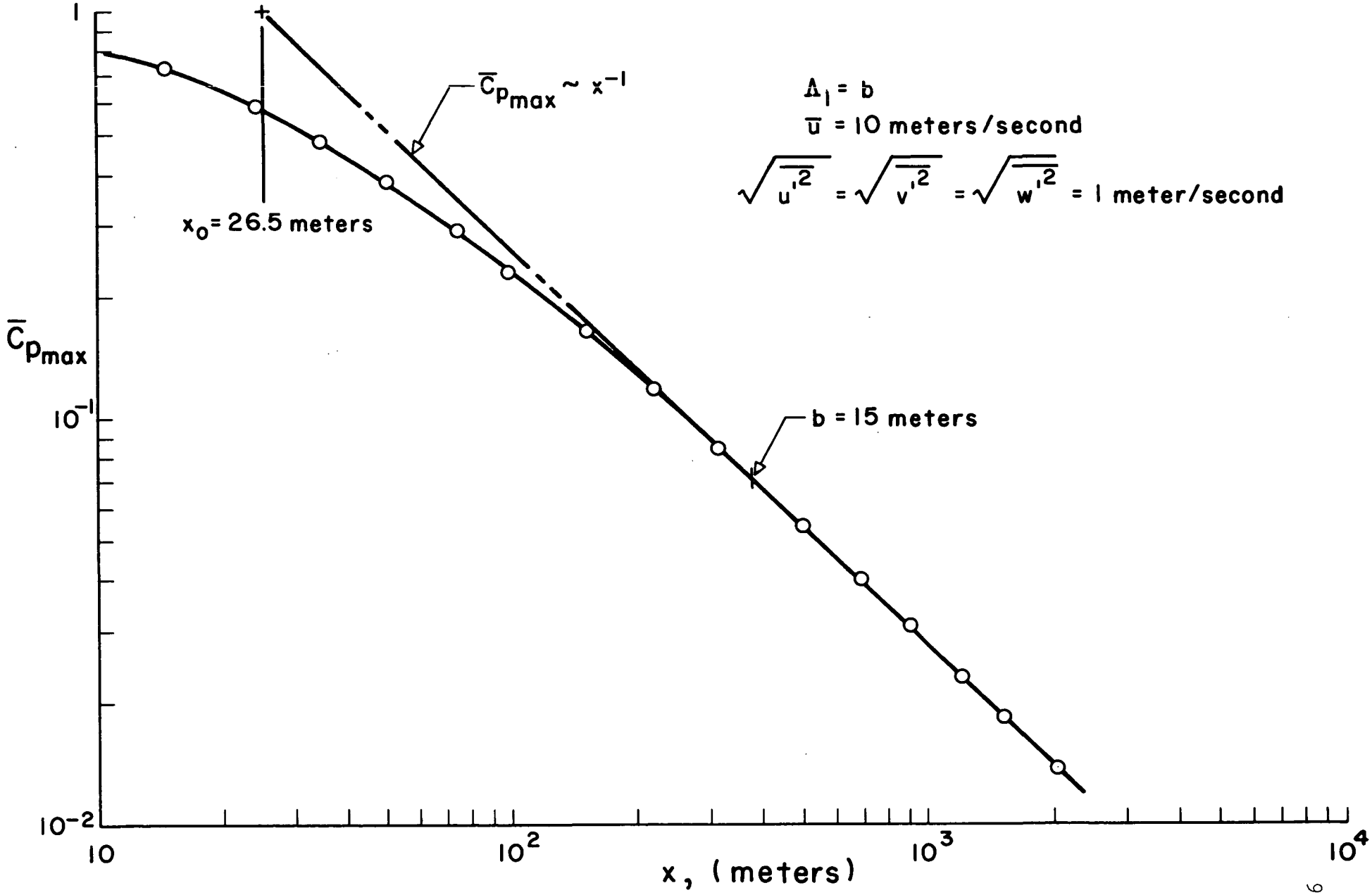

Figure 9.3. Decay of maximum concentration of pollutant with distance when the scale length Λ_1 is assumed equal to the half-breadth b of the concentration profile

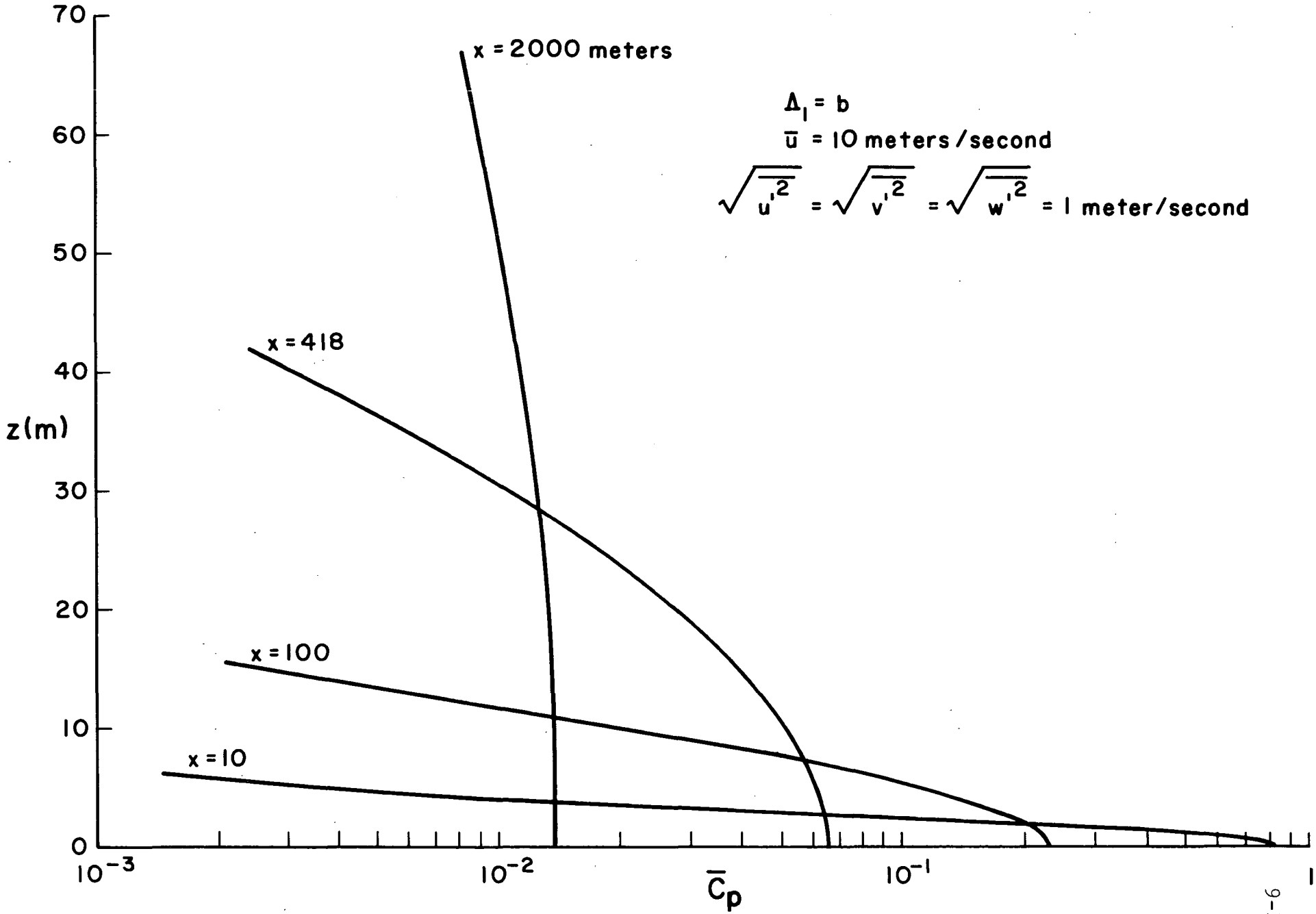

Figure 9.4. Concentration profiles at various distances downstream of a line source when the scale Λ_1 is assumed equal to the half-breadth b of the concentration profile

b is less than the Λ_1 used in the background turbulence computations and equal to this background Λ_1 when b is much larger than Λ_1 .

At this point it would appear that it is necessary to abandon the assumption of a universal Λ_1 for all the correlation equations and distinguish between the Λ_1 's in the equations for the various correlations. Therefore, we will identify a different Λ_1 for the concentration correlation equations, say, Λ_{1_c} , and for the background turbulence, say Λ_{1_t} . In terms of these new definitions, we may write the choice of Λ_{1_c} that has been suggested previously as follows: $\Lambda_{1_c} = b$ for $b \leq k\Lambda_{1_t}$ and $\Lambda_{1_c} = k\Lambda_{1_t}$ for $b > k\Lambda_{1_t}$.

In Figure 9.5 we show the behavior of the maximum concentration for the problem that has previously been discussed, using the above-noted choice of Λ_{1_c} when the constant of proportionality k between Λ_{1_c} and Λ_{1_t} is one. This figure shows the kind of decay that we desire. After a formative period of decay which depends entirely on the initial conditions applied to the problem, a mid-region of decay is found where $\overline{C}_{p_{max}}$ falls off as x^{-1} . At very large distances, $\overline{C}_{p_{max}}$ approaches a decay rate of $x^{-1/2}$. We will not present here a separate figure showing the concentration profiles for this case since, as might be expected, the profiles are identical to those of Figure 9.4 for most of the range of x considered.

It may be instructive to compare the results of all three of the calculations we have just discussed. Figure 9.6 shows the behavior of $\overline{C}_{p_{max}}(x)$ for each of these calculations. The results shown in this figure may be compared with those shown in Figure 9.7 where we have plotted the results of pollution dispersal computations using the three Λ_{1_c} models for the case of a higher relative level of turbulence, namely, $\bar{u}$ = 10 meters/second and $\sqrt{\overline{u'^2}} = \sqrt{\overline{v'^2}} = \sqrt{\overline{w'^2}}$ = 3 meters/second. It is easy to see that while the effect of higher turbulence level affects the rate of spread, it does not affect the general character of the solutions.

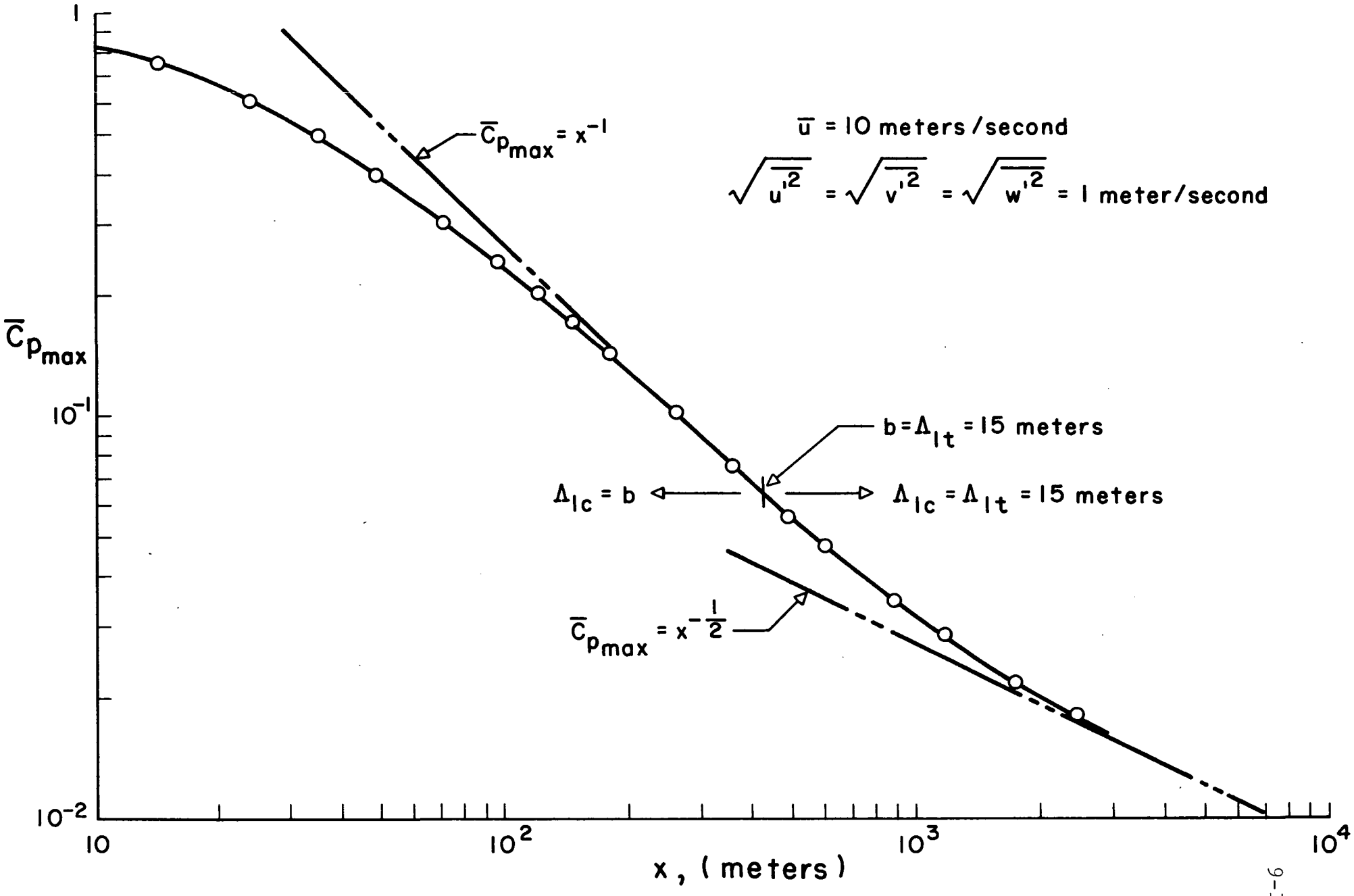

Figure 9.5. Decay of maximum pollution concentration with distance when $\Lambda_{1c} = b$ for $b \leq \Lambda_{1t}$ and $\Lambda_{1c} = \Lambda_{1t}$ for $b > \Lambda_{1t} = 15$ meters

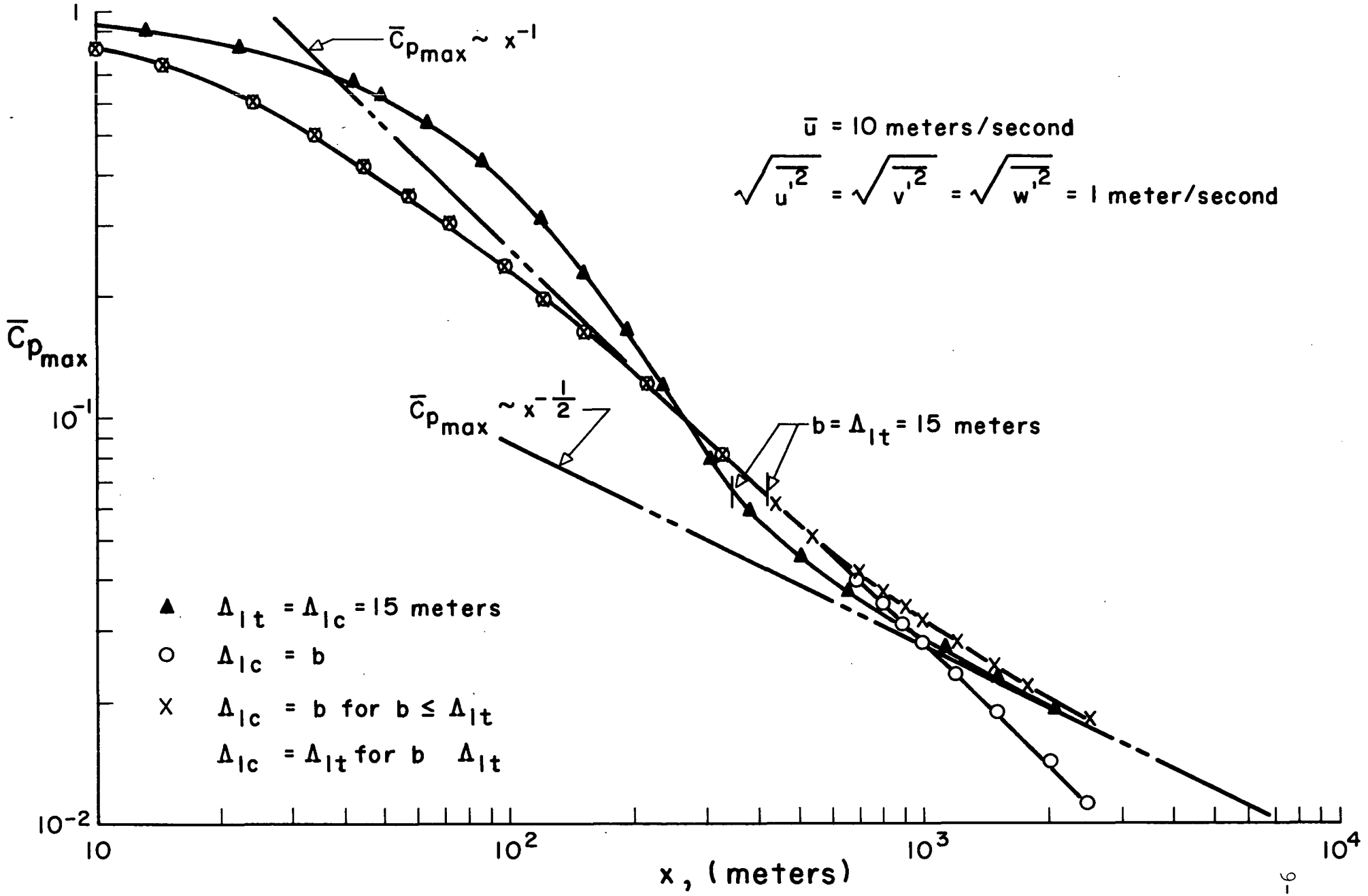

Figure 9.6. Comparison of rates of concentration decay for three choices of Λ_{1_c}

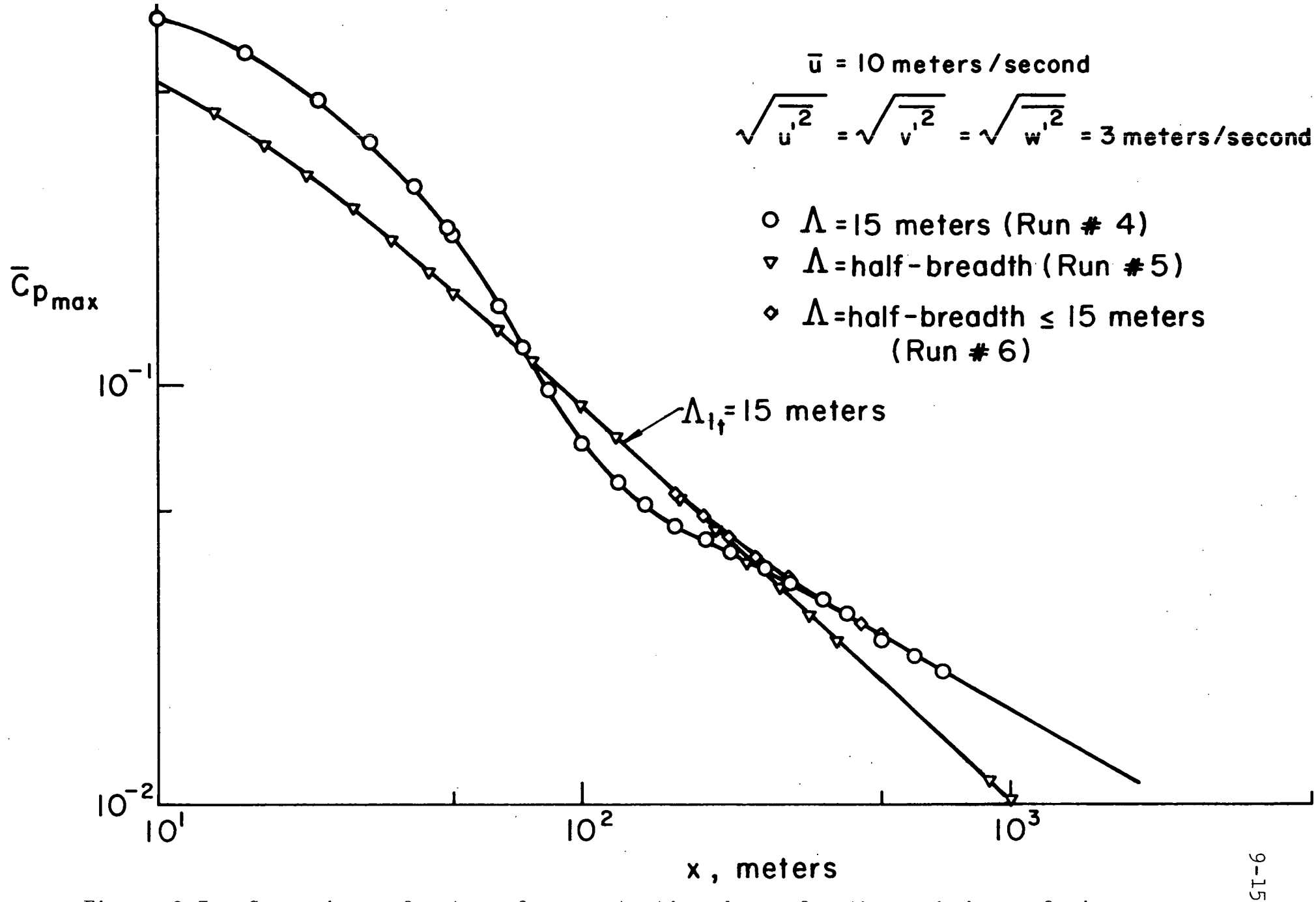

Figure 9.7. Comparison of rates of concentration decay for three choices of Λ_{1_c}

Before going on to present a calculation of the dispersal of pollutants for a more realistic atmospheric condition, a presentation of the nature of the solutions for the second-order correlations $\overline{c_p'w'}$ and $\overline{c_p'^2}$ is in order. Figure 9.8 exhibits plots of both $\bar{c}_p$ and $\overline{c_p'w'}$ at 100 meters from the source for the calculations presented in Figure 9.3. For this same condition, the variance of the fluctuation in pollutant mass fraction $\overline{c_p'^2}$ is shown in Figure 9.9. Note that the actual variance is a maximum near where the transport of pollutant is a maximum. If one computes the ratio of $\sqrt{\overline{c_p'^2}}$ to $\bar{c}_p$, it is interesting to note that this ratio has a value of 0.847 at the point where $\overline{c_p'^2}$ is maximum. As the mean concentration falls off towards the outer edges of the sheet of pollutants, $\sqrt{\overline{c_p'^2}}$ falls off less rapidly than $\bar{c}_p$ so that the ratio of $\sqrt{\overline{c_p'^2}}/\bar{c}_p$ tends to approach large values. This is what is to be expected when there is an occasional "blob" of pollutant in an otherwise unpolluted background. This behavior of $\sqrt{\overline{c_p'^2}}/\bar{c}_p$ is also shown in Figure 9.9.

Having studied the nature of diffusion calculations by second-order modeling for a very simple case, let us now turn to the calculation of pollutant dispersal from a line source under more realistic conditions. Let us consider an atmospheric boundary layer having the mean velocity and mean temperature distributions shown in Figure 9.10. We have assumed that a stabilized region exists in the region between 88 and 140 m above the earth's surface. Also shown in Figure 9.10 is an assumed distribution of the background turbulence scale Λ_{1_t}. In order to calculate the dispersal of pollutants in this layer, we first compute the field of atmospheric turbulence produced by this combination of conditions. To do this, we use the methods described in Section 8 to obtain profiles of all the turbulent correlations necessary for the solution of Eqs.(9.3), (9.7), (9.8), and (9.9). The results of such calculations are shown in Figures 9.11 and 9.12. With these results in hand, Eqs. (9.3),

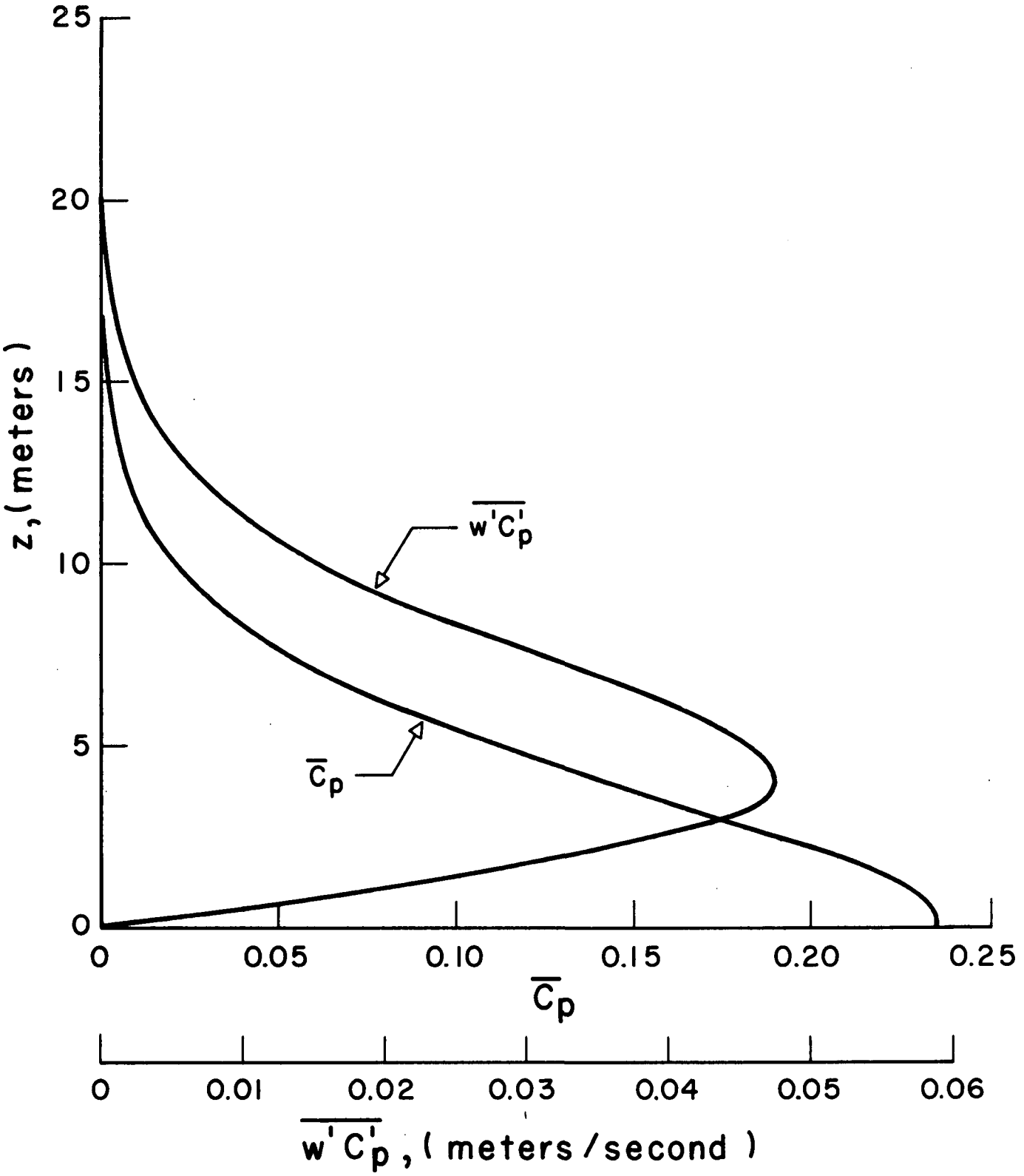

Figure 9.8. Distributions of $\overline{C}_p$ and $\overline{w'C_p'}$ as functions of z at x = 100 meters for dispersal problem shown in Figure 9.3

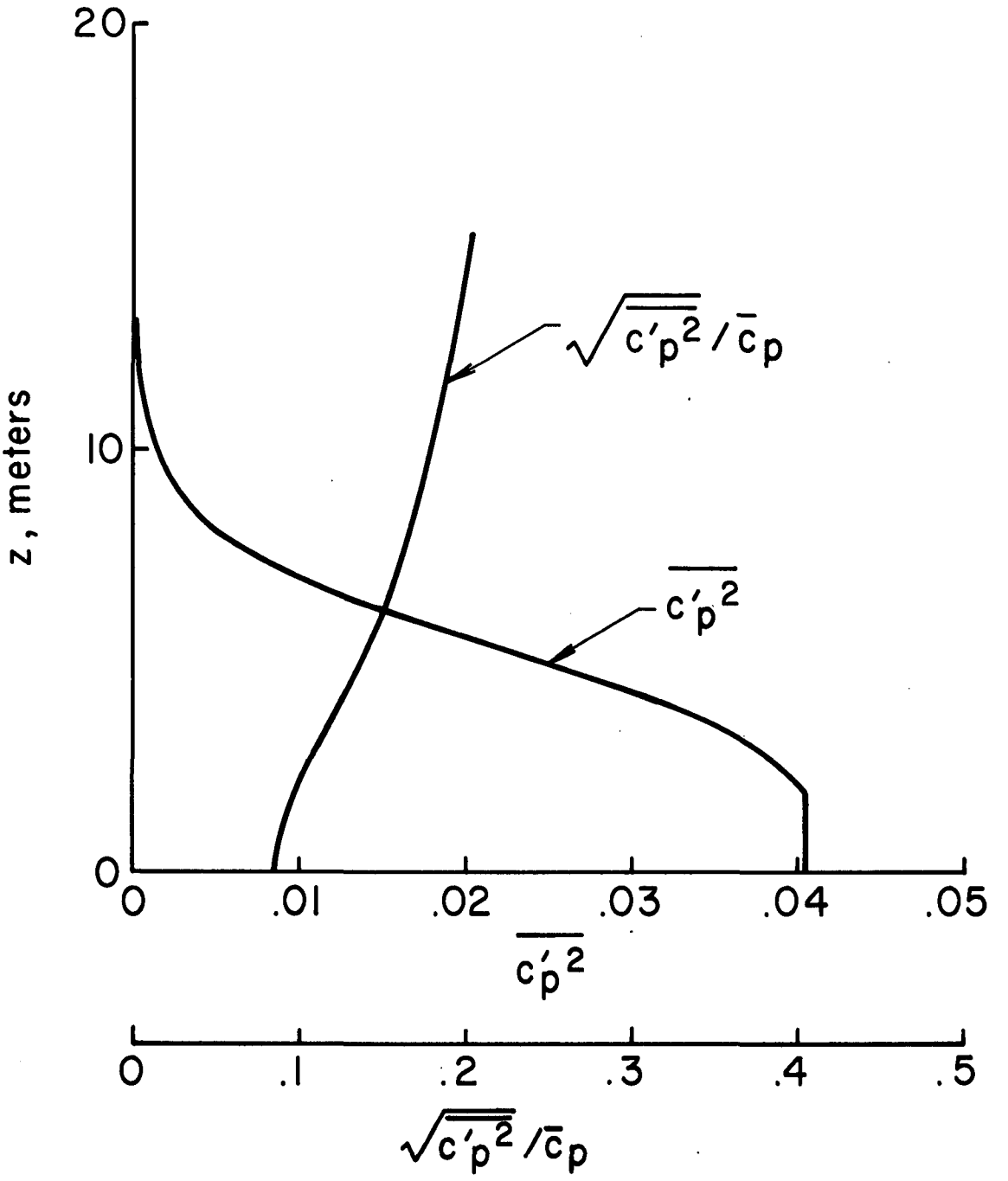

Figure 9.9. Distributions of $\overline{c_p'^2}$ and $\sqrt{\overline{c_p'^2}}/\bar{c}_p$ as functions of z at x = 100 meters for the dispersal problem shown in Figure 9.3

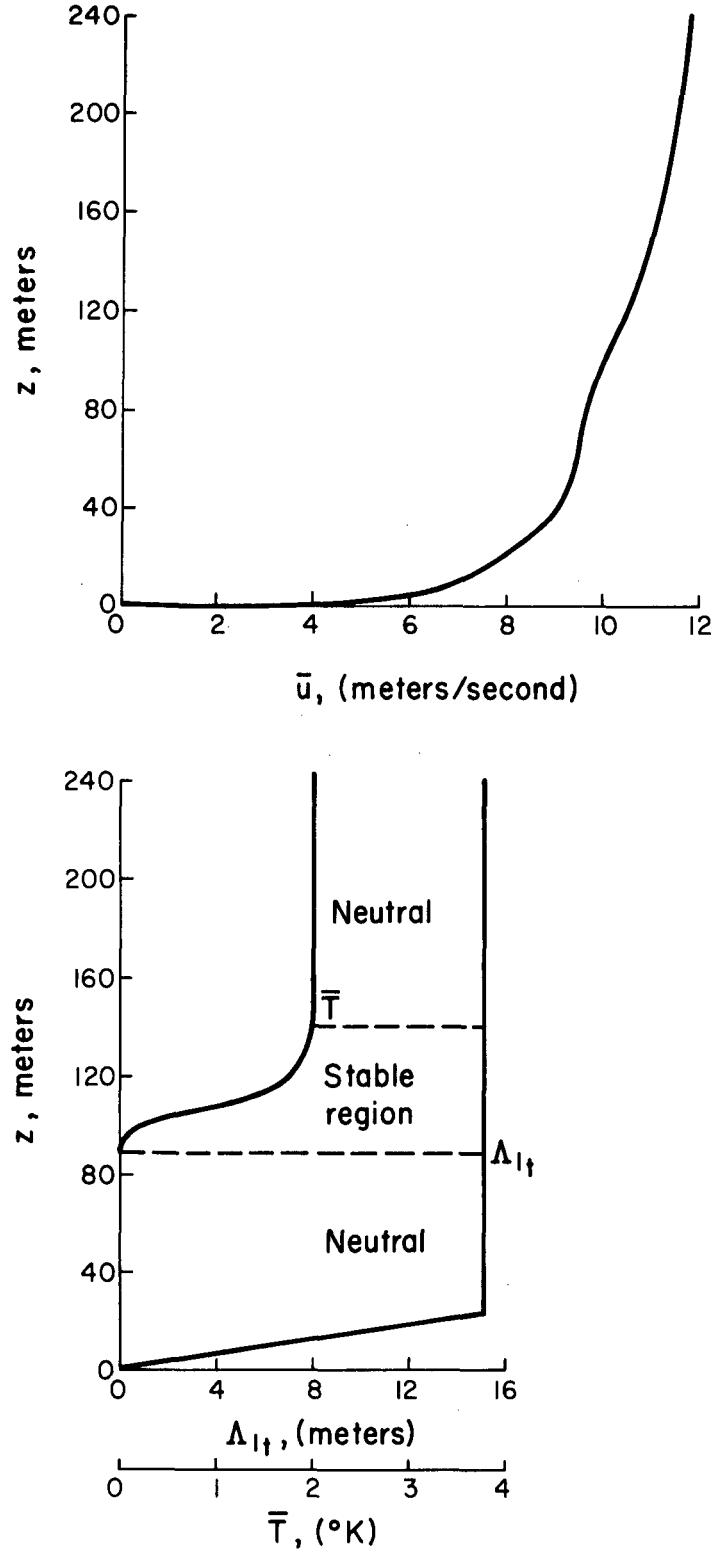

Figure 9.10. Assumed mean velocity and temperature profiles for an atmospheric boundary layer. Also shown is an assumed profile of the background turbulence scale Λ_{l_t}.

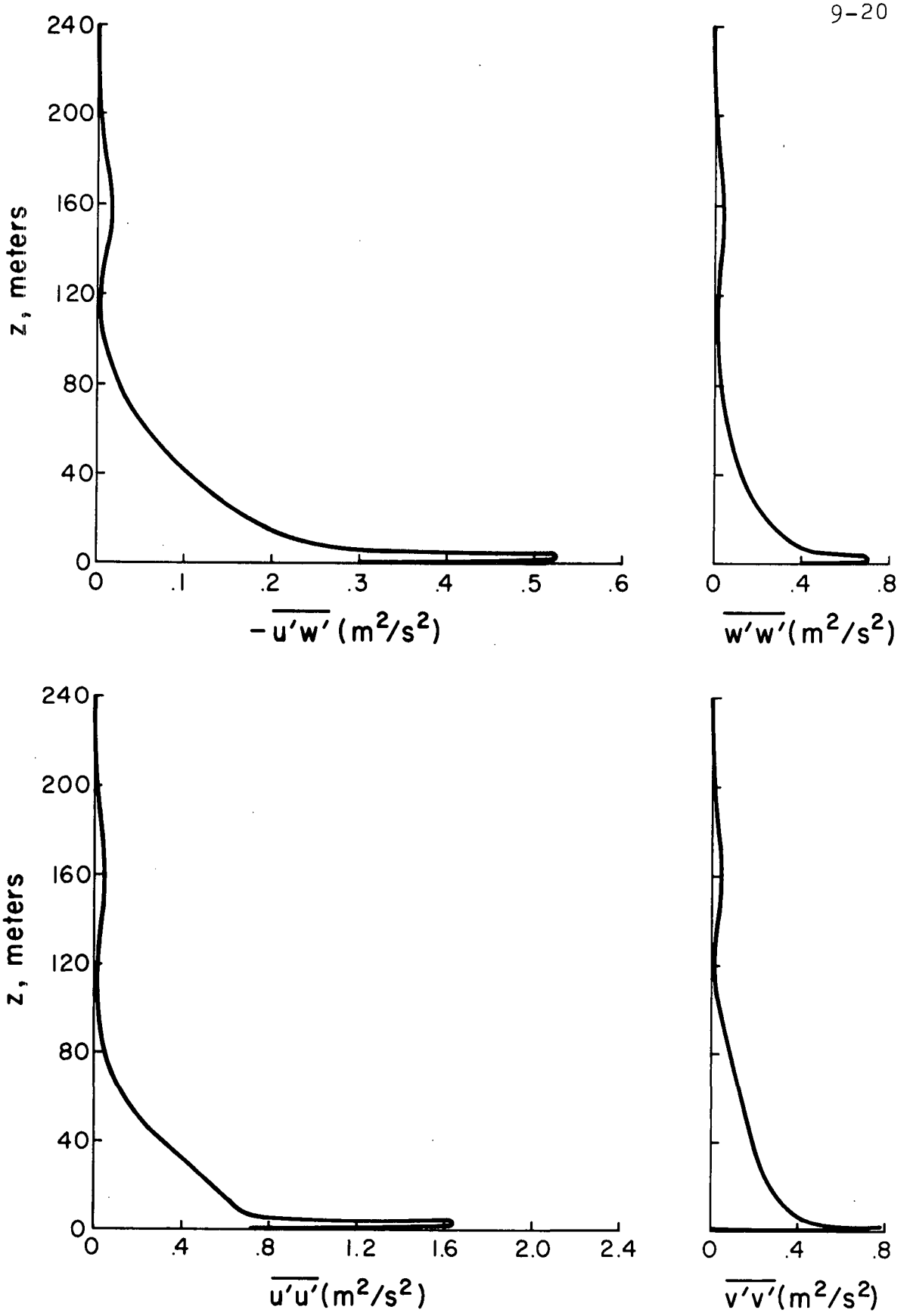

Figure 9.11. Velocity correlations computed for assumed atmospheric layer shown in Figure 9.8

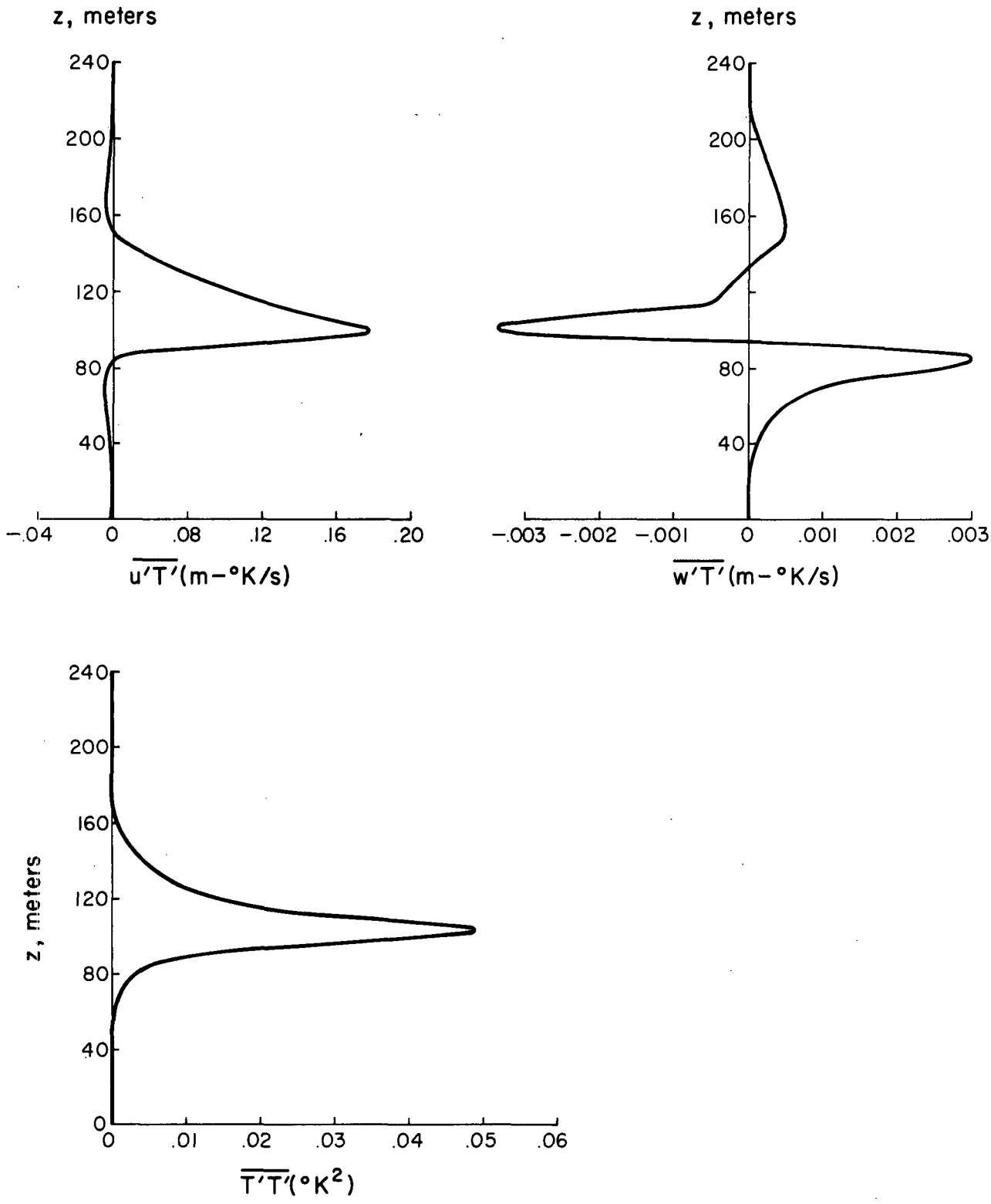

Figure 9.12. Temperature correlations computed for assumed atmospheric layer shown in Figure 9.8

(9.7) and (9.8) may be solved simultaneously for the mean concentration of pollutant $\overline{C}_p(x,z)$ downstream of a line source located at $x = 0$ and $z = z_o$.

As in our previous calculations, we assume an initial source of pollutants that has a Gaussian distribution with $\overline{C}_{p_{max}}(0,z_o) = 1$. The half-breadth of this distribution is again assumed to be .929 meters.

In view of our experience with the spread of pollutant into uniform turbulence where, for pollutant spreads less than Λ_{1_t}, we found that Λ_{1_c} must be chosen proportional to the spread b rather than equal to Λ_{1_t}, we may anticipate a difficulty with the computation we are contemplating. Since the spread above and below the maximum concentration will not remain equal because the problem is no longer symmetric, we must have a way of choosing Λ_{1_c} differently on the two sides of the concentration profile. We have selected a method for doing this which appears to be appropriate for the problem under discussion here, as well as for more complex pollutant concentration distributions. Consider for the moment the concentration distribution shown in Figure 9.13. This distribution has five extrema: 2 maxima, 1 minimum, and 2 zeroes. The range of z is broken into 4 regions which are defined by the ranges of z separating these extreme values. In each region, Λ_{1_c} is assumed to be constant and equal in magnitude to the distance between where the change in $\overline{C}_p$ is 0.25 and where the change in $\overline{C}_p$ is 0.75 times the change between the two extreme values that define the region under consideration. The Λ_{1_c} so defined are identical to the half breadth b when this method is used for the symmetric dispersals we have discussed previously, and we will use it for the computation under consideration here.

Figure 9.14 shows the behavior of solutions for the mean concentration profiles downstream of the line source we have discussed when the pollutants are injected into the atmospheric boundary layer described in detail by Figures 9.10 through 9.12. Note that the spread is initially almost symmetric, but at

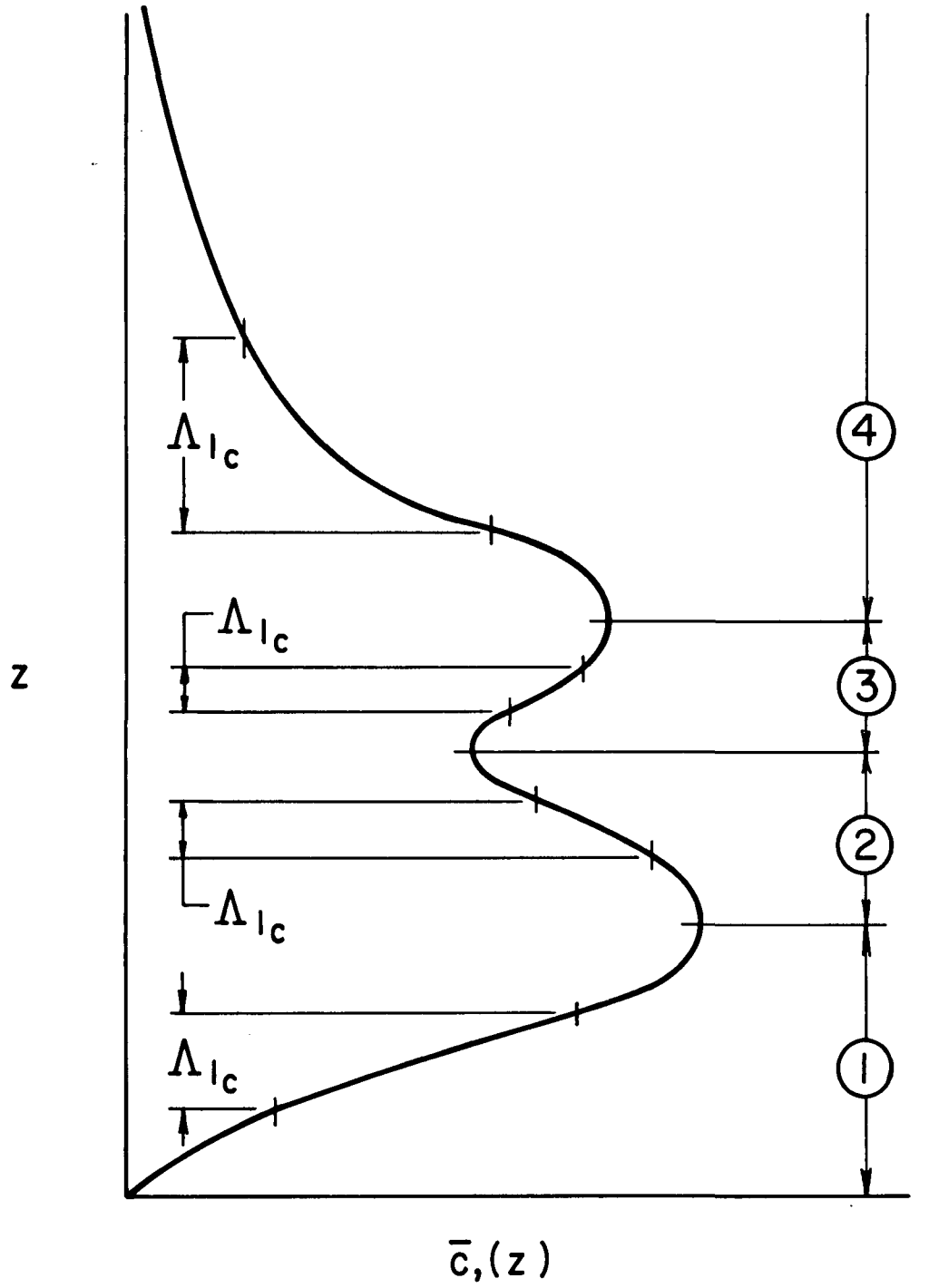

Figure 9.13. Hypothetical concentration distribution showing regions of constant Λ_{1_c} and values of Λ_{1_c} to be used in each region

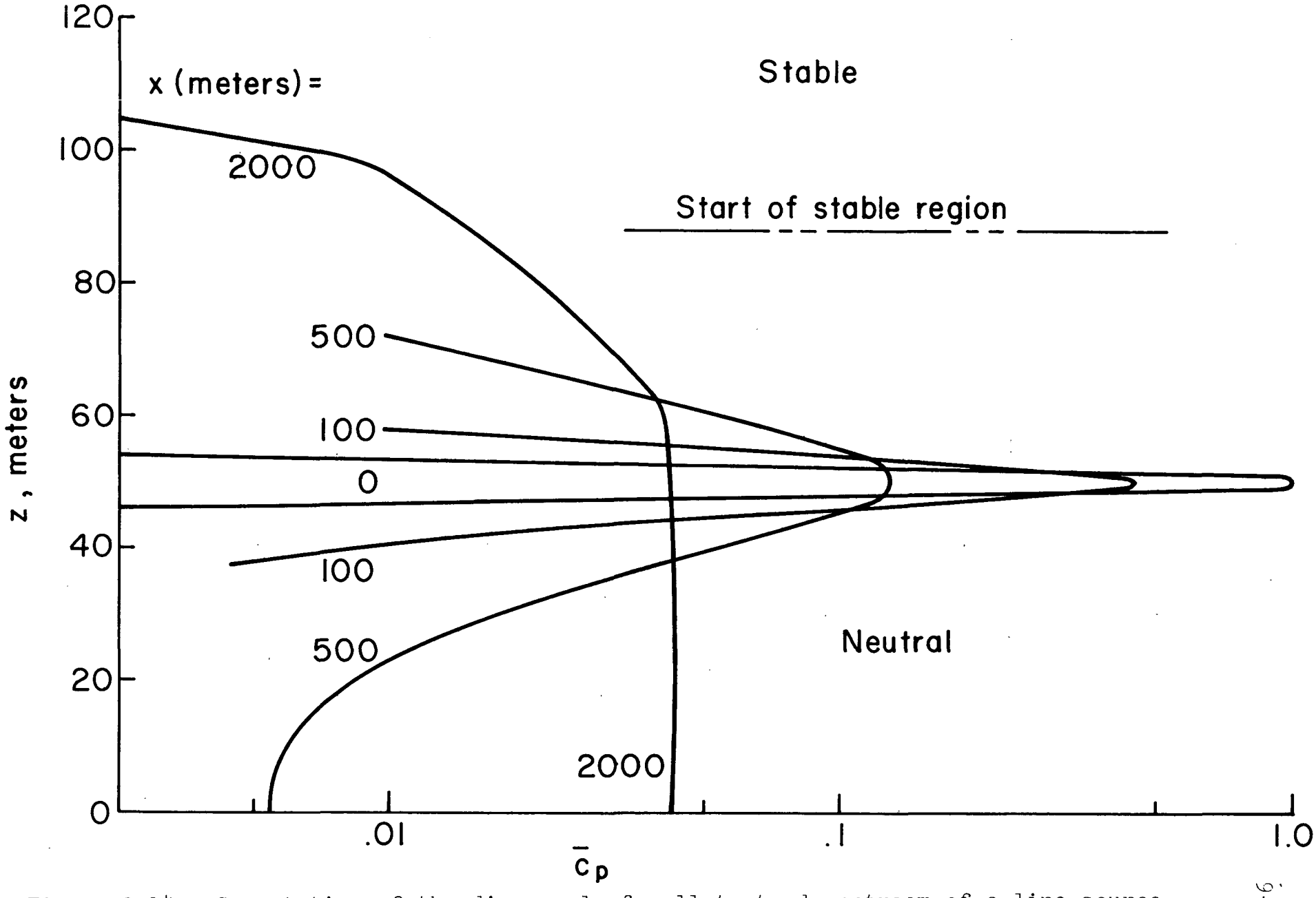

Figure 9.14. Computation of the dispersal of pollutant downstream of a line source below a layer of stable air

distances of the order of 500 meters from the source which is at a height of 50 meters, the ground has played an important role in increasing the levels of concentration. Between 500 and 2000 meters from the source, it is easy to see that the region of stable air has formed an effective lid on the dispersal of pollutants, and the distribution of pollutants has become almost uniform below this stable region at 2000 meters from the source. In order to see a significant decrease in this level of pollutant concentration, the computations would have to be run to enormous distances downstream from the source because of the very slow leakage of pollutants through the stabilized region. Indeed, for strongly stabilized regions, calculations such as those described here show that the only real hope for reduction of pollution levels is a change in atmospheric conditions.

It is hoped that this brief description of the calculation of pollutant dispersal by invariant modeling of the second-order correlation equations has served to demonstrate the power of this new method. While there are several improvements that must be added before this second-order closure method can be considered complete, there is no question but what the model will enable one to make computations of pollutant dispersal for a number of cases for which no reliable methods have been available in the past. Before discussing what some of these improvements in the overall model might be, we will complete our discussion of pollutant dispersal by considering the problem of dispersal from a point source of pollutant.

10. DISPERSAL OF POLLUTANTS FROM A POINT SOURCE

In this section we will consider the dispersal of pollutants from a point source. We will assume that the background atmosphere is given. For atmospheric boundary layers, we may again use solutions of the form used in the previous section, namely, $\bar{u} = \bar{u}(z)$, $\bar{v} = 0$, $\bar{w} = 0$, $\overline{u_i'u_k'} = \overline{u_i'u_k'}(z)$, $\overline{u_i'T'} = \overline{u_i'T'}(z)$, and $\overline{T'^2} = \overline{T'^2}(z)$. If we consider a point source of pollution for such flows, the distribution of pollutant downstream of the source is steady (if the source is steady) and is of the form $\bar{C}_p = \bar{C}_p(x,y,z)$. If we again make the boundary layer or, in this case, the thin plume assumption, we may neglect derivatives of quantities with respect to x in comparison with the same derivatives with respect to y and z. In this case the equations which govern our problem are

$$\bar{u}\frac{\partial \bar{C}_p}{\partial x} = \upsilon_o\left(\frac{\partial^2 \bar{C}_p}{\partial y^2} + \frac{\partial^2 \bar{C}_p}{\partial z^2}\right) - \frac{\partial}{\partial y}\left(\overline{C_p'v'}\right) - \frac{\partial}{\partial z}\left(\overline{C_p'w'}\right) \tag{10.1}$$

$$\begin{aligned}\bar{u}\frac{\partial \overline{C_p'v'}}{\partial x} = &- \overline{v'v'}\frac{\partial \bar{C}_p}{\partial y} + \frac{\partial}{\partial y}\left[\left(2\Lambda_{2_c} + \Lambda_{3_c}\right) q \frac{\partial \overline{C_p'v'}}{\partial y}\right] \\ &+ \frac{\partial}{\partial z}\left(\Lambda_{2_c} q \frac{\partial \overline{C_p'v'}}{\partial z}\right) + \frac{\partial}{\partial z}\left(\Lambda_{2_c} q \frac{\partial \overline{C_p'w'}}{\partial y}\right) \\ &+ \frac{\partial}{\partial y}\left(\Lambda_{3_c} q \frac{\partial \overline{C_p'w'}}{\partial z}\right) - \frac{q}{\Lambda_{1_c}}\overline{C_p'v'} \\ &+ \upsilon_o\left(\frac{\partial^2 \overline{C_p'v'}}{\partial y^2} + \frac{\partial^2 \overline{C_p'v'}}{\partial z^2}\right) - 2\upsilon_o \frac{\overline{C_p'v'}}{\lambda_c^2}\end{aligned} \tag{10.2}$$

$$\bar{u}\frac{\partial\overline{C'_p w'}}{\partial x} = -\overline{w'w'}\frac{\partial\bar{C}_p}{\partial z} + \frac{g}{T_o}\overline{C'_p T'} + \frac{\partial}{\partial z}\left[\left(2\Lambda_{2_c} + \Lambda_{3_c}\right) q \frac{\partial\overline{C'_p w'}}{\partial z}\right]$$

$$+ \frac{\partial}{\partial y}\left(\Lambda_{2_c} q \frac{\partial\overline{C'_p w'}}{\partial y}\right) + \frac{\partial}{\partial y}\left(\Lambda_{2_c} q \frac{\partial\overline{C'_p v'}}{\partial z}\right)$$

$$+ \frac{\partial}{\partial z}\left(\Lambda_{3_c} q \frac{\partial\overline{C'_p v'}}{\partial y}\right) - \frac{q}{\Lambda_{1_c}}\overline{C'_p w'}$$

$$+ \upsilon_o\left(\frac{\partial^2\overline{C'_p w'}}{\partial y^2} + \frac{\partial^2\overline{C'_p w'}}{\partial z^2}\right) - 2\upsilon_o\frac{\overline{C'_p w'}}{\lambda_c^2} \qquad (10.3)$$

$$\bar{u}\frac{\partial\overline{C'_p T'}}{\partial x} = -\overline{w'T'}\frac{\partial\bar{C}_p}{\partial z} - \overline{w'C'_p}\frac{\partial\bar{T}}{\partial z}$$

$$+ \frac{\partial}{\partial y}\left(\Lambda_{2_c} q \frac{\partial\overline{C'_p T'}}{\partial y}\right) + \frac{\partial}{\partial z}\left(\Lambda_{2_c} q \frac{\partial\overline{C'_p T'}}{\partial z}\right)$$

$$+ \upsilon_o\left(\frac{\partial^2\overline{C'_p T'}}{\partial y^2} + \frac{\partial^2\overline{C'_p T'}}{\partial z^2}\right) - 2\upsilon_o\frac{\overline{C'_p T'}}{\lambda_c^2} \qquad (10.4)$$

$$\bar{u}\frac{\partial\overline{C'^2_p}}{\partial x} = -2\overline{v'C'_p}\frac{\partial\bar{C}_p}{\partial y} - 2\overline{w'C'_p}\frac{\partial\bar{C}_p}{\partial z}$$

$$+ \frac{\partial}{\partial y}\left(\Lambda_{2_c} q \frac{\partial\overline{C'^2_p}}{\partial y}\right) + \frac{\partial}{\partial z}\left(\Lambda_{2_c} q \frac{\partial\overline{C'^2_p}}{\partial z}\right)$$

$$+ \upsilon_o\left(\frac{\partial^2\overline{C'^2_p}}{\partial y^2} + \frac{\partial^2\overline{C'^2_p}}{\partial z^2}\right) - 2\upsilon_o\frac{\overline{C'^2_p}}{\lambda_c^2} \qquad (10.5)$$

A digital computer program has been developed which can simultaneously solve (10.1), (10.2), (10.3), and (10.4) for the mean concentration $\overline{C}_p(x,y,z)$ downstream of a steady source when the background mean and turbulence fields are known. In the process, of course, the distributions $\overline{C_p'v'}(x,y,z)$, $\overline{C_p'w'}(x,y,z)$ and $\overline{C_p'T'}(x,y,z)$ are obtained. With these results in hand, (10.5) may be solved for the distribution $\overline{C_p'^2}(x,y,z)$.

As is the case for the other digital programs mentioned in this report, an outline of the numerical techniques used to construct the program is given in Appendix A which is dedicated to this subject. Here we must note that the program required to accomplish this task is a very large one and, in its development and check out, an uncommonly large number of "bugs" emerged. Most of these bugs have been eliminated, but the program is not yet operational in all possible modes and options. In particular, the existence of the cross-derivative terms in the equations for the second-order velocity-concentration correlations still leads to certain difficulties in obtaining smooth solutions.

We may demonstrate the nature of the solutions that are generated by second-order modeling at this time, however, by the choice of a special turbulence model. It is clear from an examination of (10.2) and (10.3) that if we choose a turbulence model in which $\Lambda_{2_c} = 0.1\Lambda_{1_c}$ and $\Lambda_{3_c} = -\Lambda_{2_c}$, the cross-derivative terms in (10.2) and (10.3) are eliminated. This assumption, for the two-dimensional concentration layers studied in the previous section, has an effect almost analogous to making Λ_{2_c} and Λ_{3_c} somewhat smaller compared to Λ_{1_c} than the usual value of 0.1. For this reason, it is felt that the solutions that will be discussed below are representative solutions and should exhibit the nature of pollution dispersal solutions generated by invariant modeling techniques. At present, every effort is being made to clear up the difficulty that is occasioned by the retention of the cross-derivative terms in the equations. It is hoped that this difficulty will be resolved in the very near future.

To examine the nature of these solutions and to enable one to compare the results of computations of both line and point source dispersal, we shall compute the dispersal of an initially Gaussian concentration of pollutants into the same homogeneous and isotropic turbulent background atmosphere that was used in the calculations presented in Figure 9.5. For this case, $\bar{u}$ = 10 meters/second, $\sqrt{\overline{u'^2}} = \sqrt{\overline{v'^2}} = \sqrt{\overline{w'^2}}$ = 1 meter/second, and Λ_{1_t} = 15 meters. We will again assume that no transport correlations $\overline{C_p'v'}$ or $\overline{C_p'w'}$ exist at $x = 0$. The initial Gaussian profile used has the same half-breadth as before, namely, 0.929 meters.

In Figure 10.1 we show the behavior of the maximum concentration $\bar{C}_{p_{max}}$ as a function of distance from the source of pollutants. For the case shown here, in order for the results to be comparable to one of the line source dispersals presented in Figure 9.5, we have again chosen $\Lambda_{1_c} = b$ for $\Lambda_{1_c} \leq \Lambda_{1_t}$ and $\Lambda_{1_c} = \Lambda_{1_t}$ for $b > \Lambda_{1_t}$. It is seen from Figure 10.1 that after an initial formative stage of essentially the same duration as that for the line source, the maximum concentration drops off as x^{-2}. In this mid-region of decay, the half-breadth of the plume is less than Λ_{1_t}. At a point x = 429 meters from the source, the half-breadth becomes equal to Λ_{1_t}. Shortly thereafter, the fall off in $\bar{C}_{p_{max}}$ becomes proportional to x^{-1}. This is analogous to the behavior found for the line source when $\bar{C}_{p_{max}}$ as initially proportional to x^{-1} and finally proportional to $x^{-1/2}$. In both cases, this behavior is due to the fact that the half-breadth of the sheet or plume in question grows initially as x and finally as $x^{1/2}$. In Figure 10.2, we show this behavior for both the line source and the point source by plotting the effective spread σ_z of the sheet or plume of pollutants as a function of x for the same background turbulent conditions used for Figure 10.1. Here σ_z is defined as

$$\sigma_z = \left(\frac{\int_{+\infty}^{-\infty} (z - z_o)^2 C_p(x,0,z)\, dz}{\int_{-\infty}^{+\infty} C_p(x,0,z)\, dz} \right)^{1/2} \qquad (10.6)$$

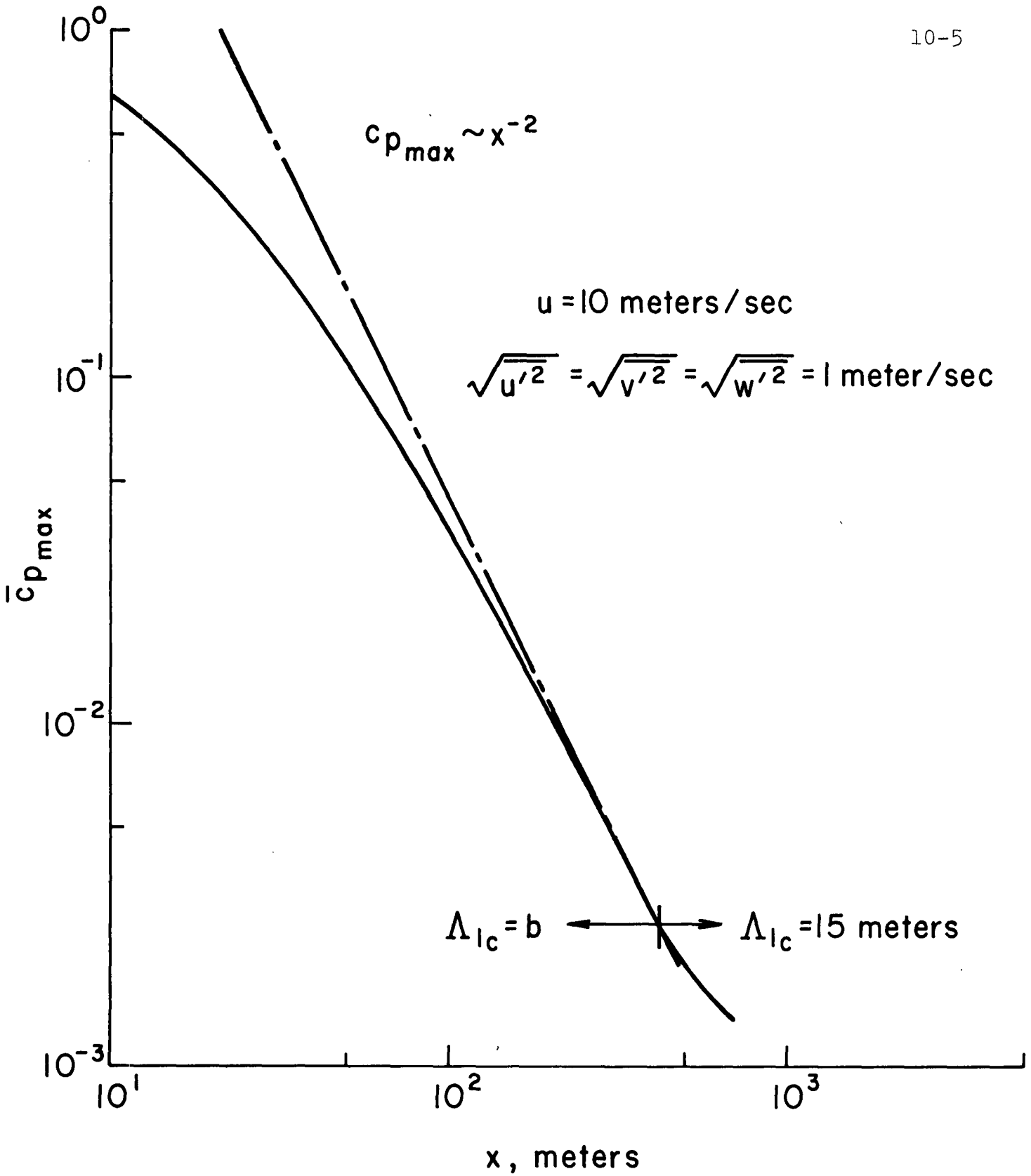

Figure 10.1. Decay of pollutant concentration downstream of a point source

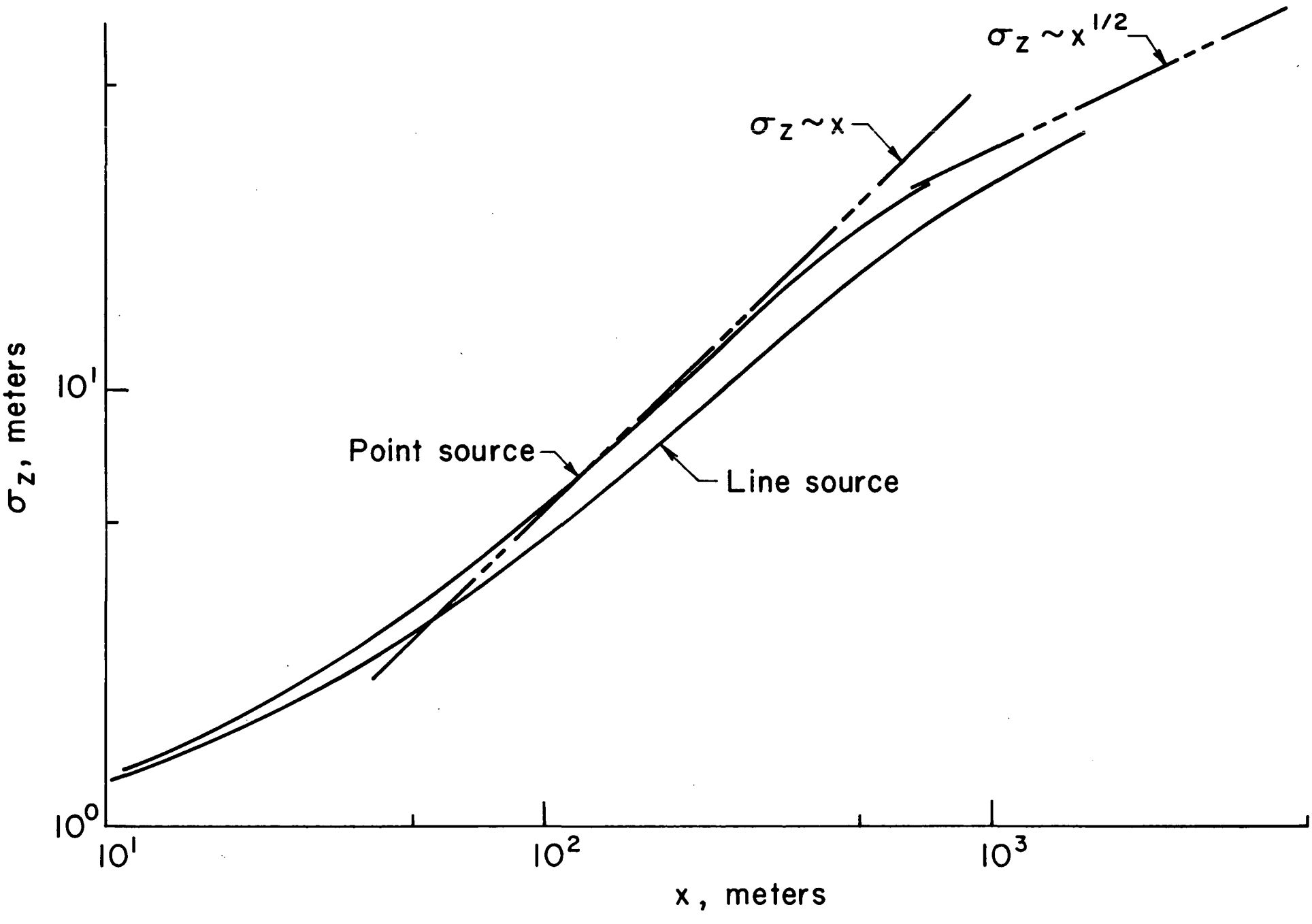

Figure 10.2. Comparison of the spread of pollutants from point and line sources for $\sqrt{\overline{u'^2}} = \sqrt{\overline{v'^2}} = \sqrt{\overline{w'^2}} = 0.1\bar{u}$ and $\Lambda_{1_t} = 15$ meters

The results shown in Figure 10.2 show the very great similarity between the spreading rates for line and point sources that is predicted by the present model of turbulent diffusion.

In Figure 10.3 are shown the central mean concentration profiles for this case of point source dispersal. Figure 10.4 shows the behavior on a traverse through the center of the plume. of $\overline{C}_p(z)$ and $\overline{C'_p w'}(z)$ at 100 meters from the source.

We may compare the results of computations such as those just presented with experimental data. In Figure 10.5, we have plotted the behavior of the spread of pollutants downstream from the source we have described for three cases of atmospheric turbulence: $\sigma_\theta \bar{u} = 2$, $\sigma_\theta \bar{u} = 1$, and $\sigma_\theta \bar{u} = 0.2$. Here $\sigma_\theta = \sqrt{\overline{u'^2}}/\bar{u} = \sqrt{\overline{v'^2}}/\bar{u} = \sqrt{\overline{w'^2}}/\bar{u}$. The results of these computations are compared in Figure 10.5 with the experimental results of Fuquay, Simpson, and Hinds [Ref. 35]. It is seen that the rates of spread predicted by the computations are within a factor of two of the experimental results in the mid-range of decay. The departure of the computed results from experiment for breadths greater than 15 meters might be due to two causes. It might be that the background scale of turbulence Λ_{1_t} was greater than 15 meters or it might be, if Λ_{1_t} is actually of the order of 15 meters, that one must assume that the proper Λ_{1_c} to use in the computations should be equal to the half-breadth of the plume until Λ_{1_c} is quite a bit larger than Λ_{1_t} before setting Λ_{1_c} equal to a constant times Λ_{1_t}. In view of our calculations of atmospheric turbulence in Section 8, it would appear that Λ_{1_t} for the experiments in questions was not greater than 15 meters. We must therefore conclude that the second reason for the departure is the correct one. In future studies it will be necessary to pin down the precise point at which the scale Λ_{1_c} departs from the half-breadth b and becomes proportional to the scale of the background turbulence and to determine the magnitude of this constant of proportionality.

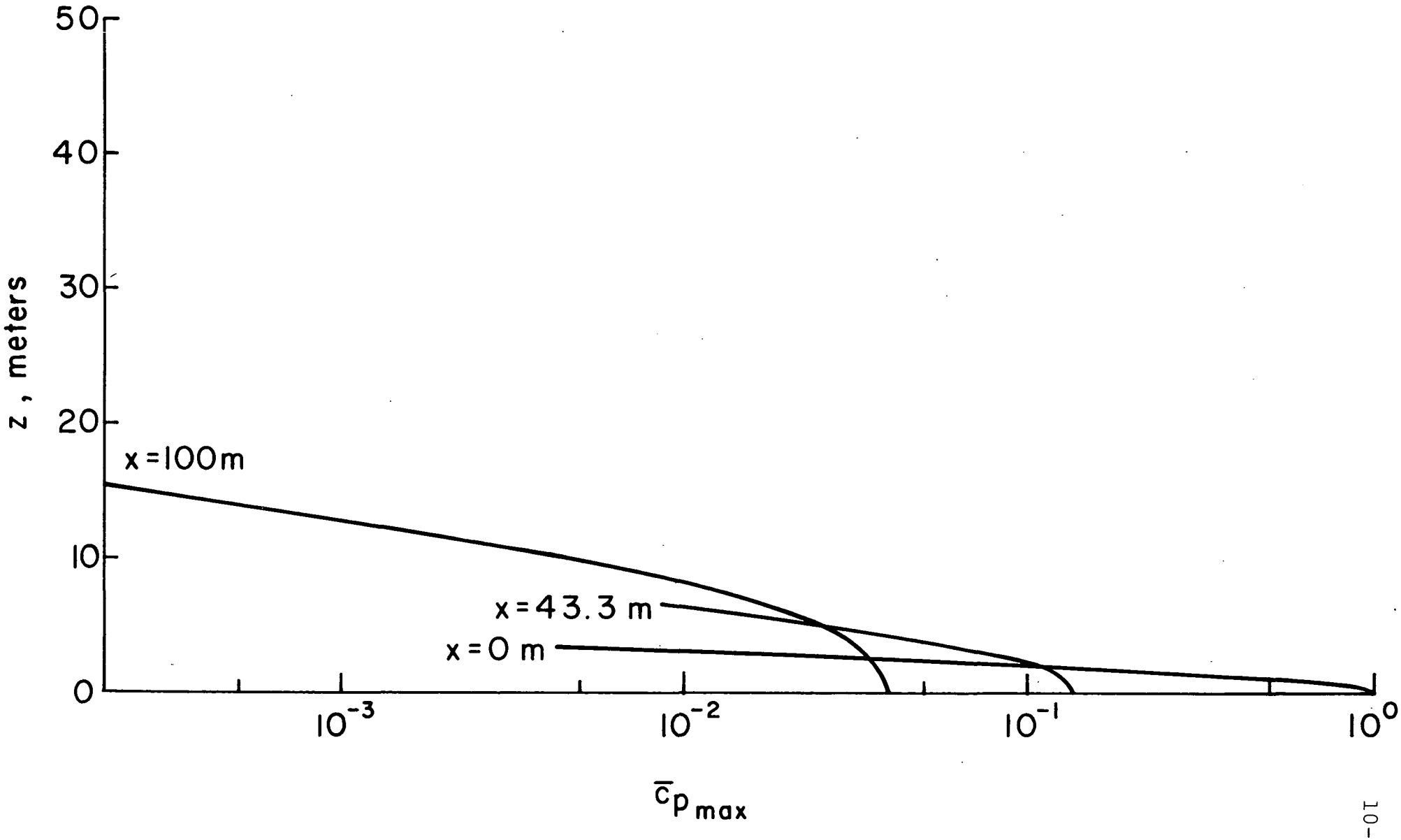

Figure 10.3. Central mean concentration profiles at various distances downstream of a source when $\sqrt{\overline{u'^2}} = \sqrt{\overline{v'^2}} = \sqrt{\overline{w'^2}} = 0.1\bar{u}$ and $\Lambda_{1_t} = 15$ meters

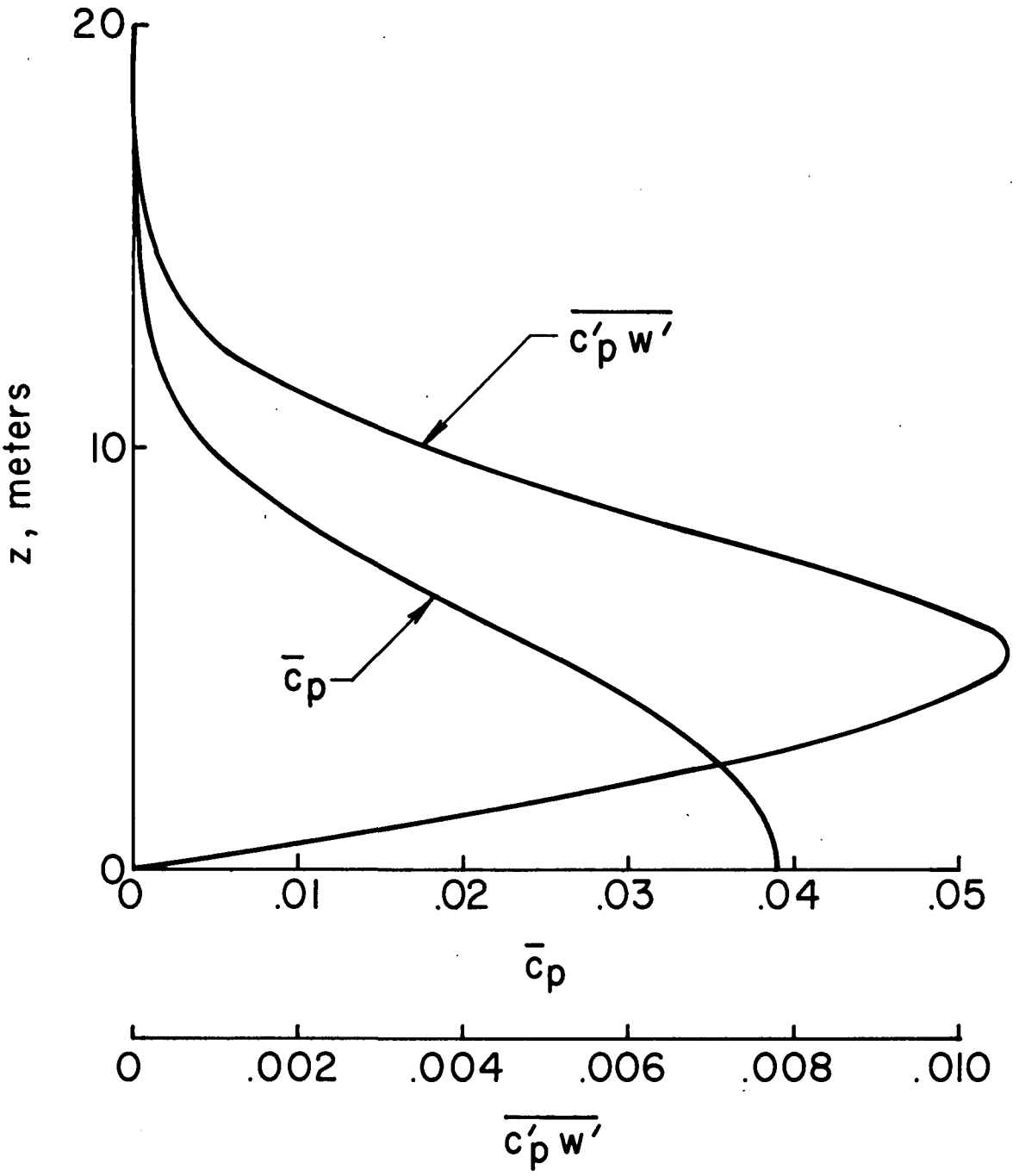

Figure 10.4. Distributions of $\bar{C}_p$ and $\overline{C'_p w'}$ at x = 100 meters for dispersal from the point source shown in Figure 10.1

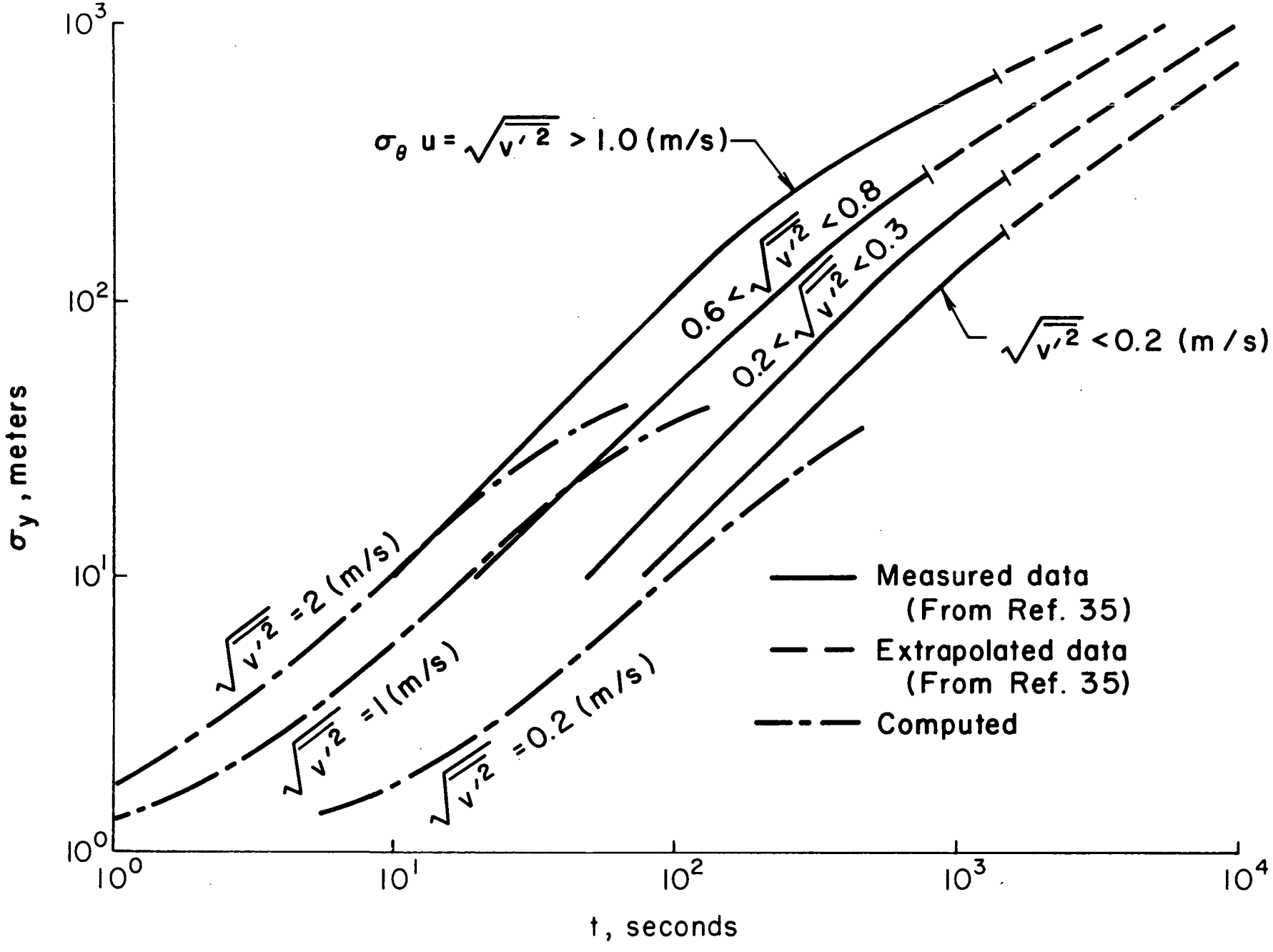

Figure 10.5. Comparison of measured and calculated lateral spreads σ_y as a function of time. Data are from Ref. 35.

11. CRITIQUE OF ATMOSPHERIC TURBULENCE AND POLLUTION DISPERSAL CALCULATIONS

In the previous three sections, we have outlined the characteristics of a new method of handling the computation of the structure of atmospheric turbulence near the surface of the earth and the dispersal of a passive pollutant in such a turbulent field. It is clear that in order to carry out such calculations, it is necessary to know the magnitude of certain scalar lengths (the Λ_1 's) that enter into the formulation of the equations for the second-order correlations necessary to calculate the mean fields of velocity, temperature, and species concentration. It was pointed out in Section 6 that it is possible to obtain equations for these lengths that can be solved simultaneously with the sets of equations we have solved in the previous three sections so as to have a closure of the turbulent problem. The construction of such equations and their incorporation into our computational programs is, of course, an item of high priority in the further development of our method. For the time being, however, we will continue to study the nature of turbulent flows by invariant second-order modeling under the assumption that we can find suitable scales associated with the distributions of the mean variables $\bar{u}$, $\overline{T}$, and $\overline{C}_\alpha$ that will enable us to make meaningful calculations of turbulent flows that are of importance in engineering and which have heretofore been intractable. In all the problems, except one, that we have discussed in the previous sections, there have always been lengths associated with the mean profiles that were available on which to base the Λ_1 's that are required for the computations. For a free jet and a two-dimensional shear layer, there were the half-breadths of the layers in question. For the classical boundary layer, the boundary layer thickness was available. Near a solid surface it was shown that the Λ_1 's involved must behave in a particular manner, namely, proportional to the distance from the surface. For the spread of a pollutant, we always have available a local breadth associated

with the mean concentration profile. Only in the case of the atmospheric surface layer, as studied in Section 8, was there no scale available on which to base a calculation as one moved away from the surface to a region where Λ_1 was no longer proportional to z, the distance from the earth's surface. Surely there must be some appropriate length. It is not the Monin-Obukhov length, for this length does not determine a solution but merely correlates solutions once the magnitudes of heat transfer and shear are known. The answer to this question is not to be found in the equations we have studied to date. It must be sought in the more complete equations that govern the motion of the atmosphere on our rotating earth. Indeed, the missing outer scale required for the surface layer calculations discussed in Section 8 must be determined by the balance of centrifugal (Coriolis) and pressure forces that determine the thickness of the Ekman layer. For planetary boundary layer calculations, it is the scale of the Ekman layer that ultimately determines, in conjunction with surface roughness, the actual values of surface shear and heat transfer under any given conditions of surface heating or cooling. The lowest surface layer can then exhibit Monin-Obukhov similarity based on the length determined from the relative magnitudes of $\overline{w'T'}$ and $\overline{u'w'}$ near the surface. This behavior is very similar to the behavior of the classical turbulent boundary layer on a flat plate. In this case, there is a similarity near the wall (the law of the wall) which is based on the level of shear near the wall (see Figure 5.15). The actual magnitude of this shear is not determined until the whole boundary layer thickness δ is known even though this thickness may be orders of magnitude larger than the region of the boundary layer where the law of the wall is valid.

In view of the above discussion, we shall take up in the next section the calculation of the entire Ekman layer by the methods discussed in this report. Before going on to this, however, we should discuss what might be done to improve the accuracy of the basic model with which the calculations reported here have been carried out.

It is clear from the way in which the model was constructed that the model was carefully tailored to give good results for the mean and turbulent velocity fields that have been carefully measured for certain classical shear flows. Due to the paucity of experimental data on the behavior of temperature fluctuations in turbulent shear flows, it was assumed that the model valid for velocity fields could, for the purposes of evaluating the potential of the method, be taken over directly to the calculation of temperature-velocity and temperature-temperature correlations. An indication that this is not true is the inability of the atmospheric turbulence calculations presented in Section 8 to properly account for the magnitude of $\overline{T'^2}$. Also, the very high value of critical Richardson number obtained in the discussion of superequilibrium theory in Section 7 is an indication that the modeling may not be quite right. It has been found that a slight reduction in the magnitude of the tendency-towards-isotropy term $\overline{u_i'T'}$ equation compared to this tendency in the $\overline{u_i'u_k'}$ equation has a pronounced lowering effect upon the critical Richardson number found by superequilibrium calculation.

The high value of critical Richardson number obtained by superequilibrium analysis cannot be taken too seriously by itself, for this analysis neglects the effect of diffusion which actually does play an important role in determining the balance of production and loss of a given correlation at a point in actual computations. All that we can say at this time is that a further study of the modeling of the temperature correlation equations needs to be made. How might this be accomplished? If, indeed, the equations we have been using contain an adequate description of atmospheric turbulence, then one should be able to obtain from these equations the Monin-Obukhov similarity theory. If this can be done, the agreement of the computed Monin-Obukhov functions with the functions derived from actual measurements might be used to select a more appropriate model.

My colleague, Dr. W. Stephen Lewellen, has recently succeeded in deriving the whole of Monin-Obukhov similarity theory and the Monin-Obukhov functions from the model equations given in the previous sections [see Ref. 36]. A complete discussion of this development is beyond the scope of this report; the reader is referred to Ref. 36 for details. It is sufficient to say here that this new development opens up a very fruitful approach to the problem of improving the modeling of the temperature correlation equations.

Let us turn now to a discussion of the calculation of the Ekman layer and the dispersal of passive pollutants in such a layer.

12. INVARIANT MODELING OF THE EKMAN LAYER

In this section we will discuss the calculation of the complete planetary boundary layer and the dispersal of passive pollutants in such a layer by the technique of invariant modeling. We will start by writing, as is customary, the equations of motion for the planetary atmosphere with respect to a Cartesian coordinate system at rest relative to a point on the earth's surface. The x axis is taken to be the direction of constant latitude and positive in an easterly direction, the y axis is taken positive in the direction of north, and the z axis positive in a direction normal to a geopotential surface at the surface of the earth. In this coordinate system (x, y, z), let the velocities be (u, v, w). The equations of motion for velocities small compared to the surface rotational speed of the earth are then [see, for example, Ref. 37],

$$\frac{\partial \tilde{\rho}}{\partial t} + \frac{\partial}{\partial x}(\tilde{\rho}u) + \frac{\partial}{\partial y}(\tilde{\rho}v) + \frac{\partial}{\partial z}(\tilde{\rho}w) = 0 \tag{12.1}$$

$$\tilde{\rho}\frac{Du}{Dt} = -\frac{\partial \tilde{p}}{\partial x} + 2\tilde{\rho}\Omega\,(v \sin\phi - w\cos\phi) + \frac{\partial}{\partial x}\tau_{xx} + \frac{\partial}{\partial y}\tau_{xy} + \frac{\partial}{\partial z}\tau_{xz} \tag{12.2}$$

$$\tilde{\rho}\frac{Dv}{Dt} = -\frac{\partial \tilde{p}}{\partial y} - 2\tilde{\rho}\Omega\, u \sin\phi + \frac{\partial}{\partial x}\tau_{xy} + \frac{\partial}{\partial y}\tau_{yy} + \frac{\partial}{\partial z}\tau_{yz} \tag{12.3}$$

$$\tilde{\rho}\frac{Dw}{Dt} = -\frac{\partial \tilde{p}}{\partial z} - \tilde{\rho}g + 2\tilde{\rho}\Omega\, u\cos\phi + \frac{\partial}{\partial x}\tau_{xz} + \frac{\partial}{\partial y}\tau_{yz} + \frac{\partial}{\partial z}\tau_{zz} \tag{12.4}$$

$$\tilde{\rho} C_p \frac{D\tilde{T}}{Dt} = \frac{\partial \tilde{p}}{\partial t} + u_j \frac{\partial \tilde{p}}{\partial x_j} + \frac{\partial}{\partial x_j}\left(k \frac{\partial \tilde{T}}{\partial x_j} \right) \tag{12.5}$$

In these equations, Ω is the angular velocity of the earth, ϕ is the latitude, and

$$\tau_{ij} = \mu \left(\frac{\partial u_i}{\partial x_j} + \frac{\partial u_j}{\partial x_i} \right) + \delta_{ij} \lambda \frac{\partial u_k}{\partial x_k} \tag{12.6}$$

In order to make contact with the studies we have made in the previous sections, we will not use these equations directly but will assume that the Boussinesq approximation that the Prandtl and Schmidt numbers are one holds, and that variations of the coefficients of viscosity will not seriously affect any computation we will make so that (12.1) through (12.6) may be approximated by

$$\frac{\partial u}{\partial x} + \frac{\partial v}{\partial y} + \frac{\partial w}{\partial z} = 0 \tag{12.7}$$

$$\frac{Du}{Dt} = - \frac{1}{\rho_o} \frac{\partial p}{\partial x} + 2\Omega \, (v \sin \phi - w \cos \phi) + \nu_o \left(\frac{\partial^2 u}{\partial x^2} + \frac{\partial^2 u}{\partial y^2} + \frac{\partial^2 u}{\partial z^2} \right) \tag{12.8}$$

$$\frac{Dv}{Dt} = - \frac{1}{\rho_o} \frac{\partial p}{\partial y} - 2\Omega \, u \sin \phi + \nu_o \left(\frac{\partial^2 v}{\partial x^2} + \frac{\partial^2 v}{\partial y^2} + \frac{\partial^2 v}{\partial z^2} \right) \tag{12.9}$$

$$\frac{Dw}{Dt} = - \frac{1}{\rho_o} \frac{\partial p}{\partial z} - \rho g + 2\Omega u \cos \phi + \nu_o \left(\frac{\partial^2 w}{\partial x^2} + \frac{\partial^2 w}{\partial y^2} + \frac{\partial^2 w}{\partial z^2} \right) \tag{12.10}$$

$$\frac{DT}{Dt} = \nu_o \left(\frac{\partial^2 T}{\partial x^2} + \frac{\partial^2 T}{\partial y^2} + \frac{\partial^2 T}{\partial z^2} \right) \tag{12.11}$$

$$\rho = - \frac{\rho_o}{T_o} T \tag{12.12}$$

where we recall (see definition (2.10)) that

$$T = \tilde{T} - T_o \tag{12.13}$$

These equations are identical to the basic equations used earlier in this report (see Section 3, Eqs. (3.4), (3.5), (3.7), (3.8)) to describe the atmospheric motion in the surface layer except for the Coriolis terms which contain the earth's rotation Ω . This being the case, we may very easily derive the terms we must add to our second-order closure model of turbulence to account for the effect of these terms.

It is clear that the terms that are added to the three mean momentum equations by the inclusion of Coriolis forces are:

In the equation for $\bar{u}$, a term on the right-hand side equal to

$$2\Omega(\bar{v} \sin \phi - \bar{w} \cos \phi)$$

In the equation for $\bar{v}$, a term on the right-hand side equal to

$$-2\Omega\bar{u} \sin \phi$$

In the equation for $\bar{w}$, a term on the right-hand side equal to

$$2\Omega\bar{u} \cos \phi$$

To obtain the term to be added to the $\overline{u'u'}$ equation, it will be recalled that the equation for $\overline{u'u'}$ was obtained from the equation for u' by multiplying this equation by $2u'$ and averaging the result. It is clear, then, that the term to be added to the right-hand side of the $\overline{u'u'}$ equation is

$$4\Omega(\overline{u'v'} \sin \phi - \overline{u'w'} \cos \phi)$$

Likewise the terms to be added to the right-hand sides of the $\overline{v'v'}$ and $\overline{w'w'}$ equations are, respectively,

$$-4\Omega\overline{u'v'}\sin\phi$$

$$4\Omega\overline{u'w'}\cos\phi$$

To obtain the term to be added to the right-hand side of the equation for $\overline{u'w'}$, recall that this equation was obtained by multiplying the equation for u' by w' and the equation for w' by u' and adding the resulting equations. Following this procedure with the new terms that must be included, we find that we must include a term on the right-hand side of the $\overline{u'w'}$ equation equal to

$$2\Omega\left(\overline{v'w'}\sin\phi - \overline{w'^2}\cos\phi + \overline{u'^2}\cos\phi\right)$$

Likewise for the equation for $\overline{u'v'}$, we have

$$2\Omega\left(\overline{v'^2}\sin\phi - \overline{v'w'}\cos\phi - \overline{u'^2}\sin\phi\right)$$

and for the $\overline{v'w'}$ equation

$$2\Omega(-\overline{w'u'}\sin\phi + \overline{u'v'}\cos\phi)$$

The equation for $\overline{T}$ is unchanged since no Coriolis terms appear in this equation. However, in the equations for $\overline{u'T'}$ $\overline{v'T'}$, and $\overline{w'T'}$, there will be terms that result from the earth's rotation. These terms are:

In the equation for $\overline{u'T'}$

$$2\Omega(\overline{v'T'}\sin\phi - \overline{w'T'}\cos\phi)$$

In the equation for $\overline{v'T'}$

$$-2\Omega\overline{u'T'}\sin\phi$$

In the equation for $\overline{w'T'}$

$$2\Omega\overline{u'T'}\cos\phi$$

Since the equation for $\overline{T}$ is unchanged, there will be no new terms appearing in the equation for $\overline{T'^2}$ as a result of the

It is evident from an inspection of all the terms that must be added to our system of equations to account for the rotation of the earth that only second-order correlations themselves appear. Therefore, the inclusion of these terms requires no additional modeling.

If these additional terms are added to the modeled equations derived in Section 4, we obtain a set of equations suitable for computing the planetary boundary layer. These equations are

$$\frac{\partial \bar{u}}{\partial x} + \frac{\partial \bar{v}}{\partial y} + \frac{\partial \bar{w}}{\partial z} = 0 \tag{12.14}$$

$$\begin{aligned}\frac{D\bar{u}}{Dt} = &- \frac{1}{\rho_o}\frac{\partial \bar{p}}{\partial x} + 2\Omega(\bar{v}\sin\phi - \bar{w}\cos\phi) \\ &+ \nu_o\left(\frac{\partial^2\bar{u}}{\partial x^2} + \frac{\partial^2\bar{u}}{\partial y^2} + \frac{\partial^2\bar{u}}{\partial z^2}\right) \\ &- \frac{\partial}{\partial x}(\overline{u'u'}) - \frac{\partial}{\partial y}(\overline{u'v'}) - \frac{\partial}{\partial z}(\overline{u'w'})\end{aligned} \tag{12.15}$$

$$\begin{aligned}\frac{D\bar{v}}{Dt} = &- \frac{1}{\rho_o}\frac{\partial \bar{p}}{\partial y} - 2\Omega\bar{u}\sin\phi \\ &+ \nu_o\left(\frac{\partial^2\bar{v}}{\partial x^2} + \frac{\partial^2\bar{v}}{\partial y^2} + \frac{\partial^2\bar{v}}{\partial z^2}\right) \\ &- \frac{\partial}{\partial x}(\overline{v'u'}) - \frac{\partial}{\partial y}(\overline{v'v'}) - \frac{\partial}{\partial z}(\overline{v'w'})\end{aligned} \tag{12.16}$$

$$\begin{aligned}\frac{D\bar{w}}{Dt} = &- \frac{1}{\rho_o}\frac{\partial \bar{p}}{\partial z} - \frac{\rho}{\rho_o}g + 2\Omega\bar{u}\cos\phi \\ &+ \nu_o\left(\frac{\partial^2\bar{w}}{\partial x^2} + \frac{\partial^2\bar{w}}{\partial y^2} + \frac{\partial^2\bar{w}}{\partial z^2}\right) \\ &- \frac{\partial}{\partial x}(\overline{w'u'}) - \frac{\partial}{\partial y}(\overline{w'v'}) - \frac{\partial}{\partial z}(\overline{w'w'})\end{aligned} \tag{12.17}$$

$$\frac{D\bar{T}}{Dt} = \nu_o \left(\frac{\partial^2 \bar{T}}{\partial x^2} + \frac{\partial^2 \bar{T}}{\partial y^2} + \frac{\partial^2 \bar{T}}{\partial z^2} \right) - \frac{\partial}{\partial x} (\overline{u'T'}) - \frac{\partial}{\partial y} (\overline{v'T'}) - \frac{\partial}{\partial z} (\overline{w'T'}) \tag{12.18}$$

$$\begin{aligned} \frac{D\overline{u'u'}}{Dt} = {} & 4\Omega(\overline{u'v'} \sin \phi - \overline{u'w'} \cos \phi) - 2\overline{u'_j u'} \frac{\partial \bar{u}}{\partial x_j} \\ & + \frac{\partial}{\partial x_j} \left[\Lambda_{2_t} q \left(2 \frac{\partial \overline{u'u'_j}}{\partial x} + \frac{\partial \overline{u'u'}}{\partial x_j} \right) \right] \\ & + 2 \frac{\partial}{\partial x} \left(\Lambda_{3_t} q \frac{\partial \overline{u'_j u'}}{\partial x_j} \right) - \frac{q}{\Lambda_{1_t}} \left(\overline{u'u'} - \frac{q^2}{3} \right) \\ & + \nu_o \frac{\partial^2}{\partial x_j^2} \overline{u'u'} - 2\nu_o \frac{\overline{u'u'}}{\lambda_t^2} \end{aligned} \tag{12.19}$$

$$\begin{aligned} \frac{D\overline{v'v'}}{Dt} = {} & -4\Omega \overline{u'v'} \sin \phi - 2\overline{v'u'_j} \frac{\partial \bar{v}}{\partial x_j} \\ & + \frac{\partial}{\partial x_j} \left[\Lambda_{2_t} q \left(2 \frac{\partial \overline{v'u'_j}}{\partial y} + \frac{\partial \overline{v'v'}}{\partial x_j} \right) \right] \\ & + 2 \frac{\partial}{\partial y} \left(\Lambda_{3_t} q \frac{\partial \overline{u'_j v'}}{\partial x_j} \right) - \frac{q}{\Lambda_{1_t}} \left(\overline{v'v'} - \frac{q^2}{3} \right) \\ & + \nu_o \frac{\partial^2}{\partial x_j^2} \overline{v'v'} - 2\nu_o \frac{\overline{v'v'}}{\lambda_t^2} \end{aligned} \tag{12.20}$$

$$\frac{D\overline{w'w'}}{Dt} = 4\Omega\overline{u'w'}\cos\phi + \frac{2g}{T_o}\overline{w'T'} - 2\overline{w'u_j'}\frac{\partial\bar{w}}{\partial x_j}$$

$$+ \frac{\partial}{\partial x_j}\left[\Lambda_{2_t} q\left(2\frac{\partial\overline{w'u_j'}}{\partial z} + \frac{\partial\overline{w'w'}}{\partial x_j}\right)\right]$$

$$+ 2\frac{\partial}{\partial z}\left(\Lambda_{3_t} q\frac{\partial\overline{u_j'w'}}{\partial x_j}\right) - \frac{q}{\Lambda_{1_t}}\left(\overline{w'w'} - \frac{q^2}{3}\right)$$

$$+ \nu_o\frac{\partial^2}{\partial x_j^2}\overline{w'w'} - 2\nu_o\frac{\overline{w'w'}}{\lambda_t^2} \qquad (12.21)$$

$$\frac{D\overline{u'v'}}{Dt} = 2\Omega\left(\overline{v'^2}\sin\phi - \overline{v'w'}\cos\phi - \overline{u'^2}\sin\phi\right)$$

$$- \overline{u'u_j'}\frac{\partial\bar{v}}{\partial x_j} - \overline{v'u_j'}\frac{\partial\bar{u}}{\partial x_j}$$

$$+ \frac{\partial}{\partial x_j}\left[\Lambda_{2_t} q\left(\frac{\partial\overline{v'u_j'}}{\partial x} + \frac{\partial\overline{u'u_j'}}{\partial y} + \frac{\partial\overline{u'v'}}{\partial x_j}\right)\right]$$

$$+ \frac{\partial}{\partial x}\left(\Lambda_{3_t} q\frac{\partial\overline{u_j'v'}}{\partial x_j}\right) + \frac{\partial}{\partial y}\left(\Lambda_{3_t} q\frac{\partial\overline{u_j'u'}}{\partial x_j}\right) - \frac{q}{\Lambda_{1_t}}(\overline{u'v'})$$

$$+ \nu_o\frac{\partial^2}{\partial x_j^2}\overline{u'v'} - 2\nu_o\frac{\overline{u'v'}}{\lambda_t^2} \qquad (12.22)$$

$$\frac{D\overline{u'w'}}{Dt} = 2\Omega\left(\overline{v'w'}\sin\phi - \overline{w'^2}\cos\phi + \overline{u'^2}\cos\phi\right)$$

$$- \overline{u'u'_j}\frac{\partial\bar{w}}{\partial x_j} - \overline{w'u'_j}\frac{\partial\bar{u}}{\partial x_j} + \frac{g}{T_o}\overline{u'T'}$$

$$+ \frac{\partial}{\partial x_j}\left[\Lambda_{2_t} q\left(\frac{\partial\overline{w'u'_j}}{\partial x} + \frac{\partial\overline{u'u'_j}}{\partial z} + \frac{\partial\overline{w'w'}}{\partial x_j}\right)\right]$$

$$+ \frac{\partial}{\partial x}\left(\Lambda_{3_t} q\frac{\partial\overline{u'_j w'}}{\partial x_j}\right) + \frac{\partial}{\partial z}\left(\Lambda_{3_t} q\frac{\partial\overline{u'_j u'}}{\partial x_j}\right) - \frac{q}{\Lambda_{1_t}}(\overline{u'w'})$$

$$+ \nu_o\frac{\partial^2}{\partial x_j^2}\overline{u'w'} - 2\nu_o\frac{\overline{u'w'}}{\lambda_t^2} \qquad (12.23)$$

$$\frac{D\overline{v'w'}}{Dt} = 2\Omega(-\overline{w'u'}\sin\phi + \overline{u'v'}\cos\phi)$$

$$- \overline{v'u'_j}\frac{\partial\bar{w}}{\partial x_j} - \overline{w'u'_j}\frac{\partial\bar{v}}{\partial x_j} + \frac{g}{T_o}\overline{v'T'}$$

$$+ \frac{\partial}{\partial x_j}\left[\Lambda_{2_t} q\left(\frac{\partial\overline{v'u'_j}}{\partial z} + \frac{\partial\overline{w'u'_j}}{\partial y} + \frac{\partial\overline{v'w'}}{\partial x_j}\right)\right]$$

$$+ \frac{\partial}{\partial y}\left(\Lambda_{3_t} q\frac{\partial\overline{u'_j w'}}{\partial x_j}\right) + \frac{\partial}{\partial z}\left(\Lambda_{3_t} q\frac{\partial\overline{u'_j v'}}{\partial x_j}\right) - \frac{q}{\Lambda_{1_t}}(\overline{v'w'})$$

$$+ \nu_o\frac{\partial^2}{\partial x_j^2}\overline{v'w'} - 2\nu_o\frac{\overline{v'w'}}{\lambda_t^2} \qquad (12.24)$$

$$\frac{D\overline{u'T'}}{Dt} = 2\Omega(\overline{v'T'}\sin\phi - \overline{w'T'}\cos\phi) - \overline{u'u_j'}\frac{\partial\bar{T}}{\partial x_j} - \overline{T'u_j'}\frac{\partial\bar{u}}{\partial x_j}$$

$$+ \frac{\partial}{\partial x_j}\left[\Lambda_{2_t} q\left(\frac{\partial\overline{u_j'T'}}{\partial x} + \frac{\partial\overline{u'T'}}{\partial x_j}\right)\right]$$

$$+ \frac{\partial}{\partial x}\left(\Lambda_{3_t} q\frac{\partial\overline{u_j'T'}}{\partial x_j}\right) - \frac{q}{\Lambda_{1_t}}\overline{u'T'}$$

$$+ \nu_o\frac{\partial^2}{\partial x_j^2}\overline{u'T'} - 2\nu_o\frac{\overline{u'T'}}{\lambda_t^2} \qquad (12.25)$$

$$\frac{D\overline{v'T'}}{Dt} = -2\Omega\overline{u'T'}\sin\phi - \overline{v'u_j'}\frac{\partial\bar{T}}{\partial x_j} - \overline{T'u_j'}\frac{\partial\bar{v}}{\partial x_j}$$

$$+ \frac{\partial}{\partial x_j}\left[\Lambda_{2_t} q\left(\frac{\partial\overline{u_j'T'}}{\partial y} + \frac{\partial\overline{v'T'}}{\partial x_j}\right)\right]$$

$$+ \frac{\partial}{\partial y}\left(\Lambda_{3_t} q\frac{\partial\overline{u_j'T'}}{\partial x_j}\right) - \frac{q}{\Lambda_{1_t}}\overline{v'T'}$$

$$+ \nu_o\frac{\partial^2}{\partial x_j^2}\overline{v'T'} - 2\nu_o\frac{\overline{v'T'}}{\lambda_t^2} \qquad (12.26)$$

$$\frac{D\overline{w'T'}}{Dt} = 2\Omega\overline{u'T'}\cos\phi - \overline{w'u_j'}\frac{\partial\bar{T}}{\partial x_j} - \overline{T'u_j'}\frac{\partial\bar{w}}{\partial x_j} + \frac{g}{T_o}\overline{T'^2}$$

$$+ \frac{\partial}{\partial x_j}\left[\Lambda_{2_t} q\left(\frac{\partial\overline{u_j'T'}}{\partial z} + \frac{\partial\overline{w'T'}}{\partial x_j}\right)\right]$$

$$+ \frac{\partial}{\partial z}\left(\Lambda_{3_t} q\frac{\partial\overline{u_j'T'}}{\partial x_j}\right) - \frac{q}{\Lambda_{1_t}}\overline{w'T'}$$

$$+ \nu_o\frac{\partial^2}{\partial x_j^2}\overline{w'T'} - 2\nu_o\frac{\overline{w'T'}}{\lambda_t^2} \qquad (12.27)$$

$$\frac{D\overline{T'^2}}{Dt} = -2\overline{u_j'T'}\frac{\partial\bar{T}}{\partial x_j} + \frac{\partial}{\partial x_j}\left(\Lambda_{2_t} q \frac{\partial}{\partial x_j}\overline{T'^2}\right)$$

$$+ \nu_o \frac{\partial^2\overline{T'^2}}{\partial x_j^2} - 2\nu_o \frac{\overline{T'^2}}{\lambda_t^2} \qquad (12.28)$$

At this point it is appropriate that we present the equations for the dispersal of a passive pollutant species C_α . Since the equation for C_α , namely, (3.6), will not be changed by the inclusion of Coriolis forces, the equations for $\bar{C}_\alpha$, $\overline{C_\alpha'^2}$, and $\overline{C_\alpha'T'}$ will be those we have previously used. We must, however, add new terms to the equations for $\overline{u'C_\alpha'}$, $\overline{v'C_\alpha'}$, and $\overline{w'C_\alpha'}$. The terms to be added to the right-hand sides of these equations are, respectively,

$$2\Omega(\overline{v'C_\alpha'}\sin\phi - \overline{w'C_\alpha'}\cos\phi)$$

$$-2\Omega\overline{u'C_\alpha'}\sin\phi$$

and

$$2\Omega\overline{u'C_\alpha'}\cos\phi$$

With these additional terms added to our previous equations, namely, (4.24), (4.25), and (4.26), we obtain the following model equations for the dispersal of a passive pollutant:

$$\frac{D\bar{C}_\alpha}{Dt} = \nu_o \frac{\partial^2\bar{C}_\alpha}{\partial x_j^2} - \frac{\partial}{\partial x}(\overline{u'C_\alpha'}) - \frac{\partial}{\partial y}(\overline{v'C_\alpha'}) - \frac{\partial}{\partial z}(\overline{w'C_\alpha'}) \qquad (12.29)$$

$$\frac{D\overline{u'C_\alpha'}}{Dt} = 2\Omega(\overline{v'C_\alpha'}\sin\phi - \overline{w'C_\alpha'}\cos\phi) - \overline{u_j'u'}\frac{\partial\bar{C}_\alpha}{\partial x_j} - \overline{u_j'C_\alpha'}\frac{\partial\bar{u}}{\partial x_j}$$

$$+ \frac{\partial}{\partial x_j}\left[\Lambda_{2_c} q\left(\frac{\partial\overline{u'C_\alpha'}}{\partial x_j} + \frac{\partial\overline{u_j'C_\alpha'}}{\partial x}\right)\right] + \frac{\partial}{\partial x}\left(\Lambda_{3_c} q \frac{\partial\overline{u_j'C_\alpha'}}{\partial x_j}\right) - \frac{q}{\Lambda_{1_c}}\overline{u'C_\alpha'}$$

$$+ \nu_o \frac{\partial^2\overline{u'C_\alpha'}}{\partial x_j^2} - 2\nu_o \frac{\overline{u'C_\alpha'}}{\lambda_c^2} \qquad (12.30)$$

$$\frac{D\overline{v'C'_\alpha}}{Dt} = -2\Omega\overline{u'C'_\alpha}\sin\phi - \overline{u'_j v'}\frac{\partial\bar{C}_\alpha}{\partial x_j} - \overline{u'_j C'_\alpha}\frac{\partial\bar{v}}{\partial x_j}$$

$$+ \frac{\partial}{\partial x_j}\left[\Lambda_{2_c} q\left(\frac{\partial\overline{v'C'_\alpha}}{\partial x_j} + \frac{\partial\overline{u'_j C'_\alpha}}{\partial y}\right)\right]$$

$$+ \frac{\partial}{\partial y}\left(\Lambda_{3_c} q\frac{\partial}{\partial x_j}\overline{u'_j C'_\alpha}\right) - \frac{q}{\Lambda_{1_c}}\overline{v'C'_\alpha}$$

$$+ \nu_o\frac{\partial^2\overline{v'C'_\alpha}}{\partial x_j^2} - 2\nu_o\frac{\overline{v'C'_\alpha}}{\lambda_c^2} \qquad (12.31)$$

$$\frac{D\overline{w'C'_\alpha}}{Dt} = 2\Omega\overline{u'C'_\alpha}\cos\phi - \overline{u'_j w'}\frac{\partial\bar{C}_\alpha}{\partial x_j} - \overline{u'_j C'_\alpha}\frac{\partial\bar{w}}{\partial x_j} + \frac{g}{T_o}\overline{C'_\alpha T'}$$

$$+ \frac{\partial}{\partial x_j}\left[\Lambda_{2_c} q\left(\frac{\partial\overline{w'C'_\alpha}}{\partial x_j} + \frac{\partial\overline{u'_j C'_\alpha}}{\partial z}\right)\right]$$

$$+ \frac{\partial}{\partial z}\left(\Lambda_{3_c} q\frac{\partial}{\partial x_j}\overline{u'_j C'_\alpha}\right) - \frac{q}{\Lambda_{1_c}}\overline{w'C'_\alpha}$$

$$+ \nu_o\frac{\partial^2\overline{w'C'_\alpha}}{\partial x_j^2} - 2\nu_o\frac{\overline{w'C'_\alpha}}{\lambda_c^2} \qquad (12.32)$$

$$\frac{D\overline{C'_\alpha T'}}{Dt} = -\overline{u'_j C'_\alpha}\frac{\partial\bar{T}}{\partial x_j} - \overline{u'_j T'}\frac{\partial\bar{C}_\alpha}{\partial x_j} + \frac{\partial}{\partial x_j}\left(\Lambda_{2_c} q\frac{\partial\overline{C'_\alpha T'}}{\partial x_j}\right)$$

$$+ \nu_o\frac{\partial^2\overline{C'_\alpha T'}}{\partial x_j^2} - 2\nu_o\frac{\overline{C'_\alpha T'}}{\lambda_c^2} \qquad (12.33)$$

$$\frac{D\overline{C_\alpha'^2}}{Dt} = -2\overline{u_j'C_\alpha'}\frac{\partial \bar{C}_\alpha}{\partial x_j} + \frac{\partial}{\partial x_j}\left(\Lambda_{2_c} q \frac{\partial \overline{C_\alpha'^2}}{\partial x_j}\right)$$

$$+ \nu_o \frac{\partial^2 \overline{C_\alpha'T'}}{\partial x_j^2} - 2\nu_o \frac{\overline{C_\alpha'^2}}{\lambda_c^2} \qquad (12.34)$$

We may now turn to the problem of computing the planetary boundary layer or Ekman layer by means of the equations we have set forth above. The simplest case we may compute in order to demonstrate the method is that of a planetary boundary layer such that all derivatives with respect to x and y vanish, and the atmospheric quantities are functions of z and t alone. For this case, in view of the continuity equation (12.14), we may take $\bar{w} = 0$.

The equations for this special case of motion in the planetary boundary layer are then

$$\frac{\partial \bar{u}}{\partial t} = -\frac{1}{\rho_o}\frac{\partial \bar{p}}{\partial x} + \bar{v}(2\Omega \sin \phi) + \nu_o \frac{\partial^2 \bar{u}}{\partial z^2} - \frac{\partial \overline{u'w'}}{\partial z} \qquad (12.35)$$

$$\frac{\partial \bar{v}}{\partial t} = -\frac{1}{\rho_o}\frac{\partial \bar{p}}{\partial y} - \bar{u}(2\Omega \sin \phi) + \nu_o \frac{\partial^2 \bar{v}}{\partial z^2} - \frac{\partial \overline{v'w'}}{\partial z} \qquad (12.36)$$

$$\frac{\partial \bar{p}}{\partial z} = -\bar{\rho}g + \rho_o \bar{u}(2\Omega \cos \phi) - \rho_o \frac{\partial \overline{w'w'}}{\partial z} \qquad (12.37)$$

$$\frac{\partial \bar{T}}{\partial t} = \nu_o \frac{\partial^2 \bar{T}}{\partial z^2} - \frac{\partial \overline{w'T'}}{\partial z} \qquad (12.38)$$

$$\bar{\rho} = -\frac{\rho_o}{T_o}\bar{T} \qquad (12.39)$$

$$\frac{\partial \overline{u'u'}}{\partial t} = 4\Omega(\overline{u'v'} \sin \phi - \overline{u'w'} \cos \phi)$$

$$- 2\overline{u'w'} \frac{\partial \bar{u}}{\partial z} + \frac{\partial}{\partial z}\left(\Lambda_{2_t} q \frac{\partial \overline{u'u'}}{\partial z}\right)$$

$$- \frac{q}{\Lambda_{1_t}}\left(\overline{u'u'} - \frac{q^2}{3}\right) + \nu_o \frac{\partial^2 \overline{u'u'}}{\partial z^2} - 2\nu_o \frac{\overline{u'u'}}{\lambda_t^2} \qquad (12.40)$$

$$\frac{\partial \overline{v'v'}}{\partial t} = -4\Omega\overline{u'v'} \sin \phi - 2\overline{v'w'} \frac{\partial \bar{v}}{\partial z} + \frac{\partial}{\partial z}\left(\Lambda_{2_t} q \frac{\partial \overline{v'v'}}{\partial z}\right)$$

$$- \frac{q}{\Lambda_{1_t}}\left(\overline{v'v'} - \frac{q^2}{3}\right) + \nu_o \frac{\partial^2 \overline{v'v'}}{\partial z^2} - 2\nu_o \frac{\overline{v'v'}}{\lambda_t^2} \qquad (12.41)$$

$$\frac{\partial \overline{w'w'}}{\partial t} = 4\Omega\overline{u'w'} \cos \phi + \frac{2g}{T_o} \overline{w'T'} + \frac{\partial}{\partial z}\left[\left(3\Lambda_{2_t} + 2\Lambda_{3_t}\right) q \frac{\partial \overline{w'w'}}{\partial z}\right]$$

$$- \frac{q}{\Lambda_{1_t}}\left(\overline{w'w'} - \frac{q^2}{3}\right) + \nu_o \frac{\partial^2 \overline{w'w'}}{\partial z^2} - 2\nu_o \frac{\overline{w'w'}}{\lambda_t^2} \qquad (12.42)$$

$$\frac{\partial \overline{u'v'}}{\partial t} = 2\Omega\left(\overline{v'^2} \sin \phi - \overline{v'w'} \cos \phi - \overline{u'^2} \sin \phi\right)$$

$$- \overline{u'w'} \frac{\partial \bar{v}}{\partial z} - \overline{v'w'} \frac{\partial \bar{u}}{\partial z} + \frac{\partial}{\partial z}\left(\Lambda_{2_t} q \frac{\partial \overline{u'v'}}{\partial z}\right)$$

$$- \frac{q}{\Lambda_{1_t}} \overline{u'v'} + \nu_o \frac{\partial^2 \overline{u'v'}}{\partial z^2} - 2\nu_o \frac{\overline{u'v'}}{\lambda_t^2} \qquad (12.43)$$

$$\frac{\partial \overline{u'w'}}{\partial t} = 2\Omega\left(\overline{v'w'} \sin\phi - \overline{w'^2} \cos\phi + \overline{u'^2}\cos\phi\right) - \overline{w'w'} \frac{\partial \bar{u}}{\partial z} + \frac{g}{T_o}\overline{u'T'}$$

$$+ \frac{\partial}{\partial z}\left[\left(2\Lambda_{2_t} + \Lambda_{3_t}\right) q \frac{\partial \overline{u'w'}}{\partial z}\right]$$

$$- \frac{q}{\Lambda_{1_t}} \overline{u'w'} + \nu_o \frac{\partial^2 \overline{u'w'}}{\partial z^2} - 2\nu_o \frac{\overline{u'w'}}{\lambda_t^2} \quad (12.44)$$

$$\frac{\partial \overline{v'w'}}{\partial t} = 2\Omega(-\overline{u'w'} \sin\phi + \overline{u'v'} \cos\phi) - \overline{w'w'} \frac{\partial \bar{v}}{\partial z} + \frac{g}{T_o} \overline{v'T'}$$

$$+ \frac{\partial}{\partial z}\left[\left(2\Lambda_{2_t} + \Lambda_{3_t}\right) q \frac{\partial \overline{v'w'}}{\partial z}\right]$$

$$- \frac{q}{\Lambda_{1_t}} \overline{v'w'} + \nu_o \frac{\partial^2 \overline{v'w'}}{\partial z^2} - 2\nu_o \frac{\overline{v'w'}}{\lambda_t^2} \quad (12.45)$$

$$\frac{\partial \overline{u'T'}}{\partial t} = 2\Omega(\overline{v'T'} \sin\phi - \overline{w'T'} \cos\phi) - \overline{u'w'} \frac{\partial \bar{T}}{\partial z} - \overline{T'w'} \frac{\partial \bar{u}}{\partial z}$$

$$+ \frac{\partial}{\partial z}\left(\Lambda_{2_t} q \frac{\partial \overline{u'T'}}{\partial z}\right)$$

$$- \frac{q}{\Lambda_{1_t}} \overline{u'T'} + \nu_o \frac{\partial^2 \overline{u'T'}}{\partial z^2} - 2\nu_o \frac{\overline{u'T'}}{\lambda_t^2} \quad (12.46)$$

$$\frac{\partial \overline{v'T'}}{\partial t} = -2\Omega \overline{u'T'} \sin\phi - \overline{v'w'} \frac{\partial \bar{T}}{\partial z} - \overline{T'w'} \frac{\partial \bar{v}}{\partial z}$$

$$+ \frac{\partial}{\partial z}\left(\Lambda_{2_t} q \frac{\partial \overline{v'T'}}{\partial z}\right)$$

$$- \frac{q}{\Lambda_{1_t}} \overline{v'T'} + \nu_o \frac{\partial^2 \overline{v'T'}}{\partial z^2} - 2\nu_o \frac{\overline{v'T'}}{\lambda_t^2} \quad (12.47)$$

$$\frac{\partial \overline{w'T'}}{\partial t} = 2\Omega \overline{u'T'} \cos\phi - \overline{w'w'} \frac{\partial \bar{T}}{\partial z} + \frac{g}{T_o} \overline{T'^2}$$

$$+ \frac{\partial}{\partial z}\left[\left(2\Lambda_{2_t} + \Lambda_{3_t}\right) q \frac{\partial \overline{w'T'}}{\partial z}\right]$$

$$- \frac{q}{\Lambda_{1_t}} \overline{w'T'} + \nu_o \frac{\partial^2 \overline{w'T'}}{\partial z^2} - 2\nu_o \frac{\overline{w'T'}}{\lambda_t^2} \quad (12.48)$$

and

$$\frac{\partial \overline{T'^2}}{\partial t} = -2\overline{w'T'} \frac{\partial \bar{T}}{\partial z} + \frac{\partial}{\partial z}\left(\Lambda_{2_t} q \frac{\partial \overline{T'^2}}{\partial z}\right)$$

$$+ \nu_o \frac{\partial^2 \overline{T'^2}}{\partial z^2} - 2\nu_o \frac{\overline{T'^2}}{\lambda_t^2} \quad (12.49)$$

We will discuss solutions for the complete atmospheric boundary layer using (12.35) through (12.49) by first considering the case of a steady neutrally stable atmospheric motion. In order to obtain a solution, it is necessary for one to specify the driving forces $(1/\rho_o)\partial\bar{p}/\partial x$ and $(1/\rho_o)\partial\bar{p}/\partial y$ which, if the flow is to be steady, must be independent of time and must be functions of z alone. Let us assume for simplicity, although

the assumption is not necessary, that these driving forces are constant and independent of height. In this case, if the surface of the earth were frictionless, a geostrophic wind would exist that would be constant and independent of height. The components of this geostrophic wind would be

$$u_g = -\frac{1}{2\Omega \sin\phi}\frac{1}{\rho_o}\frac{\partial p}{\partial y} = -\frac{1}{\rho_o f}\frac{\partial p}{\partial y} = u_o \qquad (12.50)$$

$$v_g = \frac{1}{2\Omega \sin\phi}\frac{1}{\rho_o}\frac{\partial p}{\partial x} = \frac{1}{\rho_o f}\frac{\partial p}{\partial x} = v_o \qquad (12.51)$$

To find the boundary layer due to friction at the earth's surface, we may start with this geostrophic wind condition as an initial condition at, say, $t = 0$, on our equations for the mean velocities $\bar{u}$ and $\bar{v}$ that is true at all z except $z = 0$. We put in the viscous condition at $z = 0$, namely, $\bar{u}(0,t) = 0$ and $\bar{v}(0,t) = 0$. For the neutral atmospheric case we are considering here, we must solve (12.35) and (12.36) subject to the initial conditions we have specified in conjunction with (12.40) through (12.45). We take as boundary conditions on (12.40) through (12.49) the viscous condition for a solid surface that all second-order correlations must vanish at $z = 0$. We will also assume that these correlations vanish at $z = \infty$, for we will assume that, initially, there is no turbulent production so that all second-order correlations are zero. Actually, some disturbance or turbulence (it does not matter what the disturbance is) must be introduced to start a turbulent solution to this boundary layer problem. This can be done by introducing a turbulent "spot" into the flow at time $t = 0$ or, alternatively, waiting for round-off errors in the solution of the equations to build up into a full-fledged turbulence as the simultaneous solution of the equations proceeds. The solution will proceed until, at large times, the derivatives with respect to time become infinitesimal as a balance of centrifugal, viscous, and pressure forces is reached at each point in the flow. The resulting boundary layer is the steady-state Ekman layer for the driving pressure gradients that have been assumed.

Let us consider a specific case. We wish to compute the planetary boundary layer for a case when

$$v_o(z) = \frac{1}{\rho_o f}\frac{\partial p}{\partial x} = v_g = 0$$

$$u_o(z) = -\frac{1}{\rho_o f}\frac{\partial p}{\partial y} = u_g = 10 \text{ meters/second}$$

We will assume that the surface at $z = 0$ is smooth and, further, that $2\Omega \sin \phi = 10^{-4}$ rad/sec. In order to carry out a solution of our equations, we must specify the length scale Λ_{1t}. We will assume here that Λ_{1t} may be taken equal to 0.15 times the height at which the wind speed $\sqrt{\bar{u}^2 + \bar{v}^2}$ becomes equal to the geostrophic value $\sqrt{u_g^2 + v_g^2} = |u_g|$. This assumption is very much akin to the assumption made for an ordinary boundary layer in Section 5, namely, $\Lambda_1 = 0.15\delta_{.99}$.

A calculation of the character of the Ekman layer on an absolutely smooth earth under the condition $u_g = 10$ m/sec and $v_g = 0$ carried out as described above is shown in Figures 12.1 through 12.5. Figures 12.1 and 12.2 show the computed $\bar{u}$ and $\bar{v}$ profiles, respectively. Figure 12.3 depicts the Ekman spiral for this case. It will be noted that the wind speed first reaches the geostrophic at an altitude of approximately 150 meters. It will also be noted, from Figure 12.2, that the total thickness of the Ekman layer is approximately 1500 meters. For this case, the surface angle is computed to be 13.8°. Figures 12.4 and 12.5 show the values of all the second-order velocity correlations. One notes in Figures 12.4 and 12.5 that the distributions of $\overline{u'u'}$ and $\overline{u'w'}$ are not smooth but have a "bump" between a height of 50 and 150 meters. Whether this bump is a physical reality or due to some bug in the computer program is unknown at present. As we shall see, this "bump" did not appear in the calculations carried out for a rough earth. Of some interest, insofar as the dispersal of pollutants in the atmosphere is concerned, is the fact that the root-mean-square values of the vertical and lateral velocity fluctuations run about 2% of the geostrophic wind velocity for

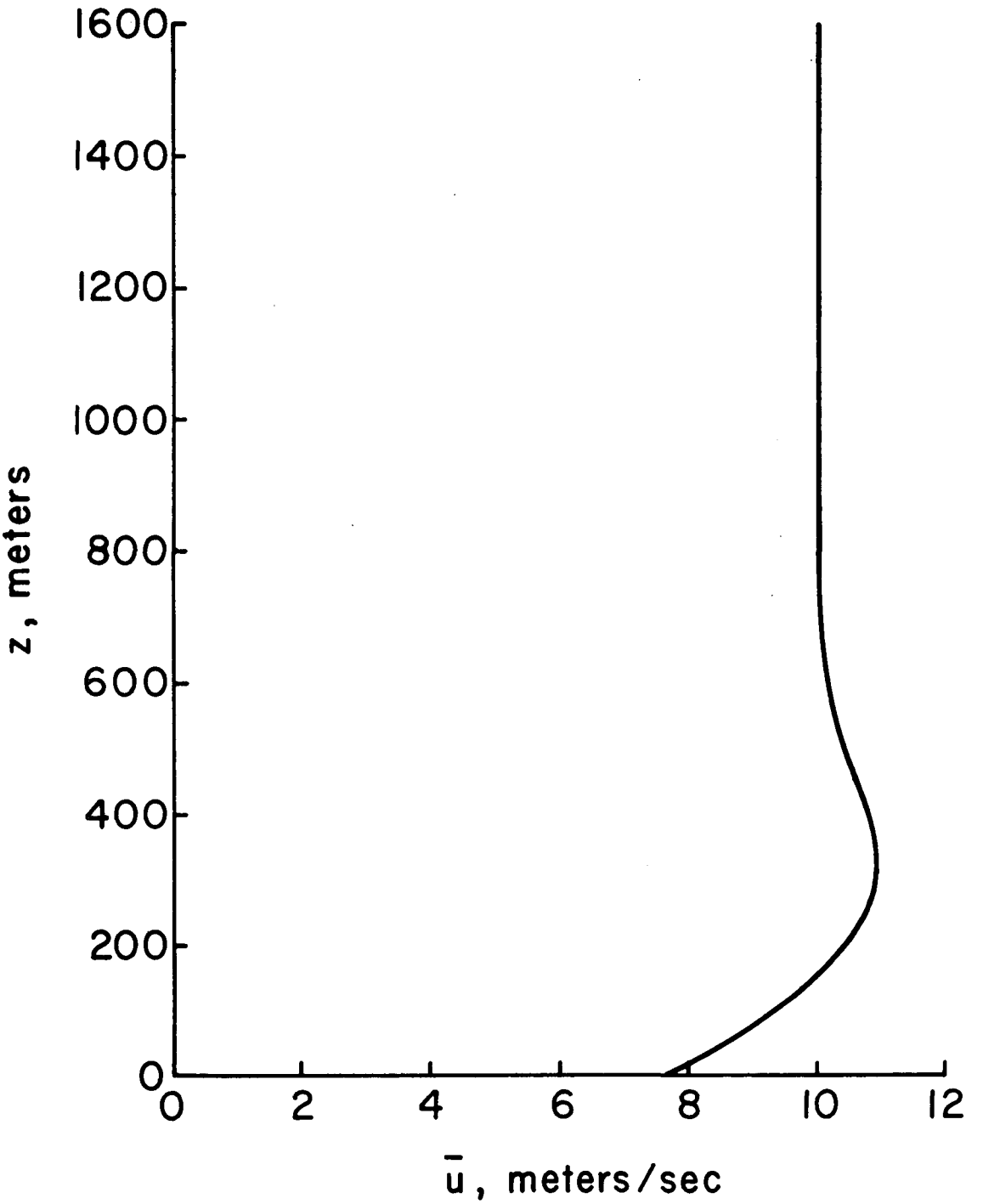

Figure 12.1. Profile of mean velocity $\bar{u}$ for steady state planetary boundary layer when $\bar{u}_g$ = 10 m/s, $\bar{v}_g$ = 0 and z_r = 0

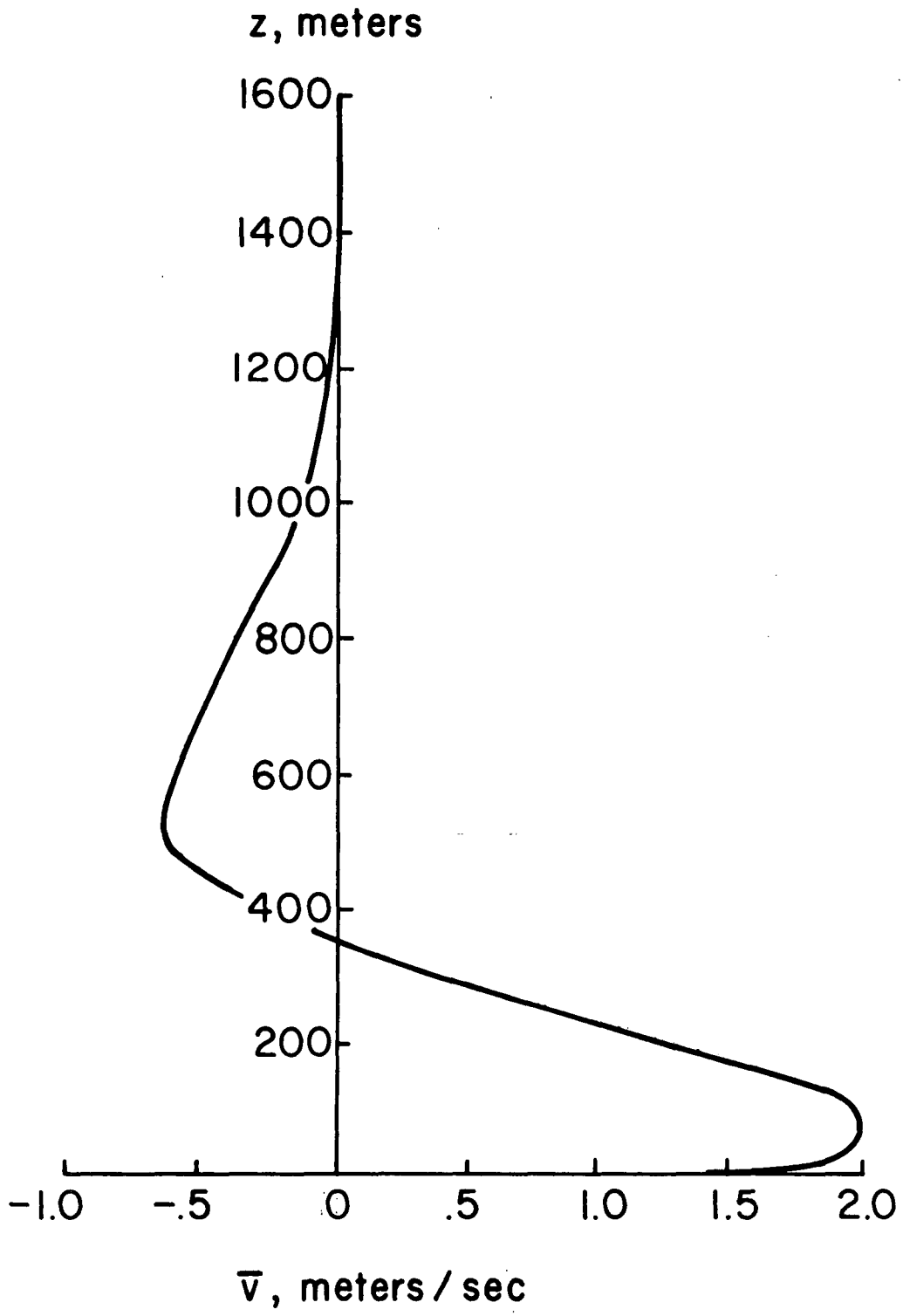

Figure 12.2. Profile of mean velocity $\bar{v}$ for steady state planetary boundary layer when $\bar{u}_g = 10$ m/s, $\bar{v}_g = 0$ and $z_r = 0$

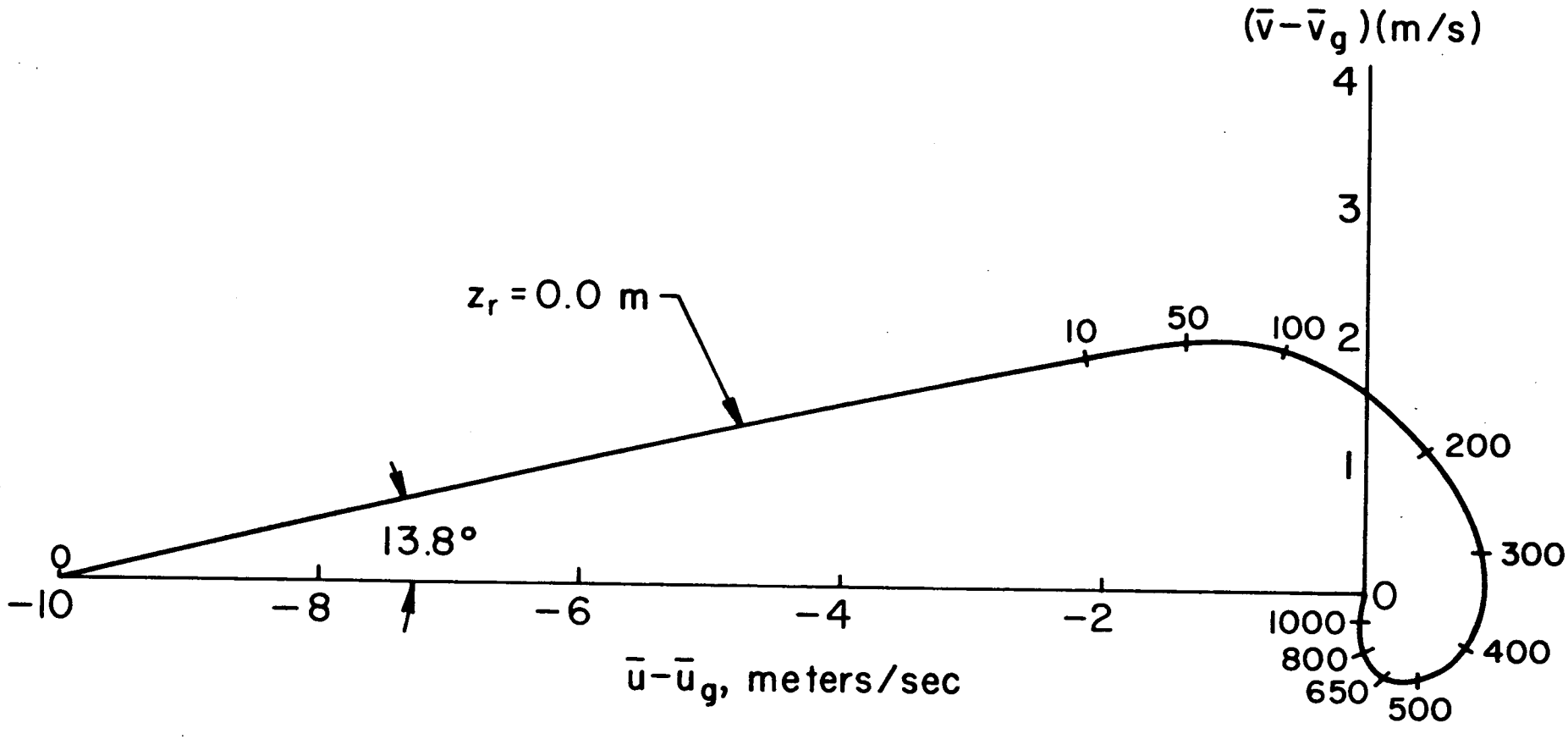

Figure 12.3. Ekman spiral for a smooth earth when $\bar{u}_g$ = 10 m/s, $\bar{v}_g$ = 0, and z_r = 0

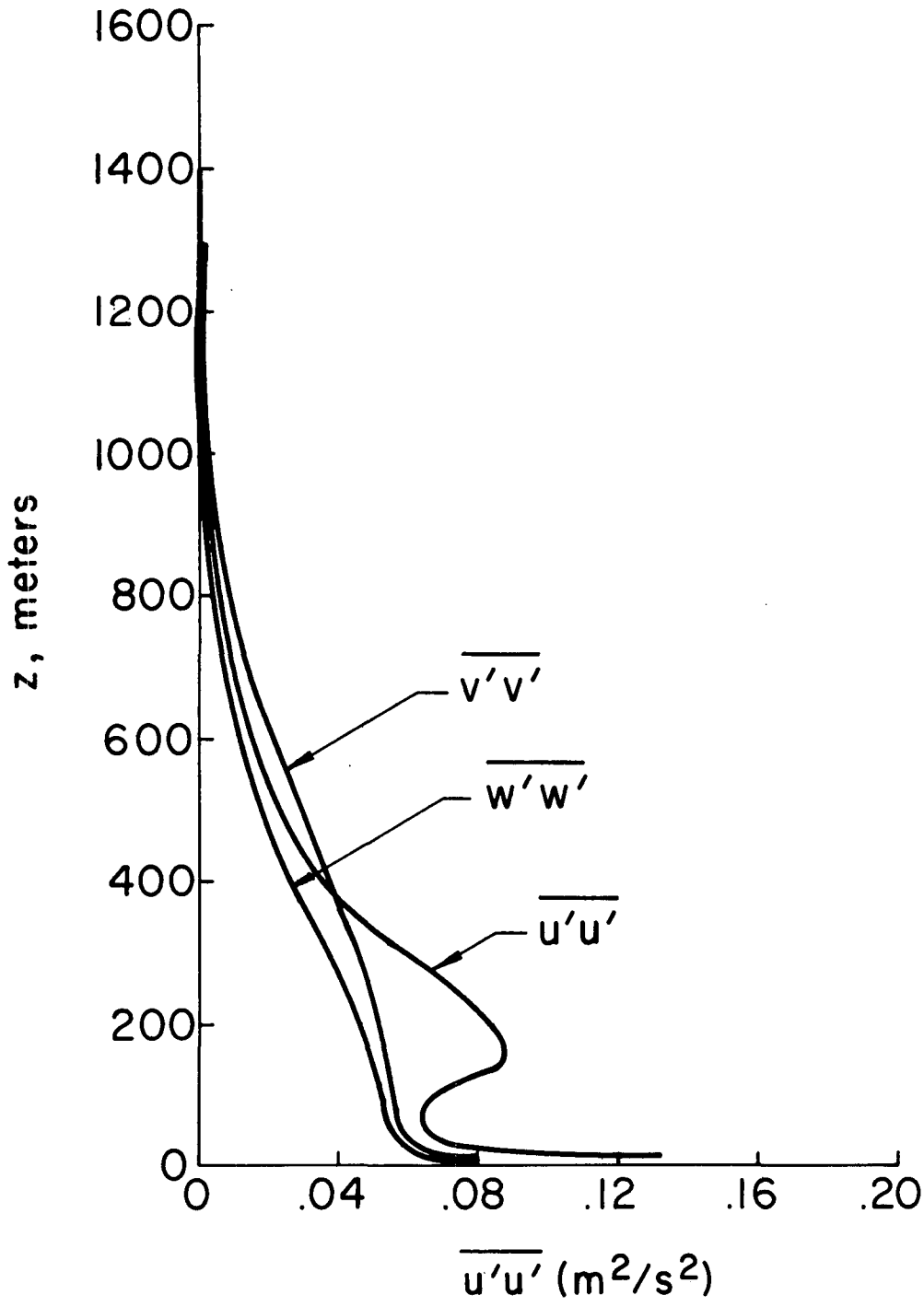

Figure 12.4. Distributions of $\overline{u'u'}$, $\overline{v'v'}$, and $\overline{w'w'}$ for the planetary boundary layer on a smooth earth for $\bar{u}_g$ = 10 m/s and $\bar{v}_g$ = 0; z_r = 0

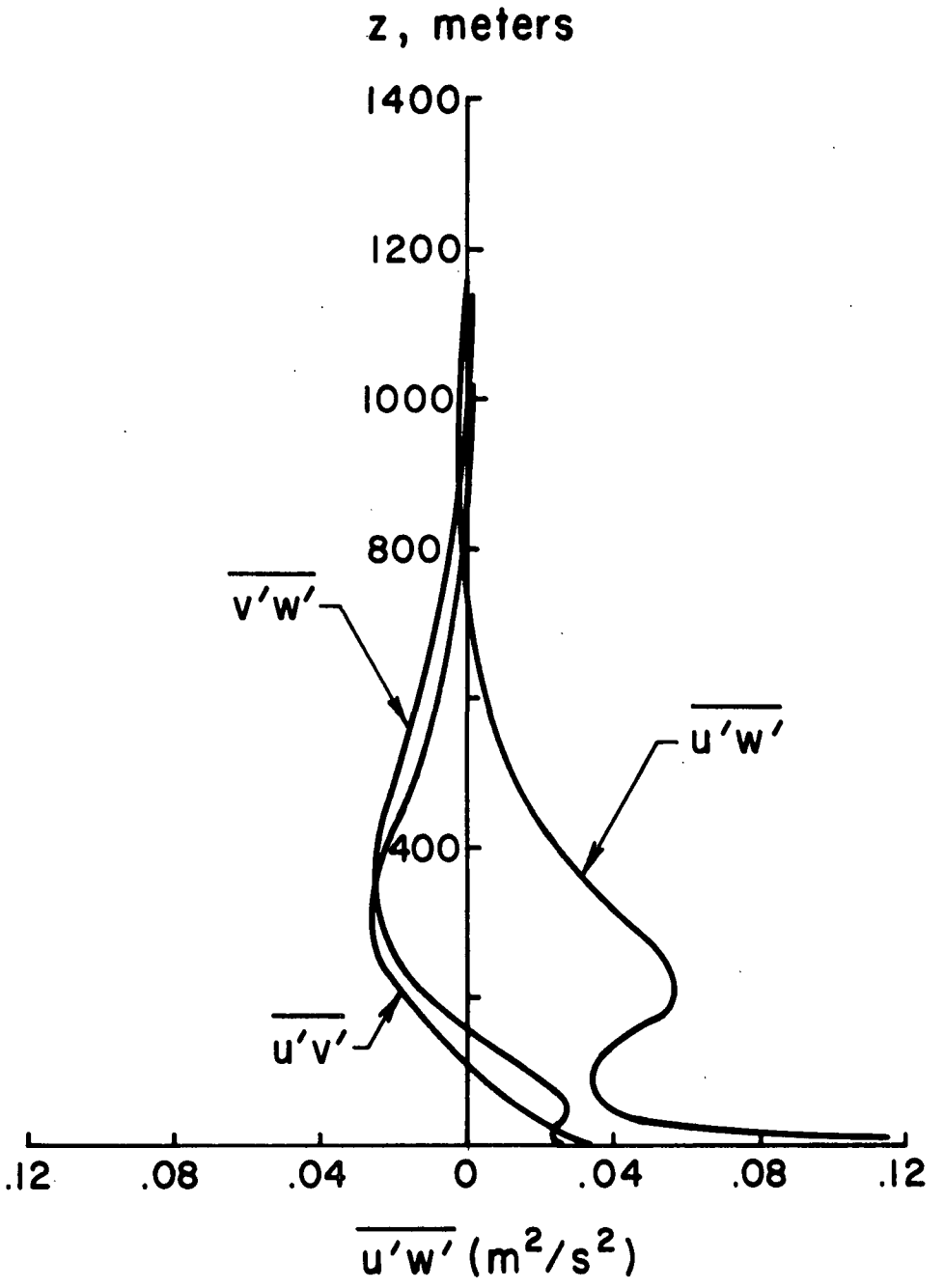

Figure 12.5. Distributions of $\overline{u'w'}$, $\overline{v'w'}$, and $\overline{u'v'}$ for the planetary boundary layer on a smooth earth for $\bar{u}_g$ = 10 m/s and $\bar{v}_g$ = 0; z_r = 0

some 200 meters above the immediate surface layer where these velocities are roughly constant for some 20 meters above the surface at about 3% of the geostrophic wind.

The angle of the flow at the surface is related to the amount of surface friction. For this particular calculation, the nondimensional friction velocity defined by

$$u_*/\bar{u}_g = \sqrt{\tau_o/\rho_o(0)\bar{u}_g^2}$$

is computed to be 0.02. Both this value and the surface angle of 13.8° are considerably lower than one usually finds. This is because we have computed our planetary boundary layer for the ideal case of an absolutely smooth earth. If we are to obtain results that are more realistic, we must compute the planetary boundary layer *on* a rough earth.

In order to take account of surface roughness in the calculations, we may proceed as follows. First we assume that the drag of the surface elements will remove momentum from the lowest layers of the boundary layer in such a way that for a region between the true surface $z = 0$ and the small height $z = z_r$, there is no mean velocity; i.e., we assume $\bar{u} = \bar{v} \equiv 0$ for $0 \leq z \leq z_r$. In this region, although the mean velocity is zero, there certainly may be small turbulent eddies. Therefore, we will assume that the viscous boundary condition of $\overline{u_i' u_k'} = 0$ still applies at the true surface $z = 0$. We may further assume that the scale of the eddies is still proportional to the distance from this true surface, so that in making the calculations, we specify that $\Lambda_{1_t} = 0.7z$ as we have done in the past. If these new boundary conditions are applied to our equations, the flow over a rough surface may be calculated.

In Figures 12.6 through 12.10 the results of such a calculation are presented for a roughness height z_r of 0.01 meters. As in the previous example, the results are presented for the case when $\bar{u}_g = 10$ m/sec and $\bar{v}_g = 0$. It will be noted from

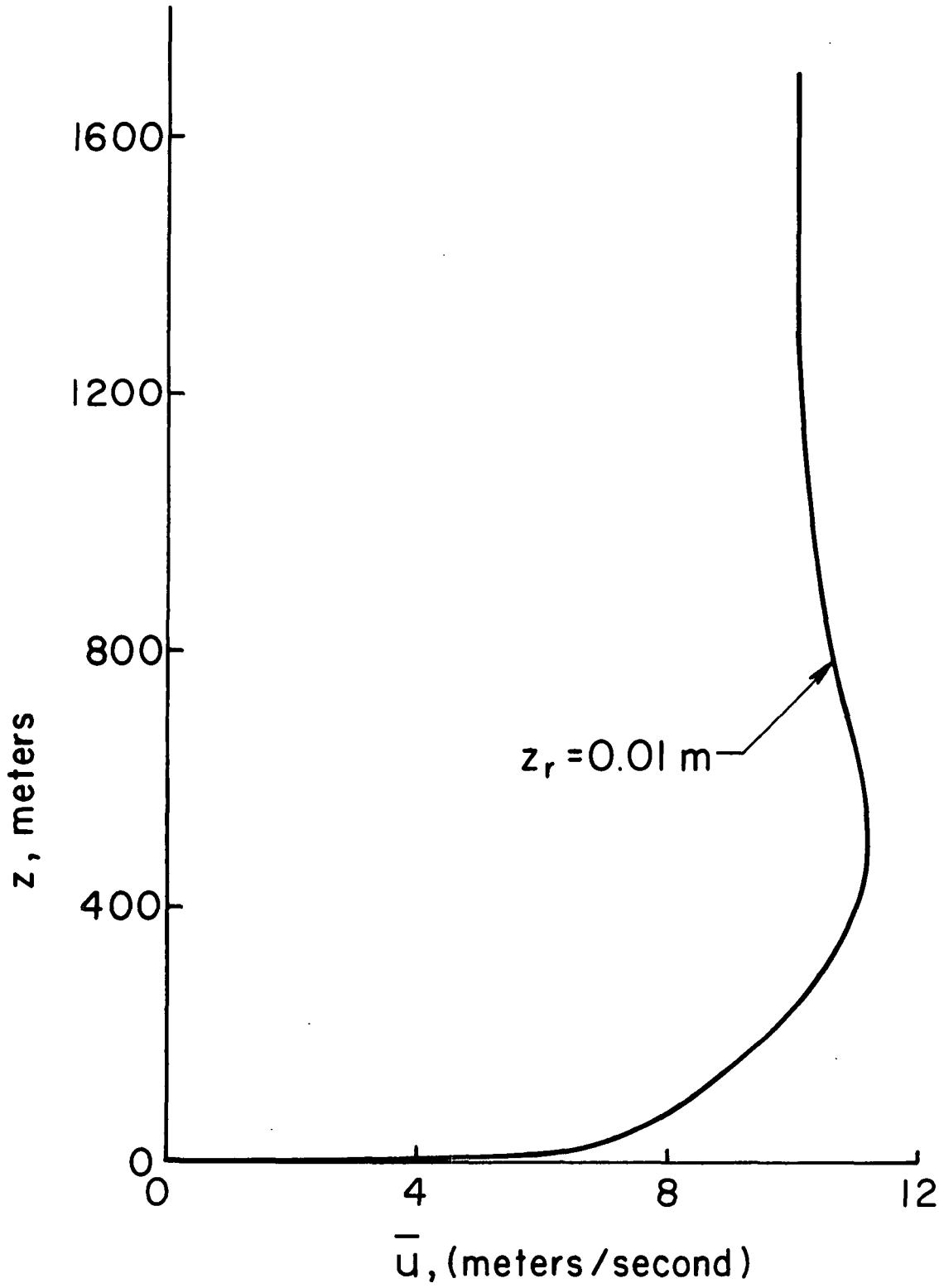

Figure 12.6. Profile of mean velocity $\bar{u}$ for steady state planetary boundary layer when $\bar{u}_g$ = 10 m/s and $\bar{v}$ = 0 for a rough earth, z_r = 0.01 meters

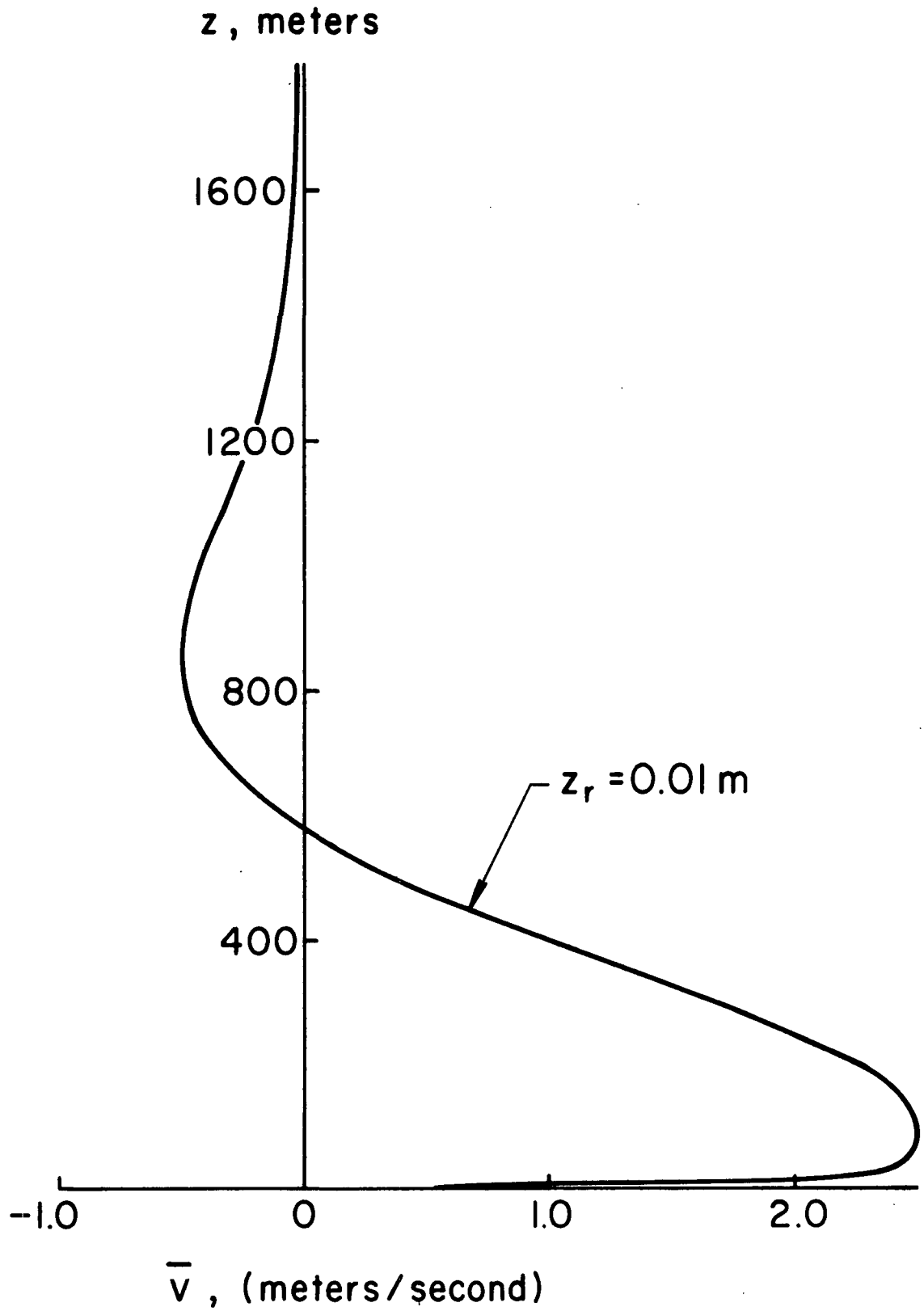

Figure 12.7. Profile of mean velocity $\bar{v}$ for steady state planetary boundary layer when $\bar{u}_g$ = 10 m/s and v_g = 0 for a rough earth, z_r = 0.01 meters

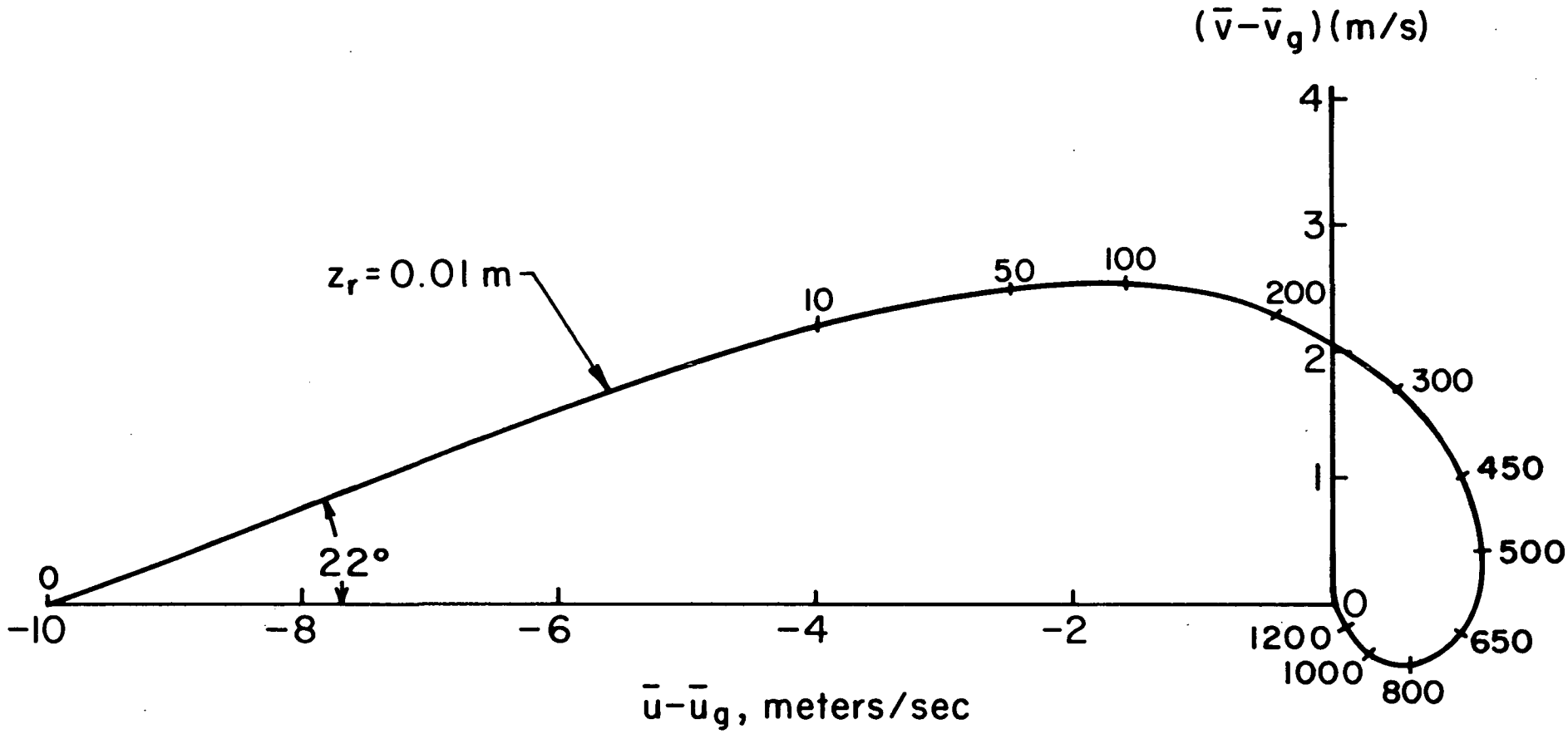

Figure 12.8. Ekman spiral for a rough earth when $\bar{u}_g$ = 10 m/s, $\bar{v}_g$ = 0, and z_r = 0.01 m

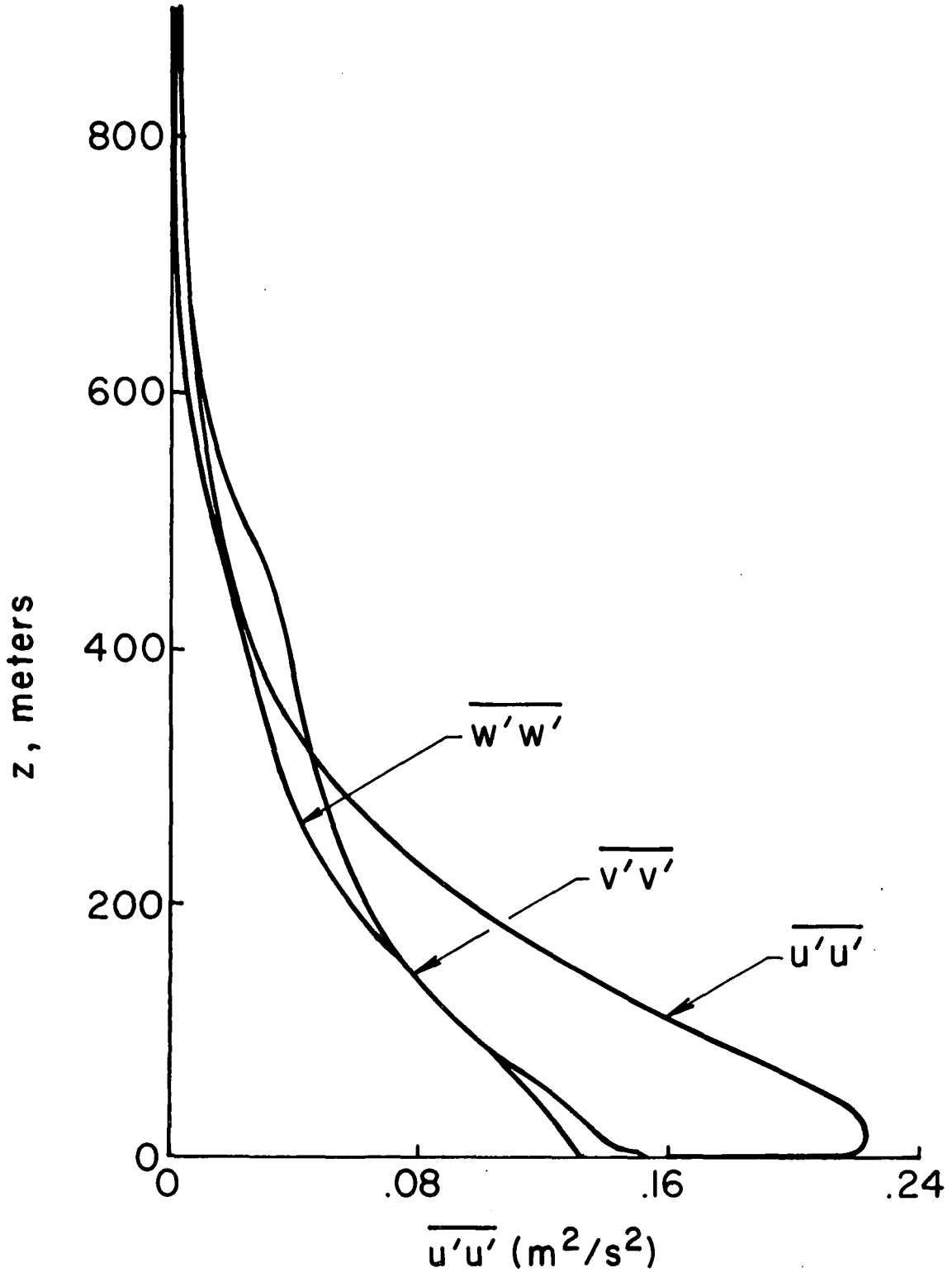

Figure 12.9. Distributions of $\overline{u'u'}$, $\overline{v'v'}$, and $\overline{w'w'}$ for the planetary boundary layer on a rough earth; z_r = 0.01 meters for $\bar{u}_g$ = 10 m/sec and $\bar{v}_g$ = 0

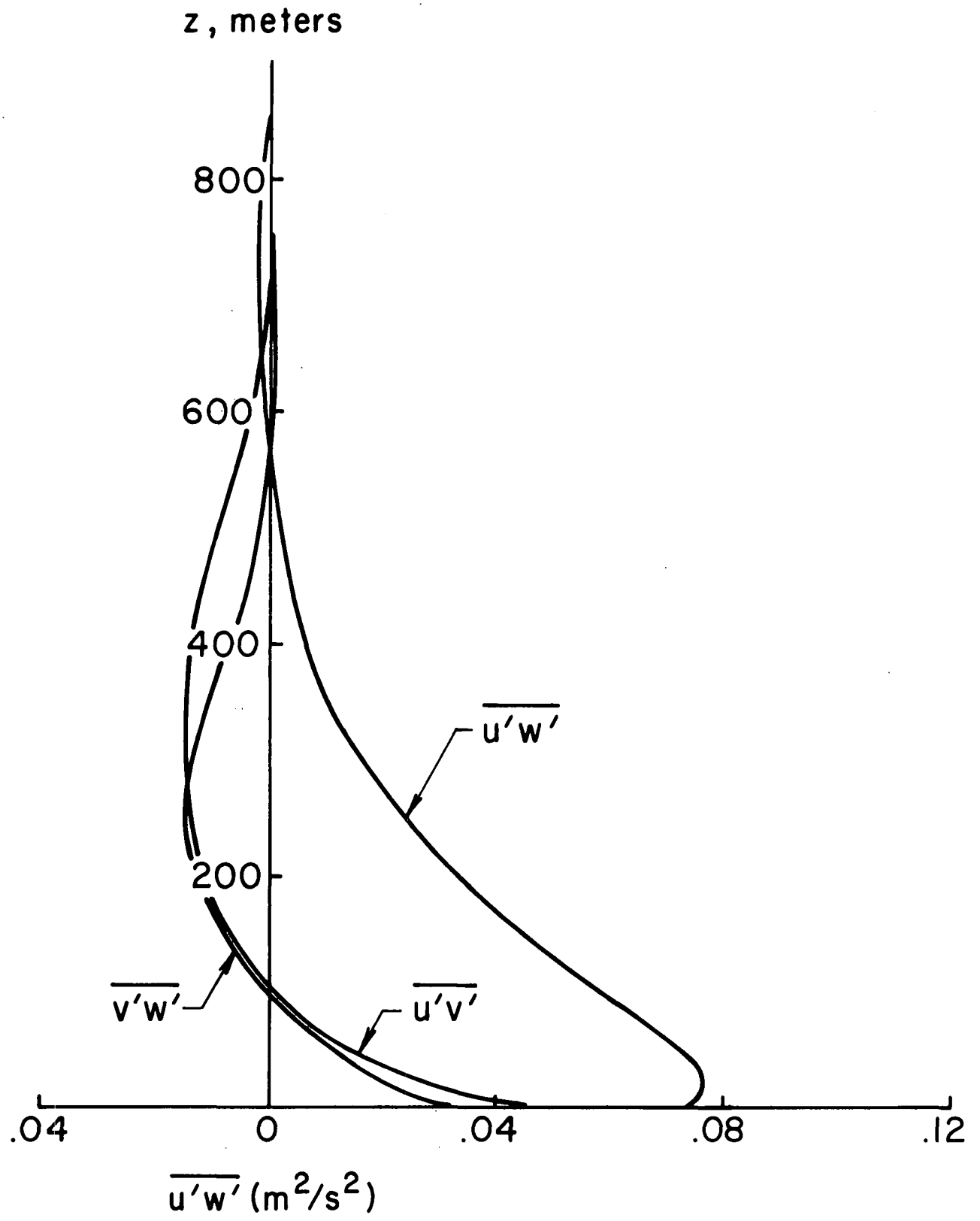

Figure 12.10. Distributions of $\overline{u'w'}$, $\overline{v'w'}$, and $\overline{u'v'}$ for the planetary boundary layer on a rough surface; z_r = 0.01 meters for $\bar{u}_g$ = 10 m/sec and $\bar{v}_g$ = 0

Figure 12.8 that the height at which the wind speed first becomes equal to the geostrophic value $\sqrt{u_g^2 + v_g^2}$ is now roughly 250 m. The height of the total Ekman layer is, according to Figure 12.7, approximately 2000 m. For this roughness condition, the nondimensional friction velocity was computed to be

$$u_*/\bar{u}_g = 0.0281$$

The surface angle was found to be 22°. These results are more in line with typical experimental results, and we shall presently compare these results with those found by other investigators.

Figures 12.9 and 12.10 show the distributions of the second-order velocity correlations that were computed. It will be noted that the level of the root-mean-square vertical and lateral velocity fluctuations in the surface layer where $\sqrt{\overline{v'v'}} \simeq \sqrt{\overline{w'w'}} \simeq 0.37$ are about 4% of the geostrophic wind speed. At about 100 meters above the surface, these fluctuations have fallen off to about 3% of the geostrophic wind speed. It will also be noted in Figure 12.10 that no "bump" appears in the energy or shear correlations for the rough earth where this "bump" had been found for the smooth earth calculations shown in Figure 12.5.

We may compare the results of these calculations with those of other investigators. For this purpose, we choose the theoretical results of Blackadar [Ref. 38], Lettau [Ref. 39], and Appleby and Ohmstede [Ref. 40]. In order to make the comparison, it is necessary for us to find the relationship between our roughness height z_r and the usual roughness height z_o defined by other investigators. The equation for the mean velocity in the immediate neighborhood of the surface when considering the classical roughness height z_o is

$$\frac{\bar{q}}{u_*} = \frac{\sqrt{\bar{u}^2 + \bar{v}^2}}{u_*} = \frac{1}{\kappa} \ln \frac{z}{z_o} \qquad (12.52)$$

where κ is von Kármán's constant. This may be used to compute z_o from the local mean velocity and the surface friction expressed

through u_*, viz.,

$$z_o = z_r^{-\kappa\bar{q}/u_*} \tag{12.53}$$

If we use the results of our calculations for the case just described where $z_r = 0.01$ meters, we find from the mean velocity profile and the friction velocity that the effective z_o was 0.0071 meters.

We may now compare our results with those of Refs. 38, 39, and 40 from which the nondimensional friction velocity $u_*/\sqrt{\bar{u}_g^2 + \bar{v}_g^2}$ and surface turning angles may be plotted as functions of the roughness Rossby number

$$R_o = \frac{\sqrt{\bar{u}_g^2 + \bar{v}_g^2}}{2\Omega \sin \phi \; z_o} \tag{12.54}$$

The results of our calculations are compared in Figures 12.11 and 12.12 with those of Refs. 38, 39, and 40. It is seen that our results are in good agreement with those of previous investigators.

Now let us consider the planetary boundary layer when there are departures from neutral stability, and it is necessary to include the temperature equations in the solution. With our present equations, if there exists a steady source or sink of heat at the boundary of our flow at $z = 0$, then there will never be a steady state solution of the equations in the sense we have just described for the neutral atmosphere. One can, however, find time-dependent solutions which are steady state in the sense that they are cyclic if heat transfer at the boundary of the flow is cyclic and the net heat added to the atmosphere is zero. Such a cyclic heating might be representative of the diurnal effect of the sun on the earth's surface. To obtain such solutions, one may start at time $t = 0$ with initial conditions obtained from a neutral solution of the atmospheric boundary

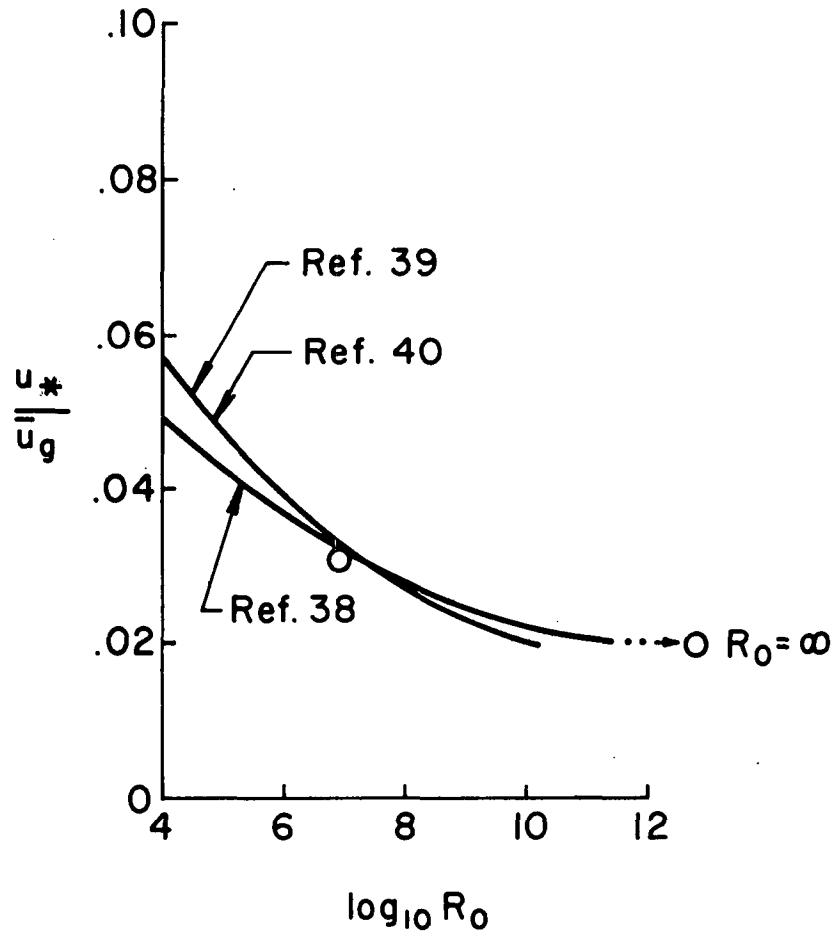

Figure 12.11. Comparison of calculated friction velocities with results obtained by Blackadar [38], Lettau [39], and Appleby & Ohmstede [40]

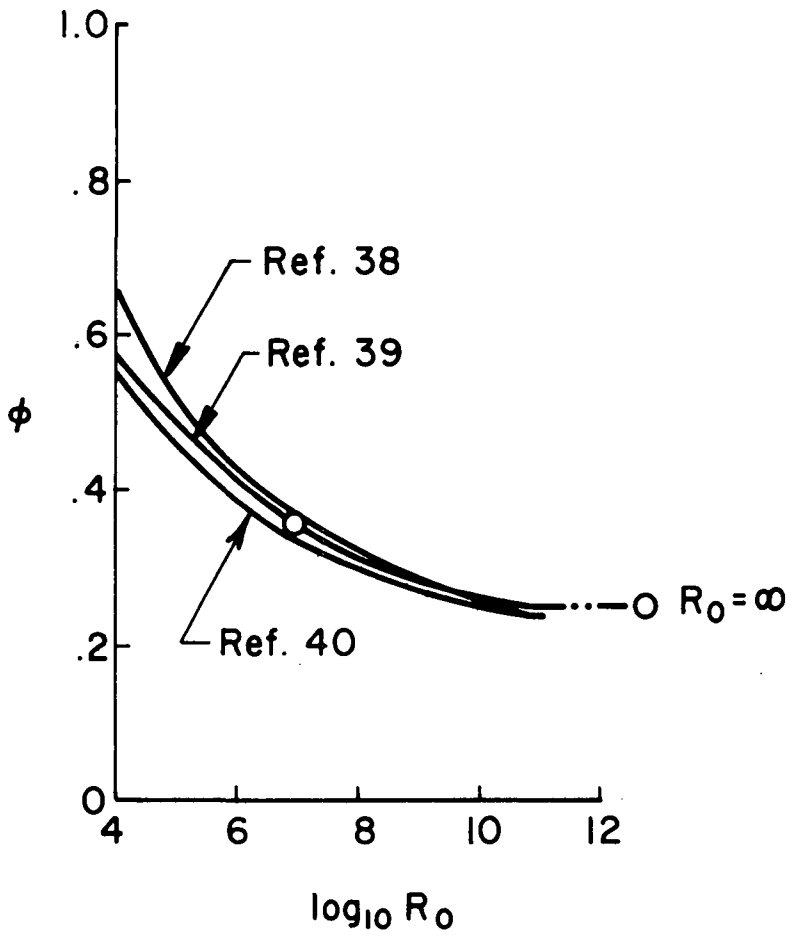

Figure 12.12. Comparison of calculated surface angles in radians with results obtained by Blackadar [38], Lettau [39], and Appleby & Ohmstede [40].

layer and apply at the surface for $t > 0$ a cyclical heat transfer. After several cycles of such heat transfer, the characteristics of the atmospheric boundary layer at each z will become cyclic in time and independent of the initial conditions that were chosen. In this way, representative atmospheric boundary layers under a very wide spectrum of stability conditions can be found. We have not, as of this writing, obtained solutions of this type to present here. Studies of this type will comprise part of our effort under EPA sponsorship during the coming year.

Before leaving this discussion of atmospheric boundary layers, we should present the equations for the dispersal of a passive pollutant in such layers that are equivalent to those which were solved in Section 10. The thin layer equations appropriate for use with (12.35) through (12.49) are the following:

$$\frac{\partial \bar{C}_\alpha}{\partial t} + \bar{u}\frac{\partial \bar{C}_\alpha}{\partial x} + \bar{v}\frac{\partial \bar{C}_\alpha}{\partial y} = \nu_o \frac{\partial^2 \bar{C}_\alpha}{\partial z^2} - \frac{\partial \overline{w'C'_\alpha}}{\partial z} \tag{12.55}$$

$$\begin{aligned}\frac{\partial \overline{u'C'_\alpha}}{\partial t} + \bar{u}\frac{\partial \overline{u'C'_\alpha}}{\partial x} + \bar{v}\frac{\partial \overline{u'C'_\alpha}}{\partial y} &= 2\Omega(\overline{v'C'_\alpha}\sin\phi - \overline{w'C'_\alpha}\cos\phi) \\ &\quad - \overline{u'w'}\frac{\partial \bar{C}_\alpha}{\partial z} - \overline{w'C'_\alpha}\frac{\partial \bar{u}}{\partial z} + \frac{\partial}{\partial z}\left(\Lambda_2 q \frac{\partial \overline{u'C'_\alpha}}{\partial z}\right) \\ &\quad - \frac{q}{\Lambda_1}\overline{u'C'_\alpha} + \nu_o \frac{\partial^2 \overline{u'C'_\alpha}}{\partial z^2} - 2\nu_o \frac{\overline{u'C'_\alpha}}{\lambda^2}\end{aligned} \tag{12.56}$$

$$\begin{aligned}\frac{\partial \overline{v'C'_\alpha}}{\partial t} + \bar{u}\frac{\partial \overline{v'C'_\alpha}}{\partial x} + \bar{v}\frac{\partial \overline{v'C'_\alpha}}{\partial y} &= -2\Omega\overline{u'C'_\alpha}\sin\phi \\ &\quad - \overline{v'w'}\frac{\partial \bar{C}_\alpha}{\partial z} - \overline{w'C'_\alpha}\frac{\partial \bar{v}}{\partial z} + \frac{\partial}{\partial z}\left(\Lambda_2 q \frac{\partial \overline{v'C'_\alpha}}{\partial z}\right) \\ &\quad - \frac{q}{\Lambda_1}\overline{v'C'_\alpha} + \nu_o \frac{\partial^2 \overline{v'C'_\alpha}}{\partial z^2} - 2\nu_o \frac{\overline{v'C'_\alpha}}{\lambda^2}\end{aligned} \tag{12.57}$$

$$\frac{\partial \overline{w'C'_\alpha}}{\partial t} + \bar{u}\frac{\partial \overline{w'C'_\alpha}}{\partial x} + \bar{v}\frac{\partial \overline{w'C'_\alpha}}{\partial y} = 2\Omega \overline{u'C'_\alpha}\cos\phi$$

$$- \overline{w'w'}\frac{\partial \bar{C}_\alpha}{\partial z} + \frac{g}{T_o}\overline{T'C'_\alpha} + \frac{\partial}{\partial z}\left[\left(2\Lambda_2 + \Lambda_3\right)q\frac{\partial \overline{w'C'_\alpha}}{\partial z}\right]$$

$$- \frac{q}{\Lambda_1}\overline{w'C'_\alpha} + \nu_o\frac{\partial^2 \overline{w'C'_\alpha}}{\partial z^2} - 2\nu_o\frac{\overline{w'C'_\alpha}}{\lambda^2} \qquad (12.58)$$

$$\frac{\partial \overline{T'C'_\alpha}}{\partial t} + \bar{u}\frac{\partial \overline{T'C'_\alpha}}{\partial x} + \bar{v}\frac{\partial \overline{T'C'_\alpha}}{\partial y} = -\overline{w'C'_\alpha}\frac{\partial \bar{T}}{\partial z} - \overline{w'T'}\frac{\partial \bar{C}_\alpha}{\partial z}$$

$$+ \frac{\partial}{\partial z}\left(\Lambda_2 q\frac{\partial \overline{T'C'_\alpha}}{\partial z}\right) + \nu_o\frac{\partial^2 \overline{T'C'_\alpha}}{\partial z^2} - 2\nu_o\frac{\overline{T'C'_\alpha}}{\lambda^2} \qquad (12.59)$$

$$\frac{\partial \overline{C'^2_\alpha}}{\partial t} + \bar{u}\frac{\partial \overline{C'^2_\alpha}}{\partial x} + \bar{v}\frac{\partial \overline{C'^2_\alpha}}{\partial y} = -2\overline{w'C'_\alpha}\frac{\partial \bar{C}_\alpha}{\partial z}$$

$$+ \frac{\partial}{\partial z}\left(\Lambda_2 q\frac{\partial \overline{C'^2_\alpha}}{\partial z}\right) + \nu_o\frac{\partial^2 \overline{C'^2_\alpha}}{\partial z^2} - 2\nu_o\frac{\overline{C'^2_\alpha}}{\lambda^2} \qquad (12.60)$$

We have not as yet generated any solutions to these equations. The development of such solutions is a task that will be carried out under future funding from EPA.

13. CONCLUSIONS AND RECOMMENDATIONS

This monograph has presented in considerable detail the work carried out to date by A.R.A.P. towards the development of an invariant model of the motion in the atmospheric boundary layer and the dispersal of pollutants in such a layer. While it is clear that much remains to be done before a final model, complete with operational programs, is available for production studies of atmospheric pollutant dispersal, it is clear that a powerful new tool for the study of such atmospheric problems is emerging. A great deal of effort over the past two years has been devoted to the coding and debugging of the programs required for the exercise of the method. Most of the programs required for such studies are now complete. It is felt that the exercise of these programs can lead to a detailed understanding of the results of many experimental studies of pollutant dispersal, many of which have been difficult to interpret in terms of the simple diffusivity models that have been used in the past. It is strongly recommended that EPA continue to support the study of atmospheric pollution dispersal by the method of invariant modeling.

14. REFERENCES

1. Donaldson, Coleman duP.: "A Computer Study of an Analytical Model of Boundary Layer Transition," AIAA Journal 7, 2, (1969), pp. 272-278.

2. Reynolds, Osborne: "On the Dynamical Theory of Incompressible Viscous Fluids and the Determination of the Criterion," Phil. Trans. Royal Society, London, A 186, (1894), p. 123.

3. Kolmogorov, A.N.: "Equations of Turbulent Motion of an Incompressible Fluid," Izv. Akad. Nauk, SSSR fiz. VI, No. 1-2, (1942), pp. 56-58.

4. Prandtl, L. and Wieghardt, K.: "Über ein neuses Formelsystem für die ausgebeldte Turbulenz," Nachr. Akad. Wiss. Goettingen 19, 6 (1945).

5. Chou, P.Y.: "Pressure Flow of a Turbulent Fluid between Two Infinite Parallel Planes," Quart. Appl. Math.3, 3, (1949), pp. 198-209.

6. Rotta, J.: "Statistische Theorie nichthomogener Turbulenz," Z. Physik 129 (1951), p. 547.

7. Glushko, G.S.: "Turbulent Boundary Layer on a Flat Plate in an Incompressible Fluid," Bull. Acad. Science, USSR, Mech. Series No. 4 (1965), pp. 13-23.

8. Bradshaw, P., Ferriss, D.H., and Atwell, N.P.: "Calculations of Boundary Layer Development Using the Turbulent Energy Equation," J. Fluid Mech. 28, 3 (1967), pp. 593-616.

9. Beckwith, I.E. and Bushnell, D.M.: "Detailed Description and Results of a Method for Computing Mean and Fluctuating Quantities in Turbulent Boundary Layers," NASA TN D-4815, 1968.

10. Donaldson, Coleman duP. and Rosenbaum, Harold: "Calculation of Turbulent Shear Flows through Closure of the Reynolds Equations by Invariant Modeling," NASA SP-216, 1968, pp. 231-253.

11. Nee, V.W. and Kovasznay, L.S.G.: "Simple Phenomenological Theory of Turbulent Shear Flows," Phys. Fluids 12 (1969), pp. 473-484.

12. Daly, B.J. and Harlow, F.H.: "Transport Equation in Turbulence," Phys. Fluids 13, 11 (1970), pp. 26-34.

13. Gawain, T.H. and Pritchell, J.W.: "A Unified Heuristic Model of Fluid Turbulence," J. Comput. Physics 5, 3 (1970), pp. 383-405.

14. Saffman, P.G.: "A Model for Inhomogeneous Turbulent Flow," Proc. Royal Soc. London A.317 (1970), pp. 417-433.

15. Rodi, W. and Spalding, D.B.: "A Two Parameter Model of Turbulence and its Application to Free Jets," Warme- und Stoffubertragung 3 (1970), pp. 85-95.

16. Donaldson, Coleman duP., Sullivan, Roger D., and Rosenbaum, Harold: "A Theoretical Study of the Generation of Atmospheric Clear Air Turbulence," AIAA Journal 10, 2 (1972), pp. 162-170.

17. Lumley, J.L. and Panofsky, H.A.: *The Structure of Atmospheric Turbulence*, Interscience Publishers, New York, 1964.

18. Spiegel, E.A. and Veronis, G.: "On the Boussinesq Approximation for a Compressible Fluid," Astrophysics Journal 131, (1960), pp. 442-447.

19. Donaldson, Coleman duP.: "Calculation of Turbulent Shear Flows for Atmospheric and Vortex Motions," AIAA Journal 10, 1 (1972), pp. 4-12. Dryden Research Lecture, 1971.

20. Donaldson, Coleman duP. and Conrad, Peter W.: "Computations of the Generation of Turbulence in the Atmospheric Boundary Layer," presented at RAeS/AIAA/CASI Inter'l Conf. on Atmospheric Turbulence, London, May 1971.

21. Wygnanski, I. and Fiedler, H.: "Some Measurements in the Self-Preserving Jet," J. Fluid Mech. 38, 3 (1969), pp. 577-612.

22. Wygnanski, I. and Fiedler, H.: "The Two-Dimensional Mixing Region," J. Fluid Mech. 41, 2 (1970), pp. 327-361.

23. Gibson, M.M.: "Spectra of Turbulence in a Round Jet," J. Fluid Mech. 15, 2 (1963), pp. 161-173.

24. Donaldson, Coleman duP., Snedeker, Richard S., and Margolis, David P.: "A Study of Free Jet Impingement. Part 2: Free Jet Turbulent Structure and Impingement Heat Transfer," J. Fluid Mech. 45, 3 (1971), pp. 477-512.

25. Tollmien, W.: "Berechnung Turbulenter Ausbrietungsvorgange," Zeitschrift für angewandte Mathematik und Mechanik IV (1926), p. 468.

26. Prandtl, L.: "The Mechanics of Viscous Fluids," in *Aerodynamic Theory* (W. Durand, editor), Stanford University Press, 1934, pp. 34-208.

27. Coles, Donald: "Measurements in the Boundary Layer on a Smooth Flat Plate in Supersonic Flow. Part 1: The Problem of the Turbulent Boundary Layer," JPL Report 20-69, 1953.

28. Grant, H.L.: "The Large Eddies of Turbulent Motion," J. Fluid Mech. 4, 2 (1958), pp. 149-190.

29. Donaldson, Coleman duP. and Sullivan, Roger D.: "Decay of an Isolated Vortex" in *Aircraft Wake Turbulence and its Detection* (J. Olsen, A. Goldberg, M. Rogers, editors), Plenum Press, New York, 1971, pp. 389-411.

30. Donaldson, Coleman duP. and Hilst, Glenn R.: "An Initial Test of the Applicability of Invariant Modeling Methods to Atmospheric Boundary Layer Diffusion," A.R.A.P. Report No. 169, 1971.

31. Rotta, J.C.: "Recent Attempts to Develop a Generally Applicable Calculation Method for Turbulent Shear Flow Layers," AGARD Conference on Turbulent Shear Flows, London, September 1971. AGARD CP-93, pp. A.1-A.11.

32. Monin, A.S. and Obukhov, A.M.: "Basic Regularity in Turbulent Mixing in the Surface Layer of the Atmosphere," Trudy Geophysics Inst., ANSSSR 24 (1954), p. 163.

33. Rose, W.G.: "Results of an Attempt to Generate Homogeneous Turbulent Shear Flows," J. Fluid Mech. 25, 1 (1966), pp. 97-120.

34. Rose, W.G.: "Interaction of Grid Turbulence with a Uniform Mean Shear," J. Fluid Mech. 44, 4 (1970), pp. 767-779.

35. Fuquay, J., Simpson, C.L., and Hinds, W.T.: "Prediction of Environmental Exposures from Sources near the Ground Based on Hanford Experimental Data," J. Appl. Meteorol. 3, 6 (1964), pp. 761-770.

36. Lewellen, W. Stephen and Teske, Milton: "Prediction of the Monin-Obukhov Similarity Functions from an Invariant Model of Turbulence," A.R.A.P. Report No. 185, November 1972.

37. Hess, Seymour L.: *Introduction to Theoretical Meteorology*, Holt, Rinehart, and Winston, 1959, pp. 161-173.

38. Blackadar, Alfred K.: "The Vertical Distribution of Wind and Turbulent Exchange in a Neutral Atmosphere," J. Geophys. Res. 67, 8 (1962), pp. 3095-3102.

39. Lettau, H.: "Theoretical Wind Spirals in the Boundary Layer of a Barotropic Atmosphere," Beitr. Phys. Atmosph. 35. 3-4 (1962), pp. 195-212.

40. Appleby, J.F. and Ohmstede, W.D.: "Numerical Solution of the Distribution of Wind and Turbulence in the Planetary Boundary Layer," Proc. Army Sci. Conf. 1 (1964), pp. 85-99.

41. von Rosenberg, D.U.: *Methods for the Numerical Solution of Partial Differential Equations*, American Elsevier Publ. Co., Inc., New York, 1969.

42. Carnahan, B., Luther, H.A., and Wilkes, J.O.: *Applied Numerical Methods*, John Wiley & Sons, New York, 1969, pp. 449-461.

43. Crow, Steven C.: "Viscoelastic Properties of Fine-Grained Incompressible Turbulence," J. Fluid Mech. 33, 1 (1968), pp. 1-20.

APPENDIX A. NUMERICAL INTEGRATION TECHNIQUE

The equations discussed in this report are parabolic partial differential equations. They are parabolic in the sense that the time derivative $\partial/\partial t$ is first-order in time and is present in every equation with at most a second-order derivative $\partial^2/\partial z^2$ in a spatial dimension. In this appendix, we will explain the approximate numerical technique used by A.R.A.P. to obtain reasonable solutions to these differential equations.

Various numerical techniques are, of course, available to solve the types of equations we have discussed in this report. For our purposes, the implicit technique [Refs. 41 and 42] seems to be best, for a number of reasons. Its main attraction is its strong stability. The computerized equations should converge to a solution, even though it may not be the correct one. The simplicity of our boundary conditions, with all values going to zero at the earth's surface or to given known values at the upper surface, makes the application of the implicit technique almost straightforward. Another reason is computer environment. A.R.A.P.'s present computer is a 16K core (16 bits/word) Digital Scientific Corp. META-4 with secondary storage on a CalComp DS-12 disk drive. The relatively slow speed of computation (as demonstrated below) requires us to use a technique that permits solution as quickly as possible to the time-dependent problem. The implicit technique gives us that solution in a time that is faster (for the number of equations we typically handle) than a standard iterative technique.

To apply any of these several numerical techniques to a continuous differential equation, we first replace the differential equation with a finite difference equation. We represent the continuum spatial dimension by a series of discrete points. Three such points in the z direction are represented in Figure A.1 by the points at $j-1$, j, and $j+1$. In the same manner, we replace continuous time with discrete time, as with the time points n and $n+1$, as shown.

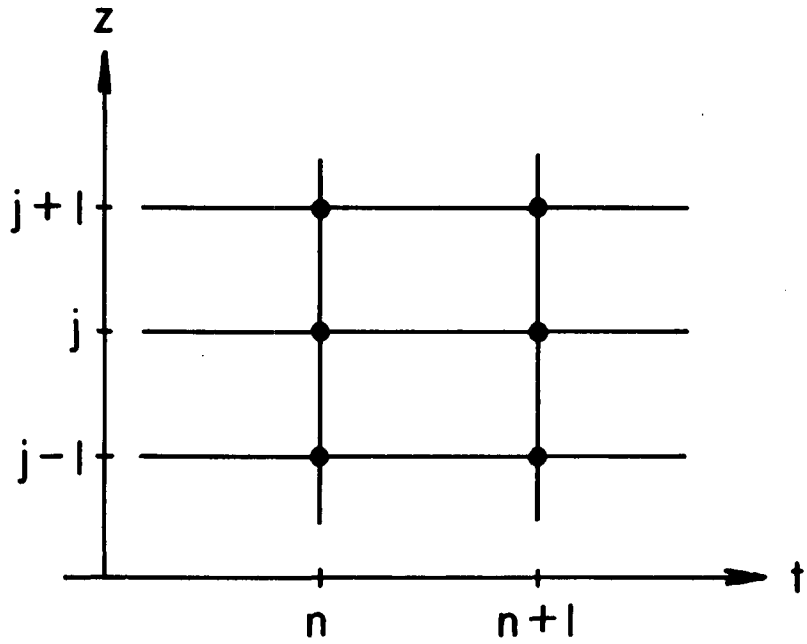

Figure A.1. The discretized time-space plane for the two-dimensional implicit solution technique

We solve the differential equations by starting with a given set of initial conditions at all z values, and then follow the solution for increasing time. We form an approximation to the continuous derivatives present in our equations. These difference approximations are then substituted into the differential equations to obtain a difference equation involving the values of the dependent variables as a function of the j and n positions. To solve this equation, we assume that the solution at t^n is known (computed from the last step or a given initial condition) and use the implicit technique given below to obtain the solution at time t^{n+1}. As we stated before, this technique is unconditionally stable, but it may not be consistent in that the difference equation may not relax to the differential equation in the limit of $\Delta z,\ \Delta t \to 0$. To ensure some success in solving our equation (since existence and uniqueness of our solutions have never been proven), we attempt internally within the computer program to maintain an "optimum" number of points in the profile in z at any one time step (a test based on curvature criterion) and an "optimum" step size in t based on maximum permitted change per step. This optimization enables us to compromise between accuracy and time considerations; as the time step decreases, the accuracy of the results increases, up to a point, but the total computation time increases accordingly. We know that our solutions are 1% accurate for the various laminar cases we have checked, and we strive to keep our turbulent solutions to an accuracy of 5%.

We must then approximate the four possible differentials $\partial/\partial t$, $\partial/\partial z$, $\partial^2/\partial z^2$, and $\partial(f(z)\partial/\partial z)/\partial z$. They become

$$\frac{\partial u}{\partial t} \doteq \frac{u_j^{n+1} - u_j^n}{t^{n+1} - t^n} \tag{A.1}$$

$$\frac{\partial u}{\partial z} \doteq \frac{\frac{h_-}{h_+}\left(u_{j+1}^{n+1} - u_j^{n+1}\right) + \frac{h_+}{h_-}\left(u_j^{n+1} - u_{j-1}^{n+1}\right)}{h_+ + h_-} \tag{A.2}$$

$$\frac{\partial^2 u}{\partial z^2} \doteq \frac{\frac{2}{h_+}\left(u_{j+1}^{n+1} - u_j^{n+1}\right) - \frac{2}{h_-}\left(u_j^{n+1} - u_{j-1}^{n+1}\right)}{h_+ + h_-} \tag{A.3}$$

$$\frac{\partial}{\partial z}\left(f(z)\ \frac{\partial u}{\partial z}\right) \doteq \frac{\frac{f_{j+1} + f_j}{h_+}\left(u_{j+1}^{n+1} - u_j^{n+1}\right) - \frac{f_j + f_{j-1}}{h_-}\left(u_j^{n+1} - u_{j-1}^{n+1}\right)}{h_+ + h_-} \tag{A.4}$$

where

$$h_+ = z_{j+1} - z_j$$

$$h_- = z_j - z_{j-1}$$

and u represents the dependent variable. With Eqs. (A.1) through (A.4) substituted into the differential equation of interest, we have replaced the equation by a forward-time-centered-space differencing that is first-order accurate in time and second-order accurate in space.

To get a feel for this technique, we now use Eq. (10.5) for $\overline{C_p'^2}$ as a very simple application. Since $\overline{v'C_p'}$, $\overline{w'C_p'}$, and $\overline{C}_p$ are presumably computed elsewhere, Eq. (10.5) contains only one dependent unknown, $\overline{C_p'^2}$, and may be rewritten as

$$\frac{\partial \overline{C_p'^2}}{\partial t} = -H + \frac{\partial}{\partial y}\left(\Lambda q \frac{\partial \overline{C_p'^2}}{\partial y}\right) + \frac{\partial}{\partial z}\left(\Lambda q \frac{\partial \overline{C_p'^2}}{\partial z}\right) + \nu_o\left(\frac{\partial^2 \overline{C_p'^2}}{\partial y^2} + \frac{\partial^2 \overline{C_p'^2}}{\partial z^2}\right) - 2\nu_o \frac{\overline{C_p'^2}}{\lambda^2} \tag{A.5}$$

where

$$H = 2\overline{v'C'_p}\,\frac{\partial \overline{C}_p}{\partial y} + 2\overline{w'C'_p}\,\frac{\partial \overline{C}_p}{\partial z} \tag{A.6}$$

and is known (in general, several equations will be coupled together to form a vector of unknowns, as shown below). For the one-space-dimensional problem, we may look at only the z and t dependence and assume that $\partial/\partial y = 0$ in Eq. (A.5). The substitution of Eqs. (A.1) through (A.4) into (A.5) yields the form

$$X_j^n u_{j-1}^{n+1} + Y_j^n u_j^{n+1} + Z_j^n u_{j+1}^{n+1} = D_j^n \tag{A.7}$$

where

$$X_j^n = -\frac{1}{h_-(h_+ + h_-)}\left\{\Lambda q_j + \Lambda q_{j-1} + 2\nu_o\right\} \tag{A.8}$$

$$Y_j^n = \frac{1}{t^{n+1} - t^n} + \frac{1}{h_+ + h_-}\left\{\frac{\Lambda q_{j+1} + \Lambda q_j}{h_+} + \frac{\Lambda q_j + \Lambda q_{j-1}}{h_-} + 2\nu_o\left(\frac{1}{h_+} + \frac{1}{h_-}\right)\right\} + \frac{2\nu_o}{\lambda^2} \tag{A.9}$$

$$Z_j^n = -\frac{1}{h_+(h_+ + h_-)}\left\{\Lambda q_{j+1} + \Lambda q_j + 2\nu_o\right\} \tag{A.10}$$

$$D_j^n = \frac{u_j^n}{t^{n+1} - t^n} - H_j^n \tag{A.11}$$

and u_{j-1}^{n+1}, u_j^{n+1}, and u_{j+1}^{n+1} are the unknown values of $\overline{C_p'^2}$ at $j-1$, j, and $j+1$. A similar linear equation may be written for every other interior point in our discrete space. Thus, if we have m points in the profile, we will have m difference equations (A.7) with $m+2$ unknowns. Since both boundaries are known, u_0^{n+1} and u_{m+1}^{n+1} are known values. We,

therefore, have a sufficient number of equations to solve for all of the u_j^{n+1} at the new time step.

We choose to use the general tridiagonal algorithm (called the Thomas algorithm in Ref. 41) to systematically solve for these unknowns. This method requires a double sweep of the z profile and is actually a straightforward Gaussian elimination. We begin at $j = 0$ knowing u_0^{n+1} and work towards the point $j = m+1$ by successively solving the following set of algebraic equations.

$$S_j^{n+1} = Y_j^n - X_j^n G_{j-1}^{n+1} \tag{A.12}$$

$$G_j^{n+1} = \left(S_j^{n+1}\right)^{-1} Z_j^n \tag{A.13}$$

$$W_j^{n+1} = \left(S_j^{n+1}\right)^{-1} \left(D_j^n - X_j^n W_{j-1}^{n+1}\right) \tag{A.14}$$

Since u_0^{n+1} is known, the first term in Eq. (A.7) is known for $j = 1$ and may be combined with D_j^n, enabling us to write $X_1^n = 0$.

The sweep is continued until $j = m$ where we downsweep back to $j = 1$ using the formula

$$u_j^{n+1} = W_j^{n+1} - G_j^{n+1} u_{j+1}^{n+1} \tag{A.15}$$

Since u_{m+1}^{n+1} is known and all the W_j^{n+1} and G_j^{n+1} are also known, the downsweep give the successive values of u at all the discrete z points j for the time t^{n+1}. The procedure is then repeated for the next time t^{n+2} and so on. For other boundary conditions, the technique needs some modification at the end points.

If u_j is a vector of unknowns $\overline{U}_j$ (as, for example, $\overline{C}_p$, $\overline{v'C'_p}$, $\overline{w'C'_p}$, and $\overline{T'C'_p}$ in Section 10), then X_j, Y_j, and

Z_j are square matrices and D_j is a vector. The inversion in Eqs. (A.13) and (A.14) is then a matrix inversion. The implicit technique is seen to be defeating if the size of the matrix (the number of unknowns) is abnormally high. In our facility, a matrix size of about 15 would appear to be prohibitive.

A typical running time for our various computer programs is one hour. If the program is small enough to fit into the 16K core, its running time would be reduced to 1/2 hour. Comparable running times on an 1108 Univac and CDC 6600 would be 5 and 2 minutes, respectively. The number of machine operations per second on the META-4 is approximately 200,000.

Equation (A.5) may also be used to demonstrate the Alternating Direction Implicit (ADI) method used to solve the spatial pollutant dispersal equations of Section 10. We now have the additional spatial dimension y with discrete points ..., k-1, k, k+1, ... as shown in Figure A.2. Our aim is to advance the plane of solution at t^n and all y and z to the time t^{n+1}. A straightforward substitution of the finite difference approximations (substituting y and k where appropriate) into (A.5) gives the form

$$I^n_{k-1,j}u^{n+1}_{k-1,j} + I^n_{k,j}u^{n+1}_{k,j} + I^n_{k+1,j}u^{n+1}_{k+1,j}$$

$$+ I^n_{k,j-1}u^{n+1}_{k,j-1} + I^n_{k,j+1}u^{n+1}_{k,j+1} = D^n_{k,j} \qquad (A.16)$$

where the I's involve the spacing factors and other known values. Each equation now contains five unknowns. With the known boundary conditions, there are as many equations as unknowns, but the difficulty of the problem has increased considerably. An elimination technique could be employed at this point, but it is far easier from our point of view to use the ADI method. In this method, every time step is split and two half-steps are performed. In the first half-step, one of the spatial dimensions is swept up

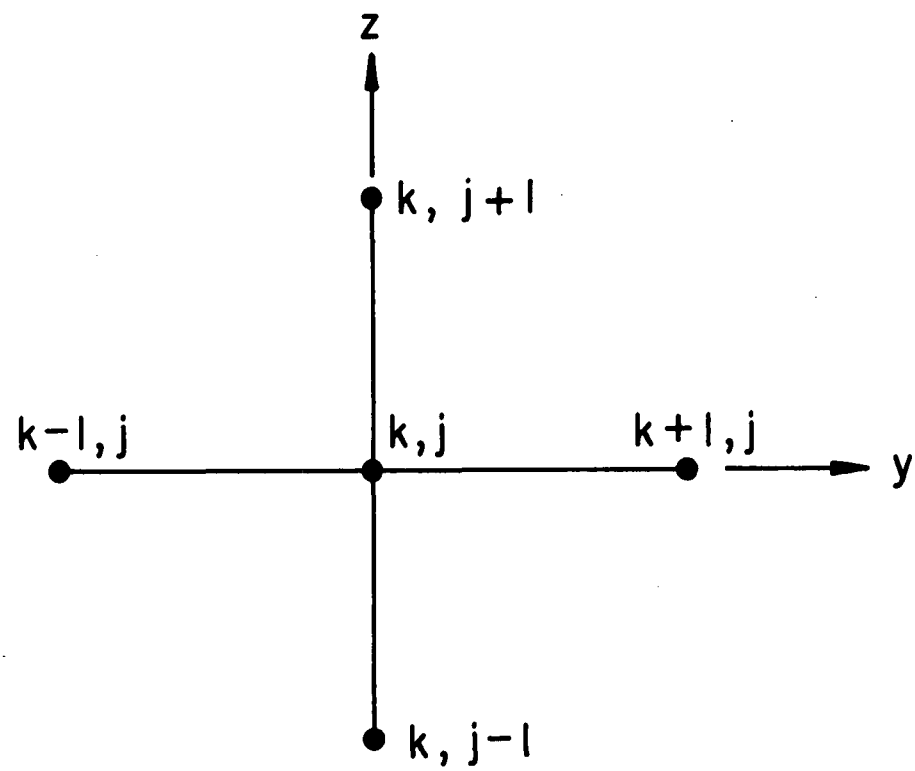

Figure A.2. The discrete spatial plane at time step t^n

and down; in the second half-step, the other dimension is swept. During the first sweep (say, z) from t^n to $t^{n+1/2}$, the y derivatives are held fixed at their t^n values. During the second sweep in y from $t^{n+1/2}$ to t^{n+1}, the z derivatives are held fixed at their $t^{n+1/2}$ values. It can be shown [Ref. 41] that while this double sweep (alternating direction) uses two sets of equations similar to Eq. (A.7), its full-step results are equivalent to using Eq. (A.16). Of course, the complexity of the computer program and its running time are increased significantly.

BIBLIOGRAPHIC DATA SHEET	1. Report No. EPA-R4-73-016a	2.	3. Recipient's Accession No.
4. Title and Subtitle ATMOSPHERIC TURBULENCE AND THE DISPERSAL OF ATMOSPHERIC POLLUTANTS			5. Report Date Approved March 1973 6.
7. Author(s) Coleman duP. Donaldson			8. Performing Organization Rept. No. 186, Vol. I
9. Performing Organization Name and Address Aeronautical Research Associates of Princeton, Inc 50 Washington Road Princeton, New Jersey 08540			10. Project/Task/Work Unit No. Element A-11009 11. Contract/Grant No. EPA 68-02-0014
12. Sponsoring Organization Name and Address U.S. Environmental Protection Agency Office of Research and Monitoring Washington, D.C. 20460			13. Type of Report & Period Covered Interim 14.

15. Supplementary Notes

16. Abstracts

A detailed derivation of the equations describing the generation of turbulence and the transport of pollutants in the atmosphere is given. The equations are closed at the order of the second-order turbulent correlations through the use of models of the higher-order correlations. The resulting invariant second-order closure model is applied to three problems: 1) the generation of turbulence in the surface layer (computed results are compared with AFCRL experimental data); 2) the transport of passive pollutants in the atmosphere (computed results are compared with experimental data and suggestions for improving the model are made); 3) the complete planetary boundary layer for the case of neutral stability for both smooth and rough surfaces. The results of computations are compared with the results of previous investigations.

17. Key Words and Document Analysis. 17a. Descriptors

Turbulence
Turbulence Models
Atmospheric Motion
Atmospheric Turbulence
Atmospheric Transport
Pollutant Dispersal
Atmospheric Boundary Layer
Atmospheric Surface Layer
Ekman Layer
Second-order Closure
Second-order Modeling
Invariant Modeling
Boundary Layers
Surface Roughness

17b. Identifiers/Open-Ended Terms

17c. COSATI Field/Group

18. Availability Statement	19. Security Class (This Report)	21. No. of Pages
Unlimited	UNCLASSIFIED	210
	20. Security Class (This Page) UNCLASSIFIED	22. Price

INSTRUCTIONS FOR COMPLETI graphic Data Sheet based on COSATI Guidelines to Format Standards for Scientific and Technical Reports Prepared by or for the Federal Government, PB-180 600).

1. **Report Number.** Each individually bound report shall carry a unique alphanumeric designation selected by the performing organization or provided by the sponsoring organization. Use uppercase letters and Arabic numerals only. Examples FASEB-NS-87 and FAA-RD-68-09.

2. Leave blank.

3. **Recipient's Accession Number.** Reserved for use by each report recipient.

4. **Title and Subtitle.** Title should indicate clearly and briefly the subject coverage of the report, and be displayed prominently. Set subtitle, if used, in smaller type or otherwise subordinate it to main title. When a report is prepared in more than one volume, repeat the primary title, add volume number and include subtitle for the specific volume.

5. **Report Date.** Each report shall carry a date indicating at least month and year. Indicate the basis on which it was selected (e.g., date of issue, date of approval, date of preparation.

6. **Performing Organization Code.** Leave blank.

7. **Author(s).** Give name(s) in conventional order (e.g., John R. Doe, or J.Robert Doe). List author's affiliation if it differs from the performing organization.

8. **Performing Organization Report Number.** Insert if performing organization wishes to assign this number.

9. **Performing Organization Name and Address.** Give name, street, city, state, and zip code. List no more than two levels of an organizational hierarchy. Display the name of the organization exactly as it should appear in Government indexes such as **USGRDR-I.**

10. **Project/Task/Work Unit Number.** Use the project, task and work unit numbers under which the report was prepared.

11. **Contract/Grant Number.** Insert contract or grant number under which report was prepared.

12. **Sponsoring Agency Name and Address.** Include zip code.

13. **Type of Report and Period Covered.** Indicate interim, final, etc., and, if applicable, dates covered.

14. **Sponsoring Agency Code.** Leave blank.

15. **Supplementary Notes.** Enter information not included elsewhere but useful, such as: Prepared in cooperation with . . . Translation of . . . Presented at conference of . . . To be published in . . . Supersedes . . . Supplements . . .

16. **Abstract.** Include a brief (200 words or less) factual summary of the most significant information contained in the report. If the report contains a significant bibliography or literature survey, mention it here.

17. **Key Words and Document Analysis. (a). Descriptors.** Select from the Thesaurus of Engineering and Scientific Terms the proper authorized terms that identify the major concept of the research and are sufficiently specific and precise to be used as index entries for cataloging.
(b). Identifiers and Open-Ended Terms. Use identifiers for project names, code names, equipment designators, etc. Use open-ended terms written in descriptor form for those subjects for which no descriptor exists.
(c). COSATI Field/Group. Field and Group assignments are to be taken from the 1965 COSATI Subject Category List. Since the majority of documents are multidisciplinary in nature, the primary Field/Group assignment(s) will be the specific discipline, area of human endeavor, or type of physical object. The application(s) will be cross-referenced with secondary Field/Group assignments that will follow the primary posting(s).

18. **Distribution Statement.** Denote releasability to the public or limitation for reasons other than security for example "Release unlimited". Cite any availability to the public, with address and price.

19 & 20. **Security Classification.** Do not submit classified reports to the National Technical

21. **Number of Pages.** Insert the total number of pages, including this one and unnumbered pages, but excluding distribution list, if any.

22. **Price.** Insert the price set by the National Technical Information Service or the Government Printing Office, if known.